Design Tool for Direct Drive Wind Turbine Generators

Proposed solutions for direct drive Darrieus generators 20MW

Leban, Krisztina Monika

Publication date:
2014

Document Version
Publisher's PDF, also known as Version of record

AALBORG UNIVERSITY
DENMARK

SEVENTH FRAMEWORK
PROGRAMME

PhD Thesis

Design Tool for Direct Drive Wind Turbine Generators

Author
Krisztina Leban

Supervisor
Ewen Ritchie

Design Tool for Direct Drive Wind Turbine Generators

Proposed solutions for direct drive Darrieus generators 20MW

ISBN: 978-87-92846-41-9

Author: Krisztina Monika Leban

Supervisor: Associate Professor Ewen Ritchie

List of published papers directly related the present thesis:

[1] Leban K, Ritchie E, Alin A. Design Tool for 5-10 MW Direct Drive Generators. Electromotion journal Vol 21 (2014) 2014, Accepted, Publication Pending; ISSN 1223 - 057X.

[2] Leban K, Ritchie E, Argeseanu A. Design preliminaries for direct drive under water wind turbine generator. Electrical Machines (ICEM), 2012 XXth International Conference on IEEE, 2012 2012:190-5.

[3] Marie-Christine Schimmelmann, Elena Charlotte Malz, Enrique Müller Llano, Lennart Petersen, Theodoros Kalogiannis, Krisztina Monika Leban, Andrew Ewen Ritchie. Alternative Parameter Determination Methods for a PMSM . Optimization of Electrical and Electronic Equipment (OPTIM), 2014 14th International Conference on 2014 , Accepted, Publication Pending.

[4] Nedelcu S, Ritchie E, Leban K, Ghita C, Trifu I. Iron losses evaluation in soft magnetic materials with a sinusoidal voltage supply. Advanced Topics in Electrical Engineering (ATEE), 2013 8th International Symposium on 2013:1-6.

[6] Nica FTV, Ritchie E, Leban K. A comparison between two optimized TFPM geometries for 6 MW direct-drive wind turbines. Advanced Topics in Electrical Engineering (ATEE), 2013 8th International Symposium on IEEE 2013.

[7] Nica FTV, Ritchie E, Leban KM. Comparison between Genetic Algorithms and Particle Swarm Optimization Methods on Standard Test Functions and Machine Design. Proceedings of the 10th Jubilee International Symposium on Advanced Electrical Motion Systems-Electromotion 2013 Cluj-Napoca, Romania 2013;Volume 20, Number 1-4 January-December 2013:ISSN 1223-057x.

[8] U.S.Paulsen, H.A.Madsen, K.A.Kragh, P.H.Nielsen, E.Ritchie, K.M.Leban, H. Svendsen, P.A. Berthelsen. The 6 MW DeepWind floating offshore vertical wind turbine concept design-status and perspective . EWEA 2014 2014;Energy Procedia, Science Direct.

[9] Uwe S. Paulsen, Helge A. Madsen, Knud A. Kragh, Per H. Nielsen, Ismet Baran, Jesper Hattel, Ewen Ritchie, Krisztina Leban, Harald Svendsen, Petter A. Berthelsen. DeepWind-from idea to 6 MW concept. Energy Procedia, Science Direct 2014;EERA DeepWind'2014, 11th Deep Sea Offshore Wind R&D Conference.

[10] Paulsen US, Vita L, Madsen HA, Hattel J, Ritchie E, Leban KM et al. First DeepWind 5 MW Baseline design. Energy Procedia Volume 24, 2012, Pages 27–35 Selected papers from Deep Sea Offshore Wind R&D Conference, Trondheim, Norway, 19-20 January 2012 2012.

The complete list of papers arising from the funding research project is presented in Appendix 1 of this thesis.

This present report combined with the above listed scientific papers has been submitted for assessment in partial fulfilment of the PhD degree. The scientific papers are not included in this version due to copyright issues. Detailed publication information is provided above and the interested reader is referred to the original published papers.

As part of the assessment, co-author statements have been made available to the assessment committee and are also available at the Faculty of Engineering and Science, Aalborg University.

For my Mother and Father…

Abstract (English)

The current work offers a comparison of the proposed machine geometries for 6 [MW] direct drive wind generator candidates with the prospective of up scaling to 20MW. The suggestions are based on a design tool especially built for this investigation. The in-built flexibility of the design tool gives the possibility of calculating a large variation of geometries using existing modules. The main goal is to be able to quickly and transparently asses the feasibility of a proposed machine for a set of requirements.

As a first step, a set of suitable machine types for the 6 [MW] design were investigated.

A comparison of the selected machine types in view of up-scaling to 20 [MW] was performed. As an example fitness criterion, the use of active materials for the generators was considered. Based on this, suggestions for 20 [MW] generators were made. The results are discussed and future work, directions and suggestions for potential improvement were listed

The design is obtained analytically at first; then visualised in 3D CAD (Computer Assisted Design) and evaluated in FEM. An analytical optimisation (Particle Swarm –PSO and Genetic Algorithms -GA) patch is available for improving the design. The tool is destined for engineers that are involved in the design of wind turbine systems.

The visualisation of the design in work is important for the overall assessment of the machine concept. The tool provides facilities for reporting on a shaped design: list of geometrical and electromagnetic quantities, pictures of the machine itself (3D particular drawing); FEM (Finite Element Model) electromagnetic profile, dynamic simulation model results and characteristic curves.

The structure of the design tool is modular and independent so that new machine types and geometries can be designed by reusing recombining and altering the different calculation modules. The design algorithm is transparent as logging of location and comments is used throughout the program. The purpose of this is to enable further development of the design tool by several contributors.

The tool was validated by both software and laboratory tests on a prototype and by comparing results with literature reporting of similar machines.

Supervisor

Ewen Ritchie

Author

Krisztina Leban

Abstrakt (Dansk)

Det arbejde giver en sammenligning af de foreslåede maskine geometri kandidater til 6 [MW] direkte drev vindmøller med henblik på en opskalering til 20 MW. Forslagene er baseret på et design værktøj specielt bygget til denne undersøgelse. Den indbyggede fleksibilitet i design værktøjet giver mulighed for beregne en stor variation af geometrier ved hjælp af eksisterende moduler. Hovedformålet er at være i stand til hurtigt og gennemskueligt at vurdere bæredygtigheden af en udviklet maskine mod en række krav.

Som det første skridt, blev et sæt af egnede maskintyper til en 6 [MW] undersøgt.

En sammenligning af de udvalgte maskintyper med henblik på opskalering til 20 [MW] blev udført. Som et muligt fitness kriterium, blev brugen af aktive materialer til generatorerne overvejet. Baseret på dette, blev forslaget til 20 [MW] generatorer foretaget. Resultaterne diskuteres og fremtidigt arbejde, udviklingsretninger og forslag til mulige forbedringer blev beskrevet.

Designet opnås først analytisk; derefter visualiseret i 3D CAD (Computer Assisted Design), og evalueret i FEM. En analytisk optimerings (Particle Swarm - PSO og genetiske algoritmer - GA) opdatering er til rådighed for at forbedre designet. Værktøjet er beregnet til ingeniører, der er involveret i udformningen af vindmølle turbine systemer.

. Værktøjet tilbyder faciliteter til visualisering: liste af geometriske og elektromagnetiske størrelser, billeder af selve maskinen (3D tegning); FEM (Finite Element Method) elektromagnetisk profil, dynamisk simulerings resultater og karakteristiske kurver.

Design værktøjet er opbygget i uafhængige moduler, så nye størrelser og geometrier at maskine typer kan designes ved at genbruge, omstrukturer og ændre de forskellige beregningsmoduler. Design algoritmen er gennemsigtig eftersom: funktions kald logges og kommentarer bruges igennem hele program strukturen.. Formålet med dette er at andre kan bidrage til fremtidig udvikling af design værktøjet.

Værktøjet er valideret ved hjælp af software, laboratorieundersøgelser på en prototype, og ved at sammenligne resultaterne med litteratur på lignende maskiner.

Supervisor

Ewen Ritchie

Author

Krisztina Leban

Foreword

The author, Krisztina Leban is a PhD Fellow at the Department Of Energy Technology at Aalborg University, Denmark. The objective of her project is to develop a design tool for direct drive electric generators for wind turbine applications.

Krisztina Leban got her BSc at Polytechnic University of Timisoara, Romania at the department of Electrical Engineering 2007. In 2009 she got her MSc diploma in Power Electronics and Drives at the Dept. of Energy Technology at Aalborg University Denmark.

This report presents work carried out for the Deep Wind project. Calculations for Work Package 3 (WP3-*Generator concepts*) of the project are reported.

The report is structured in main chapters and a set of appendices. The main report presents the problem to be solved and the proposed solutions. The appendices help the understanding of the main chapters.

Each chapter and appendix starts with a short description of the contents.

A list of the programs, with version numbers, used to develop different modules of the Design Tool is presented. The listing is important information for the contributors when further developing the tool.

Papers published/in publishing at the time of the present thesis submission that are a result of the work carried out in connection with DeepWind at Aalborg University, Institute of energy Technology are presented in the dedicated appendices.

The decision of presenting a detailed study of the proposed problems in the time given for a PhD Fellowship lead to several researchers contributing to the work. Original contribution of the author is clearly stated. Researchers that have contributed the present work by dealing with neighbouring tasks are listed and their contribution specified.

For the purpose of simplifying the text, the concept of the Deep Wind 6 [MW] and 20[MW] direct drive electrical generator for vertical axis Darrieus wind turbines will be referred to in this report as ‘Nessie’. The prototype constructed to validate de design calculations will be referred to as ‘BabyN’

Acknowledgements

Funding of the presented work was possible through the FP7 DEEP WIND no: 256769 European project.

The research was carried out at the Department of Energy Technology, Aalborg University, Denmark (IET AAU) where the Academic staff and the technical and administrative personal supported the present work

The author would like to thank supervisor Ewen Ritchie and research colleague Alin Argeseanu (Polytechnic University of Timisoara, Romania-UPT) and Florin Nica (AAU IET, UPT) for help and guidance in carrying out the work.

Special thanks to Zi Qiang Zhu, Head of Electrical Machines and Drives Group at Sheffield University, UK, for offering the possibility of a study abroad period in 2013.

Thank you to IET AAU technical staff for helping to build and set up the prototype: Jens Korsgaard , Danny Friwat, Walter Neumayr, Jan Christiansen and Mads Lund.

The author would like to thank the Deep Wind consortium

DTU: Project leader Uwe Schmidt Paulsen, colleagues Luca Vita, Helge Aagaard Madsen, Troels Friis Pedersen, David Robert Verelst, Knud Abildgaard Kragh, Per Hørlyk Nielsen, Ismet Baran);

MARINTEK (Petter Andreas Berthelsen, E.d.Ridder),

SINTEF (Harald G. Svendsen , Karl O. Merz)

TU Delft(Gerard van Bussel, Carlos Simao Ferreira, Nick Chrisocoidis),

Statoil (Wei He),

AAU(Ewen Ritchie, Ionut Trintis, Florin Nica) for a productive collaboration during the course of the research work.

The author would like to show appreciation for the interesting scientific discussions to Robert Nielsen, Norwegian University of Science and Technology, Department of Electric Power Engineering, Trifu Ion, Polytechnic University of Bucharest, Romania.

Hans-Christian Becker Jensen receives special thanks for the inter linguistic assistance rendered to the present thesis (he helped translated the abstract to Danish because he is).

Table of Contents

List of Chapters with Contents (Structure of the thesis)

Chapter 1: Introduction

In this chapter, a description of the problem to be solved is presented. Objectives, task outlines and limitations are listed. Outline of constraints and their level of flexibility are included.

Chapter 2: The Electrical Machines Design Tool

This section presents a general overview of the design tool. The main focus is set on a general description of the program, who the tool is intended for, and how the program is to be used. The implemented features and the user interface are presented and discussed.

Chapter 3: 6 [MW] Candidates

In this chapter a set of 6 [MW] designs are presented. The aim is to evaluate the designs for their suitability to be up scaled from 6 to 20 MW. As an exercise, the machines were compared with respect to the criteria of active mass usage. The design tool allows for comparison on basically any criteria chosen by the user.

Chapter 4: Discussion of Candidates – Outlook from 6 [MW] to 20 [MW]

By comparing the most suitable designs, a discussion of the 6 [MW] machines is carried out. The aim is to determine which machine type would be best suited for the 20 [MW] generator.

First, comparison criteria and issues influencing the final decision are discussed.

Suggested solutions for 20[MW] 1 [RPM] (10 [RPM]) (values suggested by the Deep Wind Project) are discussed. A set of concepts are evaluated for suitability.

Chapter 5: 20 [MW] Suggested Design

A comparison between the radial flux classic design and the double airgap suggestion is made in order to show which geometry is most feasible candidate for up-scaling.

Chapter 6: Future Work

This chapter outlines the work to be done in order to continue the development of the idea of Nessie. Tasks to be completed as well as new and possible research directions are listed.

Chapter 7: Overall Discussion and Final Conclusions

This chapter presents a discussion on the problem that was approached within this thesis. Overall conclusions are drawn based on the obtained results. The chapter is regarded as a summary of the main story line of the thesis.

Appendix 1: Publications. Contributions to the Present Work

This appendix gives information about the author and collaborators of the design tool and lists which parts of the tool they have been involved in. The list of papers arising from the research is listed. The contacts of the author and of the other researchers involved in the present research are presented.

Appendix 2: Deep Wind Project Description

This appendix gives an insight to the goals and constraints of the Deep Wind Project. The information listed is meant to aid in understanding of the approach taken in the current thesis. The solutions found during the research were tailored to the specifications of the project contract.

Appendix 3: List of Programs Used to Develop the Design Tool

This appendix lists the programs with version numbers used to develop different modules of the Nessie Design Tool. The listing is important information for the contributors further developing the tool.

Appendix 4: State of the Art SOA –Direct Drive Turbines

The aim of this appendix is to find the most suitable machine topology for Nessie. This is done by studying what industry and the scientific literature proposed [1]*,* [2]*,* [3]*. Having the set of requirements arising from the DeepWind Project (see Deep Wind Project Description in Appendix 2) the candidate is outlined.*

Appendix 5: SWOT – Most Suitable Machine for Nessie

In this appendix, strong point, Weak Point, Opportunity and Threats (SWOT) analysis was employed evaluate the available options for the Nessie generator. Rating is based on literature study.

Appendix 6: Special Issues to be Considered

In this appendix, a set of issues that turned up during the current research, but were not studied in detail within this project are presented. The importance of each element is recognised and a starting point towards their investigation is set.

Appendix 7: GUI Guide

In the following, an overview of the GUI (Graphical User Interphase) environment is given. Interfaces to the different calculation parts of the tool are presented. Familiarisation with the design tool GUI is important as the users and most of the time the developers of the program use this to initialise and run the programs behind it in a quicker and more intuitive way.

Appendix 8: Design Tool Algorithm and Equations

This appendix presents calculation steps and equations used to design various aspects of the electrical machine. The formulae used in the different modules are shown for the sake of calculation transparency; the elements of the equations are intentionally not symbols. As much as possible, the names of the code variables were used. In this way there is no need for an additional list of symbols as the long names of the elements are self-explanatory. For the coding these notations help with understanding the calculation at any point of viewing/browsing.

Appendix 9: Design Rules

This appendix discusses the different design rules for sizing electrical machines. The impact of their variation on the design is noted.

Appendix 10: Validation of the Design Tool

In the following, validation methods for the calculation results of the design tool are presented and discussed. Several methods applied for the present work are presented: comparison to literature reports, visualisation in 3d models, finite element and prototyping.

Appendix 11: BabyN Prototype

In this appendix, the Deep Wind prototype (BabyN) used to verify the design tool is presented. The idea is to have a generator and then, knowing the specification of the constructed machine (geometrical and material characteristics), to design the machine using the calculation tool. Compare the actual machine with the result of the calculation. As a result of the analysis, a verification of the accuracy of the calculation tool should be made. At first, a description of the machine is made. The laboratory tests and results are presented and discussed.

Appendix 12: Optimisation Tools

The current Appendix presents the background of the optimisation module of the design tool. The principles of the Particle Swarm Optimisation (PSO) and Genetic Algorithms (GA) are presented. Implemented elements are listed and linked to the theory.

Appendix 13: Dynamic Simulation Models for the Generator System

This section presents the simulation model used to test the machine parameters generated by the design tool.

Appendix 14: Complete Data Sheets

A complete set of values are presented for the Classic RF Benchmark (unoptimised) machine This is an example of a raw design data sheet that is produced by the Nessie Calculation Tool.

Abbreviations and Symbols

A list of abbreviations used in the thesis is given. To a certain extent, the use of symbols was avoided because they always have to be liked to their meaning in order to render the equations easy to follow. A few symbols were however used. They are listed below.

Abbreviations

AAU – Aalborg University
AFPM – Axial Flux PM Generator
BabyN – Nessie Prototype
BMOD – modulus of the magnetic flux density vector
CAD – Computer Assisted Design
DFIG – Doubly Fed Induction Generator(Radial Flux RF)
EESG – Electrically Excited Synchronous Generator (Radial Flux RF)
EMF – Electro Motive Force-induced voltage
FEM – Finite Element Model
GA – Genetic Algorithms
GUI – Graphical User Interface
IET – Institute of Energy Technology
J-Assembly moment of inertia
m – number of phases
Nessie – a machine having the Deep Wind requirements
PM – permanent magnet
PMSG – Permanent Magnet Synchronous Generator
PMSG – PM Synchronous Generator(Radial Flux RF)
POT – Magnetic vector potential
PSO – Particle Swarm Optimisation
PWM – Pulse Width Modulation
Qs – Number of Slots
SCIG – Squirrel Cage Induction Generator(Radial Flux RF)
SOA – State of the Art
SWOT – Strong points, Weak points, Opportunities and Threats
TFPM – Transverse Flux PM Generator
UPT – University Polytecnic of Timisoara
VSI(C) – Voltage Source Inverter (Converter)

Symbols

B – induction/ flux density
Bwkg, Hwkg – working point of PM
f – frequency
hx – height of x
I – current
$k_{integrator}$i – integrator constant for the current controller
$k_{Integrator}$speed – proportional constant for the speed controller
$k_{proportional}$i – integrator constant for the current controller
$k_{proportional}$speed – proportional constant for the speed controller
L_d, L_q – d and q inductances
N – number of turns
wx – width of x

Chapter 1: Introduction

In this chapter, a description of the problem to be solved is presented. Objectives, task outlines and limitations are listed. Outline of constraints and their level of flexibility are included.

Offshore wind turbines are becoming more appealing than onshore ones due to better cost efficiency [4], [5] . The trend is to go up in power and consideration of the direct drive wind turbine is proposed in industry and research literature. Advantages of the direct drive generators like the absence of the gearbox which causes reduced amounts of maintenance, better performance, lower vibration levels and high torque at low speeds make the drive an attractive candidate for wind turbines.[6], [7], [8].

The direct drive concept requires that the generator be directly connected to the shaft of the turbine rotor blades. This means that the generator rotates at a low speed, which makes it necessary to produce a high torque. Relatively large wind turbine generators are usually designed with a large diameter and a small pole pitch in order to increase the efficiency of the system, reduce the active mass and to keep the end winding losses small. [1], [9], [10], [11], [12].

The large diameter and heavy mass of the direct drive generator causes difficulty in production, transport and maintenance. With this in mind, implications of such an application have to be listed, discussed, and taken into account when designing the generator.

Basically, there are two configurations of wind turbines; horizontal and the vertical axis. For the present project, final focus will be directed only to the vertical axis turbine as stated in the DeepWind grant agreement. [4].

The Deep Wind Project (see details in Appendix 2) from which the present work arouse, commissioned a design tool that enables calculation of electric generator for direct drive wind turbines.-generically called Nessie (Deep Wind direct drive generator system for Darreius turbines)Figure 1. The goal is to go up to 20 [MW] and around 3 [RPM] through a 6 MW, 5.7 [RPM] design.

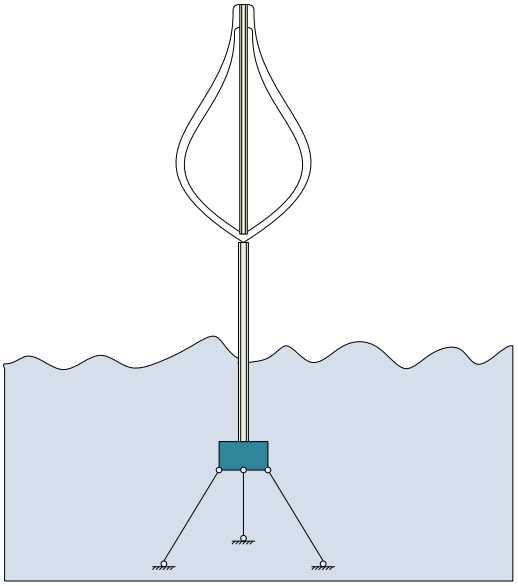

Figure 1: Nessie Concept

The overall objective of the Deep Wind project is to explore technologies for developing new and simple floating offshore vertical axis rotor wind turbines. The case of vertical axis turbines is discussed here, but if desired, the tool can easily cater for horizontal axis turbines due to the general approach taken.

The Deep Wind Project contract sets certain technological demands. From these subtasks emerge.

- floating, offshore construction
- vertical axis turbine-Darreius type-this kind of turbine is not self-starting
- the generator should be direct drive (gear ratio to be optimised: geared 1:x – could be 1:1)
- high power (5-20MW)
- as a consequence of the generator being direct drive, the rotational speed is relatively low (max 10 [RPM])

In the following, the problem that was treated in this thesis is outlined

A. Problem Formulation

Can investigation of Nessie type generator concepts be done fast and easy in order to evaluate their feasibility?

Because, at the beginning of the process the machine type for the generator is not fixed, different candidates for the generator should be discussed by the project team for a suitable 20 [MW] 3 [RPM] design.

To be able to make a decision supported by arguments, a tool with which the proposed concepts can be quantified and analysed is needed.

The goal of the present work is to make a design tool that would enable valid calculations and assessment of proposed concepts and ideas for Nessie type generators. The program should be dedicated to all researchers working with wind turbine systems. The tool should be constructed in such a way that additional models could be easily added to it by either the original or new developers. Design of new topologies of electrical machines should be made easy by using/modifying or reusing existing functions.

The approach is to move towards an analytical design algorithm using the developed design rules and scrutinise the output in different evaluation or simulation software that are interesting for wind turbine developers.

B. Objectives

The main goal is to build a design tools for development and evaluation of very large (up to 20MW) wind turbines based on the above mentioned concept [11], [1,12].

The contribution to the field of electrical machines design for generator applications is not to obtain a specific design but to enable the quick evaluation of design concept with a view to in depth design of the one considered most suitable for a certain set of requirements. Another aspect of the contribution is the ability to independently develop design modules within the tool. It is intended that several interest groups (e.g. turbine designers, material designers, generator system manufacturers) bring their contribution to the area of their interest. The design tool is able to incorporate their developments and run as a unity with minimum of effort provided the development rules for the design modules are followed.

In the following the objectives of the present work, outlining the approach taken are listed:

- Analyse the state of the art(SOA) of the field, posing the following questions
  - What machine type is best suited for the application?(feasibility, control requirements by grid codes [13], [14], [15], [16], [17].
  - How to make a flexible design tool that could be used to further investigate solutions
  - What kind of materials to use: to get the desired performance and to cope with the environment and lifetime demands?
  - How to improve the design: concept and optimisation algorithms

- As a result of the SOA analysis, decide on the most suitable generator type(s) for the DeepWind application
- Choice of software to use
- Establish design algorithms
- Construct the design tool-aim for flexibility, not best design-need to keep options open at this concept stage:
  - Design benchmark generator to compare other proposed solutions-for 6 MW
  - Propose several solution for the 6 MW
  - Compare and discuss designs in view of up scaling
  - Propose up-scaled generator concept for 20MW, 1[RPM]

  A list of programs used together with their version numbers is given in Appendix 3.
- Find methods to verify the algorithm
- Make a prototype in parallel to verify the design tool(it takes about 1,5 years for a prototype to be constructed)
- Validate the calculation
- Initiate generator topology analysis
- Document the work
- Outline and discuss future work

C. Overall Approach

In the following, the approach to solving the problem is presented. The concept behind the design tool is detailed.

Select the most suitable generator type for the DeepWind application. To reach the goal of up scaling the Nessie concept from 6 to 20 MW, several machines are considered in detail for the 6 [MW] version. Each proposed design is evaluated and a suitability comparison is carried out. As a result of the study, the 20[MW] machine is outlined. The candidates for Nessie were investigated. Appendix 4 contains the list of candidates as part of the state of the art (SOA) on generators for direct drive wind turbines. Appendix 5 shows a suitability analysis of the proposed candidates in the form of a SWOT (Strong points, Weak points, Opportunities and Threats) assessment. It was concluded that the radial flux permanent magnet PMSG and electrically excited EESG synchronous generators as well as the Transverse flux machines (TFPM) are worth investigating. The approach to solving the problem is:

1. **Make a design tool for Nessie**: Based on an analytical machines design algorithm [18], [19], [20], [21], [22], [23],[24], [25,26], obtain a first sizing of the machine. Construct the analytical design code in a modular way so that functions and sub programs could be reused for different variety of the same machine type and new types.

   A library of selectable materials was built for each element: iron, copper, permanent magnets (PM), insulation. The materials contain, characteristic curves and specific constants.

   The design process should be as automatic as possible (push button concept) but still be influenced by the user if so desired.

   Design programs for all 'best candidates' will be made incorporating design rules, sizing calculation and the associated code program. To be able to compare designs, a reference design was be calculated-ClassicNessie.

   For each calculation, a set of parameters ready to be integrated in a power systems simulation

2. **Enable analysis** of current design **using analytic approaches, CAD, FEM, Dynamic simulations** (requires specific outputs from the design process to feed to models)
3. **Validate the design tool**. Check the calculations against reports in the literature; see representation of the design in several software (CAD, FEM, Simulink) and compare results with laboratory test on the prototype built for this purpose.
4. After the design tool is validated, **several geometry proposals are made** for 5-6[MW] , 5[RPM] (values from Deep Wind Project. The proposals are the result of the same Design Tool, reusing the code so that it would fit the considered geometry.
5. Provide insight on **improving design** using different technologies(constructional concepts and materials) and by using Optimisation Algorithms; [27]; [28],[29]
6. Suggest Solutions for 20[MW] 1[RPM](values from Deep Wind Project) based on the analysis of the 5-6 [MW] machines

Conclusions

In this chapter the problem to be solved was described. The goal is to construct a flexible generator design tool to quickly test design ideas. The program could be used by both experienced machine designers and engineers from other fields working with wind turbines.

An analytical design CAD, FEM and dynamic modelling analysers is proposed to evaluate a certain concept. Validation of the calculations through the analysers, literature and prototyping is intended.

The importance of having a flexible design tool that could help in observing the validity of a certain proposed concept was underlined as the main contribution of this thesis. To be able to obtain a tool that can be expanded adapted and further developed is crucial for obtaining a fast design of novel machine geometries.

Chapter 2: The Electrical Machines Design Tool

This section presents a general overview of the design tool. The main focus is set on a general description of the program, who the tool is intended for, and how the program is to be used. The implemented features and the user interface are presented and discussed.

A. General description of the design tool

The design tool is intended for calculating electrical generators having a power rating in the range from 1 to 20MW.

The idea behind the design process considered for DeepWind is presented in Figure 2. Symbols representing main actors of the design process are depicted using icons. The communication between the programs is made available through a Design Sheet which is a list of all characterising dimensions of an iteration. Each program uses the part that is relevant from this comprehensive set of data.

A logging module was implemented to keep track of where the calculation is at a certain time(which module, which subroutine). This is useful both for debugging and observing the algorithm itself. The logging also enables writing of comments from different functions. They could be explanations, warnings or error messages.

The machines that can be calculated are the radial and the transverse flux ones. Options like choosing different slot and winding types were provided for. To create a path, for the present thesis, the PMSG, TFPM, interior rotor, number 4 type slots, double layer concentrated and distributed windings were implemented. For the other options (that are similar to the implemented ones), the ground was prepared and implementation is easy and immediate, requiring only time for the actual shift to be made.

How to use the design program

The program is dedicated to the quantification of a concept. If an idea comes into discussion (e.g distributed windings), the design tool allows for quick calculation resulting in numbers approximating the effect of the concept on the design.

The Design tool is intended to be primarily used by:

- Machine designers
- Electrical engineers
- Engineers working with electrical systems, but not electrical engineers themselves

It is intended that the user should not necessarily have deep knowledge of electrical machines to be able to interpret the results. If an idea is then found viable, or the user wishes to further develop the design in that direction, it is possible to do so by analysing in FEM, CAD Dynamic simulation or by setting up an optimisation process

To design a machine, the following steps are taken (Figure 3):

- First, an analytical design of the machine is synthesised considering the set of specified inputs
- As a result, a data set is produced having a set of standard fields.
- This list with its structure is used to transport the design values between different parts of the tool

-Optimisation -FEM -CAD - Dynamic model

- Document the design if so desired

Features of the design tool

Figure 3 shows the options given by the design tool:

- Design of radial and transverse flux machines
- The possibility to optimise, analyse and change a design with little effort by the developer
- Facilities to easily document a fixed design: generation of a design sheet complete with geometrical and electromagnetic values. A set of to-scale CAD drawings and FEM figures as well as dynamic simulation curves can be included for a more detailed presentation of the design. If desired a set of formulae can also be included to clarify the design process. Discussions comments and other specification can be added to the template.
- The option to save, load and compare designs is available
- Relatively fast design of a new concept of machine by reusing the calculation functions available in the tool

- Modular structure of the tool-allows independent further development of all functions and append new functions(see Appendix 6: Special Issues to be Considered)

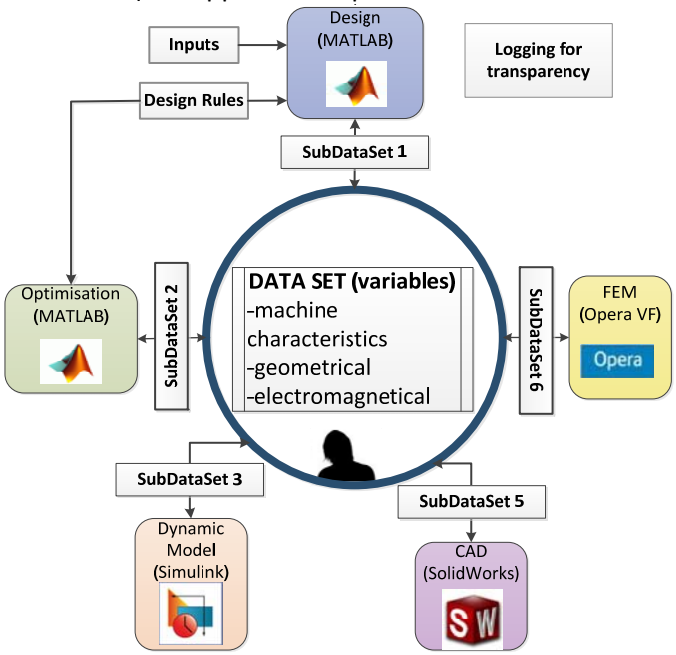

Figure 2: Deep Wind design tool concept

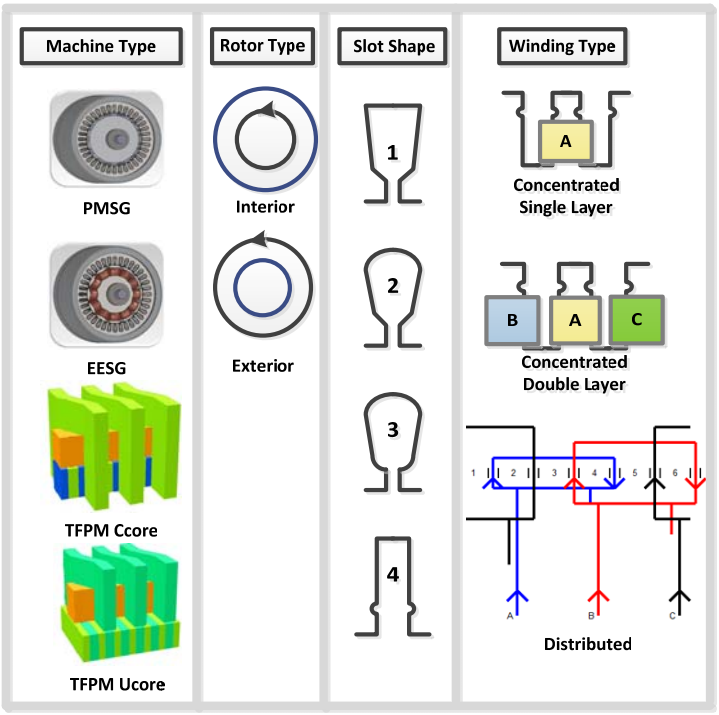

Figure 3: Design Tool Contents

Modular Design tool

Modules consist of analytical code written in Matlab and commercial software like finite element (FEM), computer assisted design (CAD) and dynamic models. All modules united form the Deep Wind Design Tool. The analytic module is composed also of different parts referred to as modules of the analytical design. In the dedicated appendix describes every module and sub module of the analytical design. Equations used are presented and by their analysis, the level of the calculations is outlined.

Main modules of the design tool (Figure 4):

- **Inputs**: contains a set of requirements, machine specifications, materials catalogue data, calculation and material constants
- **MakePM**: Calculation of the PM geometrical and electromagnetic characteristics
- **MakeWindings**: calculates the mechanical and electromagnetic dimensions of a particular type of winding
- **MakeIron**-calculates the required stator and rotor core as well as the tooth dimensions
- **MakeMagnetics**-calculates the fluxes, inductances and reactances
- **MakePerformance**-calculations for the EMFs, powers and losses
- **CheckNessieFo**r are functions that check the validity of the design. . At mathematical level : *is negative*, *out of range* or *is zero* . At conceptual level: Check if PM are demagnetised.
- **PrintDataSetTo**-functions that prepare and print initialisation files to FEM, CAD and Dynamic models.

As the design tool is developed, new sub modules may be developed. For focusing in detail on a specific issue, modules and their sub modules can be developed in depth.

As the design tool is constantly being developed, it is impractical to document each sub module at this time. To get an idea of what the functions do, all modules, sub modules and variable names used in the design code were given a self-defining name so that a list of symbols is superfluous.

How to reuse the functions:

Reusable functions have a set of inputs that are used when calling the function. An example is spf (slots per pole and phase). To make sure the program uses the updated value of a variable, spf is called each time the value for this quantity is needed. For this particular case the function can be used for several machine types.

A function has a specific set of inputs and outputs. If the function should be developed further to refine the output, additional code lines can be inserted. This can be done with or without changing the IN/OUT variables.

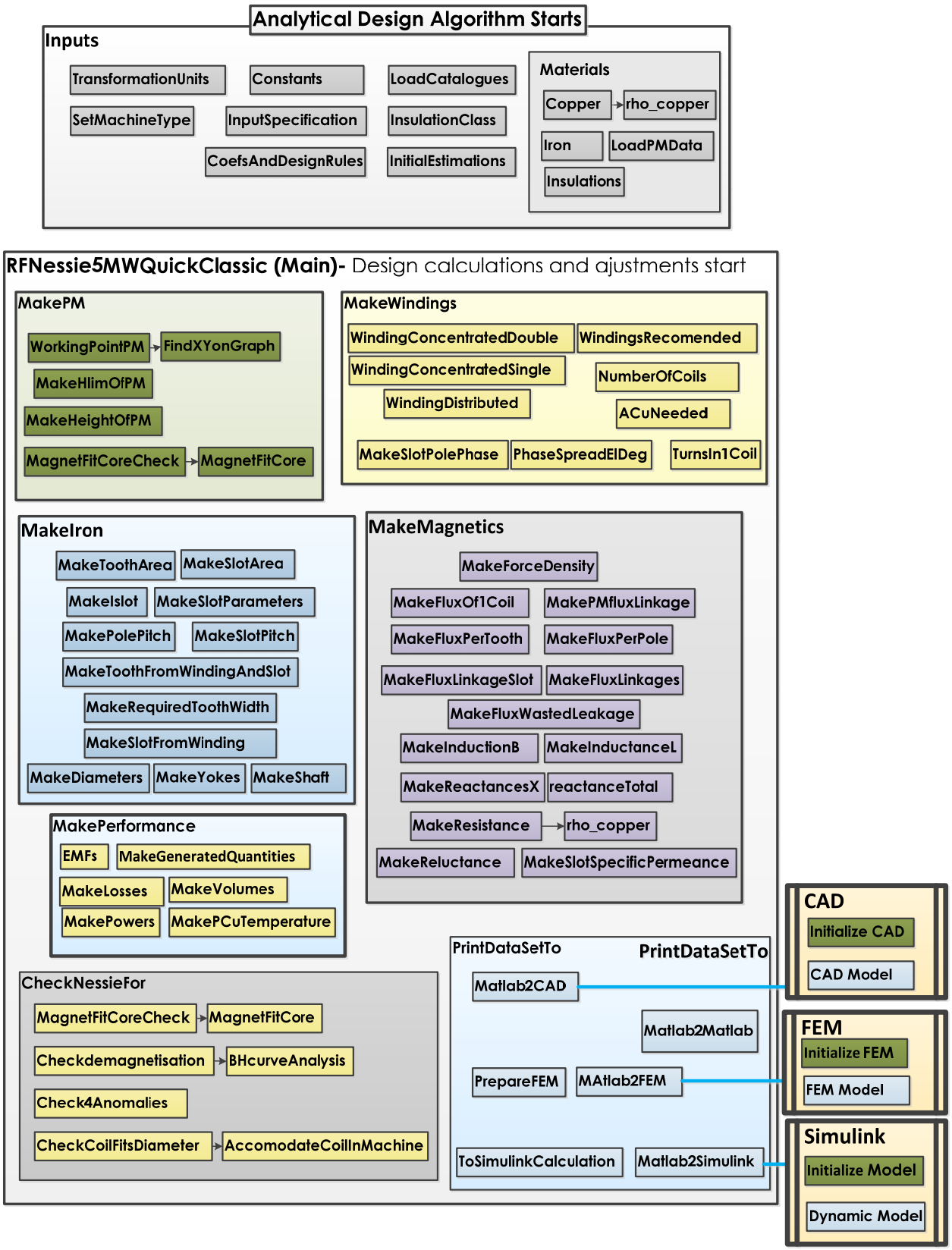

Figure 4: Design Tool Overview

Library of materials

A library of selectable materials is available for the core, permanent magnets, conductors for the windings as well as a set of constants for each material type (e.g. copper, iron). A template is used for each material type. For new material entries, the same set of parameters is introduced. This is useful when the developer of the design tool wants to consider a new material for the calculations.

The characteristics of the materials used for constructing electrical machines are important for calculations. In reality, the choice of materials of the same kind is relatively wide. Very often, the exact characteristics of the physical materials used for constructing the machine are not (exactly) known [30]. For the purpose of designing a machine at the stage presented in the present work, generic values are enough for the calculations. In Table 1 these material characteristics are presented:

Iron core	**Destination**	**Density [kg/m^3]**	**Specific hysteresis Losses $\left[\frac{W}{Kg}\right]$(50Hz)**	**Eddy Current Losses $\left[\frac{W}{Kg}\right]$(50Hz)**	**Resistivity [Ωm] at 20 C**	**Thermal Conduction $\left[\frac{W}{K}\right]$**	**Other**
• **Lamination steel**	Stator/rotor core	7700	6.2-2.9	1 at 1.5 [T]	[29-59]10^{-8}	[30-15]	Lamination factor 98
• **SMC core-Somaloy 7000**	difficult to manufacture in large sizes machines	7440	7.93	0.17	-	-	B=1.2[T],
Permanent Magnet		7600	-	-	-	-	-
Copper		8900	-	-	1.68×10^{-8}	-	-
Permeability of free space =$4\pi x10^{-7}$[H/m]							

Table 1: Characteristics of Materials used in Electrical Machines [10], [31], [30]

Analysis of current design from multiple view points

Analytic approach, CAD, FEM, Dynamic simulation (requires specific outputs from the design process to feed to models). This is made by automatically writing initialisation files from the analytical design program to the previously mentioned environments.

This approach is not strictly bound to the software used in this work but can be adapted to all comercial software that can handle initialisation files. The file must however be rewritten in the correct syntax.

User interface- GUI

The generator tool was built behind a MATLAB GUI interface. The reason for this is that the tool itself consists of a large number of files that need to be managed in an efficient way. Using the interface, the program is made intuitive and user friendly for guest users.

The user interface enables access to both running the design codes and further developing them. The design tool GUI is divided into sub-GUIs. Each sub GUI handles either a specific aspect of the design tool or the administration of it. In Appendix 7, the GUIs of the design tool are presented

B. Limitations of the design tool

1. **A general set of calculations was set up**. The design tool skeleton was constructed. Main modules were named. Only some of the modules were developed in depth (some were developed, some were only sketched and others were left for future work). See equations behind implemented calculation modules in Appendix 8: Design Tool Algorithm and Equations and Appendix 9: Design Rules.
2. The **possibility for refinement** was built into the structure of the design tool. Simple formulae were used to get a valid approximation of a certain quantity. If desired, the calculations can be carried further. The calculating function having the same inputs and certainly outputs would integrate with little or no trouble in the design tool.
3. **Limited materials library**-however, library structure is built and sample materials available. Study of the materials for the generator system was partially done. Together with a collection of available materials for

manufacturing, price and the technical advice of the manufacturers, the ideal materials to be used shall be decided on.

4. **Refined design issues postponed**: structural design of the generator box, refined manufacturing aspects and protections (e. g. corrosion and sealing) were left for future work. The importance of these issues is however recognised by the author and discussed in the thesis. (see Appendix 6: Special Issues to be Considered)

C. Validate Design tool

The calculation results given by the design tool must be validated if these are to be trusted for further consideration. One of the advantages of the relative simplicity of the modules and sub modules is that the algorithm can be monitored easily. Together with the logging functions implemented in the calculation process, the design tool is ready for debugging and validation.

To be able to spot calculation and conceptual errors that might have crept in the algorithm, several methods for validating the calculations were used. They look at the design from several points of view and in the end complement each other in finding validation issues. The following methods were used:

- PROTOTYPE test results compared to analytical estimations()
- SOFTWARE
  - Viewing of a design in several software programs CAD, FEM, Dynamic Simulation, Matlab
  - Analysing results
  - Testing: vary one parameter, keep watch the variation of other parameters. Evaluate against what the expected results should be using the theory on the subject.
- LITERATURE- design some Nessie like machines reported in the literature using the Design Tool and compare findings.

Details on the validation process may be found in Appendix 10: Validation of the Design Tool, Appendix 11: BabyN Prototype and Appendix 13: Dynamic Simulation Models for the Generator System.

Conclusions

In this chapter the approach taken when building the design tool was presented. The capabilities, limitation and the options given by the design tool were listed and discussed.

Chapter 3: 6 [MW] Candidates

In this chapter a set of 6 [MW] designs are presented. The aim is to evaluate the designs for their suitability to be up scaled from 6 to 20 MW. As an exercise, the machines were compared with respect to the criteria of active mass usage. The design tool allows for comparison on basically any criteria chosen by the user.

Design Approach

From the SWOT analysis (see Appendix 5), a set of suitable machines were chosen. Due to time limitations of the project, the radial flux PMSG and transverse flux TFPM types were selected for implementation in the design tool.

For the PMSG the winding calculations as well as the PM design issues were considered. With these the EESG can be calculated with certain adjustments. A novel geometry (double Nessie) was relatively easy to calculate by adapting and/or reusing existing functions.

The TFPM being a particular kind of machine that is essentially different from the radial flux one, had to also be implemented. Inside the TFPM tool module, two geometries were calculated(C and U core) [28], [29].

A classic benchmark design was made. The rest of the designs were compared to this.

As an example, the active mass of the generator was chosen as comparison criteria. Depending on what aspect the user wants to investigate, different fitness criteria can be implemented. The fitness criteria could be technological appropriateness, trendiness (what is done in industry), volume of active materials, etc.

It is advisable that comparison of other features be made when the machine design is close enough to the manufacturing stage for the comparison to give a valid evaluation.

For the radial flux machines (Classic RFNessie and DoubleAir-gapNessie), fractional slot concentrated windings were used. The reasons for this are that fault tolerability, a proposal for sectioning of the machine (cores built in segments) for easier transport and servicing, shorter overhang , lower cogging, and simpler windings. Together with these the other implications of using concentrated windings are accepted (see arguments in Appendix 8: Design Tool Algorithm and Equations)

All machines were given the same inputs within the permissible geometrical constraints (for the TFPM the winding type cannot of course be fractional as for the radial flux PMSG).

The following inputs were considered for the Nessie design main algorithm (Table 2):

Input	Value	[Units]
Power	6	MW
Vout rated Line	13.5	[kV]
Speed	5.63	[RPM]
Turbine Torque	10.5	MNm
Number of phases	3	[-]
Frequency	12	[Hz]
Force density	225	$\mathrm{kN/m^2}$
Power factor	cosφ= 0.95	
Current Density	6	$\mathrm{A/mm^2}$
Insulation Class	H	

Table 2. Nessie 6 [MW] Inputs

Optimised design versions are also given for the design tool machines.

Optimisation Approach

The original optimisation problem was to minimise the active mass of the generator. This is a complex task not for the optimisation tool itself but for the process of setting up a valid and comprehensive set of constraints. In other words, one should have a set of factors that stops the optimisation process from modifying a quantity in a certain direction because by continuing to do so, it would cause the degradation of the overall design. (e.g. unrealistic diameter, unacceptable saturation level). To be able to predict and monitor the relationships between different quantities and effects, the design tool has to be developed in depth in that direction.

To prove that the analytical design was successfully coupled with the optimisation tool, the minimisation of permanent magnet mass was aimed for. The shape of the magnet is relatively simple and is not directly influenced by structural and manufacturing issues as the iron or windings would be. Another justification for minimising the mass of PM used is that the cost of PM/kg is the highest of the active materials compared to that of copper or iron (see Table 38: Cost for Generator Materials (Numbers From INWIND Project)).

At the current stage, the designer must choose a safe set of inputs and outputs for the optimisation process. The implication of parameter variations must be provided by the program and made transparent in order to prove that the analytical design can indeed be coupled with the optimisation module(s) successfully. Once this validated, a more complex optimisation process can be attempted.

The design tool has a set of inputs-(see GUI Guide in Appendix 7 ; Design Equations in Appendix 8 and Design rules in Appendix 9). In the design process, some of the inputs change to suit particular design conditions; others just get initialised at the input and remain unchanged throughout the design process. Examples of unchanged parameters are mechanical power, desired output voltage, current density in the windings.

A list of 'safe' parameters for the radial flux machines was made in order to feed these values to the optimisation tool (Table 3). These will be modified by the optimisation algorithms during the calculation process. The word 'safe' refers to the possibility to modify these quantities without disturbing the logical flow of the main calculation algorithm.

Parameter	Symbol	Allowed variation interval
IN		
Working point of the PM coefficient	B_{wkg}	[0.75-0.85]
Mechanical air-gap	gap_length	$[gap_{length} \pm 10\%]$ mm
Coil width per height ratio	CoilWidthPerHeight	$[CoilWidthPerHeight \pm 10\%]$
Current Density	j	[5-7] A/mm^2
Out		
Total volume of PM per machine	$V_{PMtotal}$	ton

Table 3 : Input and Output Parameters and Associated Intervals for the Optimisation Module RF Machine

A quantity considered 'unsafe' was the frequency because by changing it the number of poles will also change for a constant speed .This is not desired because the number of slots per pole and phase has to give a valid concentrated winding design (see rules for valid concentrated windings combination in Appendix 8: Design Tool Algorithm and Equations). To achieve this, the analytical program automatically changes the poles and slot numbers to a valid combination, altering the frequency in the process. As a result, the value for the frequency is no longer controlled by the optimisation process but by the analytical design. With extra work on the design tool, this optimisation could be made possible provided the process is able to handle the issues in the manner previously mentioned.

For the transverse flux machine, inputs for the optimisation modules are given in Table 4 together with the allowed variation intervals.

Parameter	Symbol	Allowed variation interval
IN		
Mechanical speed	SpeedRating	5-5.7
Mechanical air-gap	gap_length	$[gap_{length} \pm 10\%]$ mm
Pole Pairs	PolePairs	137-157
Current Density	j	[5-7] A/mm^2
Out		
Total volume of PM per machine	$V_{PMtotal}$	ton

Table 4 : Input and Output Parameters and Associated Intervals for the optimisation Module TFPM Machine

Two optimisation methods were used: genetic algorithm (GA) and particle swarm (PSO). In Appendix 12, the methods applied are shortly presented. This lays a foundation for understanding the GA optimisation module used in connection to the machine design tool.

The GA and PSO were implemented as a module for the Nessie design tool. The question of which method is better suited for optimising the generator arises. The suitability criteria are maximum minimisation and convergence speed. To be able to determine this, the optimisation processes were analysed

The settings for the optimisation programs are (Table 5):

	PSO	**GA**	
Max Iterations	50	50	
NrIndividuals	10	50	Nr. of individuals in a generation/particles in a swarm
NrGenerations	100	100	the number of generations for the algorithm to work
Range	10	10	Nr of iteration to check if the best particle has modified its fitness value
Velocity variables	c1=c2=2	-	Social parameters, literature: typically =2
consFactor	0.729	-	Constriction factor
Operators			
Selection	-	Roulette Wheel	
Mutation	-	Random Mutation mutationProbability=6	mutationProbability= the probability of an individual to be affected by mutation [0,100]% ;
Crossover	-	BLX-alpha Crossover (alpha=0.5)	

Table 5: Settings for the GA and PSO Optimisation Modules

The magnet density chosen was the same for all machines- 7.2tons / m^3

In the following the un-optimised and optimised version of each machine are presented.

A. Radial Flux Permanent Magnet Generator-RFPM

a. Benchmark design –Classic RF Nessie; Internal Rotor (Classic RF Nessie)

The Classic RF Nessie is an inside PM rotor machine having distributed windings in the stator.

This generator is intended to serve as a benchmark for comparing the different machines suggested for the direct drive wind turbine application. The geometry is as presented in Figure 5 and Figure 6. A variation of this geometry was also prototyped. See validation of design tool in Appendix 10.

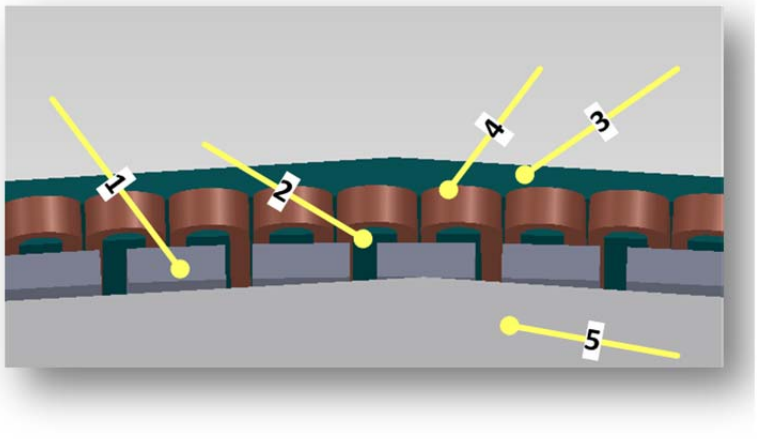

1- Permanent Magnet
2- 2-Stator Tooth
3- Stator core
4- Coil
5- Rotor Core

Figure 5: Generator Air-gap View

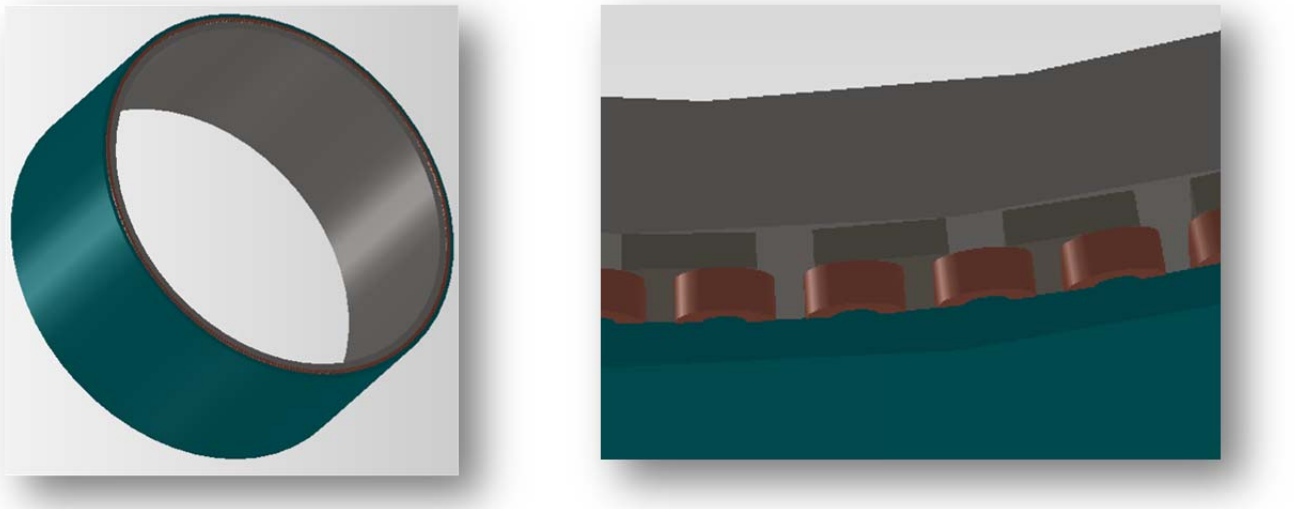

Figure 6: Classic Nessie-CAD-Unoptimised

Table 7 shows the main dimensions of the generator. For each design, a data sheet is issued automatically. An example for such a data sheet is given in Appendix 14. Table 7 is extracted from this.

Table 8 shows up to date CAD drawings of the machine components. Volumes of the materials used are also listed.

Parameter	Symbol	Value	Optimum PSO	Optimum GA
IN				
Working point of the PM coefficient	B_{wkg}	[0.75-0.85]	0.8479	8.842
Mechanical air-gap	gap_length	[6 ± 10%] mm	6.4140	5.8
Coil width per height ratio	CoilWidthPerHeight	[0.3±10%]	0.3296	0.327
Current Density	j	[5-7] A/mm^2	6.8987	5.33
Out				
Total mass of PM per machine	$V_{PMtotal}$ [ton]	9.6	8.77	8.65

Table 6 : Input and Output Values for the Optimisation Module - Classic RF Machine

Dimension Name	Symbol	Original	PSO	GA	[units]
Machine Parameters Classic Radial flux PM					
Active power generated	Pactive	6	6	5.8	[MW]
	Pmec	6.2	6.24	6.24	[MW]
number of pole pairs	PolePairs	157	157	157	[-]
actual force density	ForceDensityActual	183	207	204	[kN/m^2]
Turbine torque	Tturbine	10	10	10	[MNm]
Resulting Ratios					
	DboreToDstatorActual	0.976	0.978	0.977	[-]
	LStackToDgapAvgActual	0.691	0.504	0.656	[-]
	PM2PolePitchActual	0.85	0.85	0.85	[-]
	SlotPerSlotPitchActual	0.456	0.426	0.478	[-]
	SlotWidthPerHightActual	0.644	0.707	0.687	[-]
	CoilWidthPerHightActual	0.3	0.33	0.327	[-]
Diameters					
rotor diameter	Drotor	5.988	6.4	5.88	[m]
stator diameter	Dstator	6.145	6.561	6	[m]
bore diameter	Dbore	6	6.41	6.41	[m]
	DrotorCore	5.948	6.355	5.848	[m]
	DrotorIn	5.884	6.288	5.79	[m]
Lengths					
	gap_length	6	6.414	5.8	[mm]
	LoverallCore	4.142	3.227	3.86	[m]
Effective core length	Lusefull	3.852	3	3.59	[m]
Yokes					
	hRotorYoke	31.74	34.65	28.9	[mm]
	hStatorYoke	31.74	34.65	28.9	[mm]
Pitches					
	slotPitch	55.6	59.44	54.66	[mm]
	polePitch	60	64.17	59	[mm]
	coilPitch_slots	1	1	1	[-]
Stator Tooth					
height of tooth	hStatorToothTotal	40.6	38.69	41	[mm]
Width of tooth	wStatorToothTotal	29	32	26.8	[mm]
	Btooth	1.4	1.4	1.4	[T]
Stator Slot Open, Square slot bottom (parallel sided slot)					
number of stator slots	Qs	339	339	399	[-]
stator fill factor	slot_fill	0.5	0.5	0.5	[-]
	wStatorSlotTotal	26	27.34	28.2	[mm]
	hStatorSlotTotal	51	48.69	51	[mm]
Winding-double layer concentrated; bar conductors					
	SlotPolePhase	0.36	0.36	0.36	[-]
	Nr_coils_in_Series_per_Phase	113	113	113	[-]
	CoilsPerPole	1.08	1.08	1.08	[-]
	VdesiredPerCoil	69	69	69	[V]
	windingFactor	0.95	0.95	0.945	[-]
	ChordingColilSpanFactor	0.993	0.993	0.993	[-]
	distributionFactor	0.955	0.955	0.951	[-]
	NrTurns1Coil	8	9	8	[-]
	turnsInSeriesPerPhase	904	1017	2712	[-]
	wCoilInsulated	11	11	11.7	[mm]
	hCoilInsulated	36	33.6	36	[mm]
Permanent Magnet NDFEBO					
	Brem	1	1	1	[T]
B working	Bwkg	0.8	0.8	0.8	[T]
H working	Hwkg	-220	-220	-220	[A/m]
width of PM	Wpm	51	54.54	50.1	[mm]

height of PM	Hpm	20	22.11	19.8	[mm]
Insulation					
	Insulation Class	H	H	H	
Max insulation temperature	teta_max	180	180	180	[degC]
Currents					
1 coil, phase, line Current	Icoil= Iphase =IoutEl	259	259	259	[A]
Inductions					
	Bmax	1.7	1.7	1.7	[T]
	Bgap	0.68	0.72	0.716	[T]
	BbackIron	1.2	1.2	1.2	[T]
working point B of PM	Bwkg	0.8	0.848	0.842	[T]
Voltages					
output line voltage desired	Vout_ratedDesired	13.5	13.5	13.5	[kV]
	VgeneratedLine	17.839	17.56	16.99	[kV]
	Vdesired-generated	-0.717	-0.61	-0.232	[kV]
Generator Power					
	Pmec	6	6.24	6.24	[MW]
	Qreactive	1.9	1.89	1.89	[VAr]
	Pactive	5.7	6	5.8	[MW]
	Sapparent	6	6.270	6.116	[VA]
	powerFactor	0.95	0.95	0.95	[-]
Losses					
Copper losses	Pcu	9153	9676	7855	[W]
Eddy current Losses	Peddyst	0.77	0.77	0.77	[W]
Hysteresis losses	Physteresis	0.097	0.097	0.097	[W]
Iron losses	Piron	0.868	0.868	0.868	[W]
Additional losses	PadditionalLoss	36000	36000	36000	[W]
	PtotalLosses	45154	45676	43856	[W]
Performance					
	Pmec	6.2	6.24	6.24	[MW]
	Pactive	6	6	5.8	[MW]
	PtotalLosses	0.045	0.45	0.44	[MW]
	EfficiencyGenerator	0.965	0.958	0.932	[%]
Lumped Parameters-For Dynamic Simulation					
	Rph	0.054	0.057	0.047	[Ohm]
	Ld	0.44	0.427	0.4	[H]
	Lq	0.44	0.427	0.4	[H]
	InertiaMoment	215919	223932	178889	[kgm^2]
	FluxLinkagePM	127.3	125.21	121.22	[Wb]
Weights					
	MassCu	10.78	7.44	10	[ton]
	MassFe	35.68	32.69	30.6	[ton]
	MassPMtotal	9.6	8.77	8.65	[ton]
	MassActiveMaterialTotal	56.6	48.9	49.28	[ton]
Cost/Kg					
	costCu	15			[€/kg]
	costFe	3			[€/kg]
	costPM	50			[€/kg]
Cost of Generator Material Estimation					
	costCuGenerator	161.7	111.6	150	[k€]
	costFeGenerator	107.04	98.07	91.89	[k€]
	costPMGenerator	480	438.5	432.5	[k€]
	costActiveMaterialTotal	748.74	648.17	674.39	[k€]

Table 7: Dimensions Table for Generator –Classic RF Nessie Un-Optimised, PSO and GA Optimised

Original Machine	Original Machine		Optimised for PM Mass	
			PSO	**GA**
Active Part of the Generator 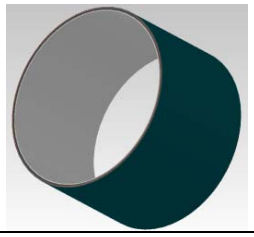	Mass = Volume = Surface area =	56.70 [ton] 8.73 m^3 930.62 m^2	48.9 [ton] 7.64 m^3 725.6 m^2	49.35 [ton] 7.57 m^3 847.49 m^2
	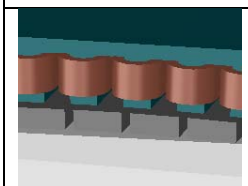	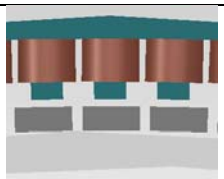		
Iron Cores	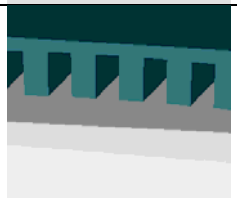	Mass Volume Surface area	35.68 [ton] 6.10 m^3 463 m^2	32.69 [ton] 5.59 m^3 369.7 m^2	30.632[ton] 5.24 m^3 422.76 m^2
Coils (Cu)		Mass Volume Surface area	10.78 [ton] 1.21 m^3 279 m^2	7.44 [ton] 0.84 m^3 200 m^2	10 [ton] 1.13 m^3 254.69 m^2
PM	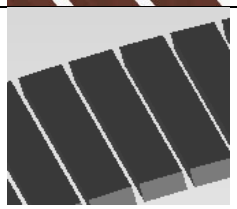	Mass Volume Surface area	9.245 [ton] 1.42 m^3 189 m^2	8.77 [ton] 1.22 m^3 155.7 m^2	8.65[ton] 1.20 m^3 170.04 m^2
Rotating part of the generator	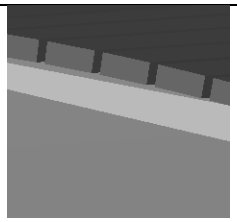	Mass Volume Surface area Moment of inertia= Mass x R_{rotor}^2 =23991 x 3^2	2.99 [ton] 3.60 m^3 344 m^2 215919 kg m^2	21.762 [ton] 3.44 m^3 285 m^2 223932 kg m^2	20.62[ton] 3.25 m^3 312.40 m^2 178889kg m^2

Table 8: Volumes and Mass from SolidWork for ClassicRFNessie

b. Double Air-gap RF

The Double Air-gap RF Nessie is an example of the design tool possibilities to design and analyse new geometries. Concept sketches are shown in Figure 7.

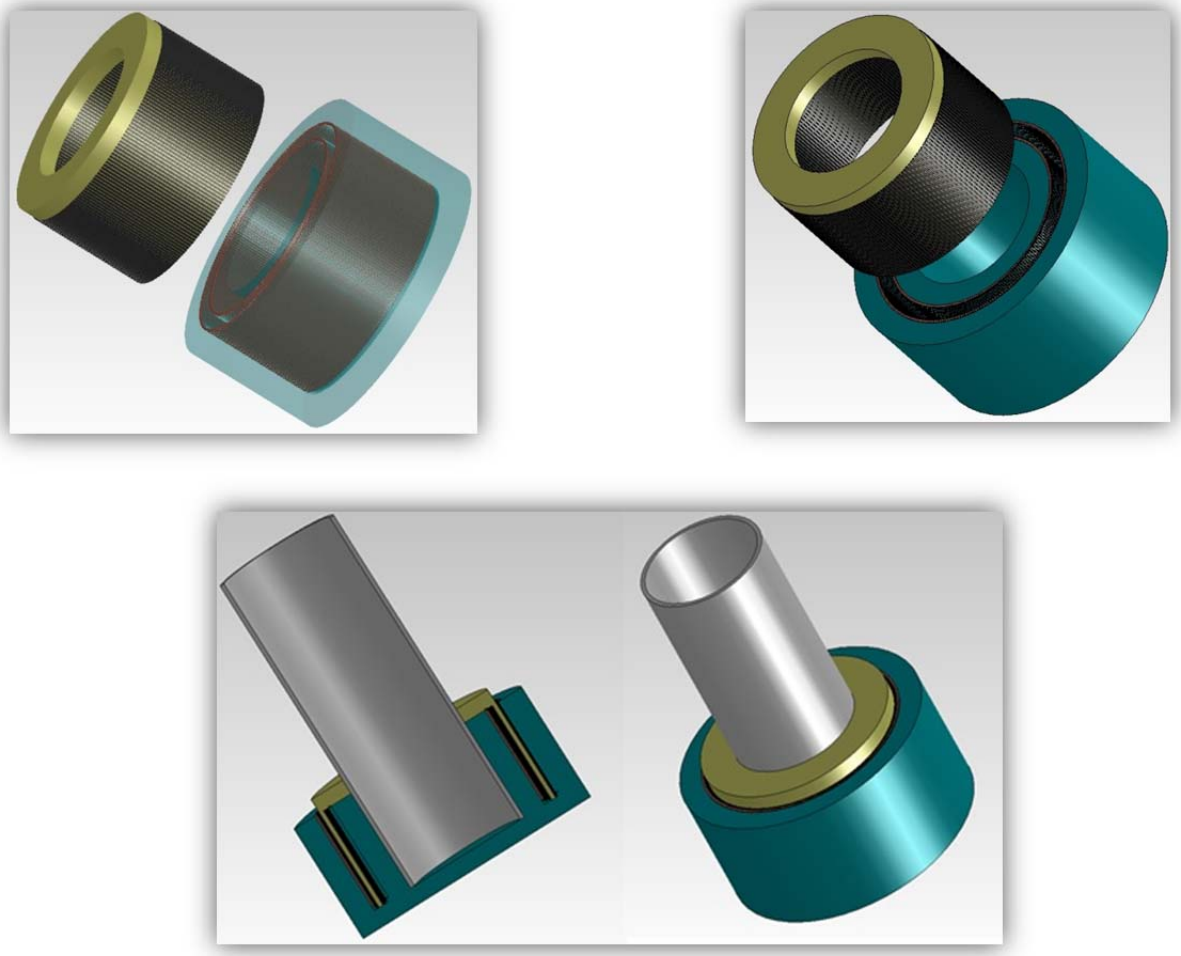

Figure 7: Double Air-gap Nessie-CAD Model-Concept

The double air-gap geometry – as a concept should offer a better use of the space inside the machine, making the outside diameter of the generator smaller. The main idea is to have two air-gaps in the machine where the permanent magnets and the windings would produce the desired voltage. It was decided that the PM are to be placed on the rotor and the windings on the stator like shown in Figure 8 and Figure 9.

On the stator sides, concentrated windings are displaced. On the rotor, permanent magnets are placed. Although a more complicated geometry was obtained (see Figure 8, Figure 9).

The question is whether or not this design would cope better with the low speed and with the active material use. Later on, this issue is investigated.

The approach of adapting the Classic RF Nessie design elements to the Double air-gap Nessie is presented in the following:

1. Design the **outer air-gap of the machine as for a Classic RF** machine was done
2. Because of the large diameter of the outer air-gap**, the inner 'machine' can be considered the same as the 'outer' one**. As an approximation the air-gap is considered to have the geometry of a linear machine (teeth and slots are the same dimension). In reality, there will be a small difference, resulting among other things in a higher saturation of the inner teeth.
3. **Each machine side** (inner and outer) will be **rated for half the full load torque and current.** The coils from the two airgaps are connected in parallel to give the machine rated current.
4. The windings of both machine sides will be connected in parallel

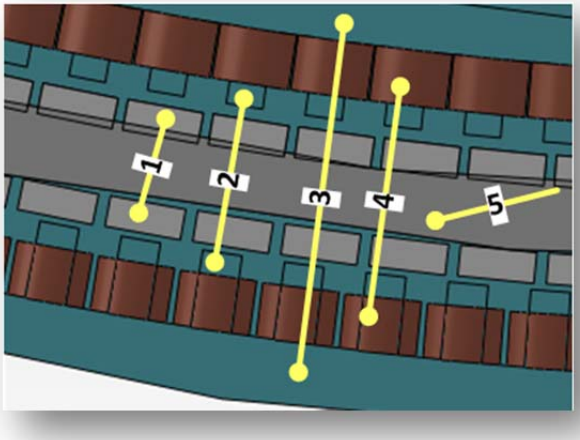

1- Permanent Magnets
2- Stator Teeth
3- -Stator cores
4- Coils
5- Rotor Core

Figure 8: Generator Air-gaps View

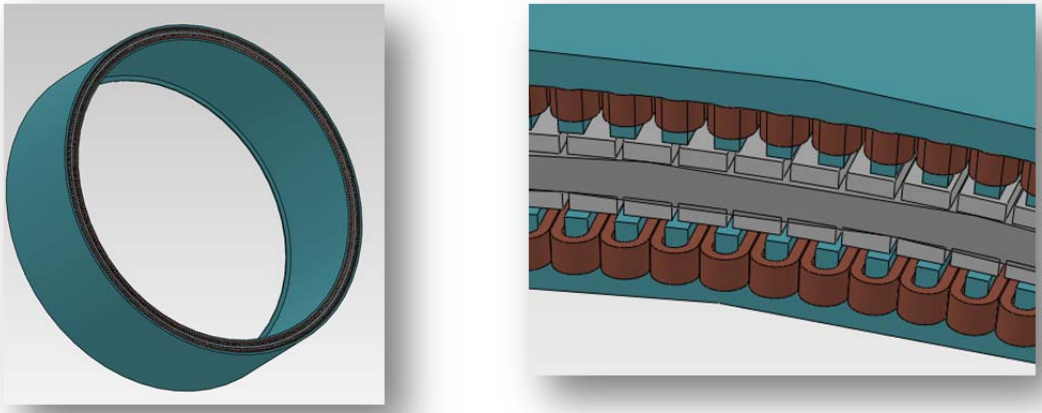

Figure 9: Classic Nessie-CAD-Original Machine

The input and output values for the optimisation problem for this machine type are given in Table 9

Parameter	Symbol	Value	Value for Optimum PSO	Value for Optimum GA
IN				
Working point of the PM coefficient	B_{wkg}	[0.75-0.85]	0.8478	0.8478
Mechanical air-gap	gap_length	$[6 \pm 10\%]$ mm	6.4155	5.7414
Coil width per height ratio	CoilWidthPerHeight	$[0.3 \pm 10\%]$	0.3185	0.323
Current Density	j	[5-7] A/mm^2	6.5	5.5837
Out				
Total mass of PM per machine	$V_{PMtotal}$ [ton]	9.6	9.1	8.81

Table 9 : Input and Output Values for the Optimisation Module Double Air-gap RF Machine

Calculation values for the original and optimised Double Air-gap machines extracted from the automatically generated design sheets are shown in Table 10.

Appreciations of weights and rotor inertia moments together with CAD drawings of the original machine are shown in Table 11

Dimension Name	Symbol	Original	PSO	GA	[units]
Machine Parameters Double Air-gap Radial flux PM					
Active power generated	Pactive	5.95	6.25	6	[MW]
	Pmec	6.24	6.48	6.4	[MW]
number of pole pairs	PolePairs	157	157	157	[-]
actual force density	ForceDensityActual	184	207	207	[kN/m^2]
	Tturbine	2x5	2x5	2x5	[MNm]
Resulting Ratios(outer Dbore)					
	DboreToDstatorActual	0.976	0.977	0.977	[-]
	LStackToDgapAvgActual	0.346	0.254	0.322	[-]
	PM2PolePitchActual	0.85	0.85	0.85	[-]
	SlotPerSlotPitchActual	0.436	0.439	0.477	[-]
	SlotWidthPerHightActual	0.644	0.684	0.679	[-]
	CoilWidthPerHightActual	0.3	0.319	0.323	[-]
Diameters					
Outer rotor diameter	DrotorOut	5.938	6.334	5.852	[m]
Inner rotor diameter	DrotorInt	5.760	6.140	5.682	[m]
Stator outer diameter	DstatorOut	6.14	6.538	6.052	[m]
bore diameter outer	DboreOut	5.948	6.346	5.862	[m]
bore diameter inner	DboreIn	5.736	6.118	5.666	[m]
	DrotorCoreOut	5.896	6.288	5.812	[m]
	DrotorCoreIn	5.8	6.186	5.724	[m]
Lengths					
	gap_length	6	6.4	5.7	[mm]
	LoverallCore	2.071	1.621	1.9	[m]
effective core length	Lusefull	1.926	1.507	1.767	[m]
Yokes					
	hRotorYoke	47.61	50	43.5	[mm]
	hStatorYoke	31.74	33.68	29	[mm]
Pitches					
	slotPitch	55.6	59.31	54.78	[mm]
	polePitch	60	64	59	[mm]
	coilPitch_slots	1	1	1	[-]
Stator Tooth					
height of tooth	hStatorToothTotal	40.67	41	41.5	[mm]
Width of tooth	wStatorToothTotal	29.4	31	27	[mm]
	Btooth	1.4	1.4	1.4	[T]
Stator Slot Open, Square slot bottom (parallel sided slot)					
number of stator slots	Qs	339	339	339	[-]
stator fill factor	slot_fill	0.5	0.5	0.5	[-]
	wStatorSlotTotal	26	28	28.2	[mm]
	hStatorSlotTotal	50	51	51.5	[mm]
Winding-double layer concentrated; bar conductors					
	SlotPolePhase	0.36	0.36	0.36	[-]
	Nr_coils_in_Series_per_Phase	113	113	113	[-]
	CoilsPerPole	1.08	1.08	1.08	[-]
	VDesiredPerCoil	69	69	69	[V]
	windingFactor	0.95	0.95	0.95	[-]
	ChordingColilSpanFactor	0.993	0.993	0.993	[-]
	distributionFactor	0.955	0.955	0.955	[-]
	NrTurns1Coil	16	19	17	[-]
	turnsInSeriesPerPhase	1808	2147	1921	[-]
	wCoilInsulated	10.7	11.5	11.8	[mm]
	hCoilInsulated	36	36	36.5	[mm]
Permanent Magnet NDFEBO					
	Brem	1	1	1	[T]
B working	Bwkg	0.8	0.8	0.8	[T]
H working	Hwkg	-220	-220	-220	[A/m]

width of PM	wpm	51	54	50.3	[mm]
height of PM	hpm	20	23	20.4	[mm]
Insulation					
	Insulation Class	H	H	H	
Max insulation temperature	teta_max	180	180	180	[degC]
Currents					
1 coil, phase, line currents	Icoil= Iphase= IoutEl	130x2	130 x2	130 x2	[A]
Inductions					
	Bmax	1.7	1.7	1.7	[T]
	Bgap	0.68	0.68	0.68	[T]
	BbackIron	1.2	1.2	1.2	[T]
working point B of PM	Bwkg	0.8	0.848	0.848	[T]
Voltages					
output line voltage desired	Vout_ratedDesired	13.5	13.5	13.5	[kV]
	VgeneratedLine	14.21	14.93	14.467	[kV]
	Vdesired-generated	-0.717	-1.43	-0.967	[kV]
Generator Power					
	Pmec	6.24	6.48	6.48	[MW]
	Qreactive	1.89	1.89	1.893	[VAr]
	Pactive	5.95	6.25	6	[MW]
	Sapparent	6.28	6.53	6.35	[VA]
	powerFactor	0.95	0.95	0.95	[-]
Losses					
Copper losses	PCu	41440	45243	39712	[W]
Eddy current Losses	Peddyst	0.771	1.542	1.542	[W]
Hysteresis losses	Physteresis	0.097	0.193	0.193	[W]
Iron losses	Piron	0.868	1.736	1.736	[W]
Additional losses	PadditionalLoss	36000	72000	72000	[W]
	PtotalLosses	77441	117245	111713	[W]
Performance					
	Pmec	6.2	6.48	6.48	[MW]
	Pactive	5.95	6.25	6	[MW]
	PtotalLosses	0.113	0.117	0.112	[MW]
	EfficiencyGenerator	0.954	0.96	0.935	[%]
Lumped Parameters-For Dynamic Simulation					
	Rph	0.246 /2	0.27/2	0.236/2	[Ohm]
	Ld	0.84	0.84	8.55	[H]
	Lq	0.84	0.84	8.55	[H]
	InertiaMoment	178060			[kgm^2]
	FluxLinkagePM	523.45/2	529.15/2	537.7/2	[Wb]
Weights					
	MassCu	10.78	8.453	10.192	[ton]
	MassFe	35.68	34.471	34.497	[ton]
	MassPMtotal	9.6	9.094	8.818	[ton]
	MassActiveMaterialTotal	56.6	52.018	53.507	[ton]
Cost/Kg					
	costCu	15			[€/kg]
	costFe	3			[€/kg]
	costPM	50			[€/kg]
Cost of Generator Material Estimation					
	costCuGenerator	161.7	126.795	152.88	[k€]
	costFeGenerator	107.04	103.413	103.491	[k€]
	costPMGenerator	480	454.7	440.9	[k€]
	costActiveMaterialTotal	748.74	684.908	697.271	[k€]

Table 10: Dimensions Table for Generator – Double Air-gap RF Nessie

Original Machine	Original Machine		Optimised for PM Mass	
			PSO	**GA**
Active Part of the Generator 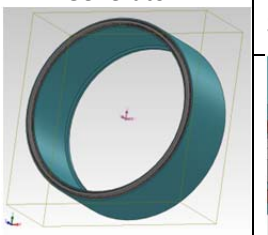	Mass = Volume = Surface area =	60.79 [ton] 9.509 m^3 842.4 m^2	54.019 [ton] 8.447 m^3 698.734 m^2	53.508 [ton] 8.267 m^3 781.819 m^2
	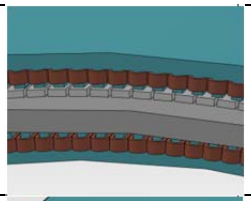	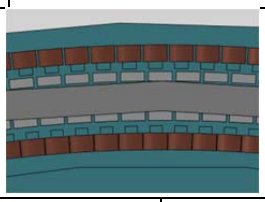		
Iron Cores	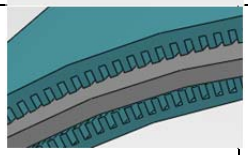	Mass Volume Surface area	41.36 [ton] 7.07 m^3 387.7 m^2	36.471 [ton] 6.234 m^3 322.092 m^2	34.497 [ton] 5.897 m^3 354.939 m^2
Coils (Cu)	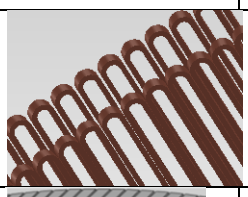	Mass Volume Surface area	9.83[ton] 1.105 m^3 268.4 m^2	8.453 [ton] 0.950 m^3 217.864 m^2	10.192 [ton] 1.145 m^3 256.904 m^2
PM	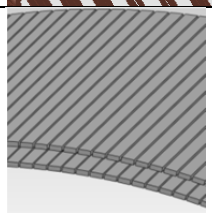	Mass Volume Surface area	9.6 [ton] 1.334 m^3 186.3 m^2	9.094[ton] 1.263 m^3 158.778 m^2	8.818 [ton] 1.225 m^3 169.976 m^2
Rotating part of the generator	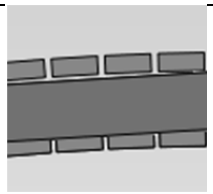	Mass Volume Surface area Moment of inertia= Mass x R_{rotor}^2	20.2 [ton] 3.146 m^3 264.168 m^2 178060 [kg m^2]	18.48 [ton] 2.868 m^3 224.272 m^2 185350[kg m^2]	17.619 [ton] 2.729 m^3 240.418 m^2 150840[kg m^2]

Table 11:Volumes and Mass from SolidWorks- Double Airgap Nessie

B. Transverse Flux Permanent Magnet Generator-TFPM

The C and U core TFPM were implemented in the design tool. Their design is presented in Figure 10 and Figure 11 and it will not be detailed in this thesis. The calculated values for these machines will be used in suitability assessment for consideration towards up scaling to the 20 [MW] design. The design and optimisation of these machines is presented in [29], [28], [32].

The iron for the transverse flux machines represents the concentrators in the rotor. The stator core is made from sintered material having a density of 7440 kg/m^3

The price for the sintered material is referenced to Wotec Industrial Co limited. This solution is theoretical as discussions on the subject revealed that sintering is not a feasible process for such large pieces at the moment. The low mechanical resistance of this material makes it extremely difficult to handle in assembling-especially in the presence of PM. This would make the manufacturing costs for this solution prohibitively high. The result would be a fragile machine that would be difficult to repair. (see combination Sintered/Fe - Chapter 4)

For the iron core of the TFPM generators made with iron concentrators and core (Fe), the cost can be seen in Table 14. In either case, the manufacturing cost would be high.

This solution was considered in the current thesis with the hypothetical scenario that if the above mentioned shortcoming were to be resolved in time and the solution became feasible; the machine resulting from the design tool calculations would be a candidate for Nessie.

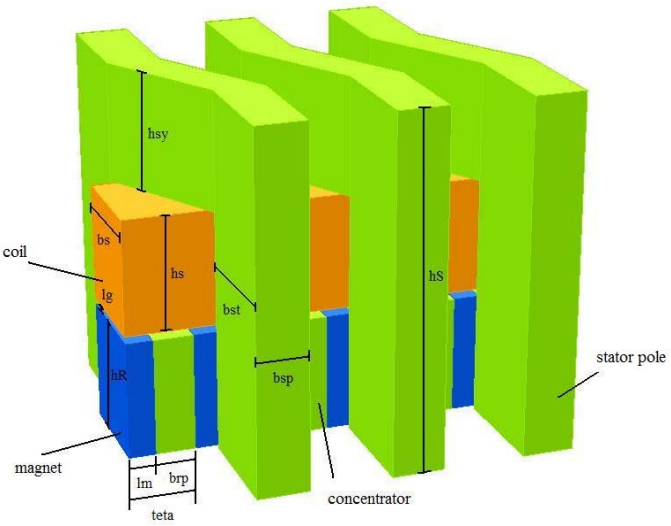

Figure 10: TFPM C core Nessie-CAD

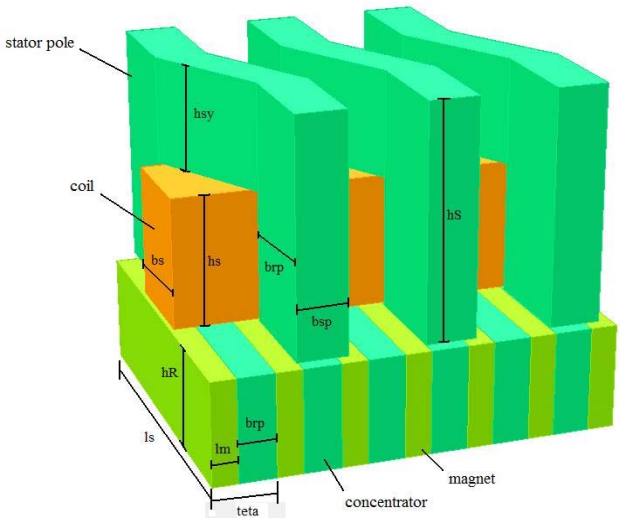

Figure 11: TFPM U core Nessie-CAD

The TFPM C core optimisation values are listed in Table 12:

Parameter	Symbol	Value	Value for Optimum PSO	Value for Optimum GA
IN				
Working point of the PM coefficient	B_{wkg}	[0.75-0.85]	0.8478	0.8478
Mechanical air-gap	gap_length	[6 ± 10%] mm	6.4155	5.7414
Coil width per height ratio	CoilWidthPerHeight	[0.3±10%]	0.3185	0.323
Current Density	j	[5-7] A/mm^2	6.5	5.5837
Out				
Total mass of PM per machine	$V_{PMtotal}$ [ton]	2.9	2.31	2.259

Table 12 : Input and Output Values for the Optimisation Module TFPM C Core

Table 13 shows the material usage of the TFPM C core machine. Optimised and un-optimised machines are presented.

Dimension Name	Symbol	Original	PSO	GA	[units]
Machine Parameters		**Machine type** TFPM			
Active power generated	Pactive	5.95	5.95	5.95	[MW]
	Pmec	6.2	6.2	6.2	[MW]
number of pole pairs	PolePairs	157	157	157	[-]
actual force density	ForceDensityActual	185	185	185	[kN/m^2]
	Tturbine	10	10	10	[MNm]
Diameter Lengths					
	DstatorOut	5.938	7.29	6.9	[m]
	gap_length	6	6.5	6.5	[mm]
Effective core length	Lusefull	0.4702	0.416	0.415	[m]
Winding- concentrated					
	NrTurns1Coil	65	65	65	[-]
	wCoilInsulated	52	43	49	[mm]
	hCoilInsulated	52	43	49	[mm]
Permanent Magnet					
	PMTypeMSG/ Brem	NDFEBO/1	NDFEBO/1	NDFEBO/1	[-]/[T]
Insulation					
	Insulation Class	H	H	H	
Max insulation temperature	teta_max	180	180	180	[degC]
Currents					
1 coil, phase, line currents	Icoil= Iphase= IoutEl	153	153	153	[A]
Voltages					
output line voltage desired	Vout_ratedDesired	13.5	13.5	13.5	[kV]
Weights					
	MassCu	0.876	0.742	0.734	[ton]
	MassFe	4.25	3.4	3.318	[ton]
	MassSintered	29.5	24	23.4	[ton]
	MassPMtotal	2.9	2.31	2.259	[ton]
	MassActiveMaterialTotal	37.526	30.452	29.711	[ton]
Cost/Kg					
	costCu	15			[€/kg]
	costFe	3			[€/kg]
	costSintered	35			[€/kg]
	costPM	50			[€/kg]
Cost of Generator Material Estimation					
	costCuGenerator	13.14	11.13	11.01	[k€]
	costFeGenerator	12.75	10.2	9.954	[k€]
	costSynteredGenerator	1062	864	842.4	[k€]
	costActiveMaterialTotal	1232.89	1000.83	976.314	[k€]

Table 13: Dimensions Table for Generator –TFPM Nessie C core

Chapter 4 discusses the candidates for up scaling from 6 [MW] to 20. As a result, a candidate for the 20 [MW] is suggested as a result of analysing the overall cost and mass of the designs.

Conclusions

In this chapter the generator candidates that were implemented in the design tool were presented. Using the modules developed for the radial flux PMSG and taking advantage of the design tool structure and flexibility, the double Nessie geometry was calculated. For comparison, a different type of machine, the TFPM machine was included. Variations on the machine types are easily possible by modifying the existing files.

The criteria for optimisation needed to be set up to obtain the direction towards which the design should tend. As an example the active mass was optimised in the current thesis and also for a TFPM generator. [28], [27]

In the future, the design of a machine needs to be adaptable to cater for other criteria that will arise from different design and construction requirements. Both optimisations algorithms were set up following a general approach. New objective functions can be handled to accommodate different optimisation directions

Although the optimisation goal was to minimise the mass of the PM, the consequence is that other parameters of the design change as well.

Chapter 4: Discussion of Candidates – Outlook from 6 [MW] to 20 [MW]

By comparing the most suitable designs, a discussion of the 6 [MW] machines is carried out. The aim is to determine which machine type would be best suited for the 20 [MW] generator.

First, comparison criteria and issues influencing the final decision are discussed.

Suggested solutions for 20[MW] 1 [RPM] (10 [RPM]) (values suggested by the Deep Wind Project) are discussed. A set of concepts are evaluated for suitability.

The comparison criteria for the present thesis focus around issues that can be grasped using the information generated by the Deep Wind research. The machines were mainly compared with regards to the mass of active materials, estimated relative cost and performance. (see Table 38: Cost for Generator Materials (Numbers From INWIND Project)).

Figure 12 shows that for up scaling, the cost of active materials increases as a function of the power, [33].

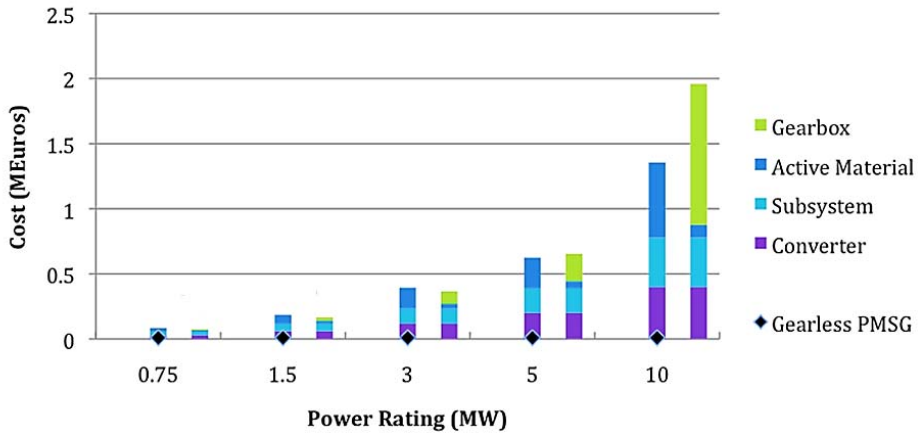

Figure 12: Cost Comparison Between Geared - Gearless PMSG with Construction Cost Ignored [33]

Regarding common practice in wind generation industry, the radial flux machines have the advantage of being well known in production and maintenance. They are more efficient and have a higher power factor than TFPM machines, because of the high leakage flux in TFPM.

It is this author's recommendation that the radial flux machine is the best suited candidate of the two for the 20[MW] generator at this time.

When looking at the overall problem several more factors intervene in deciding the most suitable candidate

- Expected inactive mass: structural elements including generator box and shaft, insulation
- Performance –an accurate criteria, the estimation of losses must be made with a greater precision
- Ease of manufacturing, transport and maintenance
- Costs estimated by taking into account the cost decrease in case of mass production

The inactive mass can only be approximated since no thorough design was made for this thesis. The performance is again estimated as a complex loss model was not set up. The active mass on the other hand was calculated as a required value for a feasible generator.

In the following the proposed machines in Chapter 3 are summarised in Table 14. The active masses and costs of original and optimised machines are included.

The transverse flux machine was calculated with the iron core being made of sintered and iron (S/Fe) and only with iron (Fe).

A summary of the results can be found in

Table 15.

By looking at the summary, the machine with the minimum cost is the TFPM using laminations for the core. This is an idealisation and not applied in industry. The alternative using sintered materials core is most expensive.

The realistic 6 [MW] machine that has the lowest costs is the Classic RF PSO.

	RFPM Benchmark			Double RF Nessie			TFPM C -Benchmark					
	Original	PSO	GA	Original	PSO	GA	Original		PSO		GA	
							S/Fe	Fe	S/Fe	Fe	S/Fe	Fe
Out Diameter[m]	6.145	6.561	6	5.938	6.334	5.852	7.2		7.29		6.98	
Active Length[m]	3.852	3	3.59	1.926	1.507	1.767	1.41		1.248		1.245	
Efficiency[%]	0.965	0.958	0.93	0.954	0.96	0.935	0.96		0.96		0.96	
MASS												
Iron [ton]	35.68	32.69	30.63	35.68	34.471	34.497	4.25	33.75	3.4	27.4	3.318	26.718
Sintered[ton]	-	-	-	-	-	-	29.5		24		23.4	
PM[ton]	9.6	8.77	8.65	9.6	9.094	8.818	2.9	2.9	2.31	2.31	2.259	2.259
Copper[ton]	10.78	7.44	10	10.78	8.453	10.192	0.876	0.876	0.742	0.742	0.734	0.734
Total Mass[ton]	56.6	48.9	49.28	56.6	52.018	53.507	37.5	37.52	30.452	30.452	29.711	29.711
COST												
Iron [k€]	107.04	111.6	91.89	107.04	103.413	103.491	12.75	101.25	10.2	82.2	9.954	80.154
Sintered Iron [k€]	-	-	-	-	-	-	1062	0	864	0	842.4	0
PM[k€]	480	438.5	432.5	480	454.7	440.9	145	145	115.5	115.5	112.95	112.95
Copper[k€]	161.6	111.6	150	161.7	126.795	152.88	13.14	13.14	11.13	11.13	11.01	11.01
Total Cost[k€]	748.74	648.17	674.39	748.74	684.908	697.271	1232.89	259.39	1000.83	208.83	976.314	204.114
REDUCED												
PM reduced by[%]	-	8.6	9.89	-	5.27	8.14	-		20.34		22.1	
Active Mass Reduced by [ton]	-	7.7	7.32	-	4.582	3.093	-		7.074		7.815	
Total Cost reduced by [k€]	-	100.57	74.35	-	63.832	51.469	-	-	232.06	50.56	256.576	55.276
Convergence[s]	-	81	273	-	91	593	-		4.79		9.126	

Table 14: Overall View of optimisation results for machines studied 6 [MW] 5.63 [RPM]

Outer Diameter		Active Length		Mass Of PM		Total Mass		Total Cost	
Min	Max	Min	Max	Min	Max	Min	Max	Min	Max
Double RF Original	TFPM Original	TFPM GA	Classic RF Original	TFPM PSO	Classic RF Original	TFPM GA	RF Original	Classic RF PSO/TFPM(FE)	TFPM Original

Table 15: Result Observations/Overview 6 [MW] 5.63 [RPM]

Conclusion

In this chapter the results of the 6[MW] machine design and optimisation were presented. It was concluded that the least costly realistic machine is the Classic RF PSO. Looking from the Nessie up-scaling to 20 [MW] from a product point of view, the most suitable candidate for up-scaling is Classic RF PSO. The Double Air-gap machine represents the second choice. In the following, the Classic and Double Airgap machines are further investigated for upscaling.

Chapter 5: 20 [MW] Suggested Design

A comparison between the radial flux classic design and the double airgap suggestion is made in order to show which geometry is most feasible candidate for up-scaling.

The up-scaling of the direct drive generator to 20 [MW] and 1 [RPM] as suggested by the DeepWind Research Project presents some challenges that cannot be completely addressed at this stage of the work. Initial steps to outline viable solutions were however made. The design trend of the Classic and Double Airgap machines were investigated over a speed range between 1 and 10 [RPM] for input frequencies of 15 and 6 [Hz]. The values for the designs obtained using the calculation tool are presented and based on these, a set of figures are generated.

The purpose of these figures is to show the trend of the design in order to approach the most suitable design for the Deep Wind 20 [MW] 1[RPM] machine. Additional considerations like manufacturing approaches and costs can be stated based on these curves.

The set of inputs for the investigation is presented in Table 16. (See also Appendix 8: Design Tool Algorithm and Equations and Appendix 9: Design Rules)

Input	Value	Units
Power	20	[W]
Gap Lenngth	10	[mm]
Speed	[1-10]	[RPM]
Vout rated Line	13.5	[kV]
Number of phases	3	[-]
Frequency	15; 6	[Hz]
Power factor	cosφ= 0.95	[-]
Current Density	6	A/mm^2
Insulation Class	H	[-]
Working point of PM	0.8xBrem	[T]
Slot Fill Factor	0.5	(Cu/Total Slot Area)
Short Circuit Coefficient	5	[-]
PM to Pole Pitch	0.85	[-]
CoilWidthPerHeight	0.3	[-]
Double Layer Concentrated Windings	[-]	[-]
Neodymium Magnets	[-]	[-]

Table 16: Classic and Double Airgap Machine-Inputs

The values for the investigated machines are presented in Table 17:1 to 10 [rpm] **Classic** 20 [MW] Overview (Unoptimised) at **15 [Hz]**; Table 18:1 to 10 [rpm] **Double Airgap** 20 [MW] Overview (Unoptimised) **15 [Hz]**; Table 19:1 to 10 [rpm] **Classic** 20 [MW] Overview (Unoptimised) at **6 [Hz]** and Table 20:1 to 10 [rpm] **Double Airgap** 20 [MW] Overview (Unoptimised) **6 [Hz]**

	1 [rpm]	2 [rpm]	3 [rpm]	4 [rpm]	5 [rpm]	6 [rpm]	7 [rpm]	8 [rpm]	9 [rpm]	10 [rpm]
D_{stator} [m]	35.655	18.714	12.702	10.156	10.194	10.224	10.263	10.299	10.336	10.365
$L_{usefull}$ [m]	1.997	3.828	5.673	6.604	5.233	4.403	3.748	3.302	2.92	2.642
PM Mass [ton]	42.128	42.143	42.161	39.204	36.118	34.631	29.484	29.155	28.59	25.868
Iron Mass[ton]	102.471	102.67	102.874	111	122.132	127.454	138.52	141.84	143.799	147.113
Cu Mass[ton]	34.037	33.623	33.46	28.927	23.944	21.154	15.396	14.415	13.25	11.015
TotalMass[ton]	178.636	178.436	178.495	178.885	182.194	183.239	183.4	185.41	185.639	183.996
PM[k€]	2106.4	2107.15	2108.05	1960.2	1805.9	1731.55	1474.2	1457.75	1429.5	1293.4
Iron [k€]	307.413	308.01	308.622	332.262	366.396	382.362	415.56	425.52	431.397	441.339
Copper[k€]	510.555	504.345	501.9	433.905	359.16	317.31	230.94	216.225	198.75	165.225
Total Cost [k€]	2924.368	2919.505	2918.572	2726.36	2531.45	2431.22	2120.7	2099.49	2059.64	1899.964
Torque[MNm]	181.818	95.238	64.516	47.619	37.736	31.746	27.027	23.81	21.053	19.048

Table 17:1 to 10 [rpm] **Classic** 20 [MW] Overview (Unoptimised) at **15 [Hz]**

	1 [rpm]	2 [rpm]	3 [rpm]	4 [rpm]	5 [rpm]	6 [rpm]	7 [rpm]	8 [rpm]	9 [rpm]	10 [rpm]
D_{stator} [m]	33.4	17.634	11.982	10.156	10.192	10.23	10.263	10.297	10.335	10.365
$L_{usefull}$ [m]	1.127	2.155	3.187	3.302	2.617	2.201	1.874	1.651	1.46	1.321
PM Mass [ton]	41.192	41.239	41.288	39.316	37.055	34.9	29.595	27.675	27.306	25.988
Iron Mass[ton]	132.313	125.046	124.077	122.889	124.995	124.477	139.85	146.557	150.338	153.031
Cu Mass[ton]	33.202	32.481	32.256	29.153	25.486	23.713	15.927	13.806	12.991	11.787
TotalMass[ton]	206.707	198.766	197.621	191.358	187.536	183.09	185.372	188.038	190.635	190.806
PM[k€]	2059.6	2061.95	2064.4	1965.8	1852.75	1745	1479.75	1383.75	1365.3	1299.4
Iron [k€]	396.939	375.138	372.231	368.667	374.985	373.431	419.55	439.671	451.014	459.093
Copper[k€]	498.03	487.215	483.84	437.295	382.29	355.695	238.905	207.09	194.865	176.805
Total Cost [k€]	2954.569	2924.303	2920.471	2771.762	2610.025	2474.126	2138.205	2030.511	2011.179	1935.298
Torque [MNm]	181.818	95.238	64.516	47.619	37.736	31.746	27.027	23.81	21.053	19.048

Table 18:1 to 10 [rpm] **Double Airgap** 20 [MW] Overview (Unoptimised) **15 [Hz]**

	1 [rpm]	2 [rpm]	3 [rpm]	4 [rpm]	5 [rpm]	6 [rpm]	7 [rpm]	8 [rpm]	9 [rpm]	10[rpm]
D_{stator} [m]	15.666	10.409	10.289	10.384	10.48	10.563	10.653	10.737	10.825	10.916
$L_{usefull}$ [m]	6.526	6.344	4.474	3.302	2.617	2.289	1.874	1.651	1.518	1.321
PM Mass [ton]	63.524	63.38	56.698	54.497	53.174	54.883	52.543	50.867	51.121	49.313
Iron Mass[ton]	132.76	134.037	158.067	171.15	179.794	181.001	187.377	189.686	192.606	194.579
Cu Mass[ton]	50.433	48.846	34.363	26.606	22.193	20.494	17.088	16.285	15.295	14.401
TotalMass[ton]	246.717	246.263	249.128	252.253	255.161	256.378	257.008	256.838	259.022	258.293
PM[k€]	3176.2	3169	2834.9	2724.85	2658.7	2744.15	2627.15	2543.35	2556.05	2465.65
Iron [k€]	398.28	402.111	474.201	513.45	539.382	543.003	562.131	569.058	577.818	583.737
Copper[k€]	756.495	732.69	515.445	399.09	332.895	307.41	256.32	244.275	229.425	216.015
Total Cost [k€]	4330.975	4303.80	3824.54	3637.39	3530.97	3594.56	3445.60	3356.68	3363.29	3265.402
Torque [MNm]	181.818	95.238	64.516	47.619	37.736	31.746	27.027	23.81	21.053	19.048

Table 19:1 to 10 [rpm] **Classic** 20 [MW] Overview (Unoptimised) at **6 [Hz]**

	1 [rpm]	2 [rpm]	3 [rpm]	4 [rpm]	5 [rpm]	6 [rpm]	7 [rpm]	8 [rpm]	9 [rpm]	10 [rpm]
D_{stator} [m]	13.499	10.19	10.273	10.365	10.458	10.54	10.627	10.707	10.794	10.883
$L_{usefull}$ [m]	7.058	6.604	4.474	3.302	2.617	2.201	1.874	1.651	1.46	1.321
PM Mass [ton]	103.13	97.873	74.99	68.177	66.733	60.416	56.895	56.536	55.66	54.207
Iron Mass[ton]	267.068	279.56	323.981	349.491	361.02	370.229	347.789	318.502	300.512	310.599
Cu Mass[ton]	79.817	67.986	38.618	29.019	25.018	20.268	17.365	16.544	15.43	14.632
TotalMass[ton]	450.015	445.419	437.589	446.687	452.771	450.913	422.049	391.582	371.602	379.438
PM[k€]	5156.5	4893.65	3749.5	3408.85	3336.65	3020.8	2844.75	2826.8	2783	2710.35
Iron [k€]	801.204	838.68	971.943	1048.473	1083.06	1110.687	1043.367	955.506	901.536	931.797
Copper[k€]	1197.255	1019.79	579.27	435.285	375.27	304.02	260.475	248.16	231.45	219.48
Total Cost[k€]	7154.959	6752.12	5300.713	4892.608	4794.98	4435.507	4148.592	4030.466	3915.986	3861.627
Torque [MNm]	181.818	95.238	64.516	47.619	37.736	31.746	27.027	23.81	21.053	19.048

Table 20:1 to 10 [rpm] **Double Airgap** 20 [MW] Overview (Unoptimised) **6 [Hz]**

The plots resulting from plotting the values from Table 17, Table 18, Table 19 and Table 20 are presented in the following. The figures are discussed and the implications of the design trend are commented on

By looking at the diameters of the machines as a function of speed (Figure 13) the curves for the 6 and 15 [Hz] machines have a sudden variation (knees) at 2 and 4 [RPM] respectively. For the 6 [Hz] there is more space to accommodate the windings (a smaller number of slots) so the knee occurs at a lower speed compared to the 15 [Hz] machines. If a 1 [RPM] machine is desired, a theoretical solution would be to decrease the frequency so that the knee would occur at ideally below 1[RPM] so that the diameter would decrease to constructionally acceptable levels. This would mean a frequency of around 2 Hz. The practicality of this solution and a design trend for different frequencies should be investigated.

For the viability of this concept of decreasing the frequency, an overall analysis of the generator, energy distribution systems and manufacturing consequences must be performed.

For speeds below these values the machines get expensive because the large diameters require extra structural support solution to maintain the required stiffness. Before the knees, the torque sets the diameter. Beyond the knees, the diameters are set by the power.

The corresponding lengths to the diameters from Figure 13 are shown in Figure 14. When the diameter increases to make the torque, the length of the machine becomes smaller. When the diameter settles to what the windings need (after the knee), the design compensated by having a shorter length.

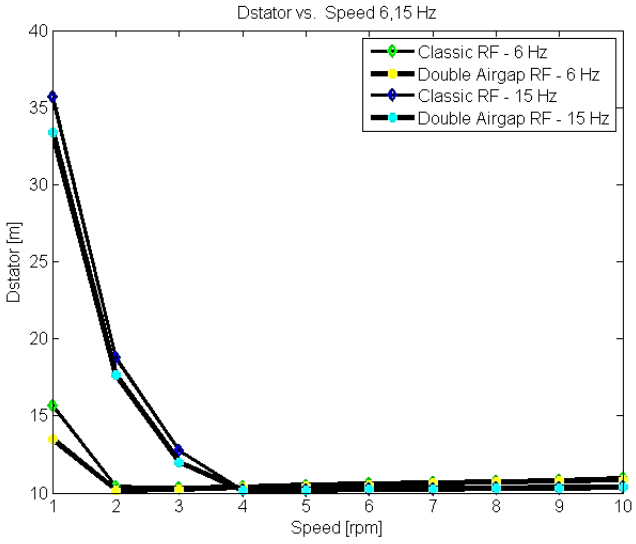

Figure 13: Speed vs. Stator Diameter

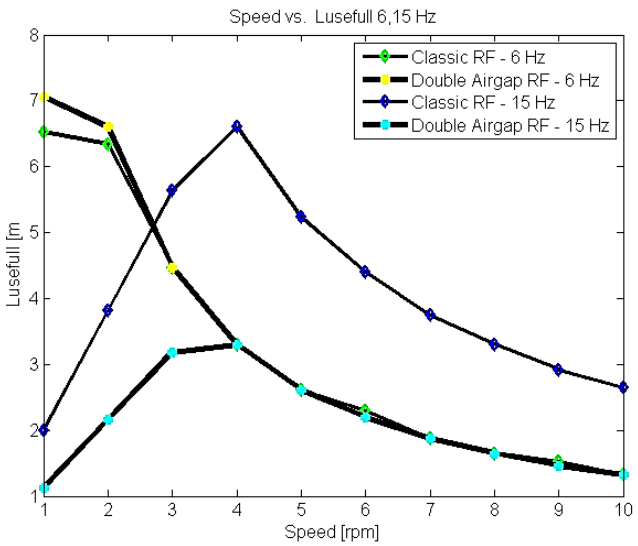

Figure 14: Speed vs. Useful Length

By looking at Figure 13, the most appropriate machine for the 20 [MW], 1 [RPM] would be the 6 [Hz] Double airgap machine because it has the smallest diameter. However, by looking at the corresponding length in Figure 14, the machine would be 7 [m] in length. For an optimum diameter to length ratio, the speed should be between 3 and 5 [RPM]. For 5 RPM, all but the Classic 15 [Hz] machine are suitable.

The torque versus speed curve of the machine is given in Figure 15

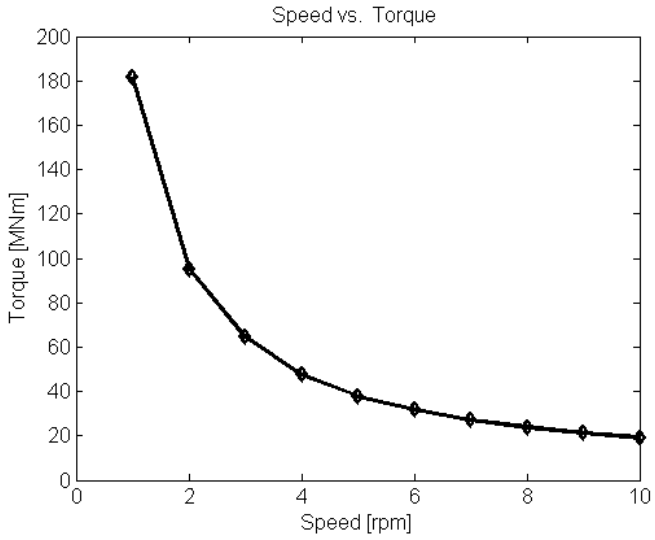

Figure 15: Speed vs. Torque

Figure 16 shows the total mass of the generator for the speed range considered. The 15 [Hz] machines have approximately the same mass. For the 6[Hz] machines, the double airgap machine is heaviest.

Correspondingly, the cost of materials for the calculated masses is shown in Figure 17. The shape of the mass and the cost curves differ respectively because the relative proportion of materials with a different kilo price also differs

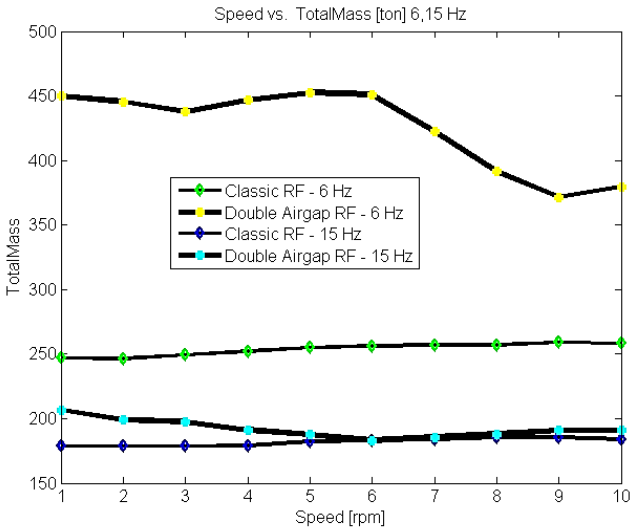

Figure 16: Speed vs. Total Mass

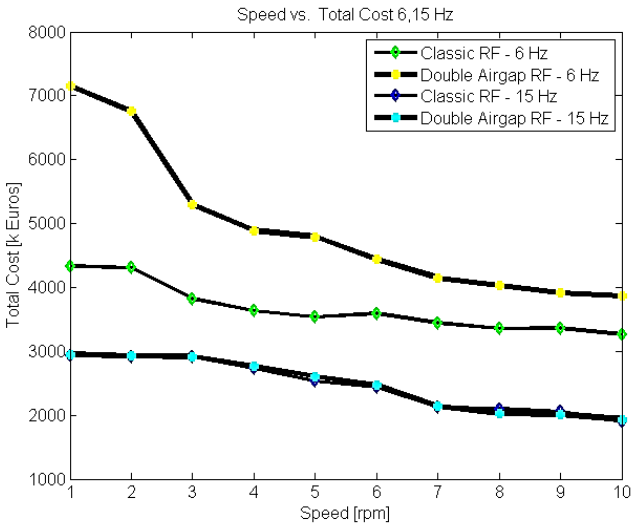

Figure 17: Speed vs. Total Cost

It can be seen that the Double Airgap 6[Hz] machine is the heaviest. When decreasing the frequency the machines get heavier and more expensive when it comes to the active materials used. On the other hand, for a lower frequency, the knee point occurs at lower speeds (Figure 13) resulting in a smaller diameter. This is expected to lower the cost of the supporting structure.

The cost and mass of PM are presented in Figure 18 and Figure 19. It can be seen that the cost of this material is predominant compared to the iron and copper. Before the knee point, the required mass of PM is proportionally more for the 6 [Hz] Double Airgap machine. After the knee point, this becomes disproportionately more.

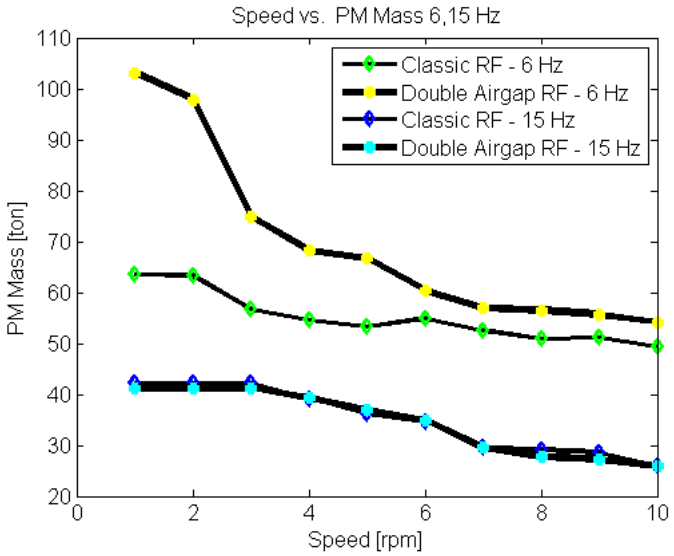

Figure 18: Speed vs. Mass of PM Used

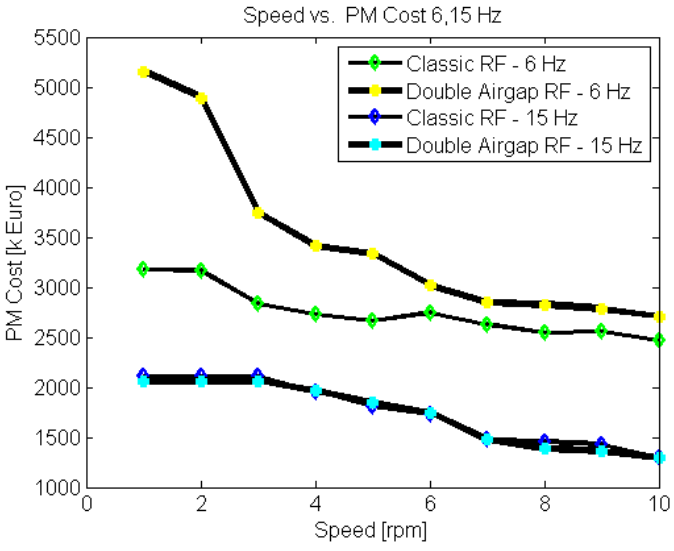

Figure 19: Speed vs. Cost of PM

Figure 20 and Figure 21 show the mass and associated cost of the useful iron. It is worth investigating as future work if the shape of the mass of individual materials varies with the frequency.

From Figure 22 and Figure 23, it can be concluded that the needed amount of copper decreases after a certain speed.

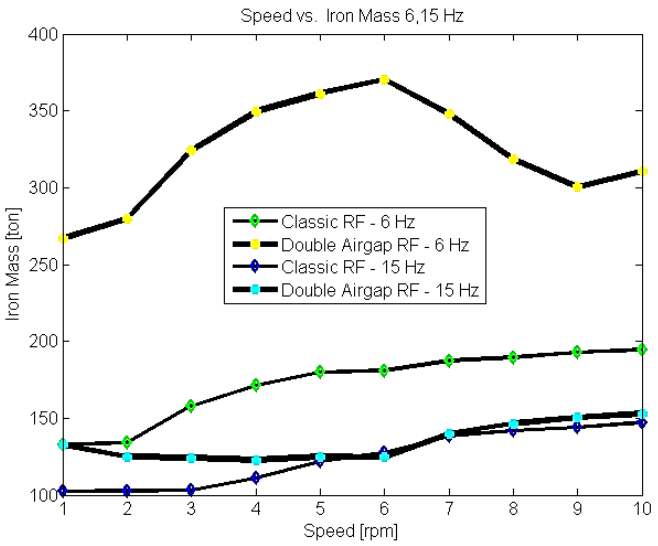

Figure 20: Speed vs. Mass of Iron Used

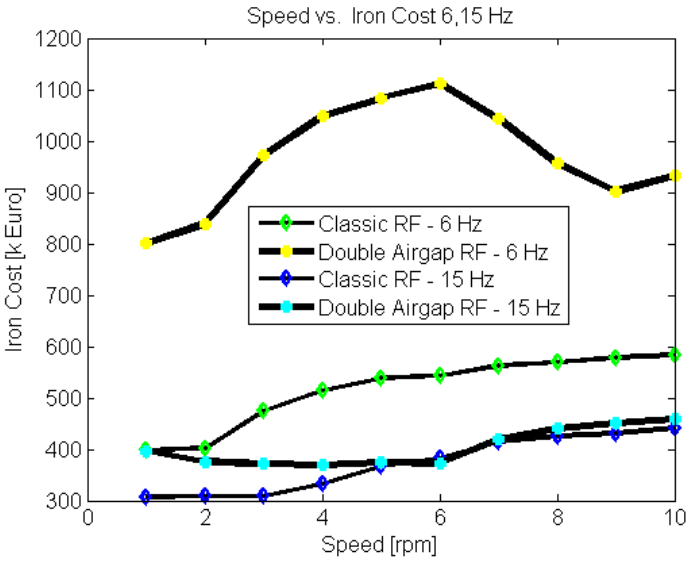

Figure 21: Speed vs. Cost of Iron

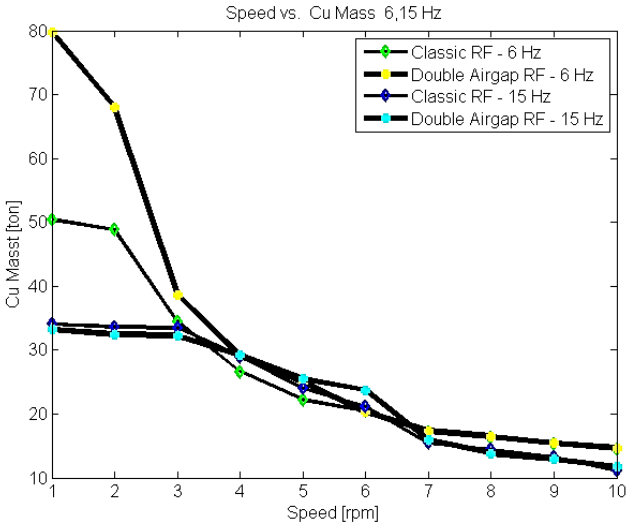

Figure 22: Speed vs. Mass of Copper Used

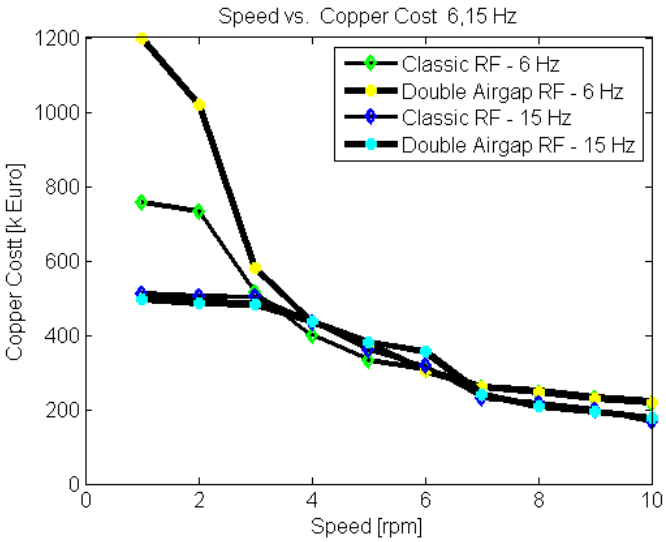

Figure 23: Speed vs. Cost of Copper

As an overview of the design tendencies, a number of abstract curves were drawn from the available data. Figure 24 shows the speed versus the machine aspect ratio. $D_{Stator}/L_{usefull}$ is sometimes used as a design rule for designing/optimising electrical machines.

Figure 25 shows the Torque/Total Mass as a function of rotational speed. It can be seen that the 15 [Hz] machines give the best performance from this point of view.

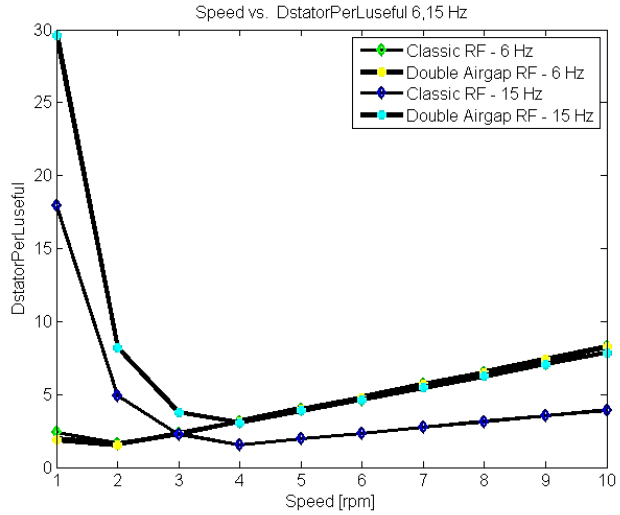

Figure 24: Speed vs. $D_{Stator}/L_{usefull}$

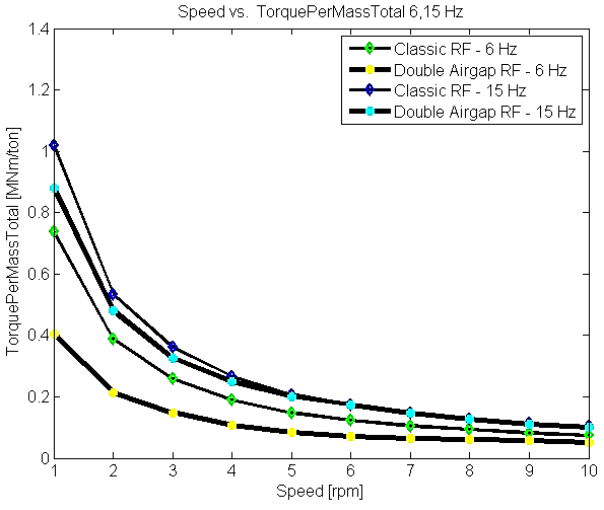

Figure 25: Speed vs. Torque Per Mass

The machine is considered as a hollow cylinder and the diameter times useful length versus the speed would give an idea of the volume (Figure 26).

Usually, when designing electrical machines, the square of the diameter times the length is considered as for a full cylinder (Figure 27). In both cases, the 15 [Hz] Classic machine ranked highest.

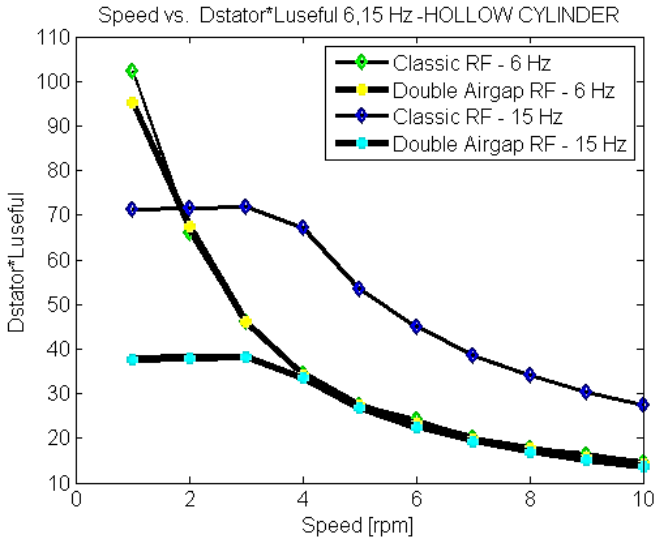

Figure 26: Speed vs. D_{Stator} x $L_{usefull}$

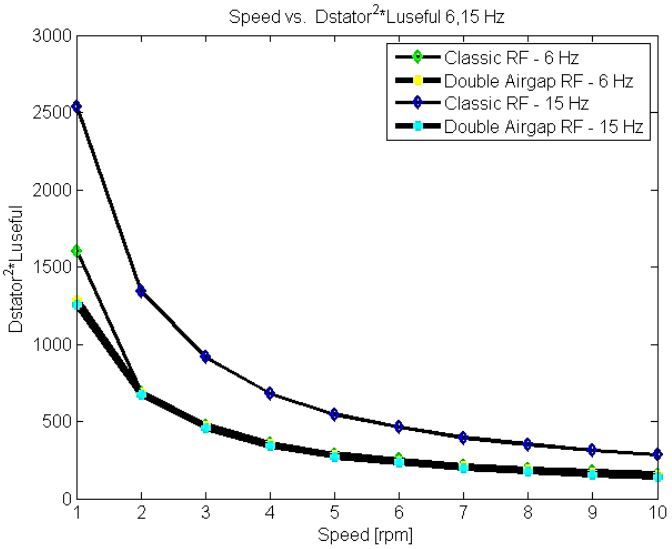

Figure 27: Speed vs. D_{Stator}^{2} x $L_{usefull}$

By looking at the figures obtained in the current analysis, the most suitable machine for the 20 [MW]1 [RPM]design (original specification) would be found by evaluating all curves. A summary of the conclusions is presented in Table 21. It is concluded as a result of this analysis that that the Double 15[Hz] machine would be the best choice if the speed was increased to 5 RPM.

Criteria/Figure	Appropriate Machine Type	Suggested alterations from original specifications	Comments
Figure 13	Double 6Hz, Classic 6 Hz	Go up to 3-5 RPM	Have smallest diameter
Figure 14	Double 6,15Hz; Classic 6 Hz		Have shortest length
Figure 16	Classic 15Hz, Double 15Hz		Have lowest mass
Figure 17	Classic 15Hz, Double 15Hz		Have lowest cost
Figure 25	Classic 15Hz, Double 15Hz		Have highest torque/mass
Best	**Double 15Hz**	**Ideal if the speed increases to 5 RPM**	

Table 21: Evaluation of the Best 20 [MW]1 [RPM]Nessie so Far-With Suggestions

Further investigations are needed to conclude a definite direction for the final design. Several considerations like the structural design and manufacturing feasibility must be taken into account before making a final decision. The design tool offers the possibility of easy analysis of the design rules and tendencies from an electromagnetic point of view.

The presented geometries do not represent the final proposals. With the design tool, more geometries can be investigated.

One suggestion for a new geometry derived from the Double Airgap geometry would be to have one row of PM instead of two. The PM would go right through the rotor iron that would forms a cage to hold them in.

Conclusions

This chapter presented the design tendencies for the 20 [MW] Nessie for 6 and 15 [Hz] input design frequencies over a speed range from 1 to 10 RPM.

Based on the presented curves and figures discussions on a suitable design for the 20 [MW]1 [RPM]can be started. All figures must be evaluated for the consequences they might have on a final design. A suggestion for the appropriate candidate was made (**Double 15Hz**).

The current analysis gave an example of the capabilities of the design tool to investigate solutions for Nessie type machines. With the available modules of the tool, several similar investigations can be set up.

Chapter 6: Future Work

This chapter outlines the work to be done in order to continue the development of the idea of Nessie. Tasks to be completed as well as new and possible research directions are listed.

A. Further develop the design tool

Table 22 lists all the issues that the author was considering in connection with the presented problem. Starting from these, the road to taking the present work to the next level is outlined.

Title of study	Purpose of study and content
Further scrutinise the calculations	• Analyse the empirical rules in the design algorithm (e.g. increasing the core length to generate the desired voltage, thus setting the *LStackToDgapAvg*- see design ratios in Appendix 9) • In the current stage, the frequency is an input to the design tool as a requirement from the converter design. Analysis of a range of frequencies suitable for the converter is to be investigated. • Analyse design curves for the Double and Classic designs (e.g. 6 and 15 Hz). Further identify design tool elements that shape these curves.
Extend the cost model of the generator	• Investigate cost of manufacturing and use • Model cost impact of mass production vs. prototyping • Analyse the cost impact of a design to neighbouring systems: control, distribution of energy
Improve design by adding e.g. more complex modules	• Approximations of design values to be calculated –e.g self and mutual inductances [34] • Cogging torque issues • Design of the insulation as a function of voltage, current , environment(salt water) and upper limit stress situations: e.g. short circuits, transients • Diagnosis and monitoring • Cooling methods • Automatic deduction/calculation of the design ratios • Expand losses calculations ,complex leakage estimation
Test design tool limits	• Test for which range of input values the design tool gives valid designs • Extend parts of the design tool to other electromagnetic designs like transformer, inductors
New geometries	• Test and improve flexibility limits of the design tool • Extend the design tool by calculating new geometries
Analysis of concepts	• Single vs double layer windings for Nessie –overall implications for 20MW • Double airgap machine geometry using a single set of magnets for the two stators (coil sets)
Geometrical optimisation	• Width of PM vs pole shoe-investigate implications • Tune geometric parameters as a result of analysis • Exterior rotor- design and analysis; compare to interior rotor solution. Analyse the influence of speed and power as well as manufacturing and servicing benefits.
New materials (see details below)	• Superconductive • Electro copper(pure copper) • Ferrofluids • other
Finish wound prototype and tests	• Assemble rotor laminations • Make windings • Test • Compare with design tool results

Investigate testing methods-prototyping	• Large scale prototyping • Scaling issues • Testing methods of different scale prototypes
Selection of fluid suitable for filling an undersea generator	If the DeepWind generator will be totally enclosed and filled with a fluid at the same pressure as the surrounding sea, this fluid will have to be suitable for filling a generator, compatible with the generator materials, compatible with the motion and temperature of the generator under all conditions, and non-polluting in case the fluid should escape into the surrounding sea.[35],[36] ,[37], [38], [39]
Evaluation of the interaction of sea water on all used materials	If the DeepWind generator is selected to be totally enclosed then the mutual effects of sea water and the outer enclosure materials must be evaluated. If the DeepWind generator is selected to be an open construction then the mutual effects of sea water and all generator materials must be evaluated.[40], [41], [42] This is because the presence of the DeepWind generator will affect the temperature and composition of the local sea water, which may affect the local life in the sea. Conversely the temperature and materials of the DeepWind generator may be affected by the local chemicals and life in the sea. For all selected topologies of DeepWind generator it will be necessary to make an appropriate study of these effects in order to obtain an acceptable lifetime of the DeepWind generator and to avoid unacceptable pollution effects on the surrounding sea.
Modelling of thermal behaviour of generator under normal & abnormal conditions	• Design detailed cooling system-concept and simulation[43] • Evaluate the thermal behaviour of the generator system-machine and converter-in normal and abnormal situations • Influence of an air filled casing (thermal insulation) vs. water/fluid filled casing
Generator immersed in salt water-flooded generator	Evaluate the concept for feasibility: cost of having a flooded machine vs. gain(elimination of sealing, pressure equalization) – see discussion in Appendix 6 Corrosion protection-evaluate possibilities For immersed windings-better cooling, but need to be protected [44]. Main effects to be considered are the increased coil capacitances(coil to ground and inter coil capacitances), increased stress on the insulation, increased windage losses because of the saltwater flow in the air-gap. This is however not that severe for low rotational seeds[45]
Further develop study on dynamic modelling	• Influence the machine design by the design and control of the converter[46], [47] • Fault analysis [48], [49], [50], [51], [25], [52], [53], [54], [55], [56] • Integration in wind power plants [48], [57], [58], [56], [59], [60], [61], [57], [62],
Cooling of the generator	• Investigate solutions • decide for an elaborate solution • design cooling • analyse cooling-general approach fitting any design • work into the design tool
Generator control requirements and methods	• Analyse the connection between generator characteristics and the converter and control design[63], [64], [65], [46], [16] Investigation of suitable control methods: [66], [67], [68], [69], [70], [71]
Use the design tool	• find parties interested in using the design tool • evaluate design proposals for different applications-not necessarily wind turbine related • integrate the machine design tool with converter and generation/distribution grids designs and applications

Table 22: Future Work Plan

In the following, a few of the issues presented in Table 22 are discussed.

a. Manufacturing process

Manufacturing and transporting of relatively large offshore-underwater generators requires thorough investigation.

Suggestions:

- **Modular structure of the stator and rotor** should be analysed [72] -Figure 28. Difficulties to assemble a large PM rotor into a large ferromagnetic stator will occur. Theoretically a sectioned machine would allow for an easier fixing of the rotor into the stator.

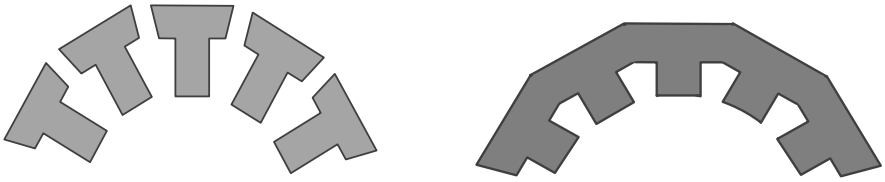

Figure 28: Modular vs Solid stator core

It is envisaged that the generator would be easier to manufacture as a set of small components that would be transported and assembled on site. Another foreseen advantage is that faulty components would be easier replaced underwater provided elevator type structures were to be fitted inside the DeepWind floater (shaft).

The downside of this solution is that additional structure elements would be needed to keep the shape of an already relatively thin machine. Magnetically, losses might occur because of the additional air-gaps introduced in the flux path. The flux leakage might pass through the air-gap rather than linking to the neighbouring teeth.

- The question of a **suitable number of modules** arises.(e.g. [72] reports 6 slices 4 6 MW)

- An in depth analysis of **suitable materials** for the application is needed. Both active and structural materials should be investigated with regards to the price, friability, lifetime and other relevant perspectives that might reveal themselves during this analysis.

- **Manufacturing methods for the 20[MW] generator components** should be investigated. A modular structure would allow for smaller machine tool to make the components.

- Complete design of the mechanical structure e.g. casing, shaft and addition **generator structure elements needed** as these might affect the design of the generator itself.

- Identify and design **additional subsystems of the generator system**: e.g. diagnostics and monitoring sensors, data and power transmission system, filtering of generated voltage, safety apparatus [73], [74].

- **Design and refinement of control modules** e.g. to comply with grid codes and functioning requirements, safety procedures in case of abnormal conditions [75],

- **Vibration analysis** of the overall structure design analysis needs to be done in order to avoid resonant frequencies between the generator and the rest of the turbine [20], [19].

As a modular concept is proposed for the large machine together with sectored core, the concentrated winding would be more desirable for the Nessie application than the distributed ones.

b. Maintenance

Due to the marine location of the turbine and generator the level of maintenance must be minimised or even avoided.

Suggestions:

- Use system identification, approximations and predictions to determine full scale generator characteristic quantities [76], [77]
- Use monitoring and diagnostics to detect incipient faults [78], [51], [79], [80], [81], [82], [83], [50], [54]
- Decide action for each fault type[84], [85], [54], [86]
- Predefine the maintenance procedure for each expected fault.
- Provide the turbine and generator with built-in maintenance features e.g. for a modular structure (justified for the 20 [MW]generator)-a controlled elevator that extracts and replaces a faulty coil with a healthy one with minimum assistance from the maintenance personnel.

c. Solutions for increasing the generator torque density

In the following, the concept of adding Ferrofluid in the air-gap to improve the performance of large direct drive generators is discussed.

The ferrofluid is a fluid containing a suspension of coated magnetic nanoparticles in a carrier fluid. When exposed to a small magnetic field (around 10 mT-depending on the fluid), its physical properties and behaviour change due to the alignment of the magnetic particles . The oily substance turns into a gel influencing its flow. For a well-designed fluid, after removing the magnetic field, the ferrofluid regains its initial state [39].

The relative permeability of the ferrofluid $\mu_{ferrofluid}$ can be between 2 and 4. By inserting this material in the air-gap of the generator, the permeability in the air-gap will change from 1 to $\mu_{ferrofluid}$, the higher the ferrofluid permeability, the greater the force produced by the magnets.[35]

By reviewing the literature and by assessing the concept, it is concluded by the author that adding ferrofluid in the generator air-gap has the potential of improving the torque density of the generator. This material is not that controversial anymore and is easily obtainable for a relatively good price. This material could be used to improve the performance of the machine [87], [88].

Ferrofluid properties are discussed in [89], [90]; [38] (impact of uniform magnetic fields on ferrofluids); [91] (force enhancement); [35] (efficiency improvement). Ferrofluid flow properties are explained in [89].

Reporting on ferrofluid in electric machines may be found in [92], [93](electromagnetic forces); [88], [94], [95].

There are only a few articles focused on generators and ferrofluids together. Most current research is aimed at adding ferrofluids to the air-gap of electric motors and not generators.

To be analysed

1. The **reduction of the generator mass**: less PM and copper needed to produce the same flux density by changing the air-gap permeability.
2. **Improved cooling** of the generator as the ferrofluid can be used as a cooling agent.
3. **Vibrations damping** using ferrofluids is a well-known application that can be applicable to the generator as well.
4. The generator with ferrofluid acts as a magnetic bearing. In this case, the order 1 levitation occurs, namely, a constant air-gap is maintained. If vibration or other similar disturbances occur and eccentricity exists between the stator and the rotor, the ferrofluid will help with centering. In this way, vibration and noise is reduced [96].

Analysis method

A PM or electrically excited electrical machine should be chosen tested as a generator using a drive machine The performance of the generator will be measured without ferrofluid in the first instance. Later, ferrofluid will be added to the air-gap and the performance measured again. The two sets of performance figures will be compared and contrasted, to establish the change in performance obtained by adding the ferrofluid.

The machine would be run at low speeds because the goal is to test the concept of direct drive generators (not at 10 [RPM] as the machine might not be designed for this low speed). The speed of a test machine would be somewhere around 100 [RPM]–special measurements may be performed. The low speed of the application works in the favour of filled air-gap as the friction losses might increase drastically at high speeds.

For the sake of accuracy, it is important to determine the permeability of the ferrofluid before testing it in the machine. Issues like the apparent viscosity as a function of the magnetic field (magnetic saturation), behaviour at different temperatures (thermal saturation-Curie point of the fluid) and reaction to salt water should be investigated for the particular fluid used.

To reduce friction in the ferrofluid flow, the stator slots of the test machine could be filed with resin thus obtaining a smoother flow surface.

Further discussion

Finding a method for measuring the relative permeability of ferrofluid is important for the experimental and theoretical work. From the literature, the-relative permeability of ferrofluids should be larger than 2 in [96], [37] If the relative permeability of the ferrofluid is 2, it is expected that the necessary volume of PM would be halved.

For first experiments proving the concept, a relatively low cost ferrofluid may be used. For more advanced experimental methods and results, a ferrofluid having better characteristics should be used.

The negative aspects of the added friction should be accounted for. Tests needed to quantify the limits of the concept.

B. Geometrical Investigations Suggestions

In the following, suggestions for future geometrical investigations are listed.

a) Outer Rotor Nessie

When discussing the connection of the generator to the turbine, the idea of an exterior rotor generator came up to avoid sealing and other connection problems. For the suggested construction, the tower would be directly connected to the rotor.

The choice for rotor-stator geometries-Figure 29- was investigated by consulting literature reports. The following issues were discovered:

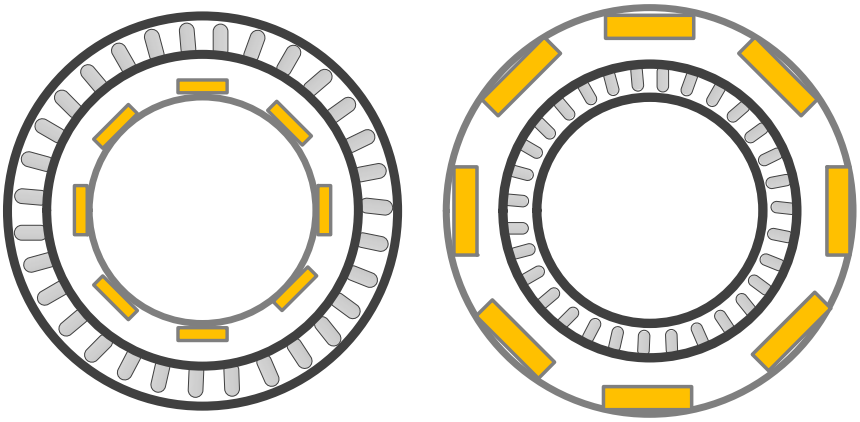

Figure 29: Interior vs Exterior Rotor

1. Interior rotor is more difficult to cool [97](natural cooling-no special provisions for cooling)
2. Ideally the torque produced by an exterior rotor machine scales by a factor of the outside radius of the machine-for a large radius. In practice, the growth is limited by the saturation of the stator and rotor back iron and the consequent reduction of B_{gap}.

Another important factor to take into account when comparing the inner vs outer rotor geometries in the winding/slot area correlated with the radius of the bore. [98]

Taking into account the saturation effects [98] concluded that the exterior rotor is capable of producing the largest torque provided an optimum winding/slot area and bore radius is set.

3. [99] concludes that

- The outer rotor machine produces higher power compared to the inner rotor one for speeds larger than 50 [RPM] for a 1.5 kW machine.
- The active weight of the machine was found to be higher the inner rotor one.
- The electromagnetic torque was higher for the interior rotor machine

4. [9] claims that no significant difference between inner and outer rotor topologies

It is interesting to investigate the scalability of these affirmations for higher powers and lower speeds. (for Nessie)

The concept of interior vs exterior rotor was discussed in the literature. Based on these reporting the problem can be discussed and weighed. For a final conclusion on whether this concept is suitable for the 20 [MW] design requires on-subject analysis for that machine scale range.

Other factors like the coupling of the generator rotor to the turbine rotor might influence the decision on the presented question. For the sake of analysis flexibility, extensive design and evaluation for the exterior rotor solution is proposed as future work for the 20[MW] generator system. The influence of the power and speed as well as manufacturing and servicing issues should be also investigated together with the performance.

b) Long Nessie

Figure 30 shows a large Diameter/Length ratio. Figure 31 depicts a machine with a small aspect ratio. The latter case is desired to some extent because the tower could be used to house the generator. The impact of the aspect ratio on the turbine and anchoring system design should be investigated.

a) Multiple Nessie

Figure 32 shows a sketch where multiple phase shifted machines set on the same shaft to form one generator. See also [100].

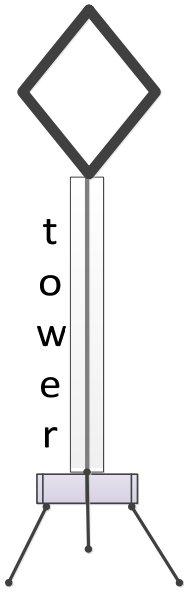

Figure 30:Original Nessie

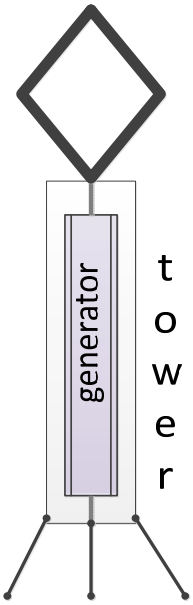

Figure 31: Long Nessie

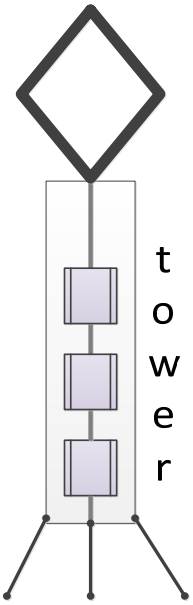

Figure 32: Multiple Nessie

C. Trends in Direct Drive Machine Concepts

Alternative direct drives generators for high power levels are discussed in the [101] review paper. The outstanding concepts that outline future trends pertinent to the Nessie concept are:

a. Superconductive materials-

The principle of the superconductor material is that when cooling down the material to a cryogenic state, the electrical resistivity of the material (e.g. copper) can be considered zero. This implies the current density in that material may also be increased. In other words, for the same volume of machine, more torque can be produced-with one third the weight and one half the losses of conventional machines. [9], [102], [103], [104], [105],.[106], [107], [108]

Significant reduction in the size and weight of 10 MW-class generators for direct-drive wind turbine systems-cost of clean energy relative to conventional copper and permanent-magnet-based generators will be reduced [109].

There are high temperature and recently developed low temperature superconductors [103], [110], [111]. Superconductive materials working above 30K are considered high temperature semiconductors. With developments in this area, the threshold is being moved to even higher temperatures. Figure 33 show the evolution through time of the functioning temperature and the coolant used for superconductive materials.

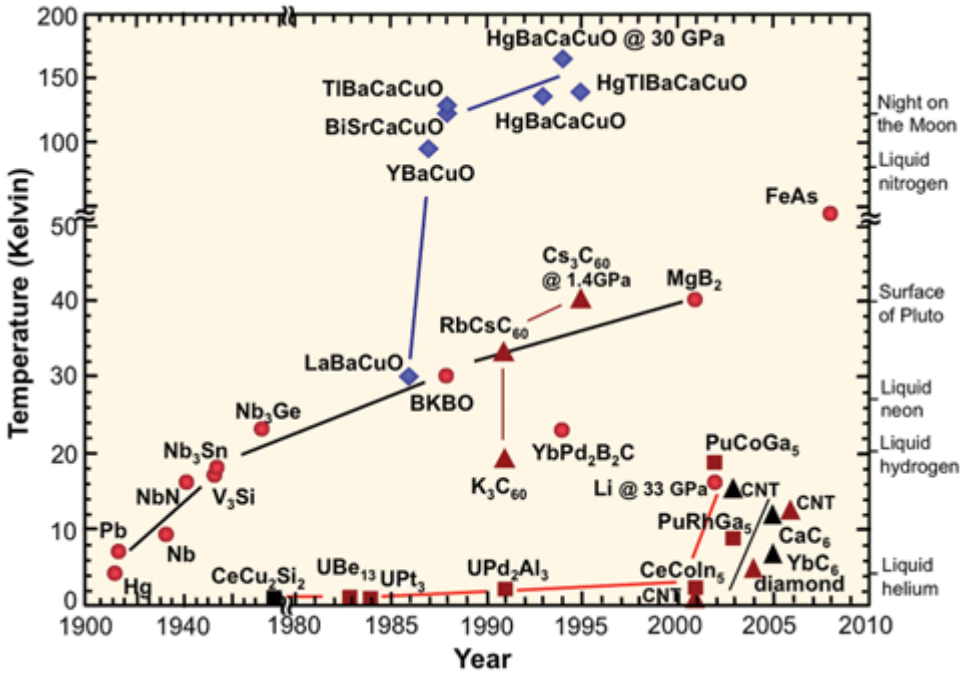

Figure 33:Temperature and Coolants of Semiconductor Materials [112]

The technology is not affordable at this point in time. The material itself, the cooling system and the maintenance of these still raise problems at exploitation level. If the cost and maintenance issues improve, the concept shows promise related to the Nessie generator.

High temperature superconductor (HTS) technology

10 [MW]HTS direct-drive wind generator was produced by NREL (National Renewable Energy Laboratory) and AMSC (American Superconductor) in the US. (see Figure 34)

The estimated mass of the HTS generator is about 120 tonnes, (that represents 30 to 40% of the mass of conventional direct-drive generators) 10 [MW] HTS generator – 6 kV; 11 [RPM] the diameter is 4.5, 5m and the efficiency at rated power is 0.96% [102].

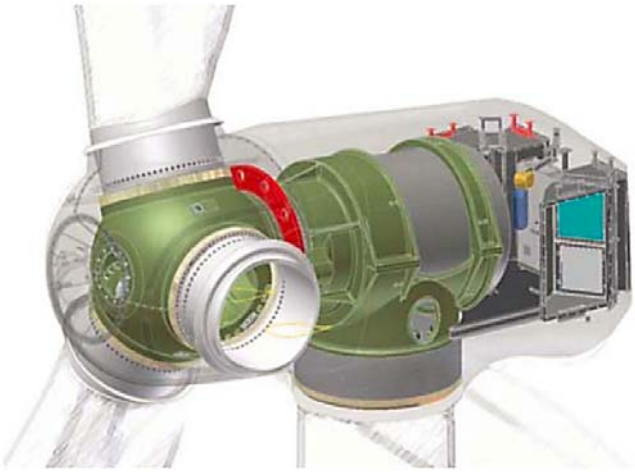

Figure 34: 10[MW]HTS Direct Drive Wind Turbine [102]

Low temperature superconductor technology

It is difficult to achieve good steady state cooling at 4 K for a mass above 10 000 kg with dimensions higher than 4 m diameter and 2.5 m length [113]

[113] treats a 10 [MW] machine using superconducting materials and proposes a cooling method for large 15-20[MW] turbines.

b. Halbach arrays

Halbach arrays are obtained by connecting PM so that the resulting structure exhibits a larger flux density one side compared to the individual magnet and almost zero on the opposite side [93], [114], [115], [116], [117], [118], [119], [120], [121]. in this way, the PM are focused towards the air-gap.

c. Magnetic gears

The magnetic gears have a high speed shaft with fewer pole pairs than the low speed one- see Figure 35

The idea is to integrate magnetic gears in the direct drive generator to artificially increase the speed and decrease the number of poles hence the diameter of the generator [101]. Design of magnetic gears [122], [123],[124], [125], [126], [127], [128] is usually for lower torques and diameters than discussed for the 20[MW] Nessie.

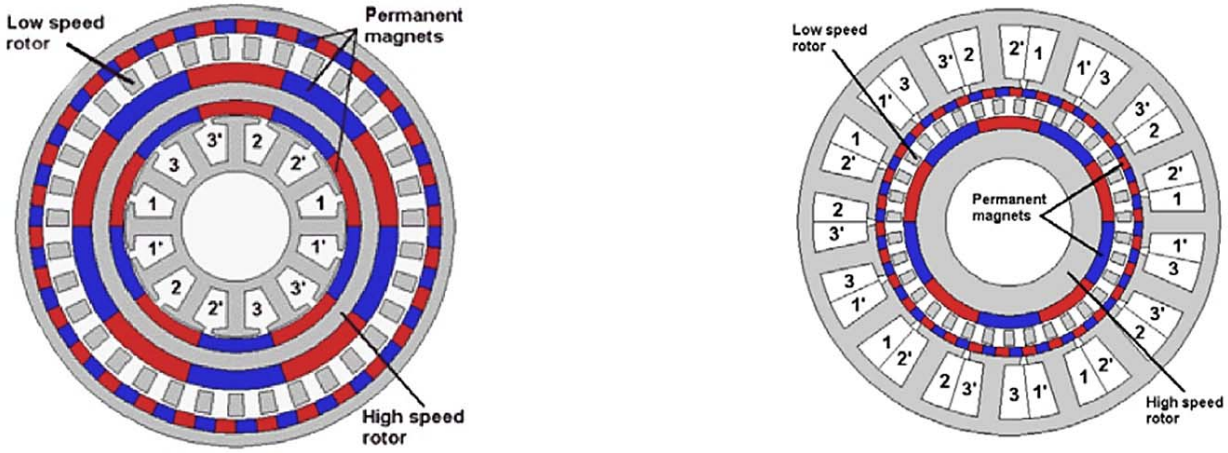

Figure 35: Integrated magnetic gears [101]

d. Ironless RFPM Machines

The ironless RFPM machine for large direct-drive wind turbines was proposed by [129] , [130]. The machine has a pair of spoked wheels which carry the rotor and the stator. The rotor is a steel rim with surface-mounted rare earth PMs. The stator consists of air-gap windings with a non-metallic support structure.

The active and total mass is reduced due to the absence of an iron core (no radial attractive forces; lightweight spoke structures.

The active and total mass of the design proposed in [129] with an ironless generator rated 5 [MW] and 13.7 [RPM] were compared to slotted and slotless RFPM generators in terms of shear stress and efficiency. The proposed machine was found lighter and requiring less maintenance [9].

Conclusions

In this chapter, research directions for future works were discussed. Further development of the design tool was recommended, influenced by the manufacturing and maintenance processes. Different concepts thought suitable for the 20 [MW] Nessie were listed.

The concept of ferrofluid filled generator air-gap was assessed as a possible solution for DeepWind to increase the torque density of the generator. This would allow a smaller generator to develop the torque required.

By reviewing the bibliography on ferrofluids and electric generators, it is concluded that this concept is of interest for increasing the torque density of the generator. Tests are needed to prove that this concept could be successfully applied to Nessie type generators.

Relevant research trends related to Nessie were listed together with literature suggestions to facilitate commencement of future work.

Chapter 7: Overall Discussion and Final Conclusions

This chapter presents a discussion on the problem that was approached within this thesis. Overall conclusions are drawn based on the obtained results. The chapter is regarded as a summary of the main story line of the thesis.

A. Verification of Calculations

Even though theoretically, all the formulae obtained from literature should give good results, within a complex design algorithm, the combination of equations must be tracked. Often during the evolution of the design tool, close to satisfactory results were obtained by one validation technique (see also Appendix 10), but errors were revealed by another. It is crucial in this author's opinion that several methods are mandatory for validation.

When literature is used for validation, one cannot be sure that facts reported are error free. Omission of certain details due to the limited publication space might raise uncertainties. These shortcomings are alleviated by a comparison of roughly the same statement reported by several independent authors/projects.

Small scale prototype validation brings the implicit disadvantage of the scalability factor. As the machine is a non-linear system it is rather difficult to exactly compare small scale designs with full scale ones. Ideally, a full scale prototype machine should be used for validation. This is very often not a possibility because of the high costs involved and the need for full scale test facilities and equipment.

FEM calculations check the electromagnetic performance of the design given the material properties. For this project, relatively little proofing exists of the FEM model. The materials for the [MW] class generators are not known as manufacturing was not considered in detail. Data from the FEM model is used in the belief that a valid solution is obtained from the software itself. As a user, one does not have a full overview of the calculations behind the interface.

So far, the CAD verification proved most valuable due to the rapid visualisation of the calculated machine. The first sign of error is that the geometry elements are invalid: e.g. the PM overlap. Very little time is needed to observe the design as the calculation tool is constructed dynamically, facilitating the active link between the analytical design and the CAD.

B. Debugging

The debugging of the design process during development is inevitable. Steps were taken to facilitate this process. Descriptive names for the variables, logging of the algorithm path, list of development rules consistently, parallel written explanation files on the approach taken are just a few of the elements used to have an clear design process. Checking if the quantities have the correct sign (positive or negative) were used as a preventative measure to avoid calculating with wrong values.

The previously mentioned developer strategies contribute to the transparency and further development of the design tool.

During the validation process several corrections to the equations and the approach were made. Questions were raised by all the validation elements.

Corrections were made as a result of comparing test results on the prototype to calculated values by the design tool. Problem areas were questioned and the approach was re-evaluated.

Conclusions

During the research documented in this thesis, the problem to be solved was defined. Focus points were identified. Objectives, tasks and subtasks were defined.

Investigation of suitable machine types and relevant issues was carried out. A selection of elements to be researched was made. Important tasks that were not handled in detail in this thesis were listed for future work.

A flexible design tool was built to investigate the direct drive generator. The concept and structure of the calculation tool was defined in such a way that modifications and adaptations are easily possible and intuitive. A comprehensive set of analyses was carried out to investigate the engineering problem of upscaling a generator to 20 [MW] 1 [RPM] from a 6 [MW], 5 [RPM] design.

A set of concepts was investigated using the design tool. A novel geometry (Double Airgap) was modelled and compared to classic and previously proposed solutions (Classic RF, TFPM).Links between the analytic module and CAD, FEM and dynamic Model were shown.

Based on the current work, investigation of large direct drive wind generator concept can be started. The calculation tool is ready to receive new models and to be coupled with other design tools relevant for sizing generator and distribution systems.

Appendix 1: Publications. Contributions to the Present Work

This appendix gives information about the author and collaborators of the design tool and lists which parts of the tool they have been involved in. The list of papers arising from the research is listed. The contacts of the author and of the other researchers involved in the present research are presented.

Original Contribution

The contributions of the author Krisztina Leban to the present thesis and work are:

1. Derived the key methodology to solving the problem; Concept of the design tool
2. -Discussed the problem and solution with the collaborators
3. Identified relevant performance metrics, interpreted the technical results based on discussion with the collaborators
4. Implemented the design tool for the Classic and Double Airgap machines
5. Involved in the design of the transverse flux topologies and their optimisation
6. Strategic decision taken
   - ❖ Machine types to consider
   - ❖ Features to design-PM, winding type, slot type
   - ❖ Geometry for the radial flux machines: e.g. slot type, rotor pole pitch for the PM
7. Design and test the prototype
8. Validation of the design tool: concept, actual validation
9. Optimisation Tool:
   - ❖ Linking the optimisation module to the design tool concept
   - ❖ Decide on the method of testing each of the PSO and GA for suitability to be integrated the design tool. Is the method suitable for electrical machines? Are the algorithms correctly implemented? Which of the algorithms gives better results?
   - ❖ Setting up the optimisation problems for a test example that gives results which are conclusive enough to show compatibility between the two modules (optimisation only of the mass of PM and not of the overall active mass)
   - ❖ Integrating the optimisation modules in the design tool by shaping the calculations to accept the optimisation module.
   - ❖ Validation of the results of the optimisation and design tool by running tests where the answer can be deduced phenomenologically.
   - ❖ Using the optimisation module on the machines in the design tool
10. Novel 2 rotor generator concept
11. Analysis and comparison of the investigated candidates for Nessie
12. Choice of future work directions as result of investigation and involvement in the Deep Wind project tasks
13. Wrote thesis

Author/Collaborators

Krisztina Leban (main contact-author)	kle@et.aau.dk; krisztina_leban@yahoo.com.au.	KLE
Ewen Ritchie	aer@et.aau.dk	AER
Alin Argeseanu	alin_argeseanu@yahoo.com	AMA
Florin Valentin Traian Nica.	nicaflorinvalentin@yahoo.com	FN

Table 23: list of Research collaborators and contact details

Contributions

Program interface	FN, KLE
Machine design-PMSG.	KLE
-TFPMG	AMA, AER, FN
optimisation algorithm -genetic algorithm -particle swarm	FN, KLE, AMA
CAD	KLE
FEM	AER, KLE, FN
Dynamic Simulation	FN, KLE

Table 24: Contribution of researchers working on DeepWind Tasks

Publications arising from the research

[1] Leban K, Ritchie E, Alin A. Design Tool for 5-10 MW Direct Drive Generators. Electromotion journal Vol 21 (2014) 2014, Accepted, Publication Pending; ISSN 1223 - 057X.

[2] Leban K, Ritchie E, Argeseanu A. Design preliminaries for direct drive under water wind turbine generator. Electrical Machines (ICEM), 2012 XXth International Conference on IEEE, 2012 2012:190-5.

[3] Marie-Christine Schimmelmann, Elena Charlotte Malz, Enrique Müller Llano, Lennart Petersen, Theodoros Kalogiannis, Krisztina Monika Leban, Andrew Ewen Ritchie. Alternative Parameter Determination Methods for a PMSM . Optimization of Electrical and Electronic Equipment (OPTIM), 2014 14th International Conference on 2014 , Accepted, Publication Pending.

[4] Nedelcu S, Ritchie E, Leban K, Ghita C, Trifu I. Iron losses evaluation in soft magnetic materials with a sinusoidal voltage supply. Advanced Topics in Electrical Engineering (ATEE), 2013 8th International Symposium on 2013:1-6.

[5] Trifu I, Leban,Krisztina Monika, Ritchie, Ewen. Influence of Closed Stator Slots on Cogging Torque. Proceedings of the 10th Jubilee International Symposium on Advanced Electrical Motion Systems-Electromotion 2013 Cluj-Napoca, Romania;Volume 20, Number 1-4 January-December 2013:ISSN 1223-057x.

[6] Nica FTV, Ritchie E, Leban K. A comparison between two optimized TFPM geometries for 6 MW direct-drive wind turbines. Advanced Topics in Electrical Engineering (ATEE), 2013 8th International Symposium on IEEE 2013.

[7] Nica FTV, Ritchie E, Leban KM. Comparison between Genetic Algorithms and Particle Swarm Optimization Methods on Standard Test Functions and Machine Design. Proceedings of the 10th Jubilee International Symposium on Advanced Electrical Motion Systems-Electromotion 2013 Cluj-Napoca, Romania 2013;Volume 20, Number 1-4 January-December 2013:ISSN 1223-057x.

[8] Nica FVT, Leban K, Ritchie E. Direct drive TFPM wind generator analytical design optimised for minimum active mass usage. 8th International Symposium on Advanced Topics in Electrical Engineering, ATEE 2013.

[9] Argeseanu A, Ritchie E, Leban K. Optimal design of the transverse flux machine using a fitted genetic algorithm with real parameters. Optimization of Electrical and Electronic Equipment (OPTIM), 2012 13th International Conference on 2012:671-8.

[10] Ritchie E, Leban K, Trintis I, Friis Pedersen T, Schmidt Paulsen U, Vita L. Design And Bench Tests of Converter Driven 1kW Underwater Induction Generator for the Deep Wind Project. Proceedings of the 10th Jubilee International Symposium on Advanced Electrical Motion Systems-Electromotion 2013 Cluj-Napoca, Romania 2013;Volume 20, Number 1-4 January-December 2013:ISSN 1223-057x.

[11] Zaidi A, Senn L, Ortega I, Radecki P, Szczesny I, Erkec M et al. 6 MW direct drive wind turbine generator design. Electrical Machines (ICEM), 2012 XXth International Conference on IEEE, 2012 2012.

[12] U.S.Paulsen, H.A.Madsen, K.A.Kragh, P.H.Nielsen, E.Ritchie, K.M.Leban, H. Svendsen, P.A. Berthelsen. The 6 MW DeepWind floating offshore vertical wind turbine concept design-status and perspective . EWEA 2014 2014;Energy Procedia, Science Direct.

[13] Uwe S. Paulsen, Helge A. Madsen, Knud A. Kragh, Per H. Nielsen, Ismet Baran, Jesper Hattel, Ewen Ritchie, Krisztina Leban, Harald Svendsen, Petter A. Berthelsen. DeepWind-from idea to 6 MW concept. Energy Procedia, Science Direct 2014;EERA DeepWind'2014, 11th Deep Sea Offshore Wind R&D Conference.

[14] Paulsen US, Vita L, Madsen HA, Hattel J, Ritchie E, Leban KM et al. First DeepWind 6 MW Baseline design. Energy Procedia Volume 24, 2012, Pages 27–35 Selected papers from Deep Sea Offshore Wind R&D Conference, Trondheim, Norway, 19-20 January 2012 2012.

[15] Argeseanu A, Nica FTV, Ritchie E, Leban K. A New Geometrical Construction using Rounded Surfaces proposed for the Transverse Flux Machine for Direct Drive Wind Turbine. Optimization of Electrical and Electronic Equipment (OPTIM), 2014 14th International Conference on Accepted, Publication Pending.

Appendix 2: Deep Wind Project Description

This appendix gives an insight to the goals and constraints of the Deep Wind Project. The information listed is meant to aid in understanding of the approach taken in the current thesis. The solutions found during the research were tailored to the specifications of the project contract.

Deep Wind Project

The Deep Wind Project focuses overall on the following issues [4], [131]. Work presented in this thesis is closely linked to work package *WP3: Generator Aspects.* The focus points for the project are:

- The turbine should be vertical-axis: Darreius wind turbine rotor-this type of turbine is not self-starting
- Direct drive; high power; low speed generator
- Design adapted to deep sea conditions- watertight generator design (*may alternatively be waterproof*)
- Known technologies are to be investigated – determine the capability of existing technologies
- Mechanical coupling, where also rotor thrust may be transferred should be investigated
- Mechanical geometry to be built into the turbine design
- Electro-magnetic functional concept should be outlined
- Cooling method to be considered
- Insulation concepts to be investigated
- Electrical coupling to the grid under the special deep sea conditions
- Torque density must be improved to address the low speed,
- Sealing in general should be addressed;
- Waterproof magnetic bearings for the generator
- Generator control–generator- grid frequency converter -electrical power regulation capabilities and protections
- No pitch control is available, The converter will be provided with protection for over and under voltages, and over current

Deep Wind Project Tasks: WP3: Generator design

The tasks for WP3 are according to [4]. Irrelevant tasks not referring to the focus of this thesis have been removed from the list.

Task 3.1 Coupling between generator and wind turbine rotor
This task refers to the 1KW demonstrator that will be set in Roskilde Fjord. The work of Task 3.1 is presented in [132]

Task 3.2 Design rules and develop tools to design the generator
-Use the results of task 3.1 (the demonstrator) to determine the Nessie design rules
-Develop Nessie design tools
-Build a dynamic simulation model for the generator system from input shaft to the gear to the network point of connection.
-Build a steady state, analytic model – provide rapid calculations: operating characteristics and material usage.
-Finite element (commercial software) analysis to optimise the geometry
-Results will be inserted in the analytic program- final performance and material usage.
-Dynamic models deliver inputs to – the control system design and operation work package,
- To the mechanical system dimensioning work package.
-Reduce the size of the 20 [MW] machine by increasing the torque density and by optimising the gear ratio.

Task 3.3 Design the generator system - Work related to the 1kW demonstrator for Task 3.3 is presented in [132]

Task 3.4 A concept for watertight journal and thrust magnetic bearings
-Develop a concept for watertight journal – mechanical design
-thrust magnetic bearings, including- mechanical design
-magnetic functional concept; cooling.
-consider and propose solutions for sealing the generator and power converter against the ingress of salt water.
-watertight bearing is intended for the 6 [MW] and 20 [MW]versions.
When scaling up the wind turbine, the inactive mass is increased more and more. [10], [1,133]
The work for Task 3.5 Converter is presented in a separate report – [134]

Task 3.6 Specification and design rules for the generator
-Determine the specification and design rules for the generator sealing part and the power controller (compliant with requirements of the wind turbine rotor, the shaft, and grid code requirements, specifies the 6[MW] and 20[MW] versions)
-design rules to enable a reliable design of generator and power electronics converter for this application and a given rating.
-The solutions will be built into design proposals for the 6 [MW]small scale wind turbine and the full scale 20[MW]wind turbine mentioned in WP8.

Appendix 3: List of Programs Used to Develop the Design Tool

This appendix lists the programs with version numbers used to develop different modules of the Nessie Design Tool. The listing is important information for the contributors further developing the tool.

In order to easily run and further develop the design tool, the programs and the versions used must be listed.

For the analytic design, MATLAB was chosen. Design formulae for the generator are written in code and results are extracted. The output of the calculations will be used as input for the final element program. Opera Vector fields is used to analyse the magnetic field in the designed machine.

Dimensions will also be used to draw a 3D model of the machine in Solid Works. Here, various sections could be derived from the original 3D model. If the need arises, different sections of the machine would be fed back to Opera VF for further analysis, if possible.

Program versions for different project tasks are listed in Table 25:

analytical design	MATLAB 2011b, C++(as secondary)
dynamic model	Simulink (MATLAB 2011b)
finite element	Opera VF 16R1
mechanical drawings:	Solid Works 2010, 2011, models upgraded to 2013
report editing	Microsoft Office 2010 (Word, Excel, Visio, Project Manager)
referencing	RefWorks 2.0, Write n Cite 3
data acquisition MATLAB	National Instruments LabView 2011 (32 bits)

Table 25: Software and versions used

Appendix 4: State of the Art SOA –Direct Drive Turbines

The aim of this appendix is to find the most suitable machine topology for Nessie. This is done by studying what industry and the scientific literature proposed [1]*,* [2]*. Having the set of requirements arising from the DeepWind Project (see Deep Wind Project Description in Appendix 2) the candidate is outlined.*

A. Short description of proposed machines (SOA)

In the following, generator types suitable for direct drive high power wind turbine applications are presented. Each generator type is shortly described with respect to functioning, characteristics and performance. This is done in order to provide a clear overview of available solutions for the studied problem.

Considered generators for Nessie are listed below:

1. SCIG – Squirrel Cage Induction Generator(Radial Flux RF)
2. DFIG – Doubly Fed Induction Generator(Radial Flux RF)
3. EESG – Electrically Excited Synchronous Generator (Radial Flux RF)
4. PMSG – PM Synchronous Generator(Radial Flux RF)
5. TFPM – Transverse Flux PM Generator
6. AFPM – Axial Flux PM Generator

In the following, these types of generator are briefly presented together with arguments of why they might or might not be a suitable Nessie candidate:

a. SCIG – Squirrel Cage Induction Generator

The SCIG has a cage in the rotor and windings in the stator (see [135] for details). The rotor cannot be controlled and electromagnetically, this machine cannot start in generator mode. This would not be a problem since the Vertical axis turbine that is intended for this application cannot start naturally. To start the system, the machine has to operate first as a motor and then to be switched to generator mode.

Advantages:

- The squirrel cage induction machine is extremely rugged; brushless, reliable, economical and universally popular.
- Uninsulated winding on rotor makes it extremely rugged.
- A controlled rectifier may be used to generate programmable excitation for the generator
- Fast transient response is possible.

Disadvantages

- Complex system control (Field Oriented Control); generator parameters actual values are needed for good performance of the controller; parameters varies with temperature and frequency [136]
- The stator side converter must be oversized 30-50% with respect to rated power, in order to supply the magnetizing requirement of the machine
- In relation to the very low speed operation required for DeepWind, the small air-gap required in a squirrel-cage induction generator will cause extremely high leakage flux

Conclusions

This type of machine, although simpler and less expensive constructionally than the other candidates, would introduce the main disadvantages that it would be difficult to control and it is not able to be fully controlled. The extremely high leakage flux would make it impractical to construct.

b. DFIG – Doubly Fed Induction Generator

The field in the air-gap is obtained by the interaction of the stator and rotor windings. The stator winding is directly connected to the network absorbing reactive power to provide the magnetising current. The rotor winding is connected to the network through a four quadrant power converter comprised of a two back-to-back PWM-Voltage Source Converter that is of a lower rating than the machine.[136], [137], [138], [139], [140].

Advantages [136], [141], [142]

- Active and reactive power may be controlled – by controlling the back to back Pulse Width Modulated (PWM)Voltage Source Converter(VSC)
- Good fault ride through capability in wind turbine applications [141]

Disadvantages

- Rotor excitation done with winding – implies copper losses [136]
- Rotor winding supply system needed

Conclusions:

This machine seems interesting due to its controllability and lower rating of the power converter.

c. EESG – Electrically Excited Synchronous Generator

For this machine both the stator and the rotor are wound. More about this machine type in [143], [144]

In the following, the advantages and disadvantages of EESG are presented:

Advantage [11], [136]:

- The efficiency of this machine is usually high, because it employs the whole stator current for the electromagnetic torque production
- losses can be minimised by controlling the flux for different power ranges, (rotor side converter)
- The main benefit of the application of wound field synchronous generator with salient poles is that it allows the direct control of the power factor of the machine. Consequently the stator current may be minimized any operation circumstances. Also allows variable speed operation of the wind turbine shaft.
- Generator speed –fully controllable over a wide range, even at very low speeds.
- The pole pitch of this of this generator can be smaller than that of induction machine. This could be a very important characteristic in order to obtain low speed multi-pole machines, eliminating the gearbox.
- No PM (permanent magnets=expensive, fragile-corrosion and handling, manufacturing) Maybe a small amount of PM would be used to magnetise the exciter generator-(brushless excited-pm on stator and winding on rotor connected to the field winding via a rotating rectifier)
- Active and reactive power – fully controlled-(during normal and fault conditions) [9]

Disadvantages [11], [136]:

- The existence of a winding circuit in the rotor may be a drawback as compared with PM synchronous generator-(extra insulated winding on a rotating part-subject to vibration-insulation wear-faults, lower efficiency due to losses in the excitation)
- Brushless exciter may be used instead of a slip rings (slip rings=disadvantage)
- To regulate the active and reactive power generated, the converter must be sized typically 1.2 x rated power
- In order to accommodate the excitation winding, the pole pitch (τ_p) of the EESG must be large enough. PM would make the machine smaller (see Figure 36-EEDG vs. PMSG-Figure 37)

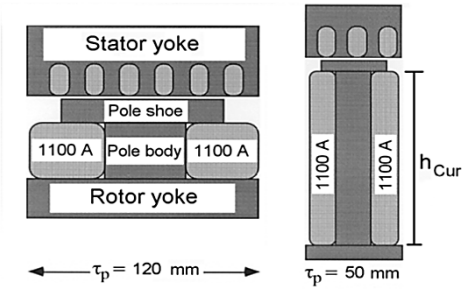

Figure 36: Increase of Pole Thickness In Electrically-Excited Coils With Short Pole Pitches [145]

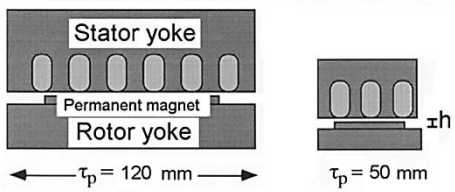

Figure 37: Constant thickness in PM-Excited Rotor Poles With Varying Pole Pitches[145]

- larger number of parts and windings – heavy and expensive
- field losses are inevitable

Conclusions:

This machine seems promising because it offers controllability. This is important to help comply with grid codes when the turbine is integrated in the generation systems.

d. PMSG –PM Synchronous generator

The rotor field is produced by PM and the stator has windings. More on this machine in [146], [147]

Advantages of PMSG system (compared to the EESG system) [9], [148], [33], [19], [19], [53], [149], [150]:

- Relatively high efficiency - no excitation winding
- Higher energy yield
- No heat losses in the excitation –May be iron losses in the PMs
- no slip rings-relatively higher reliability
- lighter and therefore higher power to weight ratio
- If it is possible to reduce the cost of a PMSG DD without diminishing the performance-the PMSG DD would be the most suitable generator system.

PMSG systems **disadvantages**:

- High cost of PM
- High cost of the converter-full rated converter Figure 38
- Difficulties to handle in manufacturing-PM
- Demagnetization of PM at high temperature and current

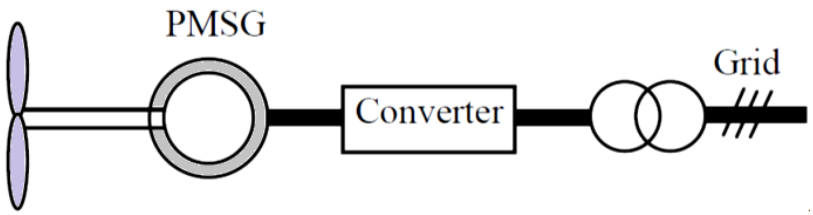

Figure 38: Scheme of DD PMSG System [151]

Conclusions:

This machine is more robust than the wound synchronous machine, but the price of magnets can be prohibitive. The flux of the PM cannot be fully controlled hence the controllability of the entire machine is less than for the EESG.

e. TFPM – Transverse Flux PM Generator

The transverse flux PM machine (TFPM) – magnetic flux is perpendicular to the direction of the rotor movement.[9], [32], [152], [153]

Advantages [154], [1]of TFPM machine

- For a 55 kW transverse flux machine the weight is about half of the total weight of an asynchronous machine with a gearbox.
- TFPM has higher force density than RFPM and AFPM machines [9]
- Simpler and smaller winding for TFPM –basically one coil; no end windings. This would make for considerably lower copper losses compared to radial and axial flux machines. The TFPM offers an increase of the space for the windings without reducing the available space for the main flux(RFPM and AFPM machines do not) [9]
- TFPM machines can be made with a very small pole pitch compared to RFPM and AFPM [9]
- TFPM has smaller active mass then the other machines to produce the same torque[9]
- A suitable machine type for direct-drive applications: high specific torque, [9]
- New TFPM topologies can be made to suit the direct-drive application [9].

Disadvantages [11], [1], [9]

- A small number of TFPM in production-mostly treated theoretically[11]
- Special methods of manufacturing and assembly (large number of individual parts)
- Complicated construction
- 3D flux path-complex model/analysis-3D flux path makes fabrication using laminations next to impossible.

- Low-force density in large air-gaps
- Low power factor, which leads to an increase in the necessary rating of the power electronic converter
- The TFPM machine less economical when the air-gap length is on the increase over 3-4 mm

TFPM disadvantages show opportunities for improvement (new topologies, flexible design)-machine will be potential and attractive for large direct-drive concept. [133]

Conclusions

At research level, there has been a lot of focus on this concept. It is concluded that this machine type should be considered as an alternative candidate for the Deep Wind application

f. AFPM – Axial Flux PM Generator

The AFPM will not be considered for vertical axis wind turbines because the difficulty of keeping the air-gap of the machine would make the system unfeasible.

B. Machine type comparison with regard to the type

In the following, the candidates are compared with each other to reveal their suitability hierarchy.

PMSG over EESG

Advantages [11]

- Higher efficiency
- Higher energy yield –see Table 26 where coefficients *a* to *k* are used to compare the two machine types
- no excitation winding
- no heat losses in the excitation –May be iron losses in the PMs
- higher reliability-no slip rings on PMSG
- PM machines are more attractive and superior with higher efficiency and energy yield, higher reliability and power to weight ratio compared with electrically excited machines. [1]
- surface-mounted PM – more suitable for direct-drive PM generator types [11]
- The PM machine is superior compared to the electrically-excited machine in terms of the mass, cost, efficiency and reliability. [11]–see Table 26

Direct Drive Generator concept	EESG	PMSG
Stator air-gap diameter	a[6 [MW]range]	a
Stack length	b	b
Active material weight		
Copper	c	c x 0.34
Iron	d	d x 0.55
PM	-	e
Total cost	f	f x 0.53
Generator active material	g	g x 0.56
Generator construction	h	h x 0.93
converter	i	i
Total cost (with margin for company)	j	j x 0.73
Annual energy yield/total cost	k	k x 1.08

Table 26: Comparison of Direct Drive Wind Generators Electrically Excited and PM [10]

Disadvantages [11]

- High cost of PM material,
- Demagnetisation of PM at high temperature and high currents.
- Fixed excitation in form of PM-voltage regulation by modifying the excitation is not possible in PMSM

TFPM over. RFPM

Advantages of TFPM vs. RFPM [11]

- TFPM provides a significant cost advantage in active material compared to RFPM machine. [1]
- TFPM allow for a larger room for optimisation than RFPM (TFPM geometries are not well developed)
- Higher force density in TFPM
- Considerably lower copper loss
- Simple windings

Disadvantages of TFPM vs. RFPM [1], [1]

- The cost advantage of the TFPM machine is reduced when the air-gap length increases over 3-4 mm. This would be the case for the large 20 [MW]machine
- Low cost-advantage and low mass-competitiveness in higher torque ratings
- RFPM generators are on the market –: well-known machine by industry and clients
- TFPM machines – difficult to manufacture-not widely used as wind generators
- construction is more complex-manufacturing
- Low power factor

On the Market

Types of direct-drive generators on the market are presented in (see also [9] for predominant generator types up to 3MW). In [155], direct drive turbines are reported to be mostly radial flux PMSG or EESG

Due to the features of the EESG these are mostly used for large direct-drive applications for wind turbines (Enercon)

Active mass-competitiveness of PM machine

The active mass is the total mass of the windings, cores and PM materials used in a machine. This is a key factor in the cost of a large generator. The lines in Figure 39 represent the linear regressions of the active mass of the three machine types (radial, axial and transverse flux). [1]. In the following, different machines are compared in order to conclude on their mass competiveness for a wind turbine application.

Figure 39 shows the active mass/torque of PM machines as a function of torque rating

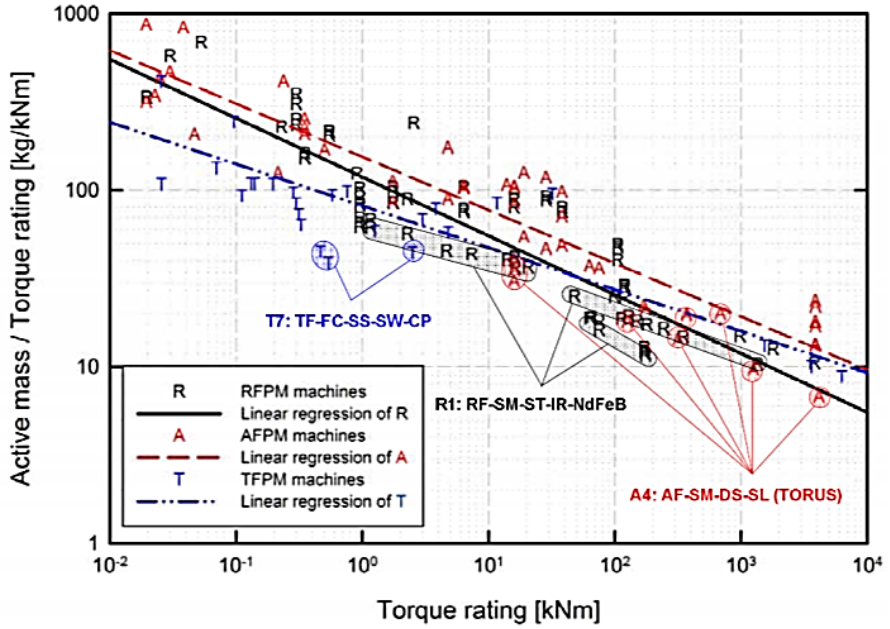

Figure 39: Active Mass/Torque of PM Machines as a Function of Torque Rating [9]

From Figure 39 [9], the following can be concluded

- TFPM lighter than RFPM machines for low torque ratings (under 50 kNm).
- RFPM machines lightest for large torque ratings (over 100 kNm).

• Active mass/torque ratios of the machines in Figure 39 decrease when the torque rating increases.

Table 27 shows the shapes of the 10 PM generators. Different generators were compared in order to rate their suitability for the Deep wind project 6 [MW]generator.
[9]suggested the following machines:

- RFPMG: slotted surface-mounted radial flux PM generator with full pitch windings, inner rotor and rare earth magnets
- TFPMG-U: single-sided, single winding flux-concentrating TFPM generator with U-core
- TFPMG-C:double-sided, single winding flux-concentrating TFPM generator with C-core
- TFPMG-U/PR: single-sided, single winding flux-concentrating TFPM generator with U-core and passive rotor
- TFPMG-C/PR: double –sided, single winding flux-concentrating TFPM generator with C-core and passive rotor

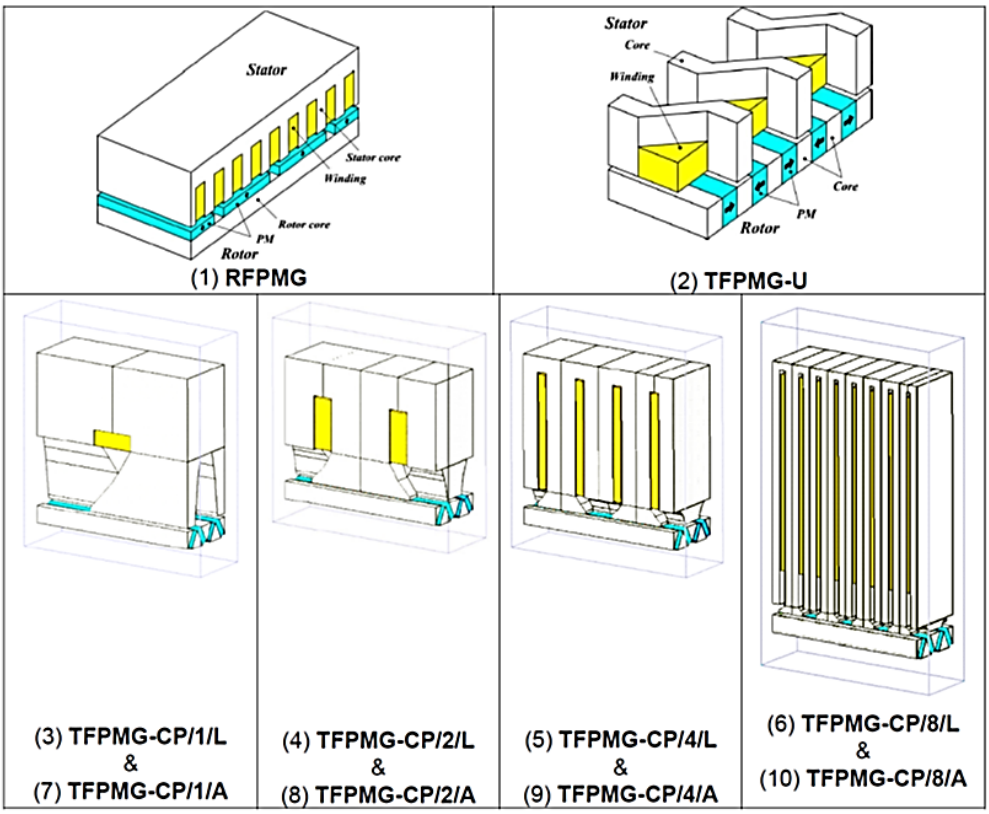

Table 27:External Shapes of the 10 PM Generators [31]

The 5 and 10 [MW]machines in Table 27 were assessed for suitability as generators for direct drive wind turbines by [31].

		RFPMG	TFPMG-U	TFPMG-C	TFPMG-U/PR	TFPMG-C/PR
Active mass	6 MW	-	++	+	Δ	--
	10 MW	++	+	-	Δ	--
Cost	6 MW	+	Δ	++	-	--
	10 MW	+	Δ	++	-	--
Efficiency	6 MW	- (96.6%)	+ (97.2%)	++ (97.4%)	Δ (96,8%)	"–(96,4%)"
	10 MW	Δ (97%)	++ (97.3%)	++ (97.3%)	- (96.9%)	"–(96,4%)"
Force density	6 MW	--	++	++	++	+
	10 MW	--	++	++	+	-

Legend:
++ very strong
+ strong
Δ middle
-weak
--very weak

Table 28: Comparison of 5 Different PM generators for 5 and 10 [MW]direct Drive Wind Turbines(Suitability) [31]

An analysis of Table 28 is presented in Table 29. The plusses and minuses are counted for each machine. A decision on the best and worst candidate is included in the last column.

•	For the 6 [MW]design:	up scaling	Active mass	Cost	Efficiency	Force density	Decision	
			(compare between 5 and 10MW)					
RFPMG	No(3-)	Not the best candidate(+)	+	2+	-	4-		-4
TFPMG-U	Good (5+)	Ok(3+)	3+	0	3+	4+		18
TFPMG-C	Best(7+)	Good (5+)	0	4+h	4+	4+	BEST	24+
TFPMG-U/PR	0	No(-)	0	2-	-	3+		-1
TFPMG-C/PR	No(5-)	No(7-)	4-	4-	4-	0	worst	-24

Table 29: Best Candidate Assessment

[31] and Table 29 show that

- the best candidates are TFPMG-U and C
- For the 6 [MW]wind turbines, TFPMG-U – lightest generator – active mass is 78 [%] of the mass of RFPMG (6 MW) suitable generator for large direct-drive wind turbines.
- For the 10 [MW]wind turbines, RFPMG lightest generator. TFPMG-U – second lightest generator-active mass is 3.3 [%] larger than the mass of RFPMG.
- TFPMG-C would have smallest losses and the lowest cost compared to the other generators for both 6 [MW]and 10 [MW]turbines.
- TFPMG-C/PR would have the largest mass, cost and losses among the five different generators for both 6 [MW]and 10 [MW]turbines.
- TFPMG-U/PR and TFPMG-C/PR most expensive than the other generators(both need large mass of PMs
- TFPMG-C and TFPMG-C/PR –sided air-gaps.-complex construction-complicated manufacturing

Active mass of different PM generators is shown in Figure 40

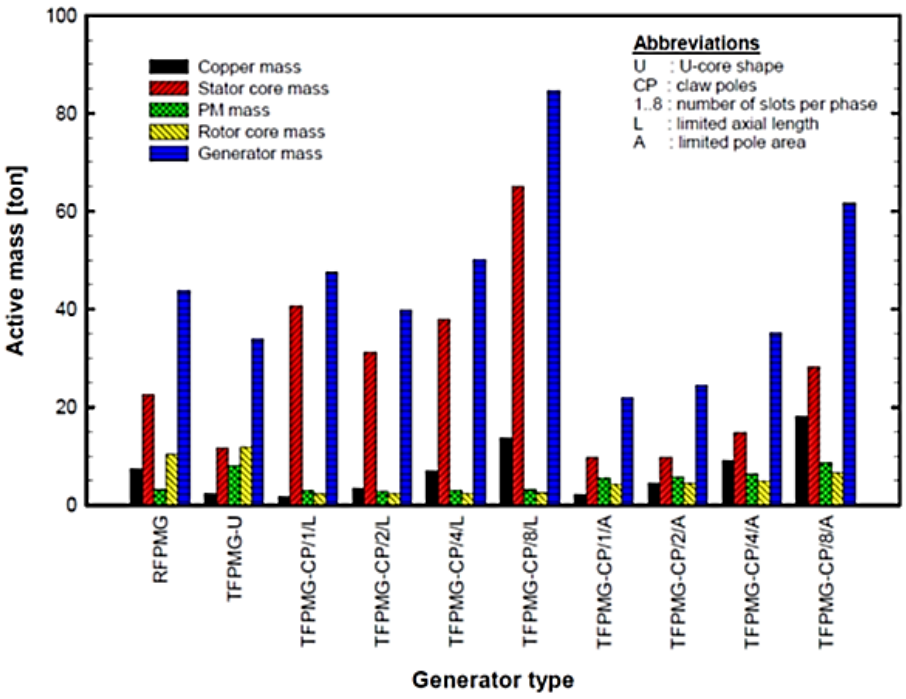

Figure 40: Active mass of different PM generators for 6 [MW]direct-drive wind turbines [31]

Figure 41 compares the different PM generators for competitiveness of efficiency, force density, cost/torque ratio and mass/torque ratio. It is concluded that the RFPMG and TFPMG-U and TFPMG-CP/1/A look most attractive (minimum active mass)

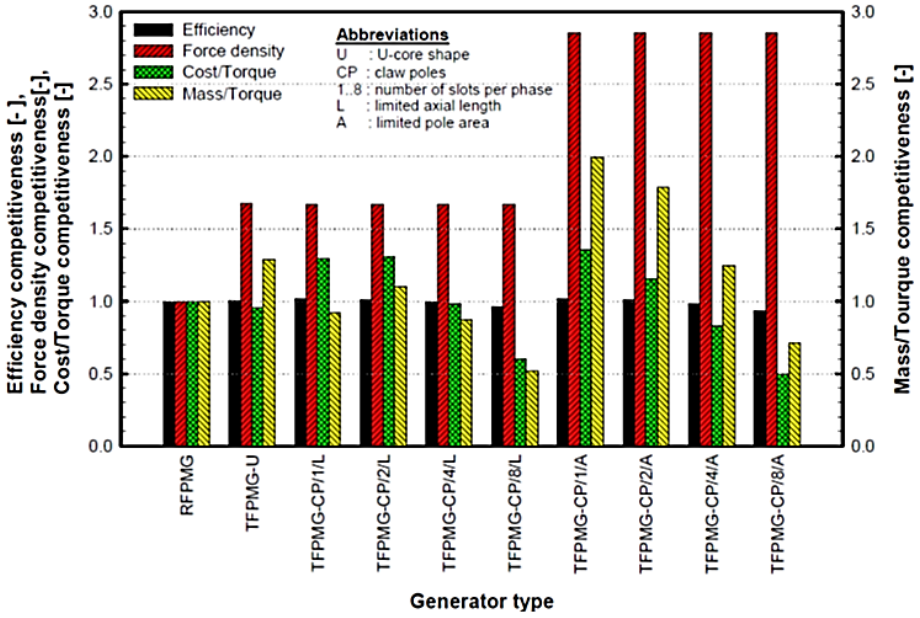

Figure 41: Efficiency, Force Density, Cost/Torque Ratio And Mass/Torque Ratio Of Different PM Generators For 6 [MW]Direct-Drive Wind Turbines [31]

Figure 41 shows that RFPMG and TFPMG-U are most attractive as a generator solution

In Table 30[31], machines from Table 27 are compared for their competitiveness as direct drive wind turbines. The highest competitiveness is rated "9" and the lowest competitiveness, "0".

		RFPMG	TFPMG-U	TFPMG-CP/1/L	TFPMG-CP/2/L	TFPMG-CP/4/L	TFPMG-CP/8/L	TFPMG-CP/1/A	TFPMG-CP/2/A	TFPMG-CP/4/A	TFPMG-CP/8/A
6 MW	**Active Mass**	4	7	3	5	2	0	9	8	6	1
	Cost	5	3	7	8	4	1	9	6	2	0
	Efficiency	4	5	9	7	3	1	8	6	2	0
	Force Density	0	5	2	3	1	4	9	9	9	9
Total 6 MW		13	20	21	23	10	6	35	29	19	10
10 MW	**Active Mass**	6	5	1	4	3	0	9	8	7	2
	Cost	7	3	8	9	5	1	6	4	2	0
	Efficiency	4	5	9	7	3	1	8	6	2	0
	Force Density	0	5	4	1	3	3	9	9	9	6
Total 10 MW		17	18	22	21	14	5	32	27	20	8
Total		43	58	64	67	34	17	102	85	58	28

Table 30: Comparison Of The Eleven Pm Generators For 6 [MW] and 10 [MW]Direct-Drive Wind Turbines [31]

The best candidate is shown to be TFPMG-CP/1/A. The worse candidate according to [31] is TFPMG-CP/8/L. The RFPMG is rated to have unsuitable force density. For the RFPMG to become a direct drive wind generator, the force density is one of the characteristics to be improved and optimised.

Active mass of RFPM machines

The following slotted RFPM machines are chosen to be characterized with respect to the active mass of the machines in scaling up the torque rating [31]. Results are shown in Figure 42 and Figure 43

	Name	RFPM Type	Rotor Type	PM Type
R1	RFSM- ST-IR-NdFeB	Slotted surface-mounted	Inner	rare earth
R2	RFSM-ST-OR-NdFeB	Slotted surface-mounted	Outer	rare earth
R3	RF-FCST-IR-Ferrite	Slotted flux-concentrating	Inner	ferrite
R4	RFFC-ST-IR-NdFeB	Slotted flux-concentrating	Inner	rare earth
R5	RFFC-ST-OR-NdFeB	Slotted flux-concentrating	Outer	rare earth

Table 31: Description of Radial Flux Machines Analysed

Figure 42 shows the torque vs. active mass of the machines surveyed in [9]

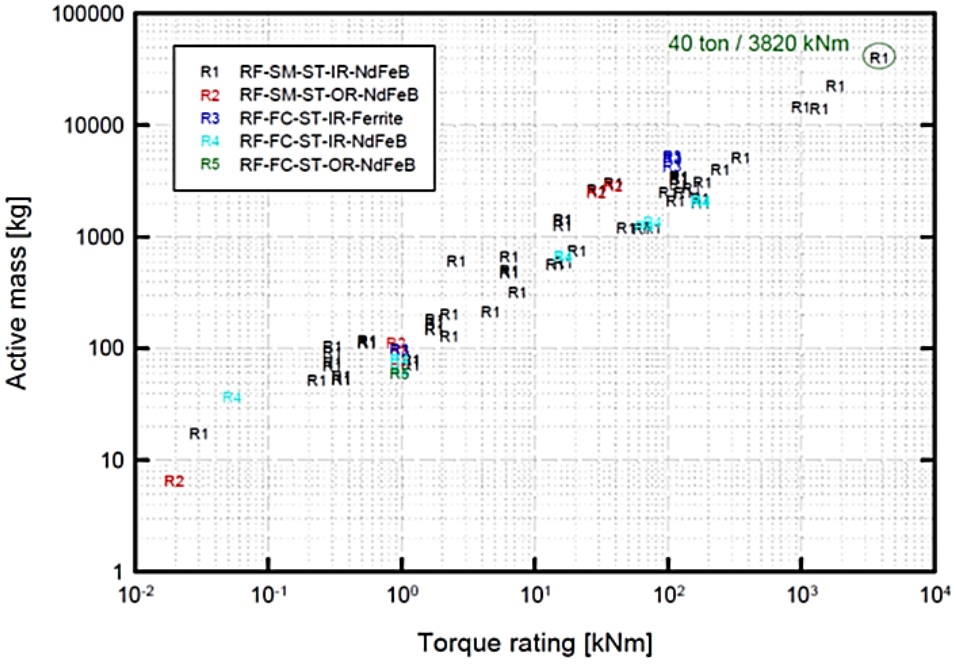

Figure 42: Active Mass Of RFPM Machines As A Function Of Torque Ratings [9]

Figure 43 shows the Active Mass/Torque of RFPM Machines as a Function of Torque Rating

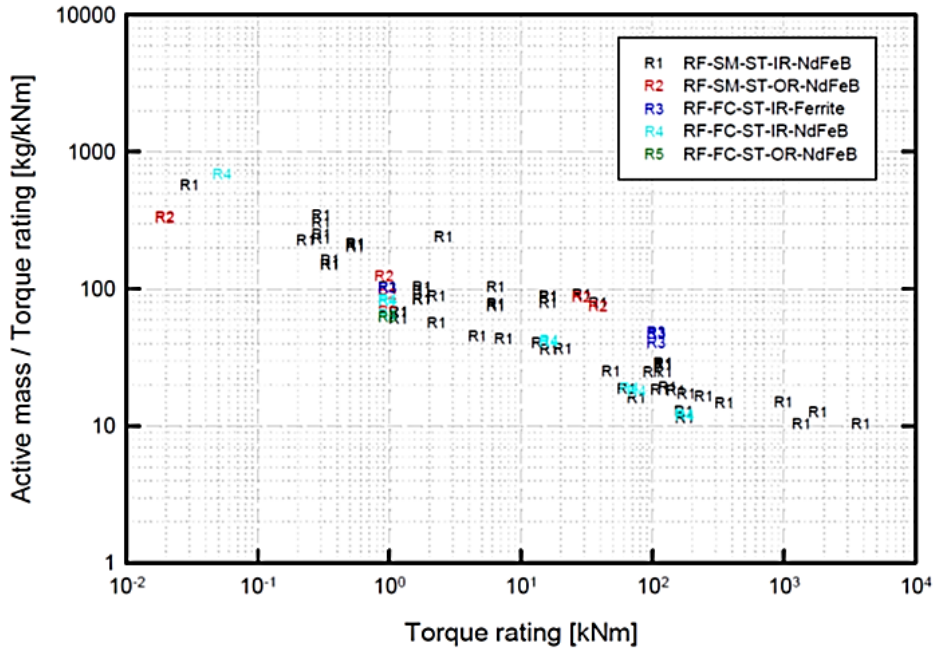

Figure 43: Active Mass/Torque Of RFPM Machines As A Function Of Torque Ratings [9]

From [9] it may be concluded that:

- There is no clear difference between slotted surface-mounted RFPM machines with inner rotor concept (R1) and outer rotor concept (R2) from an active mass point of view.
- It cannot be concluded that one concept is lighter than another for large torque machines.
- Slotted flux-concentrating RFPM machines with ferrite magnets (R3) are heavier than the machines with rare earth magnets (R4)
- It is not clear to draw the conclusion that the slotted flux-concentrating RFPM machine with outer rotor (R5) is lighter than the machine with inner rotor (R4) for large torque machines. However, the RFPM machine with *R5* concept was considered a lighter machine than the machines with R1, R2 and R3 concepts at low torque rating, about 1 kNm. [9] R1 and R4 concept seem lighter than other RFPM machines. [9]
- R1 proved to have the lightest active mass characteristics. [9]

Conclusions

It can be concluded that although some TFPM machines rated better for active mass use, the RFPM generators cannot be excluded. The downsides of the TFPM (difficult and expensive to manufacture, low power factor, uncommon in industry) for the direct drive application is kept in mind as well as the familiarity of the field with the RFPM.

From the active mass usage point of view, there is no clear difference between inner and outer rotor geometries for surface mounted slotted machines. Other factors like mechanical design of the connection system from the generator to the turbine might show the necessity of an inner or an outer rotor construction. Besides the active weight, also the inactive weight must be considered for a final design.

Machines chosen to be the most suitable from a mass assessment point of view:

- RFPM machine: Slotted surface-mounted RFPM machine with inner rotor and rare earth magnets (R1: RF-SM-ST-IR-NdFeB) [9]
- TFPM machine: Flux-concentrating TFPM machine with single windings; the best candidates are TFPMG-U: single-sided, single winding flux-concentrating TFPM generator with U-core and TFPMG-C: double-sided, single winding flux-concentrating TFPM generator with C-core [9], [31]

C. Discussion

-The PMSG DD concept has the highest energy yield compared to EESG DD concept: kx1.08 (see Table 26). [9]
-Optimum torque to mass ratio of conventional PMSG DD – 25 kg/kNm. [1]
-Up scaling, the total mass of conventional DD construction inactive mass (structural mass) is significantly increased.- see values in Figure 42, Figure 43

The PMSG DD with the minimum cost has been identified as the most suitable generator concept. [1]

- Large direct-drive wind turbines use mostly RF machines [1], [9]
- No Axial flux for vertical axis turbines
- There are no commercial TF machines for large direct-drive wind generators. [31]

The following machines were chosen as potential candidates for Nessie:

- ✓ SCIG – Squirrel Cage Induction Generator(Radial Flux RF)
- ✓ EESG – Electrically Excited Synchronous Generator (Radial Flux RF)
- ✓ DFIG – Doubly Fed Induction Generator(Radial Flux RF)
- ✓ PMSG – PM Synchronous Generator(Radial Flux RF)
- ✓ TFPM – Transverse Flux PM Generator

Reviewing the advantages and disadvantages of these machines they might be suitable for the Nessie application.

In the choice between EESG and PMSG, the latter seems to be more attractive, but neither can be dismissed at this point when the specifications of the research projects go towards up scaling with additional reduction in speed of the direct drive generator is aimed for.

Conclusions: The best candidates

From the literature consulted and the assessment and analysis performed it can be concluded that the candidates worth considering for Nessie are

- ❑ Synchronous PM(PMSG)
- ❑ Synchronous Electrically Excited(EESG)
- ❑ Transverse Flux PM (TFPMG)

The TFPM machine was considered as a backup; a comparison candidate. The author believes that because this machine is heavily encountered in the research literature for wind generator applications, it is interesting to be able to analyse the TFPM machine within the Nessie Design tool.

The AFPM –Axial Flux PM Generator was rejected due to the disadvantages it would bring for vertical axis turbines.

Other issues that could make or break the feasibility of a propose solution must be investigated. For a final decision for mass producing Nessie, the issues of the mechanical structure design, cooling, suitable insulation materials, mechanical vibrations and resonance, cogging due to the presence of PM, corrosion and fouling of the parts exposed to the elements, controllability needs and grid connection problems must be thoroughly investigated. An outlook on these issues is presented in Appendix 6.

Appendix 5: SWOT – Most Suitable Machine for Nessie

In this appendix, strong point, Weak Point, Opportunity and Threats (SWOT) analysis was employed evaluate the available options for the Nessie generator. Rating is based on literature study.

By considering the required specification (Appendix 2), a machine type must be chosen. Each machine type considered brings its own advantages and disadvantages

A SWOT (strong point-weak point-opportunities-threats –see method description in [9]) analysis is employed in order to decide on the suitability level of each machine type.

A. Issues to consider

At first, a list of suitability criteria must be outlined. Then, by investigating reports on each machine, the SWOT analysis is used to assess the candidates.

Comparison Criteria suggestions [156], [9], [10], [31]:

- outer diameter
- total length
- total volume
- efficiency
- torque density
- force density
- active material weight
- power/volume
- torque/volume
- power/mass
- torque/mass
- power/cost
- torque/cost
- functional advantages/disadvantages

The design of electric machines usually tries to optimise one or more of these criteria. Suitability of the EESG and PMSG depends on the price of PM and converters. Due to physical, functional and manufacturing restraints, a compromise must be reached-increase the specified design values without diminishing the other parameters.

For wind turbines, the rotational speed is further decreased when increasing the power rating. The mass of electrical machines depends on their torque rating. As a consequence, the torque rating (more precisely the mass to torque ratio) can be a criteria for choosing the most suitable machine for the 20 [MW] turbines.

Cost of active and inactive materials used (mass of the generator) and manufacturing cost (chosen geometry) play an important role in assessing the suitability of a machine type.

Figure 44 depicts the world market share for yearly installed power for different wind turbine generator types as well as their tendency. DFIGs seem to be the dominant type.

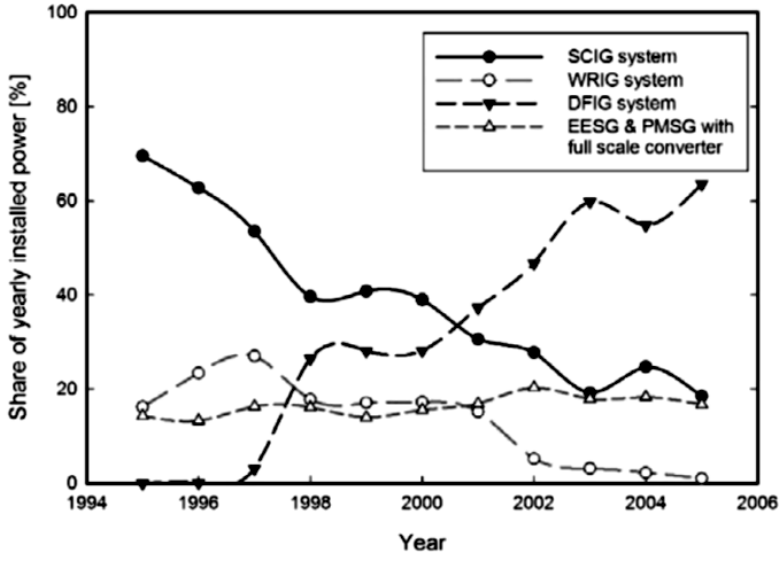

Figure 44: World Market Share For Yearly Installed Power For Different Wind Turbine Generator Types [157]

In [9], large direct-drive wind PM turbines were assessed for their active mass-competitiveness.

In Table 32, the candidates for the SWOT analysis are presented together with suitability arguments. Each argument is quantified by a value of importance. These values are assigned for each of Strong points, Weak points, Threats and Opportunities for each machine. By adding up and analysing the sum of the values, a decision is outlined

.	Strong points		Weak points		Opportunities		Threats	
	Argument	Value	Argument	Value	Argument	Value	Argument	Value
SCIG	(S1)Very robust and well established construction (S2) no insulated windings on the rotor (S3)programmable excitation (S4)Fast transient response	(S1): 10 (S2): 10 (S3):5 (S4): 4	(W1)Low speed multi-pole versions –extremely high flux leakage (W2)Requires magnetising current at all times. This causes reduced efficiency, low power factor and extra heating of the armature winding (W3):full power converter must be rated 30 to 50% more than the nominal value (W4):rotor parameters cannot be directly measured – for the control	(W1):10 (W2):8 (W3):7 (W4):3	(O1):Very robust and well established construction (O2):Magnetisation can be controlled (O3): regarding (W3)-price of converters is decreasing (O4)regarding (W4): parameters can be estimated	(O1):7 (O2):8 (O3):4 (O4):7	(T1)difficult to reduce leakage in multi-pole versions (T2)The magnitude of the leakage will increase the time constant for the torque and reduce the capability for fast response	(T1):6 (T2):4
Total /		S_{SCIG}=29		W_{SCIG}=28		O_{SCIG}=28		T_{SCIG}=10
DFIG	(S1): Active and reactive power control by controlling the rotor (S2): rotor converter is rated about 30% of the rated output (S3):good fault ride-through capability	(S1): 10 (S2): 9 (S3):8	(W1): slip rings – rotor current-will produce maintenance and functional issues (W2):insulated winding on the rotor (W3)Low speed multi-pole versions –extremely high flux leakage (W4)Requires magnetising current at all times. This causes reduced efficiency, low power factor and extra heating of the armature winding	(W1):9 (W2):8 (W3):10 (W4):8			(T1)difficult to reduce leakage in multi-pole versions (T2)The magnitude of the leakage will increase the time constant for the torque and reduce the capability for fast response	(T1):6 (T2):4
Total		S_{DFIG}=27		W_{DFIG}=35		O_{DFIG}=0		T_{DFIG}=10

.	Strong points		Weak points		Opportunities		Threats	
	Argument	Value	Argument	Value	Argument	Value	Argument	Value
EESG	(S1): Excitation can be controlled: adjustable no-load voltage [9] (S2): adjustable excitation –iron losses may be reduced at low loads. The no load voltage can be adjusted as required. (S3): usually high efficiency of this because it employs the whole stator current for the electromagnetic torque production [145] (S4): with controllable excitation, the converter +control is more flexible (S5): no PM-PM are increasingly expensive	(S1): 10 (S2):8 (S3): 6 (S4): 8 (S5): 7	(W1): have to get the excitation current from somewhere (separately excited generator) (W2): " are heavier than PM rotors and are bulky in short pole-pitch synchronous machines''[136] Figure 36, Figure 37 (W3):full power converter must be rated 20% more than the nominal value (W4): In order to accommodate the excitation winding, the pole pitch (τ_p) of the EESG must be large enough. (W5):rotor of higher mass than PM –worse if pole pitch decreases (W6):copper losses increase when number of poles increases	(W1):6 (W2): 8 (W3): 5 (W4):7 (W5):7 (W6):6	(O1):Brushless exciter may be used instead of a slip rings (O2): The pole pitch of salient pole can be smaller than that of induction machine. [145](more poles in a given diameter)	(O1): 8 (O2):8	(T1)difficult to reduce leakage in multi-pole versions	(T1):6
Total		S_{EEIG}=39		W_{EEIG}=39		O_{EEIG}=16		T_{EEIG}=6

.	Strong points		Weak points		Opportunities		Threats	
	Argument	Value	Argument	Value	Argument	Value	Argument	Value
PMSM:	(S1): -''for a given torque rating, a PMSM with a higher number of pole pairs enables a mass reduction in the stator yoke and rotor back-iron''[136] (S2): -no copper losses in rotor (S3): '' – has a total cost and a total mass lower than that of the wound-rotor SM[145]'' (S4): simple structure, good utilisation of the active materials; relatively small diameter in comparison with EESG (S5): The PM machine is superior compared to the EESM in teRMS of the mass, cost, efficiency and reliability[145] (S6): direct-drive PM machines be more attractive for large wind turbines [10][9]	(S1): 7 (S2): 8 (S3): 9 (S4): 10 (S5): 10 (S6): 10	(W1):Excitation cannot be controlled (W2):Magnets may be come demagnetised (W3):Corrosion of magnets	(W1):7 (W2):4 (W3):8	(O1):high number of pole pairs –attractive and synchronous machines with short pole pitches to be considered for cost and mass reduction[10] (O2):Different magnet arrangements [145] (O3):PM machines with a full-scale power converter may be more attractive for direct-drive wind turbines [145]	(O1):8 (O2):9 (O3):9	(T1): high cost of PM: '' specific costs of Nd-Fe-B PM material is about 5 to 15 times higher than the specific cost of copper and laminated steel''[145] (T2): PMs cause a more difficult assembly – especially for large machines.	(T1):9 (T2):8
Total		S_{PMSG}=54		W_{PMSG}=19		O_{PMSG}=26		T_{PMSG}=17
TFPM	(S1): High torque density [145] (S2): direct-drive PM machines may be more attractive for large wind turbines [31]	(S1): 8 (S2): 10	(W1): Magnets may be come demagnetised (W2):seldom seen previously in wind turbine applications [9] (W3):Complicated geometry (W4):difficult to model-3D FEM (W5):Excitation cannot be controlled (W6):Corrosion of magnets	(W1): 4 (W2):8 (W3):9 (W4):5 (W5):7 (W6): 8	(O1): room for improvement (O2): fair amount of research carried out	(O1):8 (O2):8	(T1): high cost of PM: '' specific costs of Nd-Fe-B PM material is about 5 to 15 times higher than the specific cost of copper and laminated steel''[157] (T2): PMs cause a more difficult assembly – especially for large machines.	(T1):9 (T2):8
Total		S_{TFPM}=18		W_{TFPM}=28		O_{TFPM}=16		T_{TFPM}=10

Table 32: SWOT Table for Nessie Candidates

0 1 2 3 4 5 6 7 8 9 10

Unimportant Very important

B. Evaluation of SWOT results

Table 33 summarises the results from Table 32. The decision for the investigated machine types (SCIG, DFIG, EESG, PMSG, and TFPM) is presented.

The average decision for the machines is used in order to compare the candidates by inspection. The decision from the 2nd column in Table 33 is divided by the number of arguments. The desired direction for each SWOT element is indicated in the last column.

In order to mark a candidate as suitable, the strong point $S_{machine}$ must be MAXimum-that is to say that a certain value of a strong point counts more than the same value for an opportunity $O_{machine}$ (max). in the same manner, the weak point $W_{machine}$ must be MINimum-that is to say that a certain value of a weak point counts more than the same value for threat $T_{machine}$ (min); $S_{machine}$ and $W_{machine}$ represent certainties where $O_{machine}$ and $T_{machine}$ are probabilities.

	Decision on SCIG	**No of Arguments**	**AVG decision SCIG**	**Desired**
S_{SCIG}	29	4	7.3	MAX
W_{SCIG}	28	4	7.0	MIN
O_{SCIG}	28	3	9.3	max
T_{SCIG}	10	2	5.0	min
	decision on DFIG	No of Arguments	AVG decision DFIG	Desired
S_{DFIG}	27	3	9	MAX
W_{DFIG}	35	4	8.8	MIN
O_{DFIG}	0	0		max
T_{DFIG}	10	2	5	min
	decision on EESG	No of Arguments	AVG decision EESG	Desired
S_{EESG}	39	5	7.8	MAX
W_{EESG}	39	6	6.5	MIN
O_{EESG}	16	2	8	max
T_{EESG}	6	1	6	min
	decision on PMSG	No of Arguments	AVG decision PMSG	Desired
S_{PMSG}	54	6	9.0	MAX
W_{PMSG}	19	3	6.3	MIN
O_{PMSG}	26	3	8.7	max
T_{PMSG}	17	2	8.5	min
	decision on TFPM	No of Arguments	AVG decision TFPM	Desired
S_{TFPM}	18	2	9	MAX
W_{TFPM}	28	6	4.7	MIN
O_{TFPM}	16	2	8	max
T_{TFPM}	10	2	5	min

Table 33: SWOT Results

Table 34 shows the evaluation of the results. The cells containing the desired maximum values are coloured green. The desired minimum values are outlined using orange.

The machine types chosen to be suitable candidates for Nessie are EESG, PMSG, TFPM.

	S	W	O	T	Chosen
	MAX	MIN	max	min	
SCIG	7.3	7.0	9.3	5	
DFIG	9	8.8	0	5	
EESG	7.8	6.5	8	6	X
PMSG	9	6.3	8.7	8.5	X
TFPM	9	4.7	8	5	X

Table 34: SWOT Evaluation

Conclusions

A SWOT analysis was performed to decide which machine types are the most suitable for the Deep Wind application. It is considered a good idea to explore several different types of machine before deciding on the one you will consider in depth as the solution for the problem. Another aspect was to decide on the design tool modules that need to be created in order to cater for the given system.

The machine types chosen to be suitable candidates for Nessie are EESG, PMSG, TFPM. The sufficiency for developing the tool modules is to design for PMSG, TFPM. As a result of a SWOT analysis on which machine type is most suitable for Nessie, the following resulted as viable candidates: EESG, PMSG, TFPM.

In the present thesis, the TFPM is not detailed. Information about this machine integrated in the design tool may be found in [145], [158], [100], [29].

Appendix 6: Special Issues to be Considered

In this appendix, a set of issues that turned up during the current research, but were not studied in detail within this project are presented. The importance of each element is recognised and a starting point towards their investigation is set.

A. Mechanical structure discussion

Mechanical structural design represents the sizing of the connection between the generator and the turbine. A connection element as well as an enclosure (or box) for the machine needs to be provided. These elements crave attention in choosing the material and the geometry to satisfy the conditions set by the application. The material needs to withstand the salt water, to be light enough, to provide the necessary mechanical support and to have a good cost per utility ratio. The lifetime of the structure must be related to the lifetime of the overall blade generator system. See also [159]

Due to the large diameter of the direct drive generators-support spokes could be used to connect it to the turbine shaft. [160]

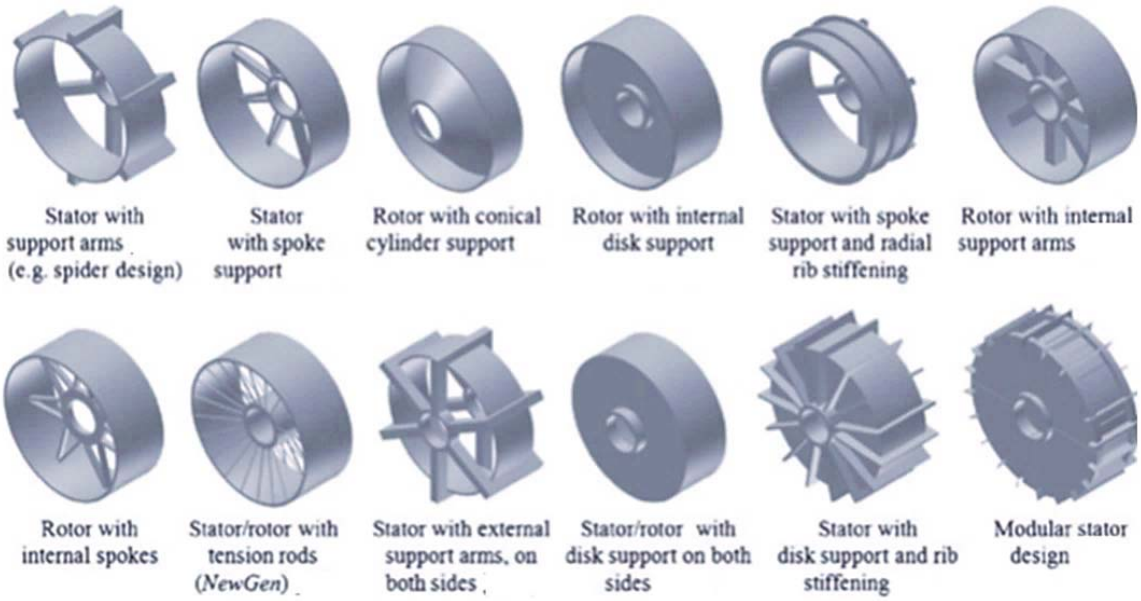

Figure 45: Inactive Structure Support Options For Rotor Or Stator Of The Generator.[7]

It is important to reduce the structural mass because

- This part does not actually produce energy
- Material is expensive to buy and manufacture
- Makes the generator system heavier

[7] and [161] propose magnetic bearings in combination with mechanical ones for the generator. The magnetic bearing increases the flexibility of the structure and of the overall system. The limits of this solution must however be thoroughly investigated.

Light substructures were proposed [162], [130], [163], [161],[164] structures in the literature.

- Ironless stators where there is no attraction between stator and rotor; not suitable for large diameters [165]
- Large diameter bearings-could become heavy and expensive for large diameter machines
- Use of light composite structural materials like grout in combination with metal sheets

At this stage, possible solutions for Nessie can be suggested. A rotor with internal support arms (spider-Figure 46 (a)) or a direct coupling of the turbine floater to the generator rotor (b).

Figure 46 (b) shows what the box would look like for the scenario where the floater is connected directly to the rotor. The mid grey inside part of the cylinder represents the generator.

The green parts represent the axial and radial bearings. It is also suggested that the box be made from special grout enclosed in plates of steel. This is needed because if the box walls would be made exclusively out of steel, it would be unnecessarily heavy.

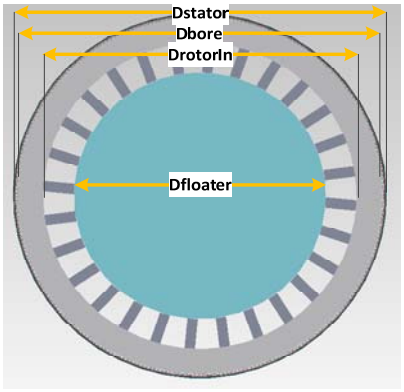

(a) Top View Of The Generator With Spider

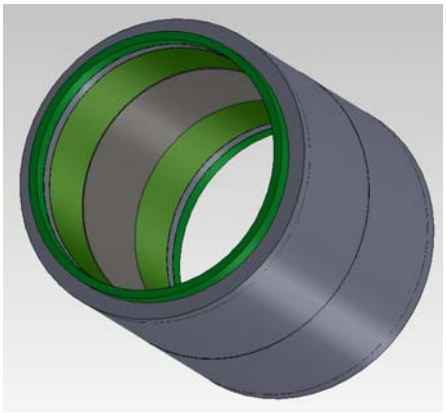

(b) ISO View Of The Generator Box-No Spider

Figure 46: Suggestions for Nessie Structural Elements

B. Cooling

In this section, the issue of generator cooling is presented. Methods available for approaching the Nessie cooling problem are discussed, but thorough investigations were left for future work

Due to losses, rotating electrical machines heat up while functioning. Dissipation of this heat by conduction and convection [129] must be ensured as an increase in temperature over the insulation class limit would speed up aging or even rapidly damage the machine.[166]

a. Cooling Methods

The types of cooling applicable to electrical machines are [18], [167], [168]

- Conduction
- Convection
  - Natural- influences (reduces) the rating of the machine. The cooler the machine is kept during functioning, the larger the design value for the current density (more current per copper crossection)
  - Forced cooling-fans and channels using cooling fluids.
- Radiation

  There are open and closed cooling systems (a closed circuit where the coolant is recirculated)

Cooling methods available for electrical machines are discussed in [169], [169], [170], [171], [172]

For large machines radial/axial ventilation channels are usually used. The disadvantage of this is that the machine gets larger to accommodate the channels. A multi inlet system is sometimes needed for large machines (for [MW] rating).

- By method

  -surface ventilation -open circuit ventilation -liquid cooled

For the 20 [MW] Nessie, the solution of having a water immersed generator is considered as a concept. This brings several questions of corrosion, fouling, lifetime and maintenance. For this solution, the sea water can be used as a coolant. To design the cooling system, a comprehensive analysis of the machine-environment interaction must be performed.

b. Thermal analysis

Before choosing the cooling method for Nessie, a thermal analysis should be carried out to define the appropriate cooling method in detail. The windings designed for a certain current density (see Appendix 9: Design Rules) produce heat that needs to be dissipated to keep the values required by the desired

insulation class (see next section for information on insulation classes). the cooling ability of the machine is lined to its geometry.

Analysis methods that can be employed to make a thermal analysis of the machine are [168]:

- Thermal network based on lumped parameters [166]; [173], [174]
- Analytical thermal-network analysis software (e.g. MotorCAD) [168], [166]
- Thermal analysis using FEM-monitoring of the temperature rise
- Air flow network –CFD (computerised fluid dynamics) [175]

c. Discussion

If a medium (gas or liquid) is used to cool the machine, the chemical structure of the coolant must not interfere with the integrity of the machine part e.g. corrosion and other damage to the insulation and active components to the machine must be handled.

The concept of water filled rotor [168], [176], [177] is considered for Nessie for the following reasons

- Anti-corrosion protection needed anyway because the exposure to salt in the sea environment is inevitable.
- The Sealing of the generator would involve a large surface as it can be seen in Figure 46. The shaft ((a) $D_{floater}$) would have a diameter of 3 m for the 6 [MW] design. The bearings (green (b)) would also have a large interior diameter to follow the shaft.
- If the generator would be sealed (air inside the generator box), a pressure equalizer would be needed to avoid ingress of salt water

The question to be further researched is whether sealing would be more difficult (in feasible, costly) then having a flooded generator.

C. Insulation Concept

In the following concept of insulation for Nessie is discussed. Issues like current, voltage, electrical and mechanical faults, temperature, wear and aging as well as corrosion are assessed.

At this stage of the work a complete (manufacturing state) design of a generator insulation is not available. A set of complex considerations that require additional investigation and work must be taken into account first. These issues are discussed in the following. An important factor to consider is the standardisation of the insulating materials and thicknesses to be used.

For the design tool calculation, the thickness of the insulation can be chosen by the designer.

a. General Description

The type of insulation chosen for the electrical machine may differ with respect to:

1) Thermal class of the designed machine

Table 35 shows the standard thermal classes for insulations of electrical machines. For Nessie, class H is chosen to allow for a high current density. The higher the current density, the better the copper is used. As a consequence the machine will become relatively smaller, providing the proper cooling for the windings is available. For the cooling, sea water that has an average temperature of 4 C will be used. A detailed design for the cooling system is required.

Thermal class	Symbol	Hot spot allowance/C	Allowed design temperature rise for $T_{ambient}$ = 40C	Allowed average winding T[C] determined by resistance measurement/C
90	Y	90		
105	A	105	60	
120	E	120	75	
130	B	130	80	120
155	F	155	100	140
180	H	180	125	165
200		200		
220		220		

Table 35 : Thermal Classes of Insulating Materials [178], [179], [180]

2) **Type of conductors used in the winding (wire or bar)-**
The cross section type of the conductor is set by the voltage planned for the coils to be insulated

a) -up to 3x690V :
   - o random wound machines-no specific placement of the conductors in the slot
   - o semi closed slots
   - o insulation along the slot lining
   - o enamelled round winding wire
   - o slot closure instead of wedges because there is no need for a complex mechanical structure to hold the conductors in place

b) for greater than 3x690V
   - o Pre formed coils
   - o Open slots
   - o Pre-insulated coils of rectangular section wire, wedged in place

Figure 47 shows the required insulation thickness of the winding in the slot as a function of the voltage.

In Figure 48 and Figure 49, slot insulation types are presented.

The primary insulation is used for the slot lining. The secondary insulation separates conductors belonging to different phases. The tertiary insulation is set on the conductor.

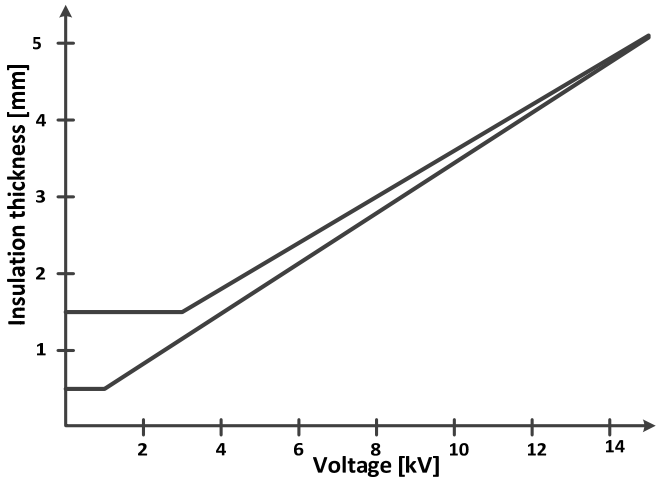

Figure 47: Insulation Thickness Of A Winding Inside The Slot [181]

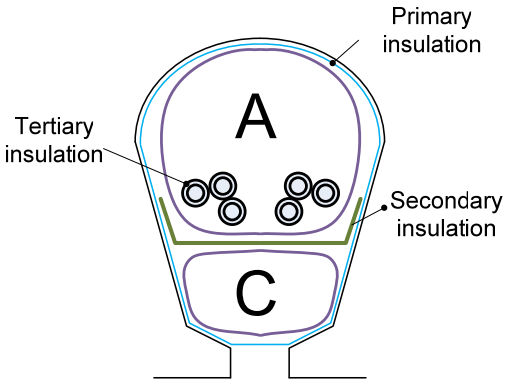

Figure 48: Insulation Random Wound, Round Bottom Slot Type

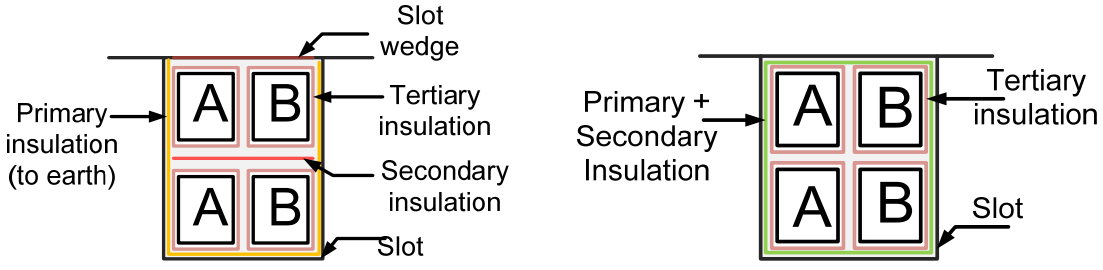

Figure 49: Insulation Pre Formed, Square Slot Type

b. Insulation Functions

The insulation for electrical machines ([30], [167], [179], [180]) must fulfil the following functions:

1. **Support the windings**

The Lorenz force (see Figure 50) acts violently on the end windings because there are no slot walls to hold the windings in place when a short circuit happens.

An aim is to move the mechanical resonant frequency range of the insulation system and winding construction to be outside the range of the electrodynamic forces. The most important frequency to avoid is the supply frequency. The direction of the forces is illustrated in Figure 50. [181]

The minimum thickness of the insulation is calculated to withstand the applied electric field strength, and is given by the ratio between the voltage over the insulation and the highest allowable field strength E_{max} in the material [18]:

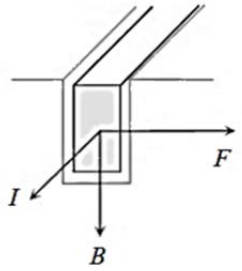

$$d = \frac{U_{onInsulation}}{E_{max}} \qquad \text{eq 1}$$

Figure 50:Lorenz force caused by the flux in the conductor in the slot on the periphery of the machine[18]

2. **Separation**

The insulation has to ensure galvanic separation between phases and between the winding and the iron core

3. **Waterproofing**

Protect from external conductive media that might create unwanted current paths.

c. Insulation Materials

Materials typically used for Nessie type machines for the different temperature classes are shown in Table 36:

Class	Materials
Y (90C)	paper, cotton, silk, natural rubber, polyvinyl chloride, etc. ; no impregnation
A(105C)	as class Y with impregnation, nylon
E(120C)	Polythylene terephthalate (terylene fibre, melinex film), cellulose triacetate polyurethanes, polyvinyl acetate enamel
B(130C)	Mica, fibreglass (alkali free alumino borosilicate), bitumenized asbestos,bakelite, polyester enamel
F(155C)	as class B but with alkyd and epoxy based resins
H(180C)	As class B with silicone resin binder, silicone rubber, aromatic polyamide(nomex paper and fibre), polyamide film (enamel, varnish and film) and polyesteramide – imide enamel
C(over 180C)	As class B but with suitable non-organic binders; Teflon (polytetraflouroethylene).

Table 36 : Insulation Materials Used For Different Temperature Classes [18]

Table 37 shows what insulation material is used for different parts of the machine with respect to the temperature class.

<table>
<tr><th colspan="2" rowspan="2">Component</th><th colspan="3">Low voltage machines</th><th colspan="2">High voltage machines</th></tr>
<tr><th>Class E</th><th>Class B</th><th>Class F</th><th>Class B</th><th>Class F</th></tr>
<tr><td colspan="2">Turn-to-turn insulation</td><td>Polyvinyl acetal for both wire & strip conductors</td><td>Polyester enamel (wire)/or phenolic bonded fibreglass (strip)</td><td>Estermide enamel (wire)/ alkyd bonded fibreglass (strip)</td><td>Phenolic bonded fibreglass (strip)</td><td>Alkyd bonded fibreglass (strip)</td></tr>
<tr><td rowspan="3">Coil-to coil and phase-to-phase insulation</td><td>Inside the slots</td><td colspan="2">Bakelized fabric strips</td><td>Epoxy fibreglass strips</td><td>Shellac or bitumen bonded mica foil/ tape on straight portions of the coils</td><td>Epoxy impregnated mica paper foil/ tape on straight portions of the coil</td></tr>
<tr><td>On overhangs</td><td rowspan="2">Melinex film bonded to press paper</td><td>Alkyd bonded mica glass sheet</td><td rowspan="2">Nomex sheet</td><td>Alkyd varnished glass tape on coil ends & alkyd bonded mica sheet between layers</td><td>Epoxy varnished glass tape on coil ends & alkyd bonded mica glass sheet between layers</td></tr>
<tr><td colspan="2">Phase/ coil to earth insulation</td><td>Mica alkyd bonded to glass cloth</td><td colspan="2">No extra insulation :phase-to-phase insulation itself is sufficient</td></tr>
<tr><td colspan="2">Slot closure (wedge)</td><td colspan="2">Bakelized fabric strips</td><td>Epoxy fibreglass strips</td><td>Bakelized fabric strips</td><td>Epoxy fibreglass strips</td></tr>
<tr><td colspan="2">Insulation for leads</td><td colspan="3">Alkyd varnished terylene or glass tape or sleeving</td><td colspan="2">Alkyd varnished glass tape</td></tr>
<tr><td colspan="2">Varnish for impregnation treatment</td><td colspan="2">Alkyd phenolic</td><td>Estermide or epoxy</td><td>Alkyd phenolic</td><td>Epoxy</td></tr>
</table>

Table 37: Insulation Materials for Electrical Machines [182]

For class H, the class chosen for Nessie, a set of materials are given in insulation catalogues from Essex Group Inc. for example. Choosing of the insulation material is left for future work as a consequence of manufacturing strategy.

D. Vibrations

The radial attraction forces between the stator and the rotor manifest themselves in the air-gap for fractional slot windings. In the design stage of the winding, the sub harmonics that create these vibrations must be avoided. These harmonics cause force waves that have a longer wavelength than that of the pole.

The forces can be estimated by integrating the force density over the surface of each tooth at given positions. The shape of the attraction force wave is related to the number of poles of the machine [182], [20].

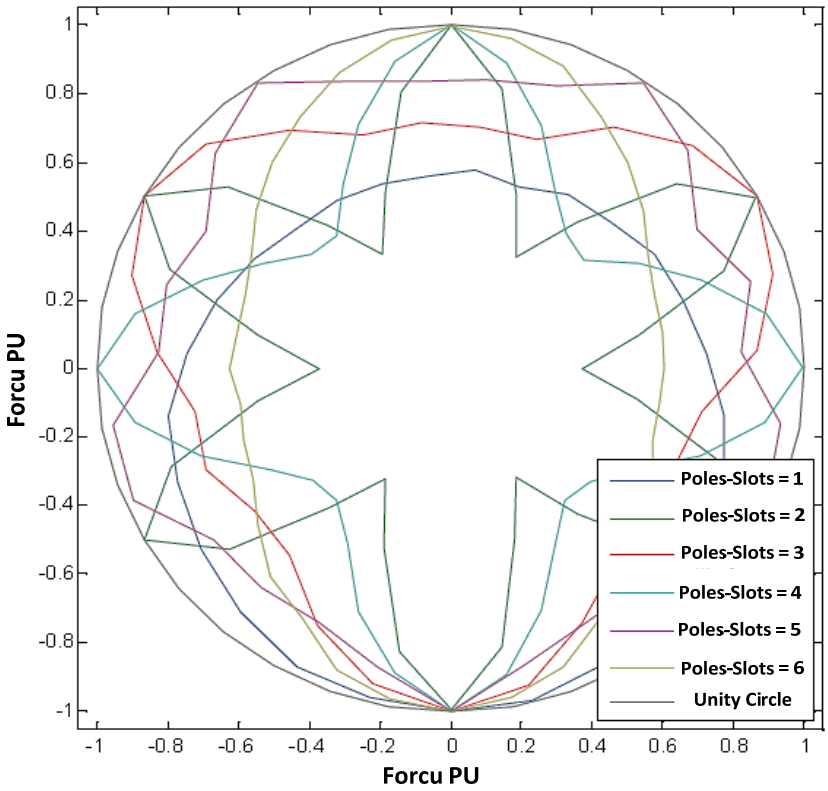

Figure 51: Normalised Force Distribution [183]

The fundamental wave length of the force is:

$$Force_{waveLength} = \frac{2\pi}{|Poles - Slots|}\,[rads] \qquad \text{eq 2}$$

The forces must be symmetrical; otherwise the machine will behave as if a mechanical unbalance existed resulting in vibrations. These vibrations must not resonate with the natural frequency of the mechanical structure. Because in variable speed drives, the vibration forces vary over a relatively wide range, the frequency spectra and resonance points must be investigated.

From FEM, an example for the 6 MW 300 slots 314 poles Classic RF Nessie type machines (Chapter 3) the force distribution is shown Figure 52: 270 A - rotor angle = 0 Radial Force Distribution due to Magnets and Full Load Current. On the y axis, the $HDB = \int HdB$ multiplied by the useful length of the machine.

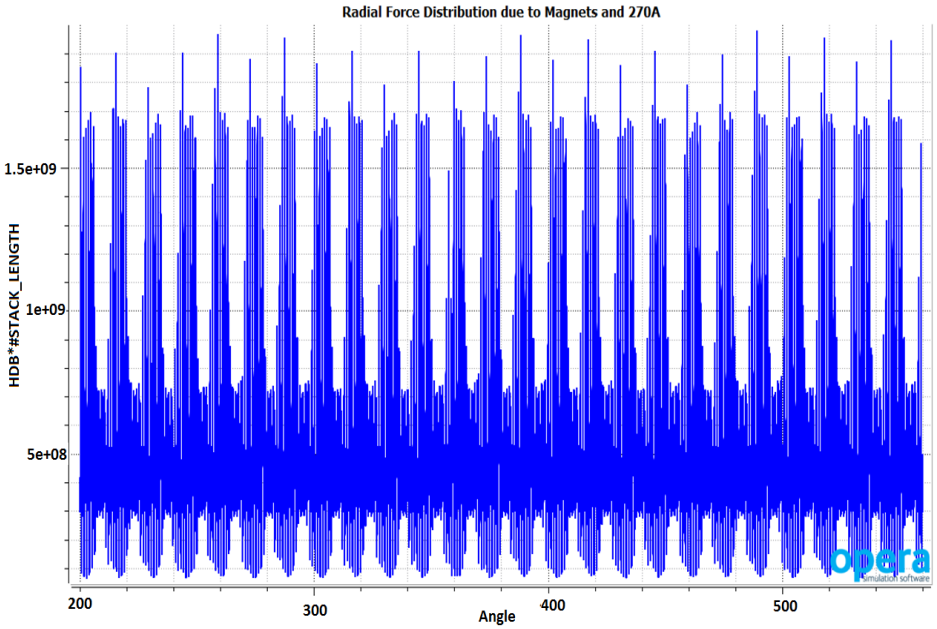

Figure 52: 270 A - rotor angle = 0 Radial Force Distribution due to Magnets and Full Load Current.

In this case there is a mixture of several harmonics with overall amplitude of 2000 MN.

Figure 53 shows the same relationship for the expected short circuit current.

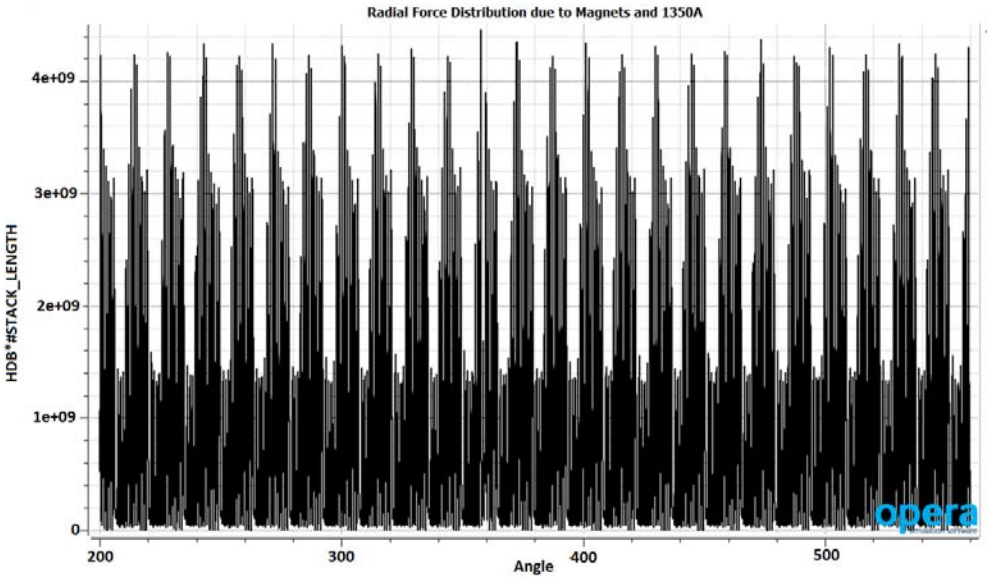

Figure 53: 1350 A - rotor angle = 0 Radial Force Distribution due to Magnets and Short Circuit Current.

The overall amplitude is 2000 MN. The Torque is **Torque = 7.832e6 x Stack Length=32.44 MNm**

C. Cogging

Cogging is the phenomenon that occurs when the permanent magnet attracts the tooth preventing the rotor to go around. It is also referred to as the no load torque. [20] [122]

A general analytic formula for calculating the cogging torque is [18]:

$$T_{Cogging} = \frac{1}{2} Flux_{Gap}^2 \frac{dReluctance_{Gap}}{dAngle_{Rotor}} \qquad \text{eq 3}$$

This phenomenon is unwanted for Nessie generators. There are several ways of diminishing or even eliminating this effect [122], [184]:

1. Insulated and non-insulated magnetic wedges and non-magnetic wedges. [185]
2. Skewing of stator slots
3. Skewing of PM on the rotor [186]
4. Adjusting the length of the arc of the PM
5. Varying the PM arc length in pairs
6. Varying the cross-section of the PM
7. Flattening of the PM where they connect to the core
8. Adjusting the slot mouth
9. Extra slots in the stator core
10. Magnetic cores between PM
11. Radial magnetisation of PM
12. Non-symmetric slot walls

E. Corrosion and fouling

Offshore wind turbines experience corrosion from the sea water and fouling where animals and plants adhere to the turbine surfaces. These must be prevented as they produce significant damage throughout the lifetime of the generator system. PM material is subject to corrosion [187], but not all magnet types suffer the same damage. Corrosion greatly affects Neodymium magnets; samarium-cobalt might be considered; ferrites (investigation needed) [147] .

Anti-corrosion protection solutions are available for the different materials involved in the construction of the system [178], [188], [189], [190], [191]. Protection of PM to avoid disintegration has been documented [192][193] .

A flooded generator would introduce additional problems so before deciding on this solution, the advantages and disadvantages must be carefully weighed [194].

For ethical and legal reasons, care must be taken that the coating materials used for protection are non-polluting.

F. Grid connection requirements

Wind generators, when integrated in the distribution system, they must be controlled to behave according to a set of rules called grid codes. These are particular to the region or country where the generator system is placed.

The grid codes discuss requirements regarding [191], [11], [17]:

- Active and reactive power control;
- Voltage and frequency control;
- Power quality, for example, flicker and harmonics;
- Fault ride-through capability: specifications on how the generator should behave during and after a fault has occurred;
- Rules are specific for each region/country, so the generator together with the control system must be designed to cope with local specifications;
- The rules can change in time due to several energy management and market factors and the system needs to comply with the new rules for an adequate integration in the supply and distribution grid.

Conclusions

This section presented important issues to be considered when designing the generator system that were not addressed in detail in the present thesis. In the view of continuing research on the Nessie generator subject, starting points have been set by listing and briefly discussing these issues.

Appendix 7: GUI Guide

In the following, an overview of the GUI (Graphical User Interphase) environment is given. Interfaces to the different calculation parts of the tool are presented. Familiarisation with the design tool GUI is important as the users and most of the time the developers of the program use this to initialise and run the programs behind it in a quicker and more intuitive way.

The GUI is a feature in MATLAB that allows masking of code using interfacing elements such as buttons and text boxes. The user of the program deals with an interactive panel that is more intuitive then dealing directly with code lines.

The purpose of the GUI is to provide the following features:

- Hide the raw code from the user. This is useful when the user is inexperienced or just wants to run the code without editing it.
- Intuitive interface – little knowledge of the program structure needed to generate a design.
- Shortcuts to features that would take more time to access in the original way e.g open documentation folder, list of variables and symbols. –a set of accessing options-access any program by writing the name in a box (rudimentary search option-no word suggestion for now. this feature is destined mostly for the developer).
- Give the user the ability to modify a set of significant and important inputs (e.g. windings connection – star or delta, the position of PM related to the iron core-buried or surface mounted, the convexity of the rotor that indicates an interior or an exterior rotor). Some quantities are chosen behind the GUI at this stage e.g. educated initial estimations (seed values) of design values.
- Decide on the values of design rules and quantities (see Appendix 9: Design Rules)
- Most values are kept between certain limits to eliminate the use of invalid values or those for which the design code has not been tested.
- -Viewing of log files and files destined for other software-e.g CAD, FEM, Simulink initialisers

The main GUI is presented in Figure 54. With this, the design process can be started.

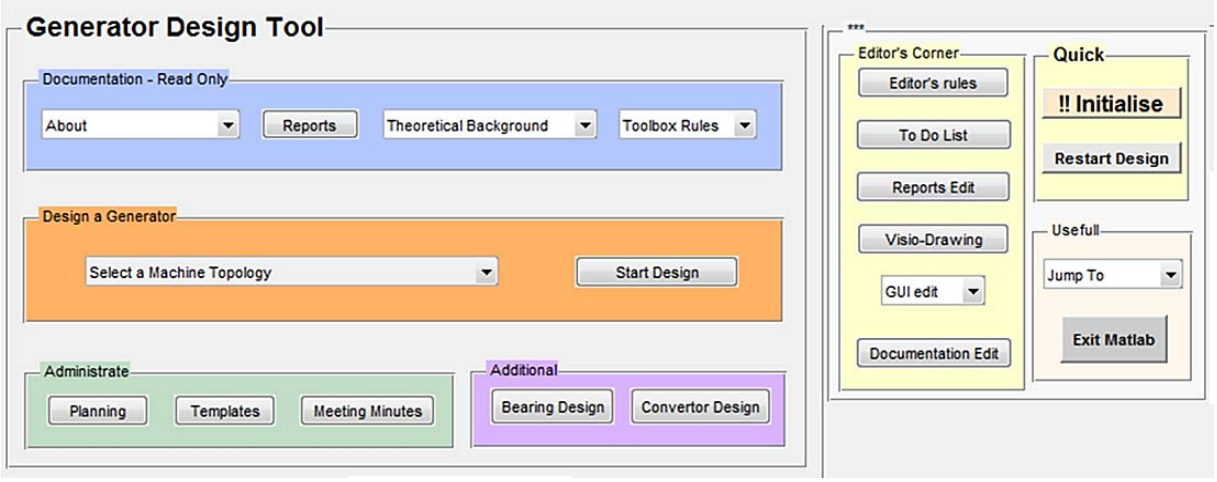

Figure 54: Main GUI

The steps of a design process are as follows (Figure 55)

1. Choose the type of machine to calculate
2. Decide on the input data – safety limits are set to ensure the validity of inputs
3. Display first analytical design
4. Update the geometry in CAD-*optional*
5. Optimise -*optional*
6. Reiterate analytically-*optional*
7. Reassess
8. Recalculate
9. Display final results

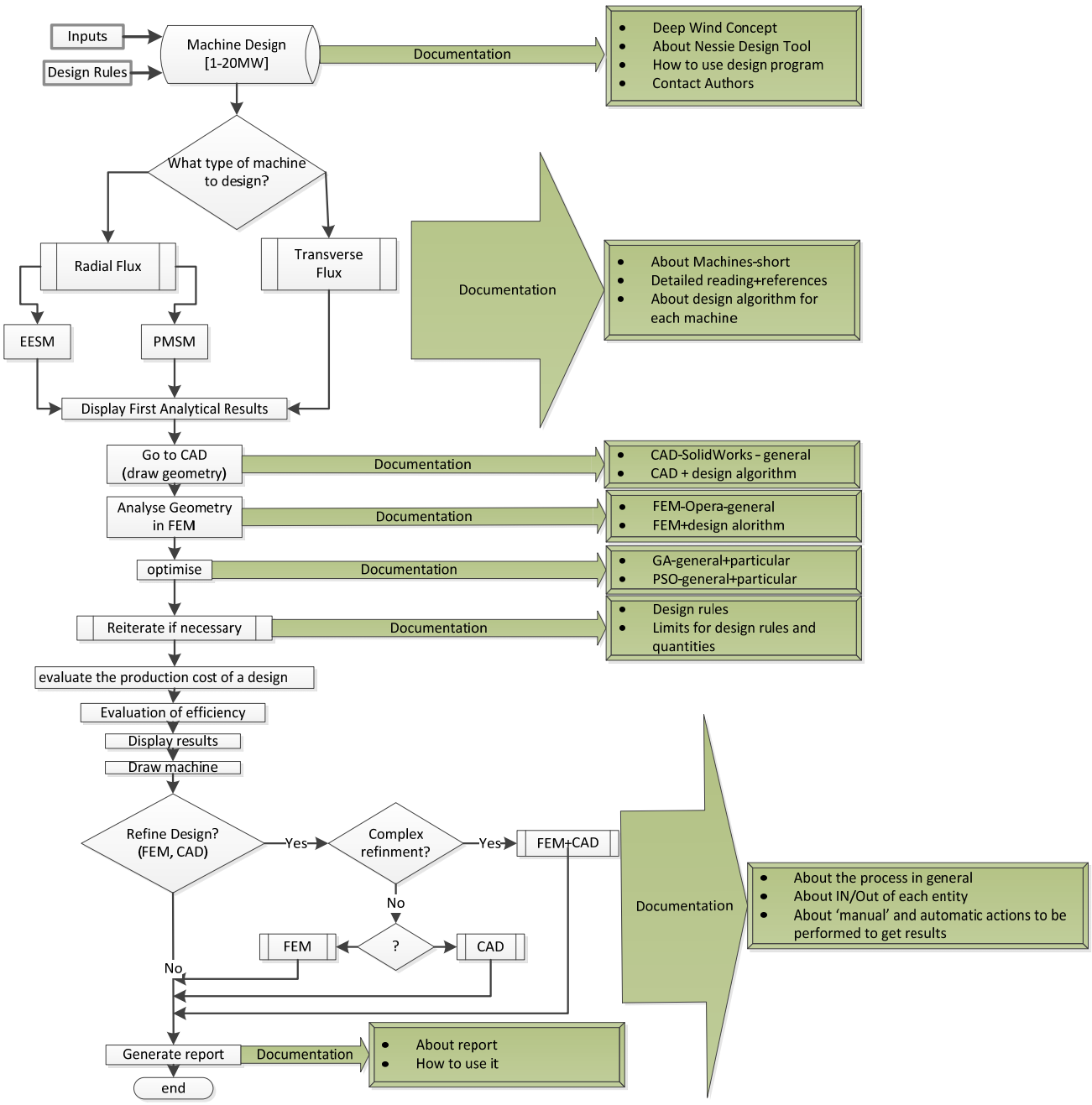

Figure 55: Deep Wind Design Tool- A Modular Approach

The diagram from Figure 55 may be followed until an acceptable design result is obtained
The adopted structure of the GUI for each machine is shown in Figure 56

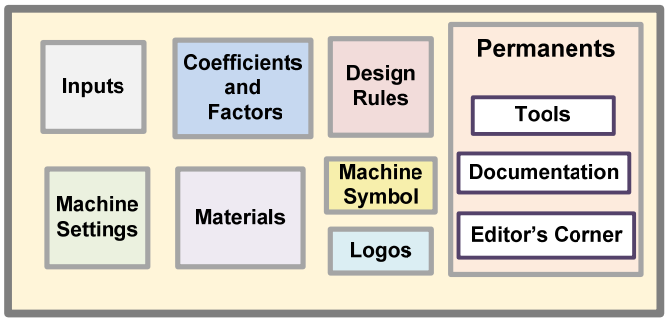

Figure 56: General Machine GUI

The sets of information generally relevant for each machine are shown.

Figure 57 depicts the interface for calculating the radial flux PM machine. Links to the optimisation module and FEM and CAD analysers are included.

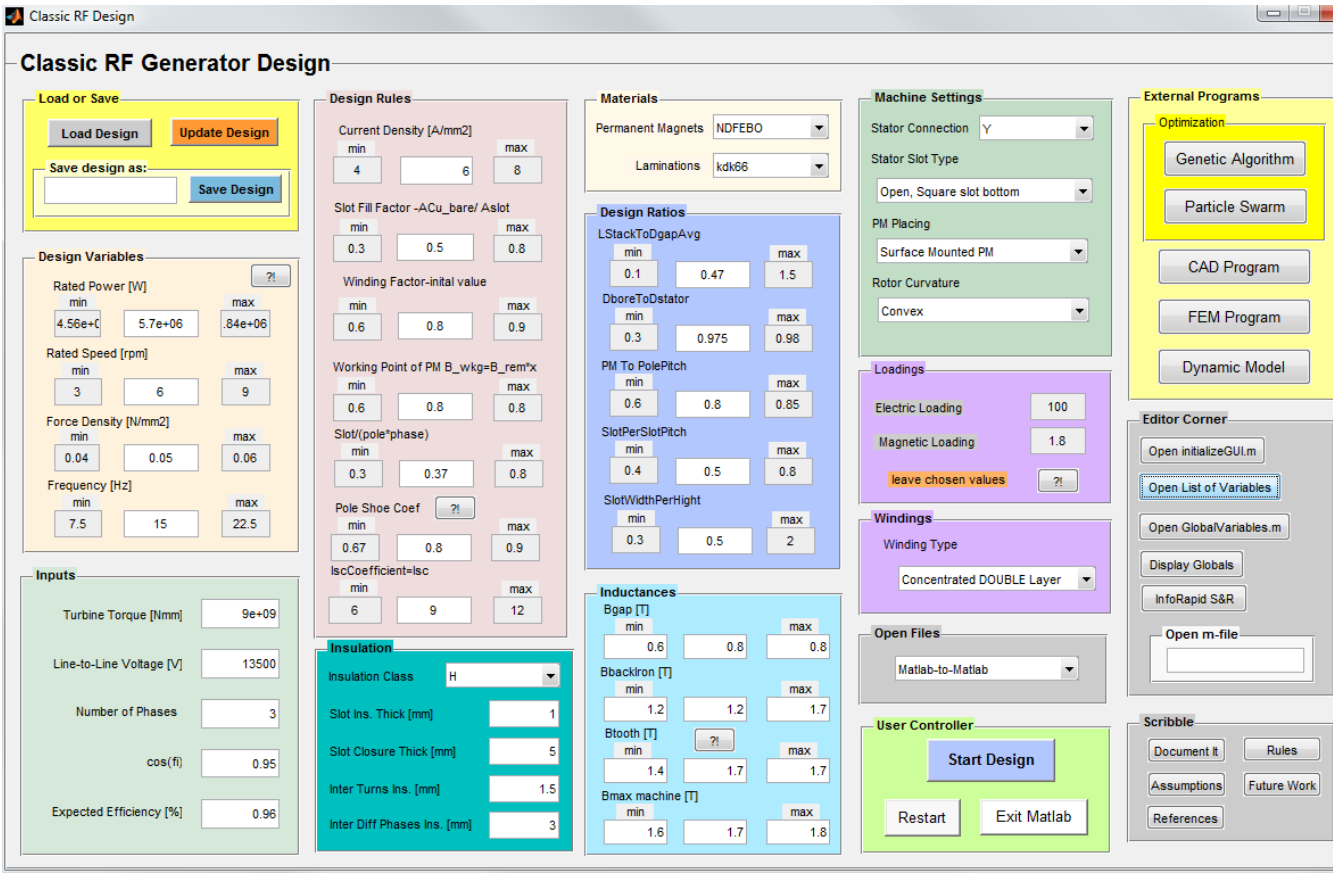

Figure 57: Classic RF Generator GUI

Because the weights of the active materials are calculated by using a feature in the CAD model, the estimated price needs to be manually calculated. Figure 58 shows the GUI that can be used for this purpose.

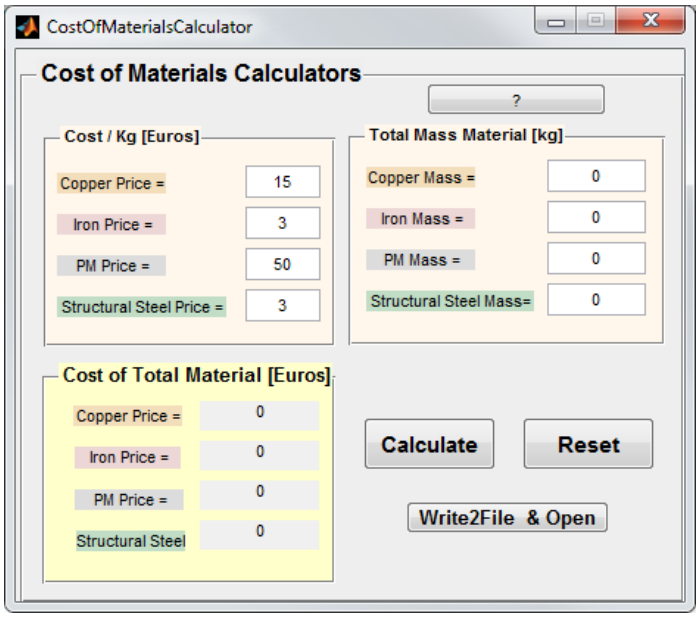

Figure 58: Cost GUI

After the first set of calculation is obtained, the user can optimise this design. Interfaces for the two available algorithms are shown in Figure 59 and Figure 60. More information about the settings can be found in Appendix 12: Optimisation Tools

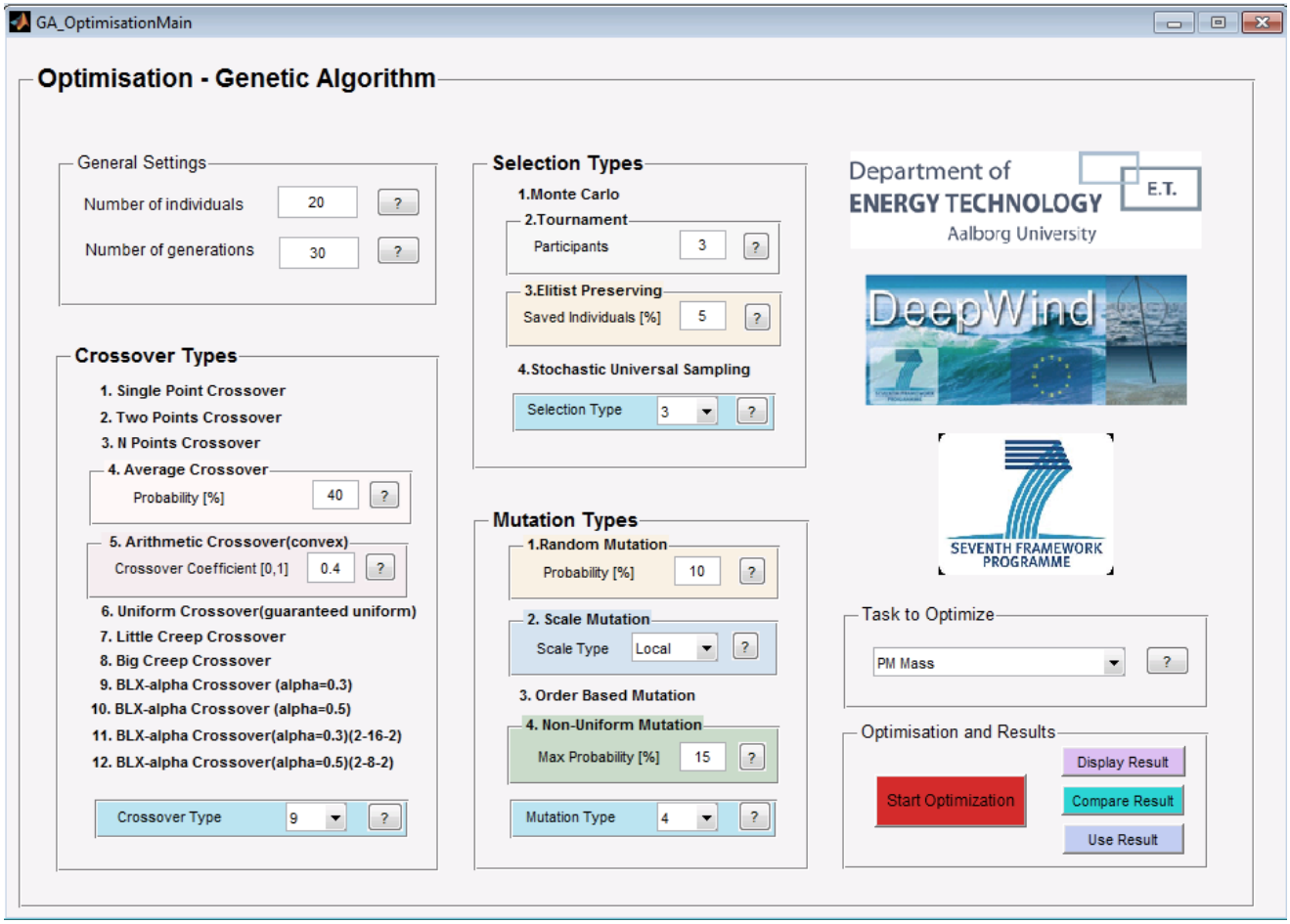

Figure 59: Genetic Algorithm GUI

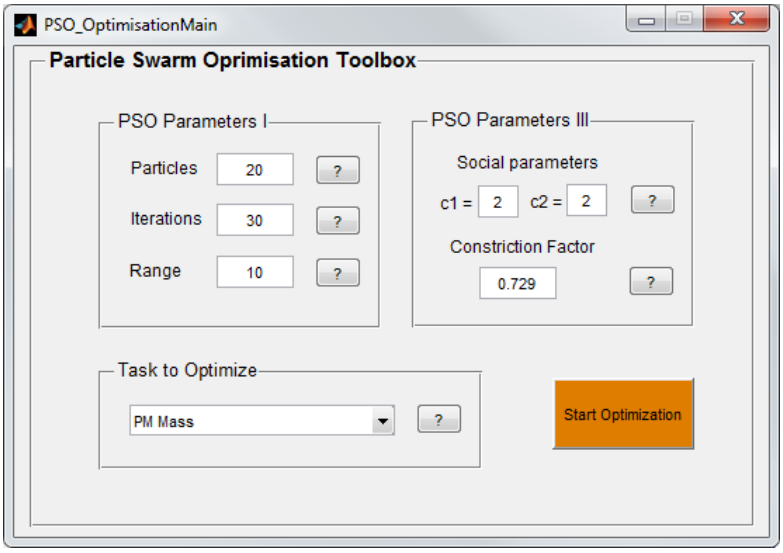

Figure 60: Particle Swarm Optimisation GUI

Appendix 8: Design Tool Algorithm and Equations

This appendix presents calculation steps and equations used to design various aspects of the electrical machine. The formulae used in the different modules are shown for the sake of calculation transparency; the elements of the equations are intentionally not symbols. As much as possible, the names of the code variables were used. In this way there is no need for an additional list of symbols as the long names of the elements are self-explanatory. For the coding these notations help with understanding the calculation at any point of viewing/browsing.

Background

As a result of the SWOT analysis (see Appendix 5) on which machine type is most suitable for Nessie, the resulting viable candidates were: EESG, PMSG, TFPM. In the following, calculation modules for the radial flux PMSG are presented. With the functions from this machine and some modifications, the EESG can also be calculated.

The following issues are to be considered when developing the calculation tool:

Specifications

It is very important to be aware of what the is desired from the machine to be designed:

- **Customer requirements** determine the type, shape and materials used in the machine. Values like the voltage and frequency determine features like the insulation that must be used for the winding and consequently the slot type. In the Nessie case, the extremely slow shaft speed from the turbine, coupled with the fairly large power requires a very high torque.
- **Standards compliance** is mandatory for equipment sold on the market. The standards may differ from the production place to where the product is to be used. For Europe and other places in the world IEC standards apply (e.g. electrical machine performance standard is IEC60034)[14]

The following inputs are considered

Inputs from adjacent systems

a) Type of machine
b) Input shaft power-mechanical power
c) Speed from the turbine
d) Line to line voltage-rated voltage RMS
e) Number of phases
f) Insulation thickness
g) Frequency
h) Cos fi –power factor of the load (related to the consumers/loads)

Inputs from the machine designer:

a) Geometrical/constructional specifications like slot shape, winding type
b) Choice of the materials
c) Insulation class
d) values for the design rules
e) Initial estimations, educated approximations

Dimensioning

The aim of the calculations is to predict the:

- **Parameters of the machine**: geometrical and electrical ; dynamic simulation parameters for models integrated in larger systems;
- **Expected Performance** : losses, temperature rise , comparison between desired and obtained quantities(e.g. power);
- **Material usage**-mass , volumes.

- **Estimated Cost;**
- **Other aspects** that the client defines as being of importance for a particular analysis. In this case, alteration of the output formats (e.g. print a certain quantity in an evaluation table) or additional modules might need developing (additional calculations and display functions adjustment).

Constraints

Constraints are imposed by different factors. One of these is material properties. Some materials cease to have a linear response to the imposed stress.

For example, magnetic materials saturate, metals lose their strength and insulation materials cease to insulate. The design algorithm needs to provide variables for these constraints that steer the calculations towards the correct values. An example of such a variable is the maximum induction in the tooth. The calculations will never give values exceeding this limit for this quantity.

Design approach

As a design example, the RF benchmark machine (see Chapter 3: 6 [MW] Candidates) type was targeted.

The first step is to **decide on the input values**. Calculation values like constants, transformation units and values for materials are loaded.

The next step is to **estimate main dimensions** to be used as seed values for future calculations. Some values like the machine diameters are recalculated as several aspects are considered during the design process. For the diameters, one factor that changes the values is the winding that need to be fitted in a slot and between teeth that have to have a certain thickness to allow the main flux to pass.

There are several approaches to start the design. The most appropriate method for the concept of a general design tool must be identified. In the following, design approaches are discussed:

1) What is the field needed to obtain the voltage to be generated

At a principle level, from Ampere's circuit law eq 4, the needed number of turns and the value of the current can be decided

$$H_m l_m + H_g gap_{length} = -turns \cdot I = MagnetoMotiveForce \quad \text{eq 4}$$

Where

H_m=magnetic field intensity in the magnetic path
H_g= magnetic field intensity in the air-gap
l_m=mean length of the magnetic circuit
I=current

The induced voltage (eq 5: EMF-to be discussed later in this chapter) is produced by the rate of change of a field going to a coil having a certain number of turns.

$$EMF = \frac{d(turns \cdot Flux)}{dt} \quad \text{eq 5}$$

Where the flux is (eq 6)

$$Flux = FluxDensity \cdot Area \quad \text{eq 6}$$

The $\frac{d}{dt}$ represents the electrical speed -eq 7

$$\frac{d}{dt} = \omega_{el} = \omega_{mec} \cdot PolePairs \quad \text{eq 7}$$

For a low speed, a large number of poles are needed (eq 7) to get the desired $\frac{d}{dt}$. This keeps the Flux density and the number of turns at an acceptable practical level.

This approach requires knowledge about the final magnetic circuit. To base the calculation on a set of guessed values is considered a risk for the fast and correct convergence of the design algorithm towards a valid output.

2) **Fix the losses, and then calculate the machine that would give those losses** [195]. This approach is considered too far away from the concept of a modular design tool because it does not allow easy access to certain quantities involved in design rules like diameters and PM working point determinators. The considered set of design rules can be found in Appendix 9.

3) **Decide on B_{gap} and try to produce that with the stator and the rotor**. Calculate the machine and check if the required field is obtained (Figure 61).

The coils are sized to produce the desired flux density in the airgap (B_{gap}). The PMs are also designed so that they would manage to transmit the desired flux density across the airgap. After both the PM and the windings are designed, the PMs are checked against the current that might demagnetise them. This current is not the load current, but the expected short circuit current that would flow in the machine. This is considered a safe approach, but with a more detailed investigation of a certain design, the demagnetising current might be estimated from the expected transient currents and a safety margin coefficient.

This machine design philosophy is considered suitable for the design tool because it can be used for calculating any machine type. From a coding point of view, one cannot calculate a formula if the values for the components are unknown. Any assumption will have to be followed by a recalculation. The goal is to avoid a large number of reiterations using uncertain assumptions.

The idea is to fix the goal field for the stator and the rotor and considering the expected losses, try to build the magnetic circuits accordingly. After the stator and rotor are designed-the geometrical and electromagnetic quantities are calculated-the interaction between the two (the EMF Electro Motive Force) is checked for compliance with the required input values. If needed, adjustments are made.

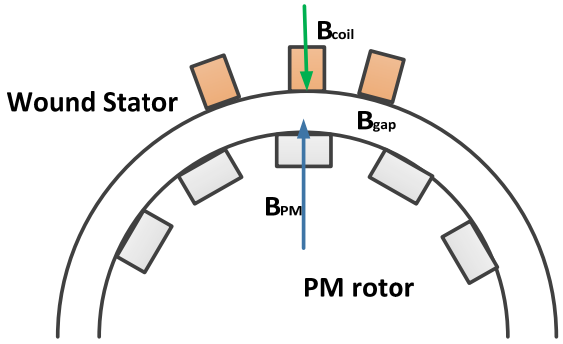

Figure 61: Magnetic Design Concept

This method is considered most suitable for the Nessie Design Tool as it required knowledge of a minimum number of machine elements. The number of reiterations and empirical estimations required can be kept low within the machine sizing algorithm.

The following, general equations for quantities calculated within method 3 are presented. The strategy behind each design element is explained.

Sizing and Calculations

a. General equations

The **bore diameter** is estimated by eq 8 as the required minimum diameter of the air-gap that is needed to produce a reciprocal electromagnetic torque to balance the mechanical torque of the turbine [22], [8]. The approximation/simplification that was made for D_{bore}=D_{gap} for the sake of simplicity: for an inside rotor the bore diameter is the inside diameter of the stator, for an outside rotor machine, the bore diameter is the inside diameter of the rotor. The difference between D_{bore} and D_{gap} is small anyway compared with the overall machine diameter, so the simplification can be used in further calculations

Dbore [mm] is defined as:

- Outside stator-Diameter of the hole of the inside of the stator
- Inside stator-outer diameter of the stator

$$D_{bore} = \sqrt[3]{\frac{2 \cdot T_{turbine} \cdot 10^3}{\pi \cdot L_{StackToDgapAvg} \cdot Force_{density}}} [mm] \quad \text{eq 8}$$

In the design algorithm for Nessie, a simpler formula was used to find the bore diameter as a first estimation [196] (eq 9). It is important for that the values for first estimations do not involved unknown values like slot dimensions or machine length because these would have to also be estimated.

$$D_{bore} = 1000 \cdot gap_{length} [mm] \quad \text{eq 9}$$

Later on, as the windings are designed, the diameter is recalculated to accommodate these. By using eq 9 in the design tool, the difference between the first estimation and the final value of the bore diameter was proven to be very small. It is very important to make good first approximations because otherwise, the error introduced in calculating related quantities would make the design algorithm unstable.

The definition of the **air-gap length** is the space between the stator and the rotor –see Figure 62

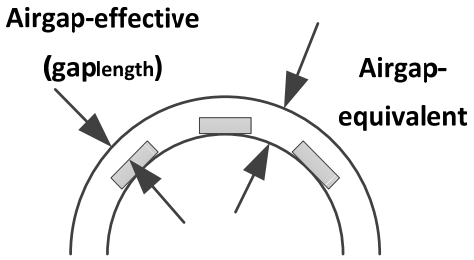

Figure 62. Lengths of the Airgap

The effective **air-gap length** is set by the mechanical clearance needed to fit the stator together with the rotor. From the design rules in Appendix 9, by using the FEM model of the machine, an empirical value for choosing the air-gap length was chosen eq 10, where the mechanical power is given in [MW]:

$$gap_{length} = \frac{P_{mec}}{10^6} [mm] \quad \text{eq 10}$$

The **equivalent air-gap** is estimated as (eq 11):

$$gap_{length_{equivalent}} = 2 \cdot gap_{length} [mm] \quad \text{eq 11}$$

As the windings and the PM are calculated, these might result in a change of the gap diameter. Only changes that increase the bore diameter are permitted by the program. The value of the machine bore diameter is not allowed to decrease under the estimated value (eq 8) because not enough EMF would get generated.

The **induction in the air-gap** is estimated from the working point of the PM B_{wkg} as eq 12

$$B_{gap} = PM2PolePitch \cdot B_{wkg} \quad \text{eq 12}$$

From the bore diameter and with Diameter/Length ratio, the core length of the machine is found as a first estimation (eq 13 and eq 14):

$$L_{overallCore} = L_{StackToDgapAvg} \cdot D_{bore}[mm] \quad \text{eq 13}$$

$$L_{usefull} = L_{overallCore} \cdot stackingFactor\ [mm] \quad \text{eq 14}$$

The stackingFactor takes account of how tight the lamination sheets can be stacked together. The value for this is given by the manufacturer of the laminations and ensured by the manufacturing process

As a recalculation, to get the desired EMF, from checking and observing the outputs of the design program, the useful **length of the machine** becomes eq 15 with eq 16:

$$Lusefull = 4 \cdot LusefullEstimate\ [mm] \quad \text{eq 15}$$

$$LusefullEstimate = \frac{4 \cdot \mu_0 \cdot T_{turbine}}{B_{gap_{avg}}^2 \cdot D_{gap_{avg}}^2 \cdot \pi}[mm] \quad \text{eq 16}$$

The number of **pole pairs** is calculated in eq 17 as a function of the frequency f that is chosen by the designer of the machine with regards to the converter that is used to control the generator and the rotational speed of the shaft n_{rpm}.

$$PolePairs = round\left(60 \cdot \frac{f}{n_{rpm}}\right) \quad \text{eq 17}$$

The number of **poles** is (eq 18):

$$poles = 2 \cdot PolePairs \quad \text{eq 18}$$

The **pole pitch** (marked in green in Figure 63) is the distance between the centre of one pole and the next and can be calculated using eq 19

$$PolePitch = \pi \frac{Diameter}{poles} \quad \text{eq 19}$$

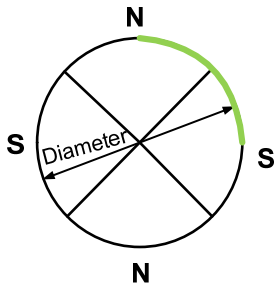

Figure 63: Pole Pitch

The number of **slots** (eq 20):

$$Q_s = SlotPolePhase \cdot poles \cdot phases \quad \text{eq 20}$$

After selecting the materials and the main dimensions, the magnetic circuit is defined and together with the dimensions, the **flux per pole** should be calculated.

The flux density in the various iron parts must be determined later on. The current in the windings will change the first estimations, so the flux must be recalculated. At this stage, the flux will be determined by the permanent magnets alone (or by the magnetising current if excitation is made by windings).(eq 21)

$$FluxPerPole = B_{wkg} \cdot S_{PM@gap}\ \ [Wb] \quad \text{eq 21}$$

The **rated torque** is (eq 22)

$$T_n = \frac{P_n}{n_{radPerSecond_{rated}}} = \frac{P_n}{\frac{2 \cdot \pi \cdot n_{rpm_{rated}}}{60}} = \frac{30 \cdot P_n}{\pi \cdot n_{rpm_{rated}}}[N] \quad \text{eq 22}$$

The expected current is (eq 23); where P_{outEl} is the rated mechanical power:

$$I_{outEl} = \frac{P_{outEl}}{\sqrt{3}\, V_{out_{rated}} cos(\varphi)}[A] \quad \text{eq 23}$$

Rated power-electrical output power

$$P_{outEl} = P_{mec} \cdot efficiency_{Expected}[\text{W}] \quad \text{eq 24}$$

b. Flux Calculations

The **flux per pole** [29] can also be calculated with eq 25:

$$FluxPerPole = PolePitch \cdot L_{usefull} \cdot B_{maxGap} \quad \text{eq 25}$$

The pole pitch calculated with eq 19.

Flux per tooth -eq 26 [18], [18] (B_{tooth} is the flux density per tooth)

$$FluxPerTooth = A_{ToothAtGap} \cdot B_{tooth} \quad \text{eq 26}$$

Where the area of the tooth at the gap is calculated considering the width of the tooth and the useful length of the core-eq 27

$$A_{toothAtGap} = w_{StatorToothTotal} \cdot L_{usefull} \quad \text{eq 27}$$

The total **Flux Linkage** per phase can in principle be calculated with eq 28[150], [197]

$$FluxLinkagePhase = turnsInSeriesPerPhase \cdot windingFactor \cdot FluxPerPole \quad \text{eq 28}$$

The flux linkage per pole is eq 29[198], [197]

$$FluxLinkagePerPole = \frac{turnsInSeriesPerPhase \cdot windingFactor}{Poles} \cdot FluxPerPole \quad \text{eq 29}$$

To determine the leakage flux crossing a parallel sided slot, this is divided into several zones because the conditions change for every section. [198], [198]

Zone 1: leakage flux across slot opening/unit length of machine

$$fluxSlotMouth = mmf_{TotalSlot} \cdot \mu_0 \cdot \frac{hSlotMouth}{wSlotMouth} \quad \text{eq 30}$$

where μ_0 is the permeability of vacuum and the total magneto motive force in a slot is calculated using eq 31

$$mmfTotalSlot = noOfConductorsInSlot \cdot IperConductor \quad \text{eq 31}$$

$$fluxLinkageSlotMouth = fluxSlotMouth \cdot noOfConductorsInSlot \quad \text{eq 32}$$

Zone 2- leakage flux across slot wedge

The leakage flux across the slot wedge eq 33

$$fluxSlotWedge = mmfTotalSlot1 \cdot \mu_0 \cdot \frac{hSlotWedge}{wSlotWedge} \quad \text{eq 33}$$

The leakage flux linkage /unit length of machine-eq 34

$$fluxLinkageSlotWedge = fluxSlotWedge \cdot noOfConductorsInSlot \quad \text{eq 34}$$

Zone3- leakage flux across wound section

$$fluxWound = mmfTotalSlot \cdot \mu_0 \cdot \frac{hSlotWound}{3 \cdot wSlotWound} \quad \text{eq 35}$$

Leakage flux linkage of the wound part of the slot /unit length of machine (eq 36)

$$FluxLinkageWound = noOfConductorsInSlot^2 \cdot IperConductor \cdot \mu_0 \cdot \frac{hSlotWound}{3 \cdot wSlotWound} \quad \text{eq 36}$$

The total leakage flux linkage per unit length of the machine is (eq 37):

$$fluxLinkagePerUnitLength = fluxLinkageSlotMouth + fluxLinkageSlotWedge + fluxLinkageWound \quad \text{eq 37}$$

The slot total permeance is (eq 38)

$$slotTotalPermeance = \frac{hSlotMouth}{wSlotMouth} + \frac{hSlotWedge}{wSlotWedge} + \frac{hSlotWound}{3 \cdot wSlotWound} \quad \text{eq 38}$$

The **leakage flux** is the flux that escapes somewhere and links only the windings or the PM that produces it and does not contribute to producing the useful field(Figure 64).

For a surface mounted PM machine with ferrite or neodymium magnets, the relative permeability of the material is close to 1 and as a result, the air-gap leakage permeance is very small (probably negligible)

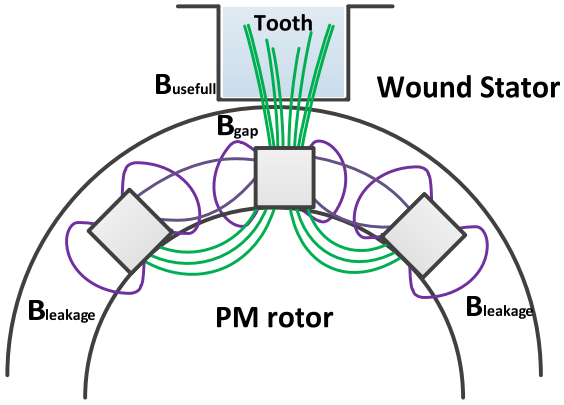

Figure 64: Useful and Leakage Flux

The **leakage flux linkage in a slot**, or wasted flux can be calculated using eq 39

$$FluxWastedInSlot = conductorsPerSlot^2 \cdot IperConductor \cdot \mu_0 \cdot slotTotalPermeance \cdot L_{usefull} \quad \text{eq 39}$$

The **leakage flux per phase** is (eq 40):

$$FluxLeakagePerPhase = \frac{FluxLeakageInSlot \cdot Q_s}{m} \quad \text{eq 40}$$

Where Q_s is the number of slots and m the number of phases

c. PM

To design the permanent magnet excitation, the following concept was used:

1. The **type of PM material is chosen**; material characteristics like magnetisation curves, densities are entered in the design tool materials library.

2. Calculate the **volume of magnet necessary** for a certain design. The volume of PM should be calculated for the current load with a view to the predicted short-circuit currents that might flow in the machine. The PM should withstand some high currents without being irreversibly demagnetised (eq 41)

3. The height of the PM must be set according to the PM function point and in view of **avoiding demagnetisation**. This combined with the desired pole pitch give the width and height of the PM

Magnet dimensions are shown in –Figure 65, where w_{pm}=width of magnet and h_{pm}= thickness of magnet

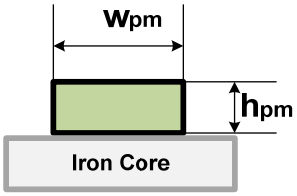

Figure 65: Magnet Dimensions

4. Calculate the **expected performance of the magnet** in the current design

- The final design is checked for demagnetisation by the short circuit current in the machine

- In the current version of the design tool it is considered that demagnetisation due to temperature will not occur

$$I_{coil_{demagnetising}} = I_{coil} \cdot I_{scCoefficient} \quad \text{eq 41}$$

Volume of the Air-gap considered a thin wall cylinder is (eq 42):

$$V_{gap} = \pi \cdot (R_{bore}^2 - R_{rotor}^2) \cdot L_{overallCore} \quad \text{eq 42}$$

Required Volume of the PM

The required total volume of permanent magnet material is calculated according to [197], [198]. This is the no load volume of the PM since it does not depend on the demagnetising current. The actual volume of the PM must be larger than this value. In the design tool, this test is carried out after the final dimensions are calculated (eq 43).

$$V_{magnetRequired} = \left(\frac{B_{gap_{avg}^2} \cdot V_{gap}}{\mu_0 \cdot B_{wkg} \cdot H_{wkg}} \right) \quad \text{eq 43}$$

where V_{gap} is the volume of the air-gap

Within the algorithm the following steps were taken to determine the required dimensions of the PM:

- The required width of the tooth for the field determined by the required winding is calculated
- Depending on the winding type, the slot width is deduced. The width and height of the winding in the slot is determined by the design rule SlotWidthPerHeight (see also design rules in Appendix 9)
- A new pole width is determined by the winding and the slot and tooth combination
- This gives a new bore diameter corresponding to the new pole pitch
- To avoid demagnetisation of PM, a minimum height is required h_{pMin} (eq 44)

$$h_{pmMin} = \frac{NrTurns1Coil \cdot Icoil_{demagnetising}}{H_c} - \frac{B_r \cdot gap_{length} \cdot PM2PolePitch}{\mu_0 \cdot H_c} - \left(\mu_r \cdot gap_{length} \cdot PM2PolePitch\right)[mm] \quad \text{eq 44}$$

where H_c is H coercive, B_r=B remanent

- For the inputs given a required volume of PM is required-eq 43

- The volume of one PM is calculated taking into account the number of poles (eq 45):

$$V_{1pm} = \frac{VmagnetRequired}{poles} \quad \text{eq 45}$$

- The required area of one PM can be deduced using the active length of the machine (eq 46):

$$A_{1pmRequired} = \frac{V_{1pm}}{L_{usefull}} \quad \text{eq 46}$$

- The width of the PM would be set by the pole pitch (eq 47):

$$w_{pm} = polePitch \cdot PM2PolePitch \quad \text{eq 47}$$

- With eq 47, the height of the PM can be calculated (eq 48):

$$hpm_{Required} = \frac{A_{1pmRequired}}{w_{pm}} \quad \text{eq 48}$$

- If $hpm_{Required} > hpm_{Min}$, hpm=hpmRequired. Otherwise hpm=hpmMin. In this case, wpm=A1pmRequired/hpm

The working point is usually [0.5 to 0.8] of B_{rem} - eq 49 (Figure 66)-(see also Appendix 9)

$$B_{wkg} = B_{wkg}Coefficient \cdot B_{rem} \quad \text{eq 49}$$

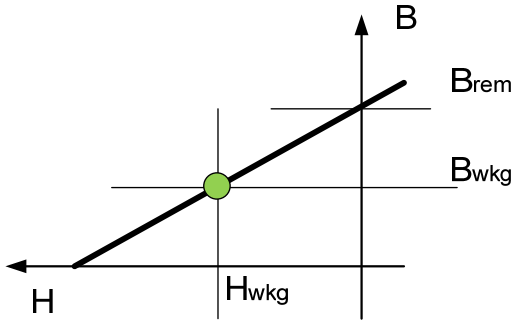

Figure 66: BH curve with Working Point

The actual B_{gap} depends on the geometry of the PM. Situations may arise when $B_{airgap} < B_{wkg}$ e.g. If the magnet is very narrow compared to the pole pitch.

Figure 67 shows a surface mounted geometry and Figure 68 depicts the buried magnets situation. For the surface mounted geometry $B_{airgap} = B_{wkg}$.

For buried PM machines, the B_{wkg} gets amplified by the iron so that $B_{airgap} > B_{wkg}$. This phenomena is quantified by field amplification factor k_b

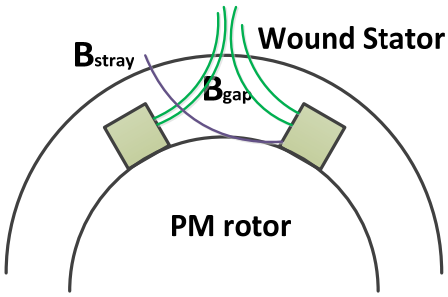

Figure 67: Surface Mounted Magnets

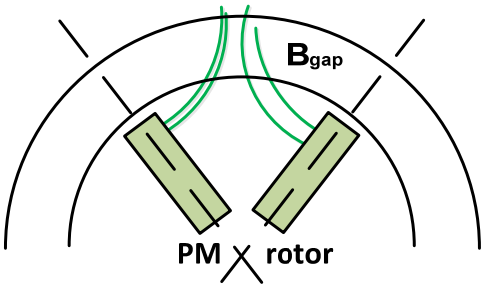

Figure 68: Buried Magnets

The actual induction in the air-gap is (eq 50):

$$B_{gap_{Actual}} = \frac{B_{rem}}{\frac{1}{k_b} + \frac{gap_{length} \cdot \mu_{rPM0}}{h_{pm}}} \quad \text{eq 50}$$

k_b, the field amplification factor is:

$$k_b = \frac{B_{gap_{avg}}}{B_{wkg}} \quad \text{eq 51}$$

For surface mounted machines Kb=1

Angle at center of PM (eq 152):

$$AngleCenterPMdeg = \frac{180 \cdot w_{pm}}{R_{rotor} \cdot \pi} \quad \text{eq 52}$$

Flux linkages of PM (eq 153):

$$fluxLinkage_{PM} = B_{wkg} \cdot Apm_{Gap} \cdot TurnsSeriesPhase \cdot Cordingfactor \cdot DistributionFactor \quad \text{eq 53}$$

Where the area of PM is (eq 54):

$$Apm_{Gap} = w_{pm} \cdot L_{overallCore} \quad \text{eq 54}$$

With the above considerations, the magnet dimensions can be estimated.

d. Windings

The winding is made having a number coils, each a number of turns. Several coils may be connected in series or parallel to make a phase winding.

The following issues need to be decided on:

- *How many turns are/should be in a coil?* The calculated number of conductors must be fitted practically in each slot together with the insulation.
- *What is the resistance and inductance of a phase winding?*
- *What is the total amount (mass and volume) of winding material used?*(active and inactive materials)

The user can decide on a winding type (distributed, concentrated single or double layer-see Figure 69, Figure 70, Figure 71) or a suitable winding type for the machine can be suggested by the program.

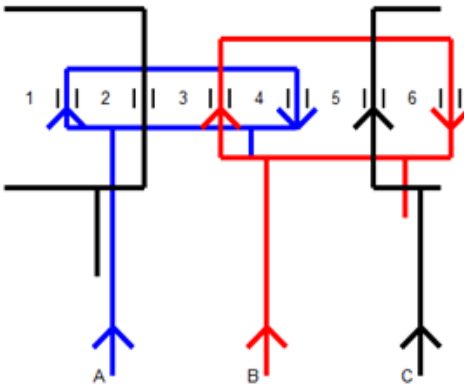

Figure 69 Distributed Winding: 2 Poles; 1 Slot/Pole And Phase

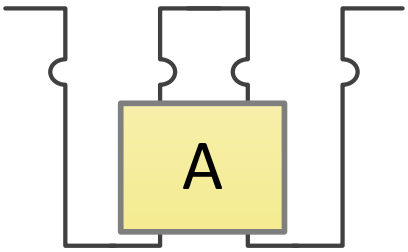

Figure 70: Single Layer Concentrated Winding/Slot/Tooth

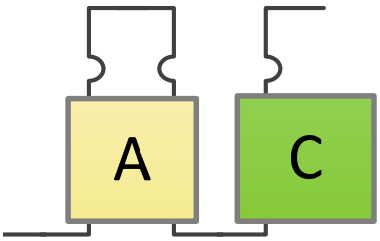

Figure 71: Double Layer Concentrated Winding/Slot/Tooth

For Nessie, the concentrated windings were considered to be most suitable because a modular construction of the stator and rotor cores is intended. This would make the machine easier to transport and service than the distributed winding design. Concentrated windings have the following other advantages [197],[19], [199], [200], [201], [148], [202], [203], [20], [21], [151], [204], [205], [206], [207]:

- Suitable for low speed high torque applications;
- Give better fill factor than distributed windings. This would make the machine smaller in in diameter and length;
- The overhang of the winding is shorter than for the distributed winding, making for smaller copper losses. The fault tolerance capability of the distributed winding is better as the machine can be made to function with faulty coils-for a short time at least. [208], [206], [20];
- Fractional slot machines have bigger EMF than integer slot machines [20]
- Number of slots and the number of poles are close in concentrated windings-more poles/slots means that the frequency can be kept relatively high;
- With concentrated windings the slot width can be decreased as they take up less space in the slot-especially single layer ones;
- Simple to manufacture, understand and replace;
- Increased fault tolerance-magnetic decoupling between phases is possible (mutual inductance very low);
- The iron core could be separated to form sections-useful in maintenance and construction of the machine;
- For single layer concentrated windings, the coils only need ground insulation as the other phase is at a sufficient distance(not in the same slot);
- The phase shift for each coil may be used to obtain multiphase machines;

- Simpler to control;

The slot, phase and pole combination must be carefully chosen for a fractional slot winding because they decide the feasibility of the winding and have influence on coil pitch, winding factor and MMF harmonics. [19], [204], [19]. Fractional slot windings can be designed to avoid cogging and get more sinusoidal MMF and EMF[20]

As not each combination of slots poles and phases gives a valid winding for the concentrated winding types, a program for excluding inadequate configurations was made [209]

The rules for giving a **valid concentrated winding** are:

1. The number of poles must be an even number
2. The number of slots must be divisible by

   -m: number of phases –for double layer concentrated windings
   -2m: number of phases –for single layer concentrated windings
3. The number of pole pairs per section are not divisible by the number of phases

The number of sections in the machine (eq 55)is defined as the greatest common divider between the number of slots and pole pairs and represents the parts the machine can be divided in so that each part can operate as an independent machine [19]

$$sections = \gcd(Q_s, PolePairs) \quad \text{eq 55}$$

4. The slots per pole and phase(spf) should be between [1.4,1.2] (120,240 degrees slot pitch)

The **winding factor** can be calculated as [20](eq 56):

$$windingFactor = distributionFactor \cdot ChordingColilSpanFactor \quad \text{eq 56}$$

Where the c**hording (pitch factor, coil span)** in radians

$$ChordingColilSpanFactor = cos\left(\frac{1}{2} \cdot ChordingCoilSpanRad \cdot SpaceHarmonicNumber\right) \quad \text{eq 57}$$

Where the coil span in radians is (eq 58)

$$ChordingCoilSpanRad = \pi - SlotPitchRad \quad \text{eq 58}$$

The slot pitch in radians is (eq 59)

$$SlotPitchRad = \frac{\pi \cdot poles}{Q_s} \quad \text{eq 59}$$

The chording or pitch is the distance between one side to the other of the same coil. Short-pitching, or chording, refers to coils with span less than a whole pole-pitch. The chording coils span factor takes account of the difference in phase of the voltages in the two coil sides (eq 60, eq 61) [20]

$$ChordingColilSpanFactor = \frac{Resultant\ voltage\ in\ a\ short\ pitch\ coil}{arithmetic\ sum\ of\ voltages\ induced\ in\ coil\ sides} \quad \text{eq 60}$$

$$ChordingColilSpanFactor = \frac{\overrightarrow{E_{coil_a}}}{2|\overline{Ea}|} = cos\left(\frac{angleBetween\ CoilSides_{el}}{2}\right) \quad \text{eq 61}$$

For sinusoidal induced voltages, the coil voltage is the phasor sum of its two coil-side voltages. Thus for coil *a* (eq 62)

$$\overrightarrow{E_{coil_a}} = \overrightarrow{Ea_-} + \overrightarrow{Ea_+} \text{ where } |\overline{Ea_-}| = |Ea_+| \quad \text{eq 62}$$

In Figure 72, an example of a distributed winding, one slot per pole and phase is shown.

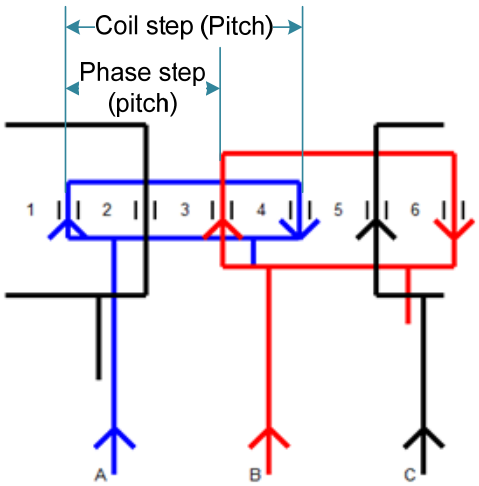

Figure 72 Distributed Winding: p=2; poles q=1 Slot/Pole And Phase

The coil step or coil pitch is defined with eq 65:

$$CoilPitch = \frac{Q_s}{PolePairs} \qquad \text{eq 63}$$

For concentrated fractional slot windings the coil step is one slot. This is inevitably a short pitched coil situation because the slot pitch is a fraction of the pole pitch.

The main reason for using chording is to reduce or suppress certain space harmonics in the phase EMFs [210]

Chording results in shorter overhang for distributed windings. The fundamental of the phase EMF is reduced because less flux is linked by a short chorded coil compared to a full pitched one.

The coil span is rarely made less than 2/3 of the pole-pitch because the additional turns necessary to obtain the desired EMF would offset the savings that may be gained in the length of the overhang.

The **distribution factor** is defined as how much of the machine is occupied by the winding of one phase -Figure 73.

The distribution factor for double layer distributed winding is shown in Figure 73 and for concentrated double layer in Figure 74. These represent the concept and not actual windings. The rules for calculating distributed windings can be found in [150], [150]and for concentrated windings in [23]

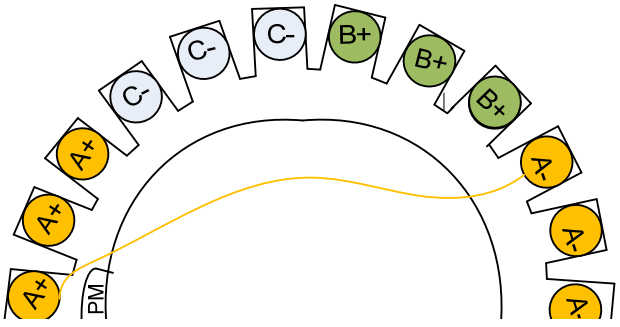

Figure 73: Distribution Factor For A Distributed Winding

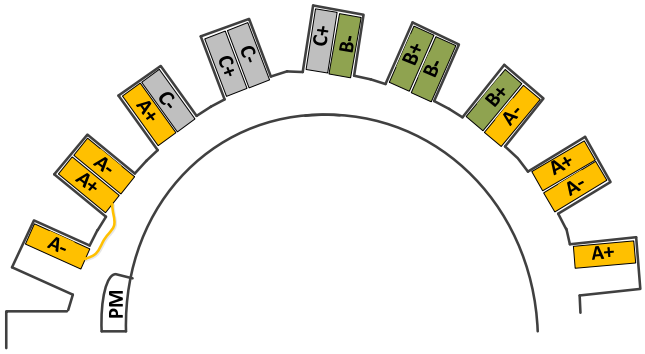

Figure 74: Distribution Factor For Concentrated Double Layer Windings

For double layer **concentrated windings** this factor may be calculated using eq 64

$$DistributionFactor_{Double} = \frac{sin\left(\frac{1}{2} \cdot SpaceHarmonicNumber \cdot PhaseSpreadElDegrees\right)}{z \cdot sin\left(\frac{SpaceHarmonicNumber \cdot PhaseSpreadElDegrees}{2 \cdot z}\right)} \quad \text{eq 64}$$

The **distribution factor for single layer distributed winding** (eq 65):

$$DistributionFactor_{Single} = \frac{sin\left(\frac{1}{2} \cdot SpaceHarmonicNumber \cdot PhaseSpreadElDegrees\right)}{z \cdot sin\left(\frac{SpaceHarmonicNumber \cdot PhaseSpreadElDegrees}{2 \cdot z/Q_s}\right)} \quad \text{eq 65}$$

Where z is the same for both single and double layer windings (eq 66)

$$z = \frac{Q_s}{gcd(NrCoils, poles \cdot m)} \quad \text{eq 66}$$

Initially, the needed cross-section of a conductor in the coil (eq 67) is calculated knowing the current in the coil and the current density j (eq 67). The current in the coil would for ClassicRFNessie be the line current, as the coils in a phase are connected in series and the machine is star connected.

$$ACuNeeded = \frac{I_{coil}}{j}; \quad AslotActive1Coil = ACuNeeded \quad \text{eq 67}$$

The coil insulated area is calculated by adding the total cross-sectional area of the insulation materials to the cross section area of the uninsulated copper coil.

The **slot fill factor** is used to quantify the amount of copper that can be included in a coil that is able to fit in the given slot. This factor is a measure of the manufacturability of the winding.

There are several ways to determine the slot fill factor;

b. determine the acceptable slot fill factor;
c. calculate the total available area of the slot and subtract the area occupied by the insulation;
d. impose a value for the slot fill factor and build the core around that.

The fill factor is dependent of the winding and core geometry: e.g. two coil sides are placed in a single slot, the insulation between the two sides will have a big impact on the value of this factor

Primarily, the slot fill factor is influenced by the voltage and current of the winding, the slot, winding and conductor cross section type, but also by the manufacturing process can also influence this quantity.
The active area of the slot, or the area of the copper is (eq 68):

$$AslotActive1Coil = AConductorActive \cdot NrTurns1Coil \quad \text{eq 68}$$

The number of turns in a concentrated coil [211] (eq 69):

$$NrTurns1Coil = \frac{V_{desiredPerCoil}}{4.44 \cdot fluxPerPole \cdot f \cdot windingFactor} \quad \text{eq 69}$$

The flux per pole is given by eq 29 and the winding factor from eq 56:

$$NrTurnsTotal = NrTurns1Coil \cdot Q_s \quad \text{eq 70}$$

The number of turns connected in series per phase is an important design value (eq 71):

$$turnsInSeriesPerPhase = \frac{Q_s}{m} \cdot NrTurns1Coil \quad \text{eq 71}$$

Active Area of one coil

$$A_{slotActive1Coil} = A_{ConductorActive} \cdot NrTurns1Coil \quad \text{eq 72}$$

Width and Height of the coil in the slot (eq 73, eq 74)

$$w_{1Coil} = \sqrt{A_{TotalInsulated1Coil} \cdot CoilWidthPerHeight} \quad \text{eq 73}$$

$$h_{1CoilBare} = \frac{A_{TotalInsulated1Coil}}{w_{1Coil}} \quad \text{eq 74}$$

For Nessie, the double layer concentrated winding was chosen as most suitable as they use the machine circumference better, produce less sub harmonics (and a more sinusoidal EMF) and allow for more slot pole combinations[18], [19]. Additional analysis is required to determine the impact of using single and double layer concentrated windings on the overall generator system. This study was left for future work.

The length of the winding elements are important for the calculation of the winding resistance and contributes to assessing the amount of material that needs to be ordered to make the machine (eq 75-eq 80)

Alternative in [151]

$$L_{conductor1ConcentrCoil} = 2L_{endSupplyToCoil} + 2\left(w_{Tooth} + 2slotInsulThick + 2(w_{wire} + interTurnsInsul)\right) + 2\left((L_{overallCore} + NrTurns1Coil + interTurnsInsul)\right) \quad \text{eq 75}$$

$$L_{conductorConcentrPerPhase} = L_{conductor1ConcentrCoil} \cdot NrCoilsInSeriesPerPhase \quad \text{eq 76}$$

$$L_{conductorTotal} = NrCoilsInMachine \cdot L_{conductor1ConcentrCoil} \quad \text{eq 77}$$

$$NrCoilsInMachine = Q_s \; for \; double \; layer \; concentrated \; windings = \frac{Q_s}{2} \; for \; single \; layer \; concentrated \; windings \quad \text{eq 78}$$

spf=numerical value of Slot per pole and phase (eq 79)

$$spf = \frac{Q_s}{m \cdot poles} \quad \text{eq 79}$$

$$L_{wirePhaseDistributed} = turnsperphase \cdot (2 \cdot L_{Core} + L_{overhangDistributed})\,[m] \quad \text{eq 80}$$

Calculation of the winding overhang (End Winding Overhang)

Winding Overhang –-is the part of the coil outside the core at one end of the core; other name end winding. For the concentrated winding (Figure 75) the length of the end winding can be approximated as eq 81

$$L_{overhangConcentrated1Coil} = 2 \cdot \left(h_{Overhang} + w_{tooth} + w_{coil}\right)[m] \quad \text{eq 81}$$

where

$$h_{Overhang} = w_{coil}[m] \quad \text{eq 82}$$

An exact calculation of the length implies exact knowledge and consideration of the displacement of each coil.

For the distributed winding (Figure 76) the length of the overhang is

$$L_{overhangDistributed1Coil} = 2 \cdot \left(2 \cdot h_{Overhang} + coilsteplength\right)[m] \quad \text{eq 83}$$

The coilsteplength is calculated with eq 84 (see also Figure 72 and Figure 76):

$$coilsteplength = coilstep(w_{slot} + w_{tooth})[m] \quad \text{eq 84}$$

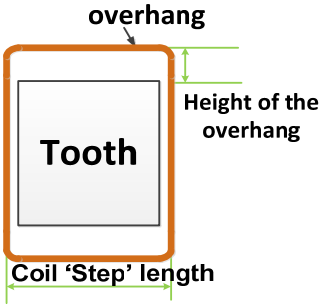

Figure 75: Concentrated Winding Overhang

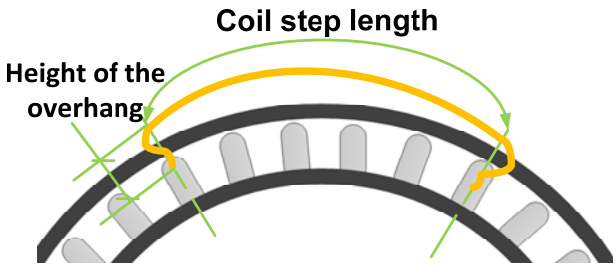

Figure 76:Overhang For Distributed Windings

e. Iron Design

The stator and rotor cores, made of soft magnetic materials (laminations for Nessie) provide a return path for the magnetic field produced by the windings and permanent magnets.

In an electrical machine, the slots carry the electric current and the teeth carry the magnetic flux. The flux links the current producing the effect of flux linkage. Of a slot pitch some of the available space belongs to the slot and the rest belongs to the teeth. The ratio between the two is an important design rule (see design rules in Appendix 9).

The main elements of the iron core are the teeth and the stator and rotor yokes (also called back iron) Figure 77. The iron design sizes these elements magnetically and mechanically.

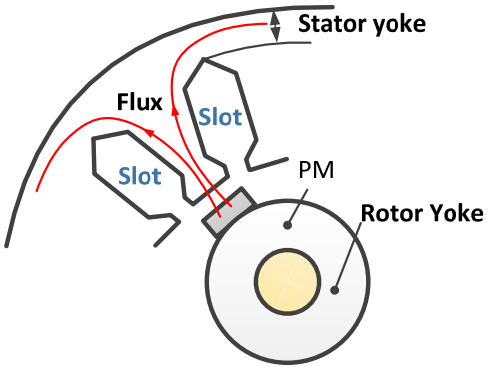

Figure 77: Stator and Rotor Yokes

The cross section of the iron parts must allow the flux to pass without saturating. The saturation value of the core depends on the material used. As calculation values, the following generic values were chosen

$B_{saturationLamination} = 1.7\ T$; $B_{saturationSintered} = 0.7\ T$.

A variety of alloy materials exist for laminations and sintered materials.

In the following, the calculation of the stator and rotor cores is explained.

The flux per pole is calculated using eq 25. For concentrated double layer windings, the flux in one pole is equal to the flux in one tooth eq 26. From eq 26, the area of the tooth at the air-gap can be calculated with eq 85.

$$A_{ToothAtGap} = \frac{FluxPerTooth}{B_{tooth}} \quad \text{eq 85}$$

And from another point of view the tooth area at the gap is expressed with eq 86

$$A_{ToothAtGap} = w_{tooth} \cdot L_{OverallCore} \quad \text{eq 86}$$

The mid **width of the tooth** is calculated with eq 87. The height of the tooth is equal to that of the slot.

$$w_{tooth} = \frac{FluxPerCoil}{B_{tooth} \cdot Lusefull} \quad \text{eq 87}$$

If during the design process the width of the tooth becomes such that for the corresponding design length the flux density is unacceptable. If the tooth area at gap is too small, the flux density is too high and saturation problems will arise. On the other hand if the tooth area is too large, the flux density will be too small and the machine will be unnecessarily too large.

By analysing eq 86 and eq 87 adjustments have to be considered to ensure the validity of the design. If the $FluxDensityPerTooth(obtained) < B_{tooth}(desired)$ then by keeping the value for w_{tooth} (because the diameter of the machine tends to be large and needs to be kept as small as possible), the active length of the core will be decreased to achieve $FluxDensityPerTooth = B_{tooth}$.

The same argument is made for $FluxDensityPerTooth > B_{tooth}$ thus increasing the length of the core.

On the other hand if the width of the slot (w_{slot}) becomes much larger than the width of the tooth, the magnetic field in the air-gap will be distorted –more leakage flux associated with the magnets will occur.

If the w_{slot} becomes too wide compared with the w_{tooth} (max 1.2 times-SlotPerSlotPitch=0.6 max-see a list of design rules in Appendix 9), then any required increase of the area should be obtained by increasing the slot height. This results in the design algorithm changing the SlotWidthPerheight design ratio.

If this fix cannot change the design enough so that the current density and the flux density in the tooth are acceptable, then the bore diameter is adjusted.

The **rotor and stator yokes** (Figure 77) must be able to carry the flux. For the ClassicRFNessie machine one idea would be to function at a relatively high saturation level because the machine is large and extra unused material (corresponding to a low saturation design) is to be avoided. Constructionally, extra back-iron would be needed to aid in bonding of the lamination.

The height of the stator yoke destined for electromagnetic purposes (and not mechanical ones) is approximated as being half as wide as the stator tooth (eq 88). This is the minimum width to accommodate the flux that is going through the tooth and splitting up in the yoke-see Figure 77

$$h_{StatorYoke} = \frac{w_{StatorToothTotal}}{2} \qquad \text{eq 88}$$

The rotor yoke is considered to be equal to the stator yoke eq 89

$$h_{StatorYoke} = h_{RotorYoke} \qquad \text{eq 89}$$

f. (Stator) Slot Design

The slot width should be able to accommodate the windings that create the B_{gap} need (designed for), that is to accommodate the windings that can carry the full load current and generate the voltage.

The current that the windings are designed for is set by the power and the required voltage. The area of conductors required is determined by the permissible current density and the full load current per coil.

There are several slot shapes that are used in electrical machines. The slot shape can be in general:

- Radial Sided Slots –Figure 78(teeth parallel) – slot walls at an angle α
- Parallel Sided Slots –Slot walls are parallel resulting in an iron geometry as in Figure 79

The slot geometry influences the leakage phenomenon.

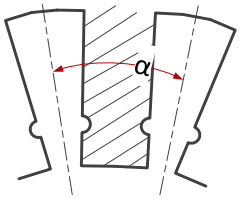

Figure 78: Radial Sided Slots(Parallel teeth)

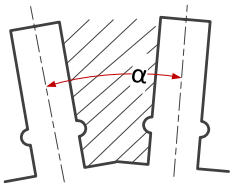

Figure 79: Parallel Sided Slots

The slot shapes proposed for the design tool are shown in Figure 80.

a. Semi-closed, Square slot bottom

b. Semi-closed, Round slot bottom-version1

c. Semi-closed, Round slot bottom-version2

d. Open, Square slot bottom

Figure 80: Nessie Design Tool Slot Shapes

The parameterisation of the slot dimensions notations for slot types B and D are presented in Figure 81 a and b. following the same logic, any slot type can be parameterised in this manner.

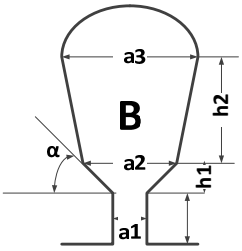

a. Slot Type B

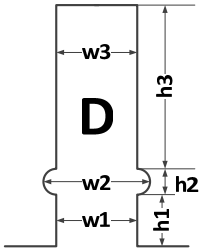

b. Slot Type D

Figure 81: Slot Dimensions

For the ClassicRFNessie, slot D was chosen to fit the preformed coils chosen for the machine.

In the following, the method for calculating of the slot is presented.

The slot width and height is influenced by the winding and slot types. A design rule that influences the slot shape is the **CoilWidthPerHeight** design ratio (see design rules in Appendix 9).

For concentrated double layer windings, the width and height of the slot can be calculated with eq 90 and eq 91 (with eq 73and eq 74):

$$h_{StatorSlotTotal} = h_{1Coil} \quad \text{eq 90}$$

$$w_{slotTotal} = 2 \cdot w_{1Coil} + spaceBetweenNeighbourCoils \quad \text{eq 91}$$

g. MMFs

The MMF produced by the current I and N turns of a single concentric coil is analysed in Figure 82(By cutting and unfolding the coil, the MMF is shown). [30]

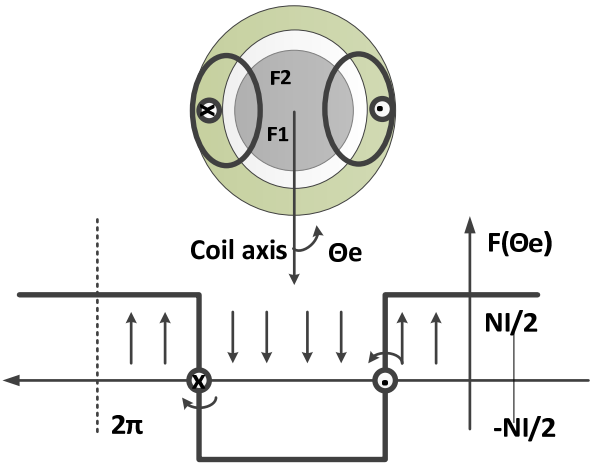

Figure 82: MMF due to Current Flowing in a Single Concentric Coil. [210]

Ignoring the reluctive drop in iron, Ampere's law is written eq 92:

$$F_1 - F_2 = NI \qquad [Aturns] \qquad \text{eq 92}$$

By symmetry of the chosen path, the MMF across the two gaps in the closed path is equal and opposite, that is, $F_2 = -F_1$ (eq 93).

$$F_1 = \frac{NI}{2} \qquad \text{eq 93}$$

The direction and magnitude of the air-gap MMF on either side of the two coils may be deduced from the figure and eq 92. For one coil of N turns, the air-gap MMF distribution can be approximated to a square wave having the magnitude of $NI/2$. The fundamental component of the Fourier analysis of this is given by eq 94:

$$F_{a1} = \frac{4}{\pi}\frac{N}{2} I\cos(\theta_e) \qquad \text{eq 94}$$

The expression for the corresponding fundamental component of the air-gap flux density in a uniform air-gap machine is (eq 95):

$$B_{gap} = \mu_0 \frac{F_{a1}}{gap_{length}} = \frac{4}{\pi}\frac{\mu_0}{gap_{length}}\frac{N}{2} I\cos(\theta_e) \quad \left[Wb/m^2\right] \qquad \text{eq 95}$$

Where the air-gap length is assumed to be constant round the rotor circumference

Coils may be short or long pitched (chording-see the Windings section above for more information on the chording factor). The full pitched coils have a span of 180 electrical degrees and the short pitched ones have less.

It is more common to have short-pitched coils as a solution to reduce the MMF space harmonics[210].

h. EMFs-the induced voltage

The induced voltage (EMF) and developed torque of an electric machine are a function of the amount of flux per pole. When the flux density distribution (B(angle)) in a pole is known, the flux per pole can be determined by integrating the flux density distribution over the pole area. Figure 83 shows a sinusoidally distributed flux density over two poles with a magnitude of $B(\theta_e)=\hat{B}\cos(\theta_e)$

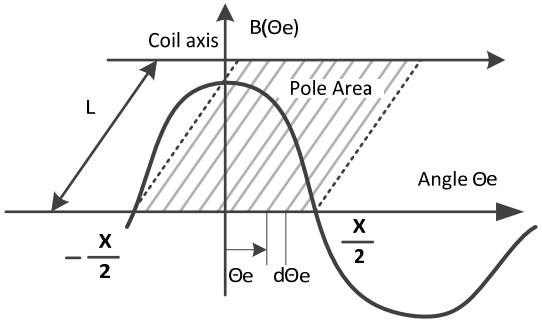

Figure 83: Flux Per Pole [19]

The flux per pole is

$$FluxPerPole=\int_{-\pi_e/2}^{\pi_e/2}\hat{B}\cos(\theta_e)L_{usefull}R_{bore}d\theta_e \qquad [Wb] \qquad \text{eq 96}$$

$\frac{\pi_e}{2}$ is the angular span of a full pole width in electrical radians. The flux per pole varies with the position, but for steady state, the FluxPerPole can be considered constant. For this, the induced voltage is

$$EMF=-\omega_e\cdot N\cdot FluxPerpole\cdot\sin(\omega_e t) \qquad \text{eq 97}$$

Where N is the number of turns and $\omega_e=\frac{\partial\theta_e}{\partial t}$

The value of the flux per pole for a sinusoidal distribution is eq 98 [210], [198]:

$$FluxPerPole=B_{avg}\times\left(\frac{2\cdot\pi\cdot L_{usefull}\cdot R_{gap}}{poles}\right)=\frac{4}{\pi}\cdot L_{usefull}\cdot R_{gap}\cdot\hat{B}_{gap} \qquad \text{eq 98}$$

The **EMF-electromotive** force is the internally generated voltage and was calculated in the design tool as with eq 99[197], [150], [198]:

$$EMF=4.44\cdot Turns_{seriesPerPhase}\cdot FluxPerPole\cdot f\cdot windingFactor \qquad \text{eq 99}$$

where f is the frequency

The number of **turns per phase** is calculated using eq 100 for a desired EMF (eq 99) and FluxPerPole (calculated with eq 25). The winding Factor is calculated with eq 56:

$$Turns_{seriesPerPhase}=\frac{EMF_{desiredPerPhase}\cdot\pi}{2\cdot n_{radPerS}\cdot FluxPerPole\cdot windingFactor}\ [-] \qquad \text{eq 100[18]}$$

$EMF_{desiredPerPhase}$ is estimated from the desired output line voltage of the generator. From that, the voltage to be generated from a coil $V_{desiredPerCoil}$ can be set.

Within one phase of an AC winding a set of serial or parallel coils may be found. For distributed windings: Figure 84 and Figure 85 show the voltages induced in the component coils forming the phase winding occupying adjacent slots will be phase displaced from one another by the slot angle separating them, β- the electrical angle subtended by the arc between two adjacent slots.

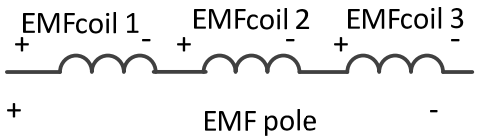

Figure 84: Coils Of A Pole Showing The Voltage Generated In Each Coil

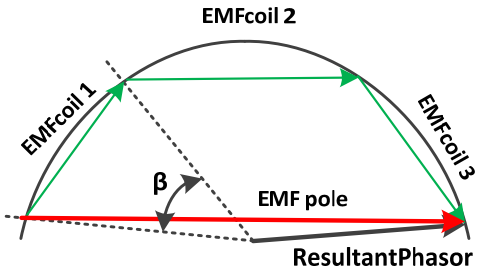

Figure 85: Resultant Phasor Voltage from Several Distributed Coils Under a Pole. [18]

The EMF generated in one concentrated coil can be calculated as (eq 101):

$$EMF_{in1ConcentratedCoilGenerated} = \frac{EMF_{VphaseGenerated}}{NrCoilsInSeriesPerPhase} \quad \text{eq 101}$$

The EMF generated per coil is checked against the desired value with eq 102

$$V_{(desired-Generated)_{coil}} = V_{desiredPerCoil} - EMF_{in1ConcentratedCoilGenerated} \quad \text{eq 102}$$

In the same manner, the generated output voltage is checked against the required value with

$$V_{(desired-Generated)_{line}} = Vout_{ratedDesired} - EMF_{LineGenerated} \quad \text{eq 103}$$

i. Inductance

Inductance is the ratio between flux linkages and the current and is the phenomenon caused by an electromagnetic field in a medium. It is a lumped circuit constant representing the effect of magnetic fields.

The total inductance per phase is calculated with eq 104 [210], [198] :

$$L_{totalPhase} = L_{leakagePerPhase} + L_{magnetisingPerPhase} \quad \text{eq 104}$$

The magnetising inductance $L_{magnetisingPerPhase}$is (eq 105):

$$L_{magnetisingPerPhase} = \frac{D_{bore} \cdot L_{usefull} \cdot \pi \cdot \mu_0 \cdot (TurnsInSeriesPerPhase \cdot windingFactor)^2}{4 \cdot gap_{equivalent_{length}} \cdot PolePairs^2} \ [H] \quad \text{eq 105}$$

Leakage inductance per phase is calculated with eq 106 [197], [197] and with $FluxLeakagePerPhase$ from eq 39 and eq 40:

$$L_{slotLeakagePerPhase} = \frac{FluxLeakagePerPhase}{I_{phase}} \ [H] \quad \text{eq 106}$$

The total leakage inductance can be calculated with eq 107

$$L_{leakagePerPhase} = L_{slotLeakagePerPhase} + L_{LeakageOverhangPhase} + L_{airgapLeakagepPerPhase} \quad \text{eq 107}$$

The overhang leakage can be calculated with eq 108

$$L_{LeakageOverhangPhase} = \frac{2 \cdot overhangLength \cdot TurnsInSeriesPerPhase \cdot k_{empirical}}{poles} \quad \text{eq 108}$$

Where

$k_{empirical} = 1$ for concentrated windings

$k_{empirical} = 1.5$ for distributed windings

In the design tool analytical calculation, for concentrated windings, the air-gap and the overhang leakages were neglected as a simplification.

j. Lumped Parameters

For modelling the machine and the analysis of its dynamic response, the lumped parameters characterising a certain design are given by the analytical calculation module of the design tool.

As a simplification, the **d and q axis induc**tances were considered equal for a surface mounted PM rotor machine.

With eq 104 [198]:

$$L_d = L_q = \frac{3}{2} L_{totalPhase} \quad \text{eq 109}$$

The **resistance per phas**e is (eq 110):

$$R_{phase_{DC}} = \left(\frac{rho_{CuFunction_{Temperature}} \cdot Length_{Wire}}{CrossSection_{Wire}} \right) \quad \text{eq 110}$$

The temperature used to calculate the resistance ($rho_{CuFunction_{Temperature}}$-the resistivity) was the steady state temperature given by the insulation class chosen. (See more on insulation classes in Appendix 6: Special Issues to be Considered)

The frequency dependency of the resistance value was ignored because of the low value for the design frequency.

The **flux linkage** of the PM (eq 111):

$$FluxLinkagePerPole = \frac{turnsInSeriesPerPhase}{PolePairs} \cdot FluxPerPole \quad \text{eq 111}$$

The **moment of inertia** is calculated for a hollow cylinder

$$InertiaMoment = \frac{RotorWeight \cdot R_{rotor}^2}{2} \ [kg \cdot m^2] \quad \text{eq 112}$$

k. Adjustments

The originally estimated values of the length and the diameter of the generator must be adjusted to keep the required force density.

The diameter is set according to the slot dimensions (w_{slot}). The diameter D_{gap} varies to accommodate the windings. The machine has to produce the required torque eq 113

$$T_{elm} = \frac{\pi \cdot D_{gap}^2 \cdot L_{usefull} \cdot F_{density}}{2} \; [N \cdot m] \qquad \text{eq 113}$$

The force density can be expressed as a function of the air-gap induction B_{gap} (eq 114):

$$F_{density} = \frac{Force}{A_{gap}} = \frac{B_{gap}^2}{2 \cdot \mu_0} \left[\frac{N}{m^2}\right] \qquad \text{eq 114}$$

Where the force in the air-gap is (eq 115):

$$Force = A_{gap} \cdot F_{density} \; [N] \qquad \text{eq 115}$$

And the cross-section area where the flux is flowing is eq 116

$$A_{gap} = \pi \cdot D_{bore} \cdot L_{overall_{Core}} \; [m^2] \qquad \text{eq 116}$$

The force density is calculated to ensure the required value for T_{elm}. If the gap diameter D_{gap} varies (increases) then the electromagnetic torque varies (increases) with the square of the diameter (eq 113).

To keep the T_{elm}. value, the following three possibilities exist for varying the force density:

1. Choose another PM that would give a different B_{gap}

2. Make the air-gap length smaller to reduce leakage of the PM flux.

3. Change the PM2PolePitch until the leakage becomes excessive-this requires thorough investigation and the value for this design rule will be changed carefully

These solutions are not applied however because they conflict with the desires of the designer (mechanical and economic constraints). What remains to be changed is $L_{usefull}$. This is adjusted to give the required area for the torque.

From eq 117, the needed area of the air-gap can be calculated knowing $D_{gap}$and the required torque

$$A_{gap_{needed}} = \pi \cdot D_{gap_{fixed}} \cdot L_{usefull} [m^2] \qquad \text{eq 117}$$

Rearranging eq 117, the length is expressed:

$$L_{usefull} = \frac{A_{gap_{needed}}}{\pi D_{gap_{fixed}}} [m] \qquad \text{eq 118}$$

The needed air-gap area can be expressed from eq 119

$$A_{gap_{needed}} = Force \frac{2\mu_0}{B_{gap}^2} \; [m^2] \qquad \text{eq 119}$$

Where the force is derived from the torque equation eq 120:

$$T_{elm} = T_{turbine} = Force \cdot \frac{D_{gap}}{2} \qquad \text{eq 120}$$

$$Force = 2 \cdot \frac{T_{turbine}}{D_{gap}} [N] \qquad \text{eq 121}$$

Substituting eq 121 in eq 119, eq 122 is obtained:

$$A_{gap_{needed}} = \frac{4\mu_0 T_{turbine}}{B_{gap}^2 \, D_{gap}} \; [m^2] \qquad \text{eq 122}$$

With this, eq 118 gives the required length for the machine (eq 123)

$$L_{usefull} = \frac{4\mu_0 T_{turbine}}{B_{gap}^2 \, D_{gap}^2 \pi} \; [m] \qquad \text{eq 123}$$

l. Losses Calculation Efficiency, and Power Factor

Losses in electrical machines occur due to several phenomena. In normal operation it is at least difficult if not impossible to identify the sources of the losses observed (measured). The losses can be measured at [212], [23]:

- No load –claimed to be independent of the current
- Short circuit (load) losses –quadratic current dependency

Figure 86 shows the powers and losses diagram. For a generator the input power is the mechanical power P_{mec} and the output power is the electrical $P_{el.}$ The losses in the stator and rotor are shown. The iron losses P_{Fe}, copper losses P_{Cu}, the losses in PM P_{PM}, the mechanical losses, $P_{mecLoss}$ are the major classes of losses in electrical machines.

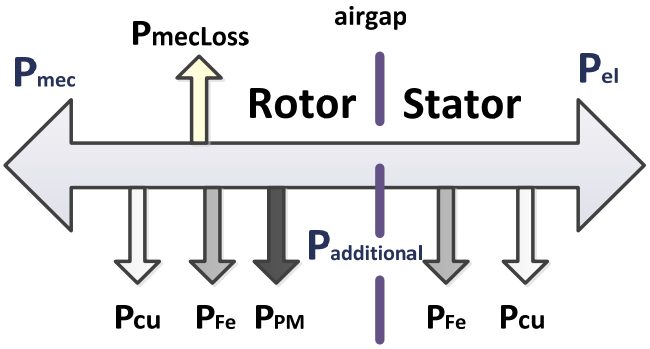

Figure 86:Power Flow Diagram: Electrical Machines-General

It is important to quantify losses in electrical machines. Estimation/calculation/measurements of losses give a view of the machine performance and can point to areas where optimisation is needed and worth it.

Because of losses, there will be a discrepancy between the input and output power of the generator. To quantify this discrepancy, the efficiency parameter is used (eq 124)

$$Efficiency_{Generator} = \frac{P_{el}}{P_{mec}} \qquad \text{eq 124}$$

In the following, the losses in electrical machines are discussed [30]. Formulae used in the design tool are given.

Copper Losses

Copper losses are due to the resistance of the windings and can vary widely with the load (I^2) (eq 125). These losses can be reduced by using high grade copper and having an increased cross sectional area of the winding conductor. [23]. It varies typically from 0.5% of the output (large machines) to 5% (medium size machines).[213]

$$P_{Cu} = m \cdot I_{rated}^2 \cdot R_{Phase} \qquad \text{eq 125}$$

Additionally, the machine can be verified with eq 126

$$P_{Cu_{Verify}} = \left(\frac{m \cdot EMF_{actallygenerated}^2}{R_{phase_{DC}}}\right) - \left(\frac{m \cdot V_{out_{rated}}^2}{R_{phase_{DC}}}\right) \qquad \text{eq 126}$$

Value from eq 125 and eq 126 should be roughly the same for a correct calculation.

The copper losses can be influenced also by the geometrical placement of the conductors as this influences the current path shape. Details may be found in [214].

Simplifying assumptions

- a uniform current path was assumed in the coil
- conductors are clean of any alien substances(oil, sea water, etc)

Iron Losses

Time-changing magnetic flux creates magnetization losses and consequently heating. These losses called iron losses are given for each material as a sum of Hysteresis and Eddy Current losses [30], [30]

They are difficult to determinate accurately. Losses due to the main flux are mostly constant for a given voltage. They are independent of the load [215]

The iron losses were calculated as a sum of the hysteresis and eddy current losses (eq 127):

$$P_{iron} = P_{hysteresis} + P_{eddy} \quad \text{eq 127}$$

The **hysteresis losses** keep account of the magnetisation parameters of the lamination [216]:

$$P_{hysteresis} = kh \cdot \frac{1}{iron_{density}} \cdot f^{fHysExp} \cdot Bin^{BHysExp} \quad \text{eq 128}$$

Where

$$B_{in} = \frac{B_{max} + B_{tooth}}{2} \quad \text{eq 129}$$

kh=hysteresis factor. For laminations used in ClassicRFNessie dk66, $kh = 2$
B_{max} is the maximum allowed flux density in the machine. The value is set by the designer
$fHysExp$ =2 is the exponent for frequency in hysteresis loss estimation
$BHysExp$ =1.2 is the exponent for peak magnetic induction in hysteresis loss estimation

The alternating magnetic flux induces an EMF in the iron. This produces currents that flow in any closed path available. These currents are called Eddy currents and they produce losses and reduce the flux capacity of the machine [217]. The **Eddy current** manifests itself as heat in the iron material

$$P_{eddy} = \frac{\frac{1}{iron_{density}} \cdot \pi^2 \cdot f^{fEddyExp} \cdot (lamThick \cdot mm2m)^{lamThkExp} \cdot Bin^{BEddyExp}}{6 \cdot rho_{iron}} \quad \text{eq 130}$$

Where

$iron_{density}$ = 7870 kg/m^3
$fEddyExp$ = 2 is the exponent for frequency in eddy current loss estimation
$lamThkExp$ = 2 is the exponent for lamination thickness in eddy current loss estimation
$BEddyExp$ = 2 is the exponent for peak magnetic induction in eddy current loss estimation
rho_{iron} = 61.9·10^{-9} is the ohm/m at 20 deg. C

In the design tool, all losses except iron, copper and the ones in PM[217] are incorporated under the generic name of additional losses $P_{additional}$.

Mechanical losses (additional)

The mechanical (additional) losses comprise losses due to friction (e.g. bearings) and windage (air-gap friction, cooling) and are generally difficult to assess. They are mainly a function of machine speed, they are assumed constant for a small variation of the speed [218]

The literature suggests that they are considered 0.5-1% theoretically. Experimentally they were found to be greater [213]. In the design tool, eq 131 was used to approximate the additional losses for Nessie.

$$P_{additionalLoss} = 0.05 \cdot P_{mec} \quad \text{eq 131}$$

The total losses were expressed with eq 132

$$P_{totalLosses} = P_{iron} + P_{Cu} + P_{additionalLoss} \quad \text{eq 132}$$

Losses in PM

The PM losses can be iron losses in PM:

- eddy current-induced currents in the material
- hysteresis-because of the changing level of magnetisation

The demagnetisation of PM [23] depends on the demagnetising element and the time of exposure to these elements:

- High magnetic fields that exceed the coercitivity of the PM. The value of this field is specific to each magnet. The demagnetising field can be produced by the windings.
- High temperatures. Above the Curie temperature (NdFeB magnets 310-400C) demagnetisation occurs. Unallied NdFeB may not be used at temperatures exceeding 60C.

When Dysprosium is added (Br is decreased and the price of PM in increased), the allowable temperature could increase to 200C and over.

The PM losses were not implemented in the calculation tool.

m. MakePowers

The active, reactive and apparent powers are given in eq 133, eq 134 and eq 135[147]

$$P_{active} = \left(\sqrt{3} \cdot EMFactallygenerated \cdot I_{line} \cdot cos(fi)\right) - P_{totalLosses} \text{ [W]} \quad \text{eq 133}$$

$$Q_{reactive} = \sqrt{3} \cdot Vout_{rated} \cdot I_{line} \cdot sin(fi) \text{ [VAr]} \quad \text{eq 134}$$

The apparent power is calculated using eq 135

$$S_{apparent} = \sqrt{P_{active}^2 + Q_{reactive}^2} \text{ [VA]} \quad \text{eq 135}$$

The efficiency can be calculated with eq 136

$$EfficiencyGenerator = \frac{P_{generated}}{P_{mec}} \quad \text{eq 136}$$

The obtained power factor is (eq 137):

$$cosfi_{Obtained} = \frac{P_{active}}{Q_{reactive}} \quad \text{eq 137}$$

n. Checkers

Checkers are functions that evaluate whether a calculation result is what is expected. The three main checkers are

- **Demagnetisation of PM**

The PM is designed to have a certain length that would keep it under an expected overcurrent (eq 44).

The PM can be checked against the expected short circuit current. The operating point will move towards $H_{coercive}$ on the magnetisation curve, but not past H_{lim}, the limit point irreversible magnetisation.

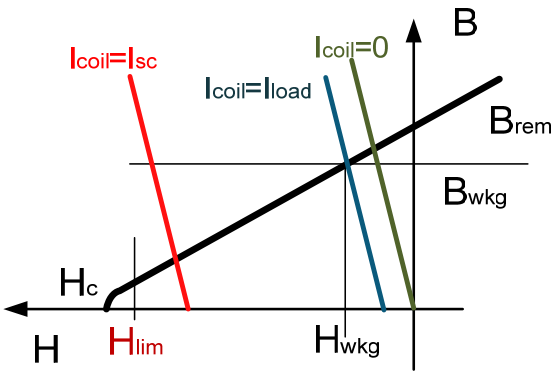

Figure 87: BH Curve - Demagnetisation

- **enoughEMFgenerated**

The EMF generated by the designed windings is compared against the desired value. Due to the fact that the machine has a large number of coils and that the turns in each coil can only be an integer number, one extra turn per coil resulting from rounding the required number of turns per coil will have a big impact on the machine.

The program is set up so that if the voltage generated by a coil is less than the desired one, the program will stop. In this case, adjustments need to be made. This situation is not normally encountered for tested and well known geometries, but when the user attempts to go outside the 'safe' interval for the input values or a new geometry is designed, this function is most useful.

- **isNegative**

Key geometrical values are kept positive by using the *isNegative* function.

At all times, the algorithm checks for inconsistencies, even if they are not normally expected. With this, the calculation tool, although simple and flexible, is kept on track by using checker functions.

o. Weights and volumes

The calculation of weight of active and inactive materials is done using a dedicated SolidWorks feature that calculates the volume and mass of parts that had a material assigned to them. The use of active material was assessed for each design. The determination of the inactive mass requirements was left for future work.

p. Cost Evaluation

The cost for manufacturing depends a lot on the quantity of products. The cost for a prototype is highest. The more turbines of the same kind are manufactured, the less their manufacturing cost will be. For the materials-for a purchase of a large amount of material, the price can be reduced by negotiation. The price paid by a turbine manufacturer is usually kept secret. As an in depth structural design of the generator was not the focus of the present work, the cost of the additional mechanical structure and the machine design alterations due to this were not evaluated.

Considering these facts, it is difficult to estimate the

-cost of active materials -cost of inactive materials

-expected cost of transport -expected cost of maintenance

An attempt to estimate the cost was made using the INWIND project values see cost estimation in Table 38. With this the cost of the materials can be roughly calculated. The overall cost of the turbine will be influenced by added costs like manufacturing and transport.

Copper	15 €/kg
Ferromagnetic iron	3 €/kg
Sintered iron	36€/kg
Permanent magnets	50 €/kg
Structural steel	3 €/kg

Table 38: Cost for Generator Materials (Numbers From INWIND Project)

The design tool is prepared to receive up to date numbers for up to date calculations as the cost and performance of materials and services varies in time. (see Figure 88, Figure 89)

Structural steel: (includes the nacelle structure, does not include the steel that is meant to be introduced into salt water.

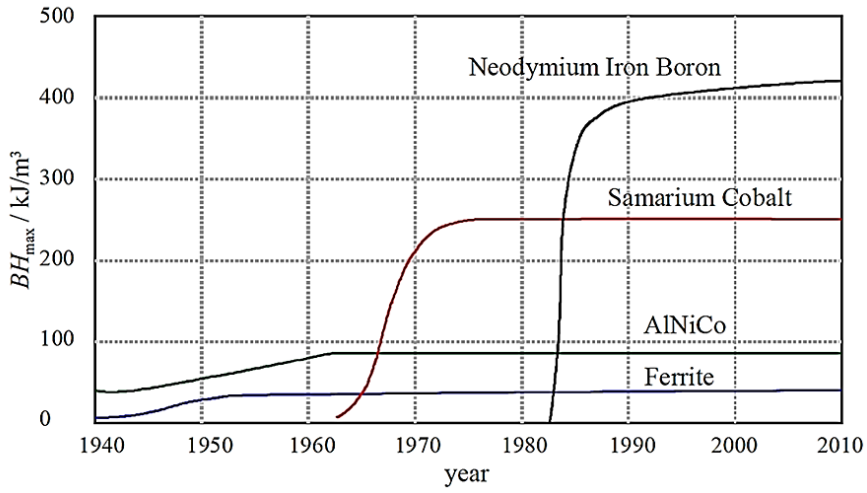

Figure 88: Maximum Energy Product Development Of PM Materials[213]

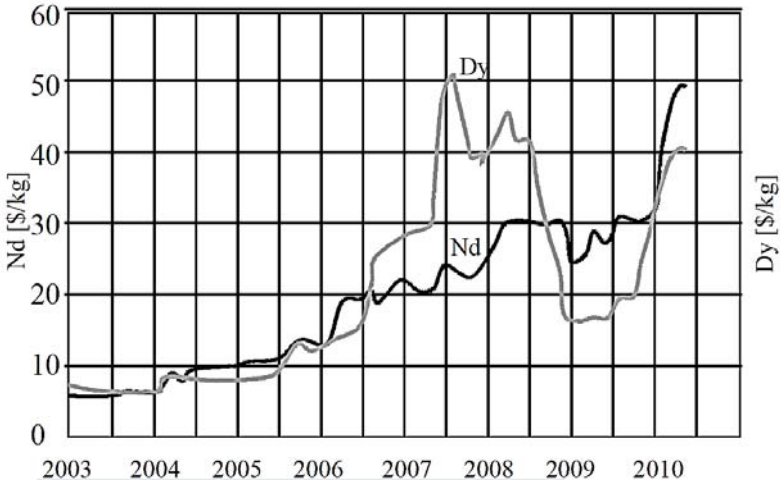

Figure 89: Price Development of Neodymium and Dysprosium in 2003 – 2010 [147]

The prices in Table 38 are not just for the raw materials, but contain manufacturing costs.

For the permanent magnets, the price is for Neodymium magnets without Dysprosium is given. The magnets that do not contain Dysprosium can have a maximum working temperature of around 80 C. this is considered the case for Nessie. If the working temperature is higher (120, 150 C), magnets containing Dysprosium are recommended [147], [219], [147], but the PM becomes much more expensive

Conclusions

The main equations used to construct the design tool sub modules were presented. A mix of theory and formulae were grouped in conceptual sections so that the reader would easily find the design concepts for a specific element e. g. iron, PM, windings.

Based on the presented equations, the radial flux machines presented in this thesis were calculated.

Appendix 9: Design Rules

This appendix discusses the different design rules for sizing electrical machines. The impact of their variation on the design is noted.

The design rules, quantities and ratios impact the design but with different intensity. The design rules and quantities are more or less fixed and it is recommended that only an experienced machine designer change the values as they have strong impact on the algorithm and results. They are tightly linked to physical properties of the materials and to the practical manufacturing process. The ratios can be modified by either the user by the algorithm itself.

A. Rules

- The distance between the PMs has to be around 5 times greater than the length of the air-gap. With FEM, the distance can be adjusted for a particular machine geometry.
- The PMs decide the air-gap flux density B that depends on the relationship between the tooth width and the slot width
- -In the stator tooth and core, the maximum flux density should not be more than 1.5 [T] when using usual lamination materials. Allowance should be made for the insulation material between laminations. Bgap=max 0.7.
- -Insulation material should withstand the operating voltage ranges. For Nessie, class H is considered appropriate. Given the fact that 20 [MW]Nessie is to be placed 200m under the sea, the 5C temperature should be taken advantage of for cooling purposes.(see also Appendix 6 for more about insulation, cooling and corrosion).
- One must account for the spatial interaction of the travelling magnetic wave and the winding.

The winding factor accounts for the angular displacement of the coil sides in a single phase. It has two components: one, takes account of the span of the coil as a fraction of the pole pitch. The other, for how the coil is distributed-how many coil sides makes a pole group.

B. Design quantities

Current density is used in designing the windings. It represents how much current will flow through the cross section of the conductor [A/mm^2]. It is set by temperature limitations of the winding, insulation and core. The cooler the machine is kept, the higher current density that the machine can be designed for. The higher the current density, the smaller the machine becomes.

Usual values are from 2 [A/mm^2] , but with a properly cooled Nessie 10 [A/mm^2] could be attempted. The value of the current density also affects copper losses, the higher the current density, the higher the copper losses.

b. The importance of **choosing numbers of slots and poles**-: It is important to avoid some combinations as they do not give feasible windings (concentrated windings). The unfeasibility might lie in unacceptable cogging torque, MMF harmonics and torque ripples. The combination for a concentrated winding is feasible if[150], [204]:

- number of poles must be an even number
- number of slots must be divisible by
    - m: number of phases –for double layer concentrated windings
    - 2m: number of phases –for single layer concentrated windings
- number of pole pairs/section are not divisible with number of phases
- Slots per pole and phase should be typically between [1/4,1/2] (120,240 degrees slot pitch)

Air-gap length

From a manufacturing point of view, the air-gap is desired to be as large as possible so that the precision needed for constructing the stator and rotor would be low. Also, with a large air-gap, fitting the rotor and stator together would not pose such a big problem.

Magnetically, the air-gap is desired to be small so that the field could be transmitted efficiently between the rotor and the stator.

With these considerations in mind, the question of the ideal air-gap arises. A FEM model of the machine can show the behaviour of the field for different air-gap lengths. An example for the 6 [MW] machine is shown in Figure 90. To have a flux density of 0.5 in the air-gap, for the machine in Table 39, the air-gap should be 10 [mm]

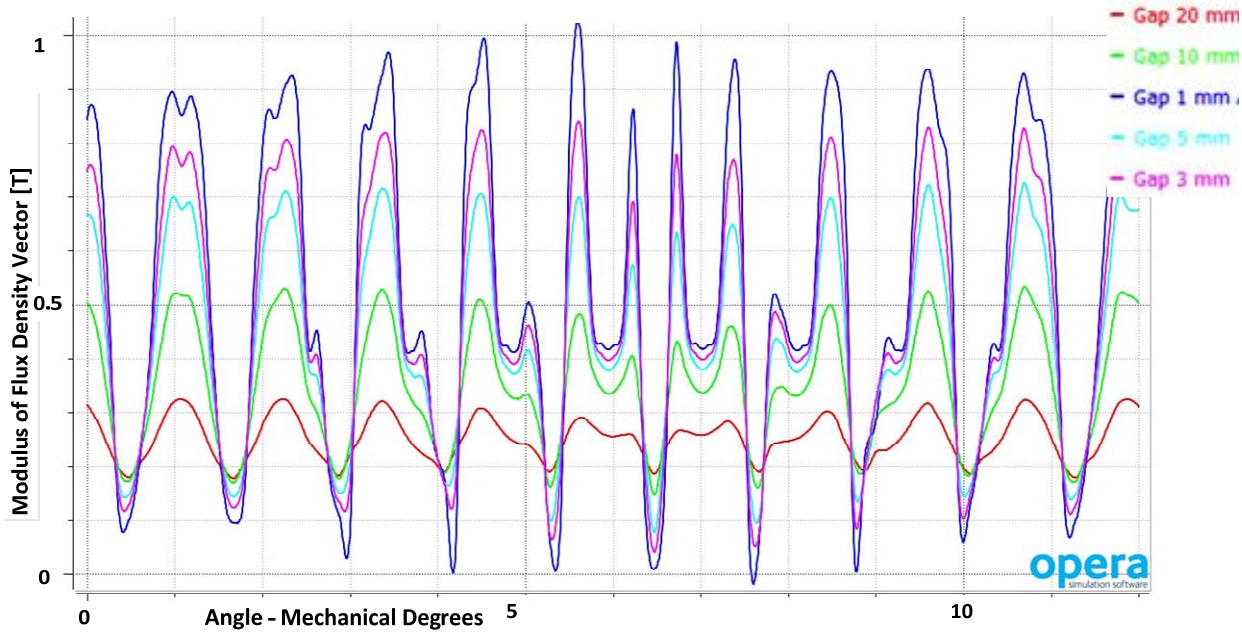

Figure 90: FEM ClassicRF Nessie 6 [MW]–NoLoad FluxDensity Bmod (pole same direction in graph)

The set of inputs from was considered

Number of pole pairs	150
Frequency [Hz]	15
Stator Bore Diameter [mm]	5811
Stator Outer Diameter [mm]	5633
Stack length [mm]	2648
Stator Slot Dimensions (Semi-closed, Square slot bottom (parallel tooth))	
Stator slot opening [mm]	32
Stator slot depth [mm]	70
Stator slot Width [mm]	32
Stator slot wedge height as air[mm]	3
Stator slot per slot pitch	0.5
Stator coil height/width	55/14
Stator slot per slot pitch	0.5
Interior rotor, Surface mounted PM rotor	
Magnet fill	0.7
Magnet rad height	18

Table 39: 6 [MW] Radial Flux- Set of Inputs For Determining The Ideal Air-Gap From The FEM Model

BwkgCoefficient

For a certain PM with the associated magnetisation curve, the working point of the PM should be chosen. With this value the field produced by the PM will be designed. The value must be chosen carefully and the demagnetisation due to the winding current must be considered. This current would move the functioning point from the working point of the PM towards the irreversible demagnetisation point. (see more on the working point of PM in Appendix 8). The value for this coefficient is typically 0.8

IscCoefficient

This coefficient represents how many times the current is expected to rise over the rated value in a short circuit situation. For large machines, the short circuit current is approximated between 5-10 times the rated current.

C. Design Ratios

In the following, design rules used in the calculation process are discussed. The design tool is open to other design rules being added, that may arise based on experience gained during manufacturing and the design process.

The design geometry ratios are very important because they give the possibility to change the aspect ratios of the machine. The values for the ratios that are set as inputs serve in the first instance for initial estimations. Due to several constructional considerations they may or may not change. The design algorithm does not oppose the change of the design ratios without a good reason.

There are situations where two design elements should change the same quantity. In this situation, the developer chooses the dominant element. Usually both design elements are alternatively available. The inactive rule is commented out and/or signalled by the logger function.

In the following, the design ratios used are explained.

SlotPerSlotPitch

This quantity represents how much of the slot pitch should be slot and how much should be tooth. The slot accommodates the winding and the insulation (see winding factor). The tooth allows the flux to circulate without saturating. It is important to consider the appropriate ratio. As a start a 50% slot 50% tooth is considered (SlotPerSlotPitch =0.5).

If the space allocated for the slots is reduced, the amount of copper that can fit in the slot is reduced, thus increasing the resistance of the winding and the copper loss. Because the overall copper usage has decreased, the cost associated with this material will also decrease.

If the tooth air-gap area is increased, the cost stays virtually the same for the material because the customer pays for the entire sheet and not just for the lamination itself. Magnetically the flux density required to provide a given flux per pole can be reduced. This would most likely reduce the iron loss up to a certain point when the material (iron) becomes saturated. The delicate balance of copper /iron may be investigated by varying the value of *SlotPerSlotPitch.*

LStackToDgapAvg

This determines the length over gap diameter ratio. By modifying this quantity, the machine can be made longer or shorter modifying the diameter accordingly to keep the same bore volume. By making the diameter smaller, the space for the number of poles and consequently the windings becomes smaller.

Since in normal operation the turbine is expected to tilt, the centre of gravity could become an important driving quantity for the overall structure design. The centre of gravity of the generator, and thus the turbine, can be moved by changing this ratio.

DboreToDstator

The bore to stator diameter ratio quantifies the geometrical proportion of the stator. By modifying this quantity, the effective stator yoke height can be changed.

PM2PolePitch

Because PM are expensive materials that produce a part of the rated field at the side edges of the pole, the idea of not covering the entire pole with magnet is introduced (eq 138):

$$PM2PolePitch = \frac{w_{PM}}{PolePitch} \quad \text{eq 138}$$

Where w_{PM} is the width of the magnet.

By having a shorter PM pitch than the pole pitch, the fringing flux is attempted to be used as useful flux while using less magnet material (

Figure 91). The range for this ratio is recommended to be around 0.8 of the pole pitch.

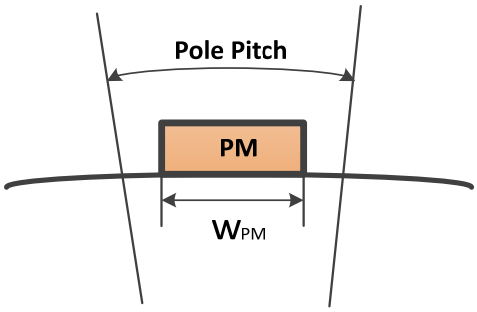

Figure 91: Smaller Width Of PM Than The Pole Pitch To Allow For Fringing

For BabyN, the PM2PolePitch was 0.46 and the results of this can be seen in the harmonic content of the phase and line generated voltages at no load and 500 [RPM](apparent in

Figure 92):

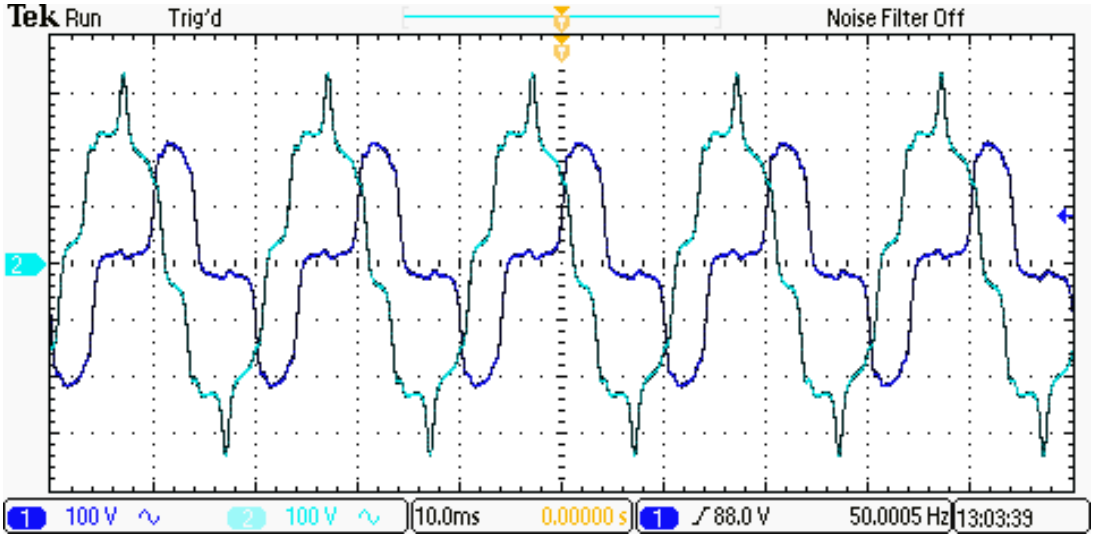

Figure 92: Line(green) and Phase(blue) Voltages Generated by Baby N at No Load

The PM2PolePitch must be large enough for the machine to generate a sinusoidal voltage, but not as large as would cause excessive leakage flux.

SlotWidthPerHight

Defines the relationship between the slot width and height dimensions. It is important to correctly asses the leakage field taking into account the length of the slot. Ideally, to have a smaller diameter, this coefficient should be as small as possible (height larger than the width). A stopping factor is the space needed for the winding and insulation. All the turns needed to produce the flux together with the insulation must fit keeping a satisfactory slot fill factor.

CoilWidthPerHeight

Defines the aspect ratio of the coil cross section. The resulting slot is linked to the type of the winding chosen (e.g. difference between single and double layer concentrated windings). For a small value, the coils are set high into the core and the outside diameter of the machine becomes smaller.

SlotPolePhase

Slot per pole and phase (eq 139) represents how many slots are allocated to each pole in a phase.

$$SlotPolePhase = \frac{Q_s}{poles \cdot m} \quad \text{eq 139}$$

For concentrated windings this is an important design rule as this variable defines the validity of a certain combinations of slot poles and phases

The feasibility region is defined for SlotPolePhase [19].

$$SlotPolePhase \in \left[\frac{1}{4}, \frac{1}{2}\right] \quad \text{eq 140}$$

Conclusions

In this appendix the design rules, quantities and ratios used for designing Nessie were presented. Appendix 8 shows how these elements are used in the design process.

For a comprehensive list of design elements, working voltage, the insulation system, the current density, the flux density, the acceptable abnormal operation, the limits of normal operation should also be included. Due to newer manufacturing technologies (compared to the time when [20] was written) and taking into account that Nessie requires design peculiarities, alterations to the designs in the literature will be necessary.

Appendix 10: Validation of the Design Tool

In the following, validation methods for the calculation results of the design tool are presented and discussed. Several methods applied for the present work are presented: comparison to literature reports, visualisation in 3d models, finite element and prototyping.

The design tool, even though it generates a set of numbers composing a design, steps must be taken to verify the validity of the output quantities. This cannot be done by only one means of validation. The design tool calculations have been checked against several elements. Adjustments were made as a result of this analysis. In the following each validation method is presented.

The main objective is to extract all the concept errors from the equations and approach of the design tool. This is the first step of building a foundation for a reliable design tool that has a larger number of modules and that are more complex than the presented version.

A. Literature

The approach is to calculate reported machines using the design tool and compare for active mass elements like copper, iron core and permanent magnet mass.

A machine for a given set of requirements will differ geometrically from designer to designer due to the different approaches taken. The cause of this difference may be either the intent of the designer/manufacturer or the impact of an optimisation algorithm. In view of this, the literature comparison is not expected to report a perfect match between the result of the design tool and literature reports. It is however expected that the compared quantities-diameter, lengths, active mass to be in the same range.

Main literature sources are [22], [164], [163],[220], [28]. The type of literature machine would be ideally un-optimised radial flux PM machines. The total active mass of the two machines was compared.

Table 40 compares two radial flux machines. The literature machine [221] and the Classic RF Nessie have close enough **LstackToDgapavg** ratios for the 10 [MW] machine. For the 20 [MW] machine, Nessie is shorter, thus making the aspect ratio smaller. The length calculated with design tool is adjusted by checking if the needed torque is generated. The diameter is set by the windings needed to produce the field in the air-gap.(details in Appendix 8: Design Tool Algorithm and Equations k.)

	PMSG [221]		**PMSG Classic RF Nessie**	
Rated power [MW]	10	20	10	20
Rotor speed [rpm]	10	7	10	7
Air-gap diameter [mm]	8000	10300	8000	1000
Axial length [mm]	2400	4100	2225	2034
Air-gap length[mm]	8	10	8	10
LstackToDgapavg	0.3	0.4	0.27	0.2

Table 40: RFPMG Direct Drive Literature Compare 10, 20 MW

For lower powers [221] gives the set of results in Table 41 to compare to the design tool equivalents. It can be observed that the active masses and the mass/torque ratios for machines of same power are fairly close in value.

	PMSG [221]			**PMSG Classic RF Nessie**		
Rated power [MW]	2	3	5	2	3	5
Rotor speed [rpm]	19.5	16	12.5	19.5	16	12.5
Torque rating [kNm]	0.979	1.790	3.820	0. 9794	1.7905	3.8197
Air-gap diameter [mm]	4.3	5.1	6.1	4.3	5.1	6.1
Air-gap length [mm]	4.3	5.1	6.1	4.3	5.1	6.1
LstackToDgapAvg[-]	0.2	0.22	0.27	0.18	0.2	0.19
Active mass [ton]	14.6	22.4	39.9	13.85	20.91	34.5
Mass/torque [kg/kNm]	14.91	12.51	10.44	14.14	11.67	9.03

Table 41: RFPMG Direct Drive Literature Compare 2, 3, 5 [MW][221]

Table 42 shows a comparison between a literature reported axial flux machines with high power ratings (up to 20MW) [221] to a surface mounted RFPM machine with the design tool (un-optimised Classic RF Nessie-see also Appendix 8: Design Tool Algorithm and Equations and the machine concept in Chapter 3: 6 [MW] Candidates). This literature report was chosen because it delivers a relevant set of values to machines that are close to what Nessie should be. The power and speed are stated together with geometrical characteristics.

	Axial Flux [164]			**Classic RF Nessie (Basic)**		
Power [MW]	5	10	20	5	10	20
Rotational speed [rpm]	12.1	8.6	6.1	12.1	8.6	6.1
Air-gap diameter [m]	6.3	8.9	12.6	6.3	8.9	12.6
Air-gap length [mm]	6.3	8.9	12.6	6.3	8.9	12.6
Number of pole pair [-]	99	140	198	99	140	198
Frequency [Hz]	20					
slots per pole per Phase[-]	1	1	1	0.35	0.36	0.36
Stator slot width,[mm]	15	15	15	34	36	52
Stator tooth width [mm]	18	18	18	58	56.5	139
Stator slot height,[mm]	80	80	80	63	63	85
Stator yoke height, [mm]	40	40	40	58	56.5	139
Rotor yoke height, [mm]	40	40	40	58	56.5	139
Magnet height, [mm]	17	23	31.5	30	34.2	65.5
Rotor pole width,[mm]	80	80	80	85	84.8	177
Mass						
PM[ton]	3.2	8.9	25.2	4.9	11	20.3
Copper [ton]	8	15.1	28.8	4.2	8.1	9.1
Stator iron [ton]	21.8	42.7	85.8	15.3	29.5	64.1
Rotor iron [ton]	10.1	20.9	40.2	9.7	19	44.7
Total [ton]	43.1	87.6	180	34.2	67.64	138.3

Table 42: Literature vs Design Tool Parameters [164]

The total mass of active material needed to produce the required power at the given speed is close values for the axial and radial flux machines. For the individual materials, values differ more widely as the geometry of each machine type is different.

Table 43 shows machine designs from [164] and the design tool for 5 and 10 MW. It is observed that again the values for both design sources are in the same range.

	Optimised PM[222]		**Un-optimised Classic RF Nessie**	
Rated Power [MW]	5	10	5	10
Rated rotor speed nr [rpm]	14.8	10	14.8	10
Generator system dimensions				
Air-gap diameter [m]	7.5	10	7.48	9.98
Stator length [m]	1.5	1.81	0.85	1.4
Pole pitch [mm]	81.5	95.2	117	111
Stator slot height [mm]	68.2	83.3	75	70
Stator sloth width [mm]	12.1	14.3	42	41
Stator tooth width [mm]	14.9	17.5	55	79.5
Stator yoke width [mm]	17.1	28.2	55	79.5
Magnet height [mm]	12.5	23.2	45	43
Magnet width [mm]	56.8	66.8	123	111
System weight [ton]				
Iron	19.6	44.9	16.8	51.1
Copper	5.46	10.8	4.5	6.58
PM	2.35	7.02	4.9	10.5
Generator active material	27.4	62.8	26.4	55

Table 43: Main Dimensions and Performances of the Optimized PM Generator System [222]

Figure 93 shows total mass estimations for different existing generators [222]. (The DFIG has a 3 stage gearbox).

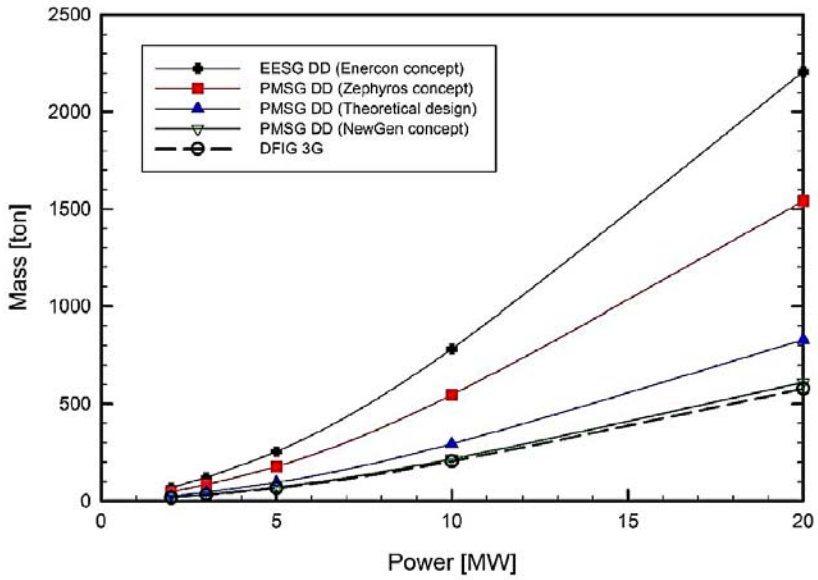

Figure 93: Total Mass Estimation Of Five Different Generators Currently In Use [164]

Even though the design tool does not estimate the inactive mass of the generator, the active mass can be obtained. Figure 94 shows the estimated active mass of [2-20 MW] un-optimised ClassicRFNessie for 12 [rpm] speed. Results were obtained by redesigning the machine for the same speed, but different powers.

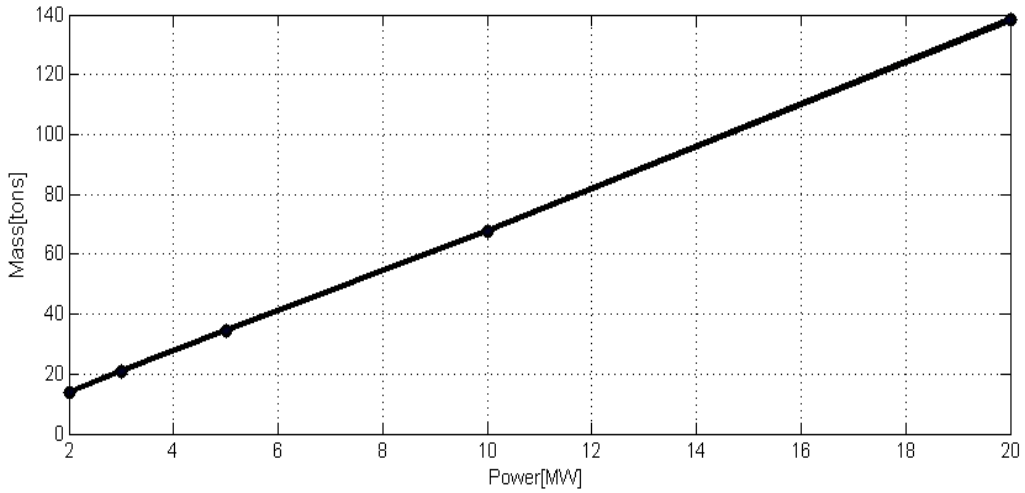

Figure 94: Literature reporting vs Nessie- Active Mass for Un-Optimised Classic RF Nessie(12 [RPM])

By having the estimation of active mass material given by the design tool , with calculations of what the mass of the structural elements would be(future work-see Chapter 6: Future Work) and by taking into account the environmental constraints of the turbine siting(under sea placing), the overall weight of the designed generator can be evaluated.

Conclusions

Classic RF Nessie was compared with literature reports. The design tool received the inputs suggested by each literature item. The weights of the active materials obtained from the CAD model associated to each Nessie design were compared with the reported ones. Although the machines are different geometrically, roughly the same material should be used to cater for the application they were designed for.

Based on the comparison between literature reports and design tool outputs, it is concluded that the design tool generates designs that are close to the reported ones.

B. Software

The communication language between designers and manufacturers are complex electronic models. These help parties involved to observe, discuss and modify the design according to a various set of specifications and standards required by all sides.

Analytical calculation and FEM results have a great impact on shaping the design. However, manufacturing issues have the ultimate say. Work drawings were needed to be delivered to the workshop for the making of the prototype and will be needed to commission the full scale generators as well.

Besides these issues, the software models were used to check the validity of the (analytical) design during its development process. In the following, analysis and validation using the CAD, the analytic design itself and FEM are discussed.

a. CAD Computer Assisted Design

A 'finished paper design' must be viewed in 3D and discussed with the workshop. In order for a set of final technical drawings (+DXF files) to be made, a CAD design is necessary. Alteration suggestions that come from the manufacturers of the machine are to be taken into account by modifying the CAD drawing of the 'finished paper design'.

The model is assembled out of part drawings united in an assembly model. The program used was Solid Works 2011.

The analytic program (code) outputs a list of dimensions for the current design. Using these dimensions that are 'publicly defined', the geometry of the machine is drawn.

The CAD has the following main purposes:

1. To **observe the geometry of the current design**. A first analysis on the feasibility of the design can be made. Geometrical aspect ratios can be very easily seen and investigated.

2. To **produce a set of work drawings** for the workshop to use in order to program their machine tools that shape the components of the generator and for personal orientation.

3. To **allow for adjustments** that are to be made. Parties involved in the design of the overall turbine/generator system will come with suggestions to change the design so that is easier, better or cheaper to construct.

4. **Produce a new set of geometrical dimensions** that are based on the analytical design, but are (maybe) altered as a result of the CAD design. These refined dimensions may be transferred to the FEM for magnetic field analysis. The actual bidirectional communication however is left for future work

5. The generator **CAD model can be further integrated** in a turbine CAD model if so desired

6. Use the CAD models to **communicate with design partners**:

- **Turbine designers**-need to know the estimated weight of the generator. This assessment can get difficult to make analytically when refined design of the generator components is made.

- **Structural mechanics**: generator box, bearing designers. Evaluation of mechanical parameters like inertia and weights of a group of subsystems can be used. Because the generator has to stay submerged up to a defined level, the turbine designers have suggested a floater. This has to cancel out part of the turbine rotor weight (generator rotor, bearings, tower blades and additional constructions linked to the rotational part). During the design process, as subsystems change, the impact of these changes can be easily evaluated. Judgment on whether or not connecting elements should be changed can be taken. Design reiterations of the subsystems can be made based on the conclusions.

- **Others**: for dissemination and marketing purposes. A 3D picture is easier to understand than a text description or a 2D sketch

7. The CAD model obtained through the design tool may be completed by **adding auxiliary parts** e.g. casing, endplates, bearings, shaft

To obtain a usable model, material properties must be assigned to each component.. The densities of the materials used in the CAD models are listed below in Table 44.

Material	Mass Density [kg/m^2]	Comments
Iron Core Lamination	5850	Value from the BabyN validation
PM	8200	Neodymium Iron Boron
Copper	8900	Solid Works Materials database

Table 44: Generator Materials Density Used In the CAD Model

b. Matlab Design Evaluation

For the benchmark Classic RF Nessie, a set of curves demonstrating the behaviour of the design tool were generated using a dedicated function of the design tool.

By analysing these curves, one can appreciate whether or not the calculations give the logically expected values. Original and fitted curves are displayed for each graph.

Figure 95 shows the stator diameter variation as function of shaft speed. This is expected as the lower the speed, the more poles are needed.

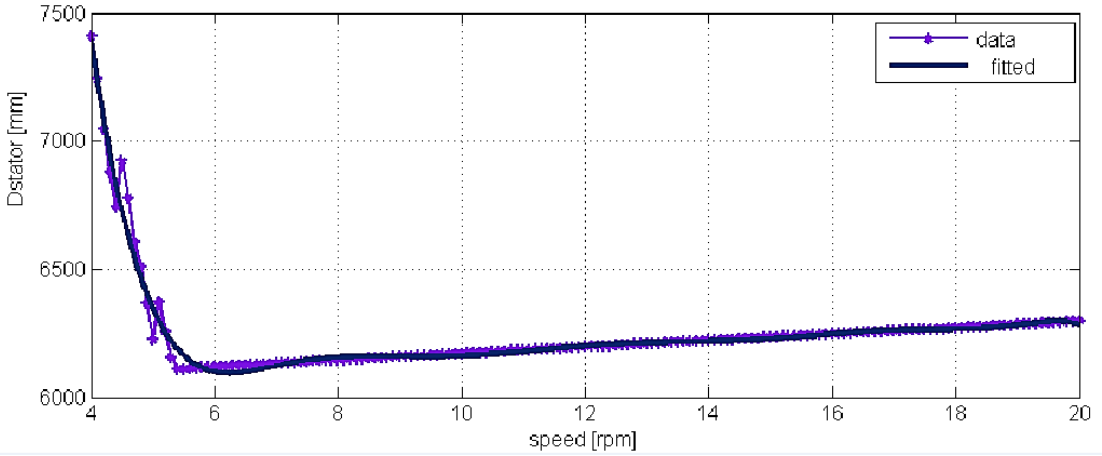

Figure 95: Stator Diameter as Function of Speed

For an increase in speed, the length of the generator decreases .A rapid fall in diameter can cause slight increase in Lusefull (Figure 96)

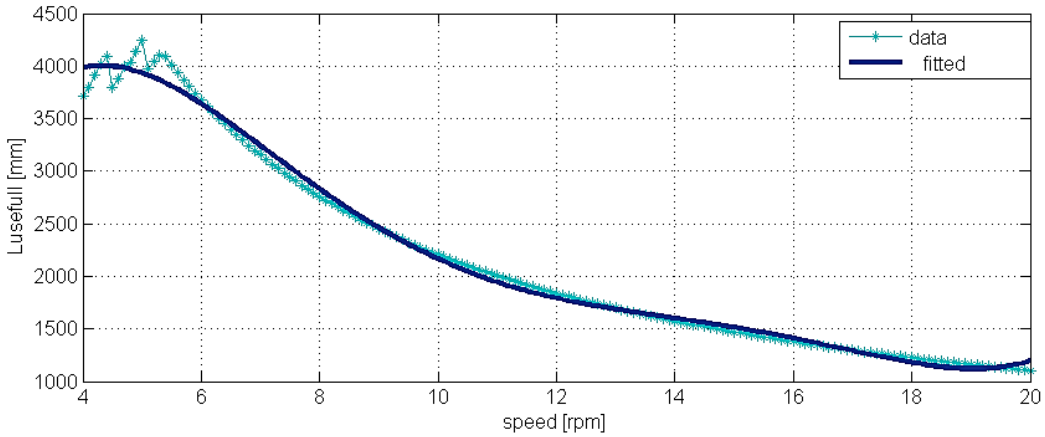

Figure 96: Useful Length vs Speed

Figure 97 shows that the mass of the PM also decreases if the speed increases.

The rise in diameter (Figure 95) after 6 [RPM]is caused by the aspect ratio adjusting itself. It can be seen from Figure 95 and Figure 96 that as the diameter increases, the useful length of the machine decreases.

Figure 97 shows that for a relatively constant diameter and decreasing machine length, the mass of the PM is falling as expected.

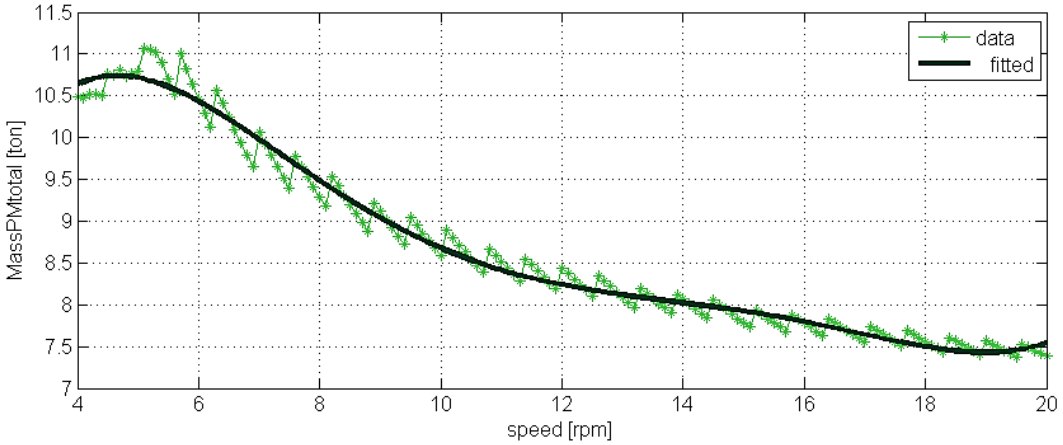

Figure 97: Mass of PM as Function of Speed

The electromagnetic torque that needs to be produced by the generator to balance out the turbine torque decreases if the speed increases (Figure 98)

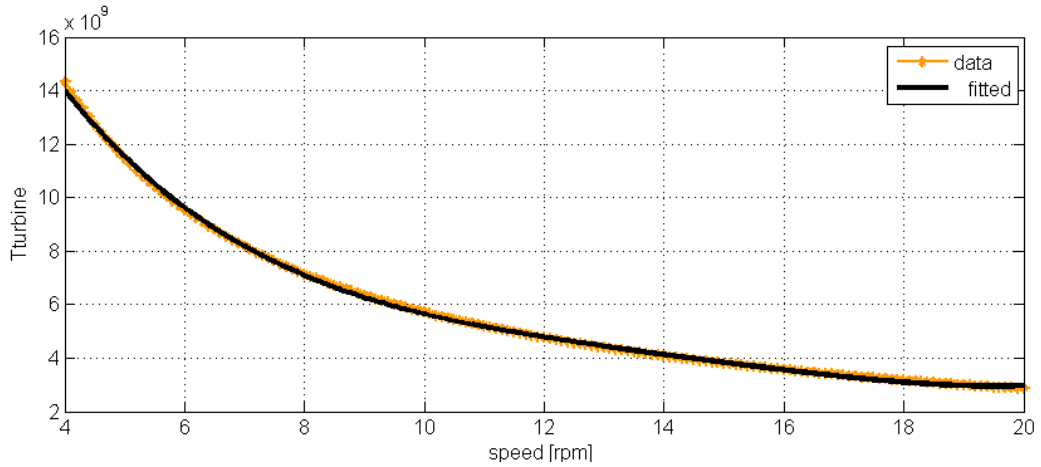

Figure 98: Torque as Speed

The number of poles vs speed is presented in Figure 99

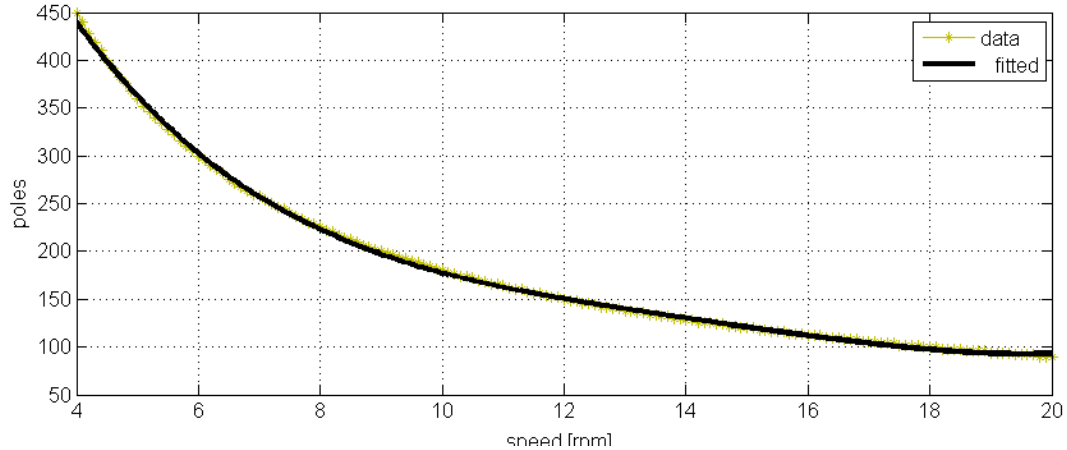

Figure 99: Poles as Speed

The number of slots gets reduced as the speed increases (Figure 100)

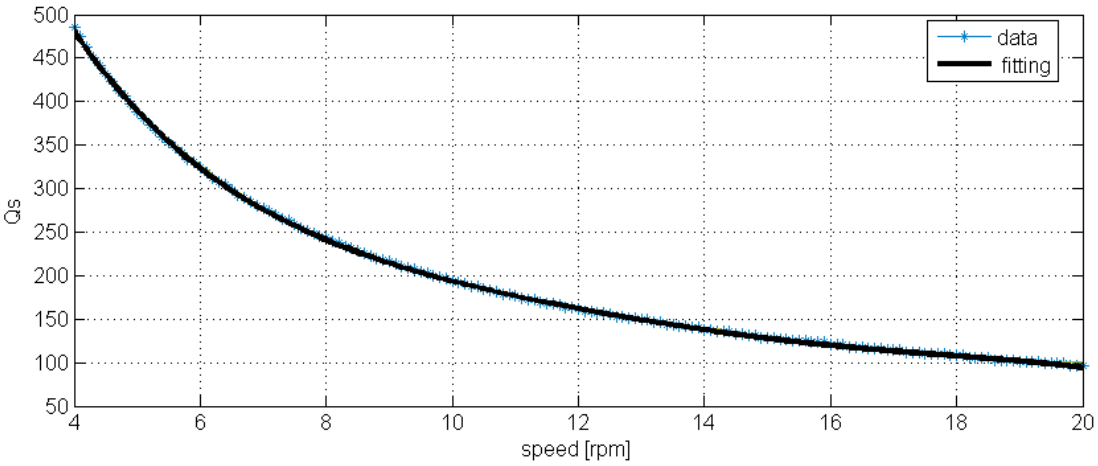

Figure 100: Number of Slots as Function of Speed

Consequently of Qs being reduced, the flux per coil increases (Figure 101):

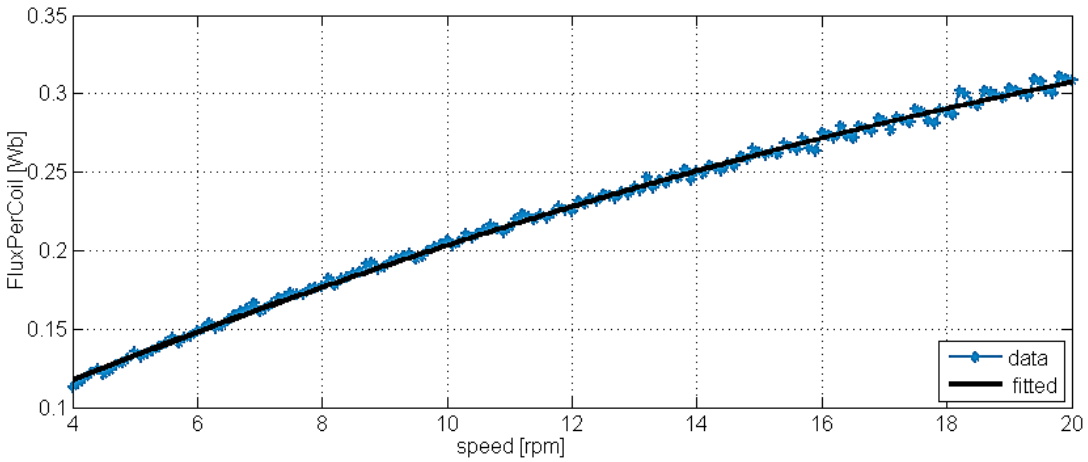

Figure 101: Flux per Coil as Function of Speed

The area of each pole will increase as the diameter is relatively constant and the number of poles decreases (Figure 95, Figure 99). With this, the pole area increases for a constant flux density as shown in Figure 101.

The number of turns in the coil (Figure 102) depends on the flux per coil x speed/volts per coil. If the Qs decrease, the volts per coil will change Figure 103

The number of coils Qs decreases as the speed increases (Figure 100), at a constant diameter (Figure 95), the turns per coil must increase to maintain the required EMF.

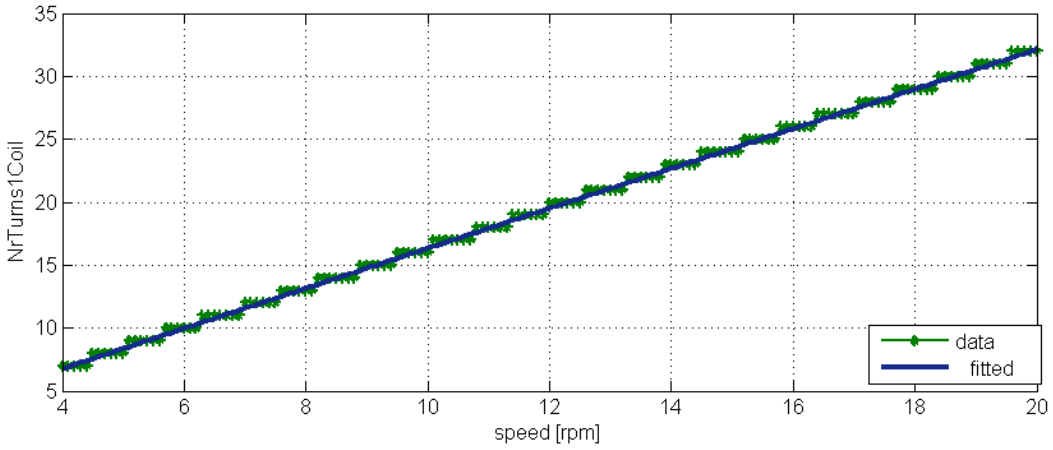

Figure 102: Turns in One Coil as Function of Speed

As expected Figure 103 shows that the EMF per coil rises steadily with speed -Figure 103.

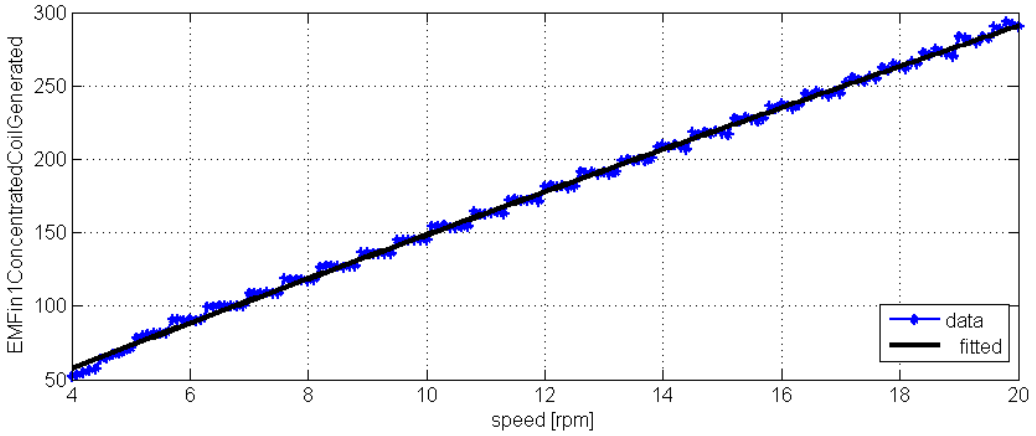

Figure 103: EMF as Speed

As the number of slots decreases (Figure 100), and the frequency is constant, the EMF of one coil must increase to get the same phase EMF.

By observing the curves given by varying the speed, the conclusion was taken that the plotted quantities vary as expected.

In the following section, *C. Prototyping-BabyN,* the use of FEM analysis to determine the machine parameters for Baby N as well as how the formulae were validate din partly by FEM is discussed.

c. FEM Model

By looking at the geometry together with the field distributions and magnitudes, FEM helps give ideas on changes to be made to the machine geometry and electromagnetic characteristics. Examples: use of another material; changing the iron geometry.

A file is written by the analytic program that initialises a corresponding parameterised FEM model. In this way, new designs having the same geometry could be investigated.

Simulation results are highly dependent on the material properties as well as on the geometry and conditions considered. Exact knowledge of the material is usually difficult to obtain. Often approximated values are used. If set up correctly, the model gives reliable results.

Investigated quantities are typically:

- Flux linkage.
- Leakage flux
- Distribution of magnetic radial force around the periphery
- Cogging
- Eddy currents

The FEM models were used to calculate parameters for both the prototype and the large scale turbines. For the literature validation, a generic model was setup.

Baby N FEM model

The prototype Baby N FEM model is presented in Figure 104 - Magnetic vector potential (POT -lines) and the modulus of the magnetic flux density vector (BMOD-coloured zones). See also description of BabyN in Appendix 11: BabyN Prototype.

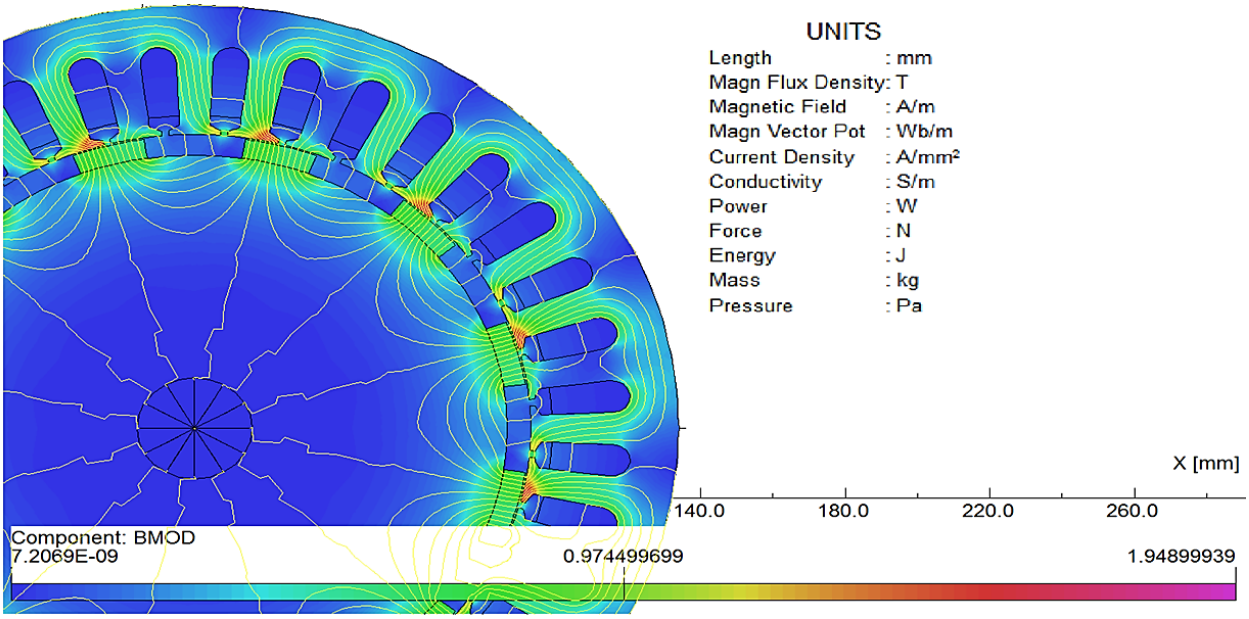

Figure 104:Baby N FEM Model-Magnetic Vector Potential(Lines) and the Modulus of the Magnetic Flux Density Vector(Coloured Zones)

Figure 105 shows the coils belonging to phase A. Figure 106 displays the materials defined in the model:

- Pale blue- stator iron;
- Dark blue -rotor iron;
- Grey -air;
- Red - winding; green- PM.

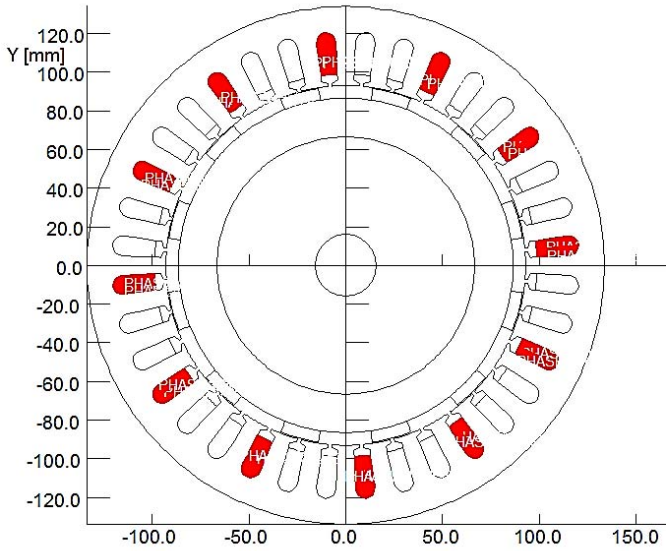

Figure 105: BabyN FEM Model - Phase A in Red

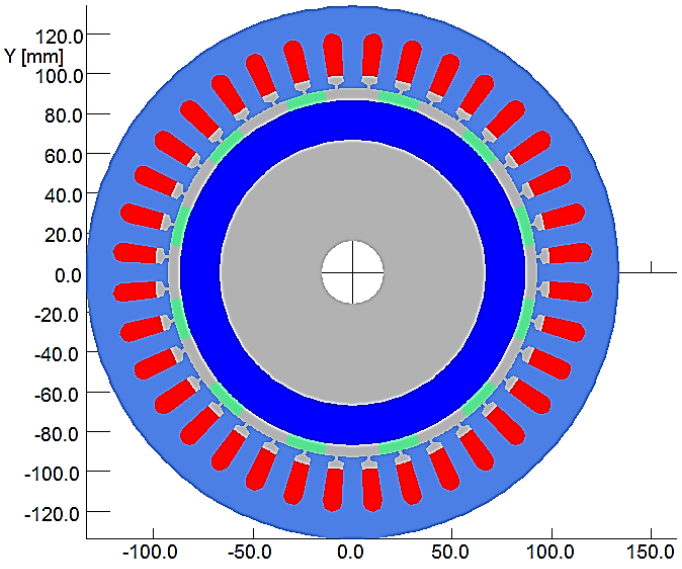

Figure 106: BabyN Materials.

Results related to figures showing the POT at different angles for 30.8 [A] RMS ($30.8 \cdot \sqrt{2} \cdot cos(angle)$))(Figure 107-Figure 112) are shown in Table 45:

Rotor angle[deg]	Flux linkages phase A [Wb turns]	The Torque [Nmm/mm]	Phase Voltage
0	0.0687	-711	
22.5	0.0683	-384	
45	0.0678	-670	
67.5	0.0687	-710	
90	0.098	1836	
112.5	0.193	1408	
135	0.3055	1402	
157.5	0.4067	1402	
180	0.4331	595	
202.5	0.4228	58	430
225	0.4265	-403	433.6
247.5	0.432	-684	440
270	0.375	-1937	381
292.5	0.260	-1410	273
315	0.157	-1389	159
337.5	0.0764	-1271	77.7
360	0.0764	-711	69.9

Table 45: POT Plots from BabyN FEM Model For Different Rotor Positions

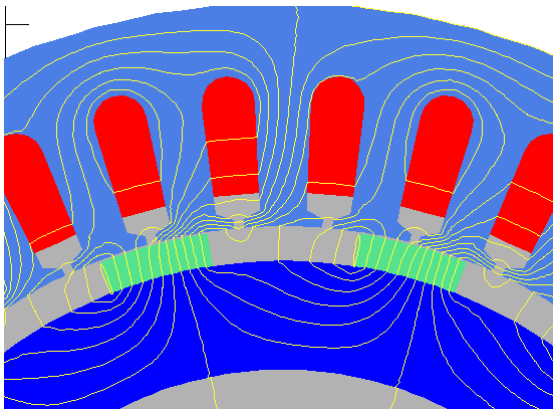

Figure 107: POT Position 0 deg 30.8 A RMS

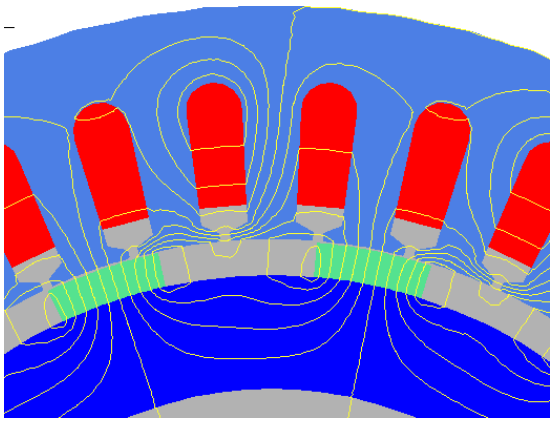

Figure 108: POT Position 22.5 deg 30.8 A RMS

.

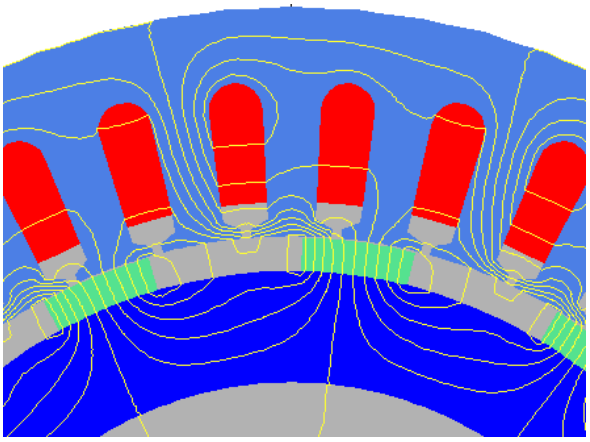

Figure 109: POT Position 45 deg 30.8 A RMS

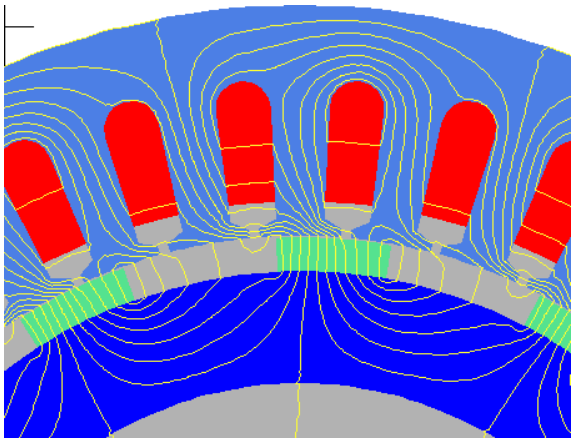

Figure 110: POT Position 67.5 deg 30.8 A RMS

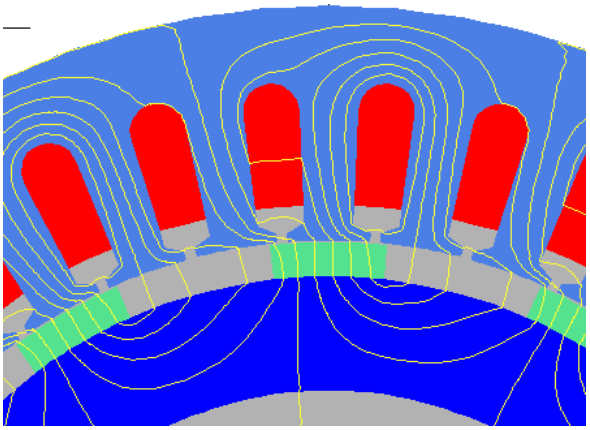

Figure 111: POT Position 90 deg 30.8 A RMS

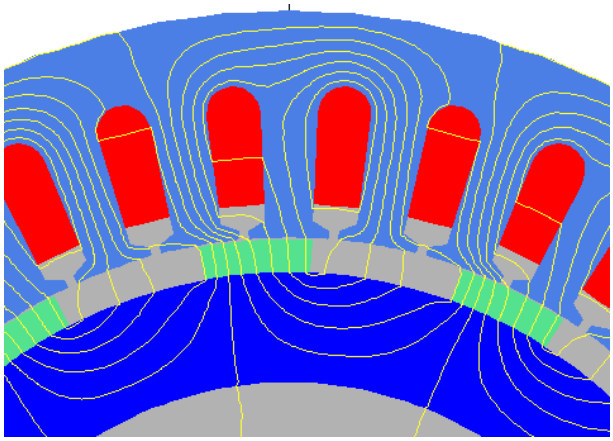

Figure 112: POT Position 112.5 deg 30.8 A RMS

The BMOD for all 12 poles of Nessie is shown in Figure 113.

The flux linkages in one phase due to the permanent magnets only at 0 deg rotation = 0.186 Wb turns

Phase Voltage RMS= 189.6 [V]

Torque = 0.0939 [Nmm/mm]

This torque represents the peak cogging torque of the machine. The value is relatively high as no provisions were made to minimise the cogging torque of the machine during the design process. This was done intentionally to provide experimental conditions for cogging torque investigations. With a large cogging

torque, measurements can be made more accurate using a torque transducer and a stepper machine. This investigation was left for future work. (Please see preliminary work in [164], [186])

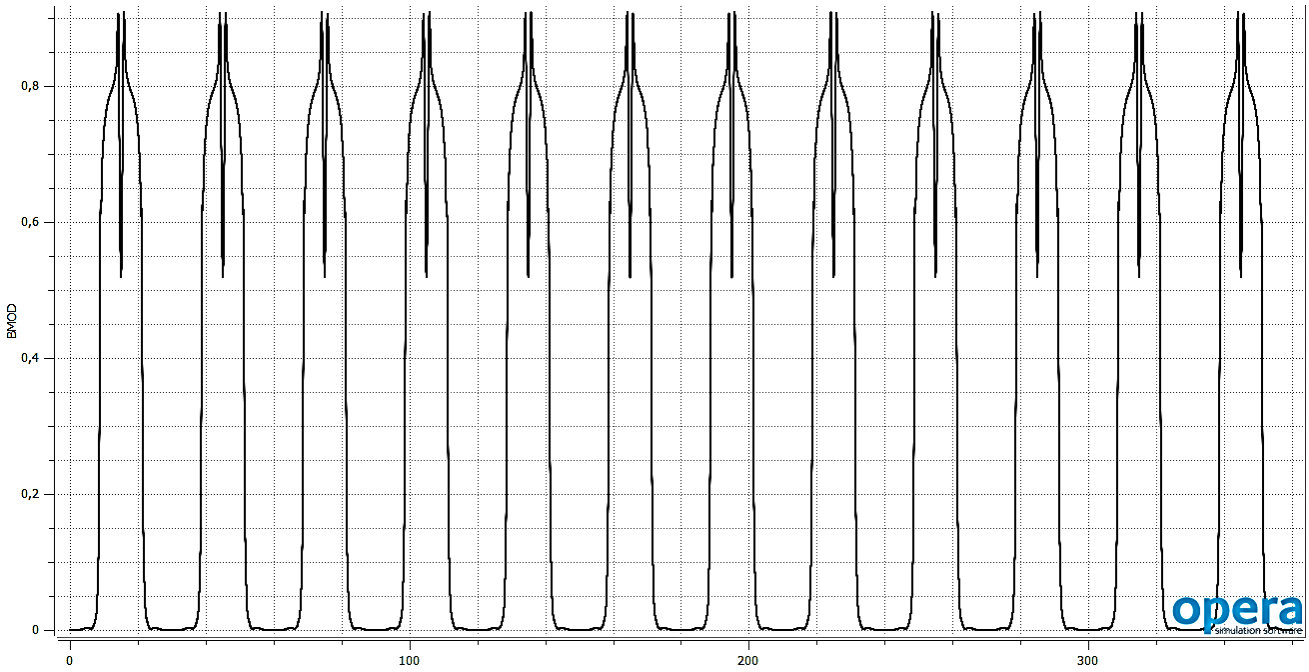

Figure 113: BMOD for the Whole BabyN 12 Poles-no Load at 0 deg

In this section, the FEM model used to analyse BabyN was presented.

Literature Validation FEM Model

For values in Table 42 for the [6 MW], 20 [Hz], 12.1 [rpm], 216 [A], Classic RF Nessie machine, a FEM model was built. The analysis of this machine in FEM was done because of the complete list of comparison data provided by the literature.

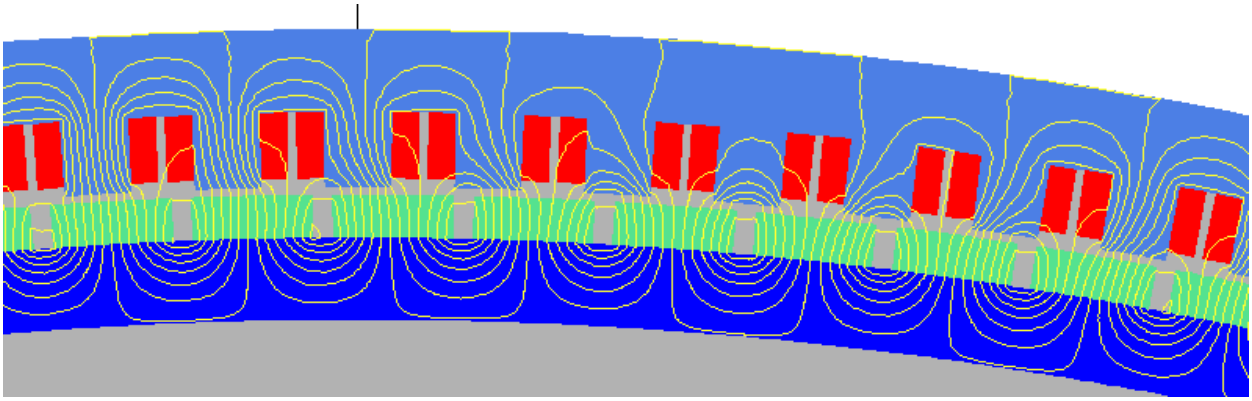

Figure 114: POT ClassicRF Nessie No-load 216 Slots 198 Poles

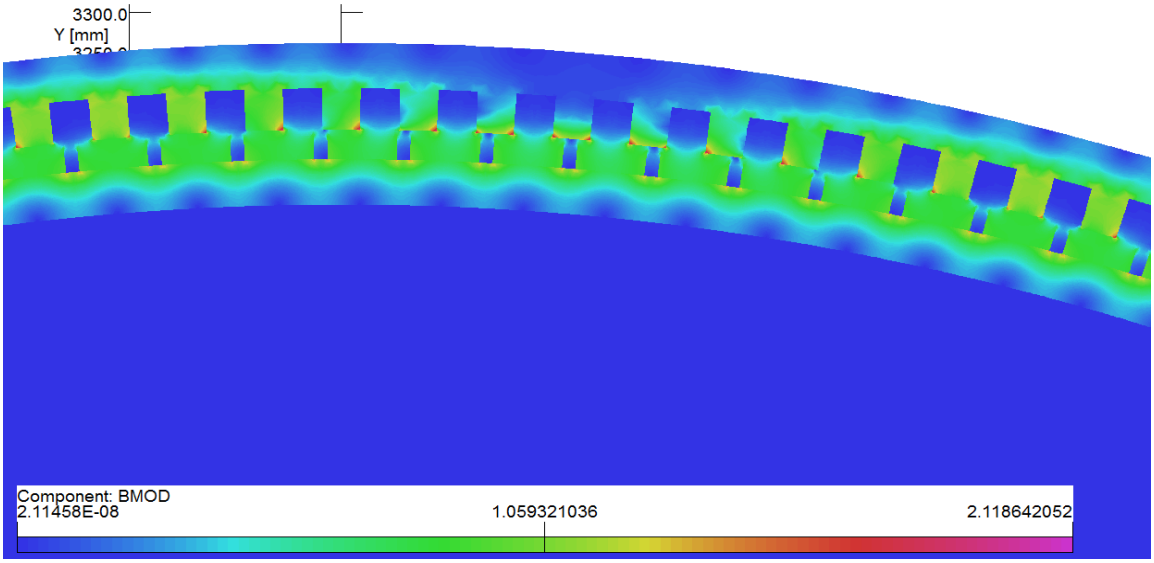

Figure 115: BMOD No-load 216 Slots 198 Poles

Flux linkage for one phase 41.677e-6 [Wb-Turns]

Voltage produced by one coil = 5.49 [V]

Voltage produced by one phase = 396.32 [V]

For the machine loaded with 216 A Figure 116 and Figure 117 were obtained.

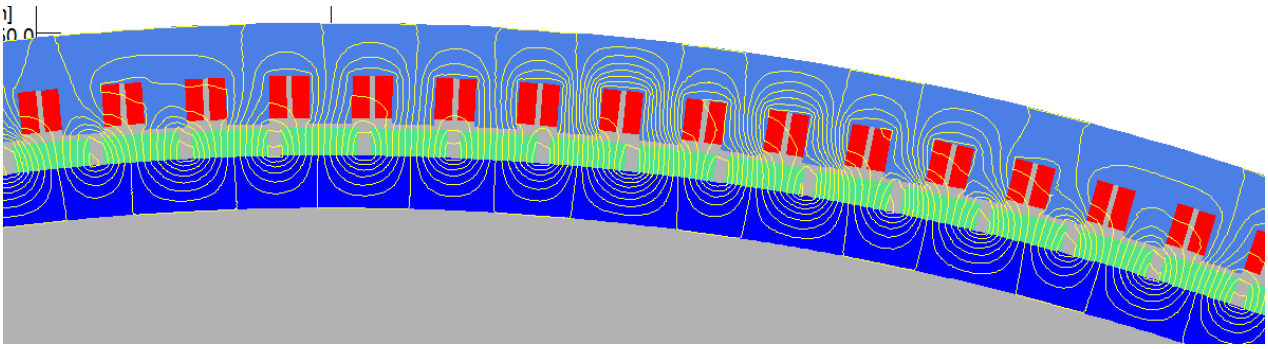

Figure 116: POT ClassicRF Nessie 216 A 216 Slots 198 Poles 22.5 deg. El = 90 deg. El

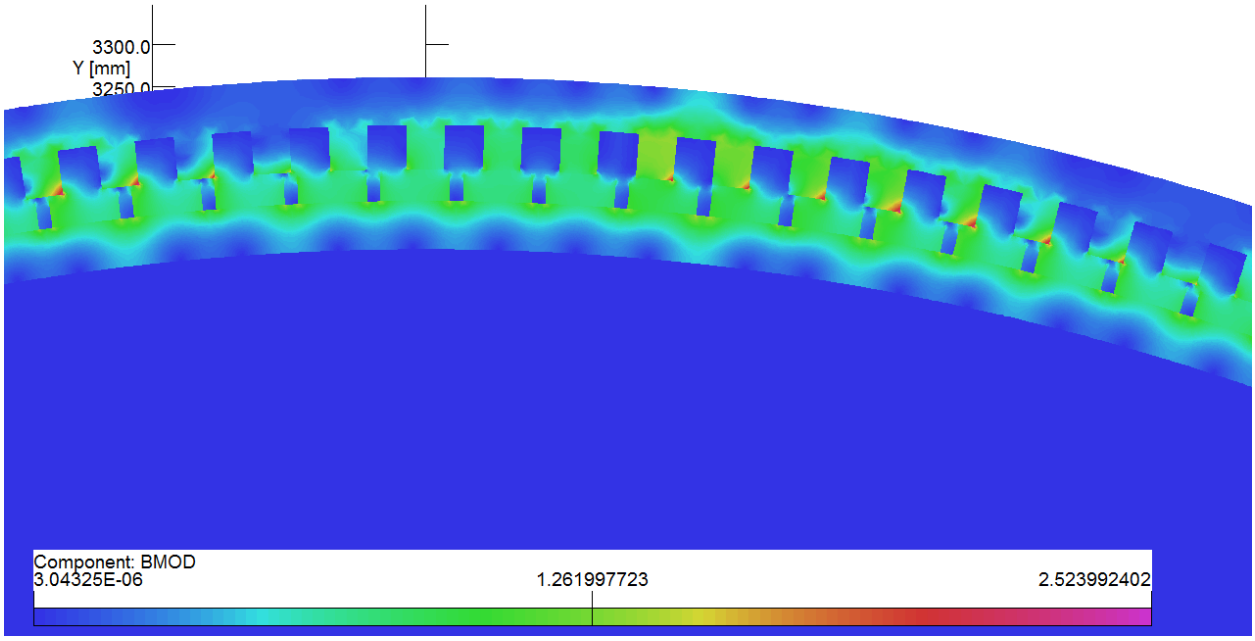

Figure 117: BMOD 216 A 216 Slots 198 poles 22.5 deg. El = 90 deg. El

Peak torque 2.94 [MNmm/mm] of core length

Flux linkage per coil 30.2e-6 [Wb-turns]

The voltage per coil is 39.8 [V]

The voltage per phase 2864 [V]

The presented evaluation shows mainly that various machines can be analysed using the design tool. With reports of machine parameters, a bigger picture can be created by using evaluation modules like FEM.

d. Dynamic Model

The purpose of this validation method is to check whether the machine parameters generated by the design tool give the expected behaviour/performance when used in a dynamic simulation. A secondary purpose is to show that the link between the analytic calculation and machine model is valid.

Once the parameters generated by the calculation tool are validated, they can be used with confidence in a more complex simulation that comprises a converter and a load with the associated control.

The model of the generator is presented in Appendix 13. To validate the parameters calculated by the design tool for the Classic RF and Double airgap Machines (see Chapter 3: 6 [MW] Candidates) the following steps were taken:

1. The parameters of each machine were calculated buy the design tool. The values are presented in the design sheets in Chapter 3. Prototype validation of the numbers obtained was performed-see next section.
2. A simple mathematical model of the machine was created to receive the parameters;
3. A field oriented control (FOC) strategy was implemented to control the speed of the machine;
3. The PI (proportional integrator)controllers were tuned using the Matlab app- 'Control System Tuning'
4. The performance rendered by the simulation model was compared to that from the design sheet. A deviation margin was allowed for the parameters as the main goal was to eliminate grouse inconsistencies.

Table 46 show the set of inputs to the simulation model. For booth generators, the desired parameters are taken from Chapter 3: 6 [MW] Candidates. Power: 5.8 [MW], rated voltage 13 [kV], rated current 236.8[A].

Symbol	Description	Classic RF	Double Airgap
P_n [MW]	Active Power -from parameter identification	5.8	5.8
V_n [kV]	Phase Voltage -from parameter identification	12.72e3	19
I_n [A]	Rated Current -from parameter identification	236.87	114.7
n_n[rpm]	Rated Speed	5.63	5.63
R_s [ohm]	Stator Resistance	0.054	0.123
L_d=L_q [H]	Synchronous Inductance	0.44	0.84
lambda_mpm [Wb]	PM Flux Linkage	127.3	261.72
p [-]	Nr. of pole pairs	157	157
J [kg x m2]	Assembly Moment of Inertia	215919	178060
Tn= [MNm]	Rated Torque	10	10

Table 46: Nessie Dynamic Model Inputs

Figure 118 and Figure 119 show the dynamic response of the studied machines (for power-P, torque Te and speed-n). Expected steady state values were reached. The link between the analytic design tool and the dynamic model was proven functional.

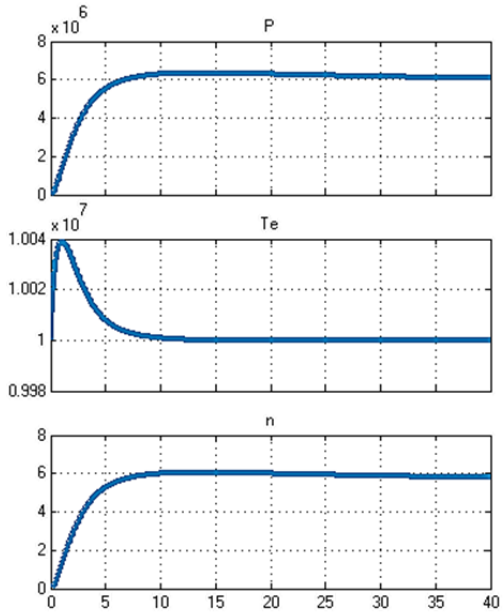

Figure 118: Classic RF Nessie Simulation Response

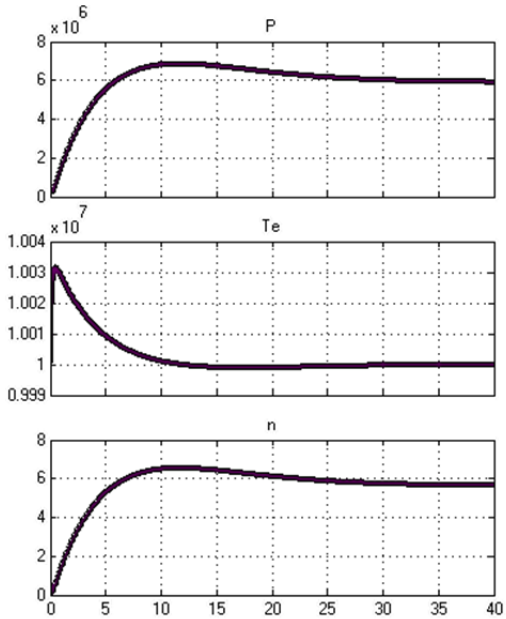

Figure 119: Double RF Nessie Simulation Response

C. Prototyping-BabyN

Because it is important to test the code, provisions for designing a prototype were made. There is a possibility of designing a prototype. A description of the prototype is made in Appendix 11

To validate the design tool the following steps were taken:

- Redesign BabyN with the final version of the design tool;
- Test the prototype-measure available quantities;
- Aim matching of the calculated performance elements vs. measured ones.
- Parameters like the resistance and inductance can be measured experimentally. The calculation of these parameters does not pose a complicated problem for the design tool, but they embody the consequences of a certain geometrical design. Comparison between calculated and measured quantities gives an idea of the design tool capabilities. Simplifying assumptions will give mismatch between calculations and measurements, but to some extent the numbers should match. The value of this comparison lies in the fact that the L and R calculated parameters are the result of the winding design and the parameter calculator modules. So the results of the validation apply to both these;
- Try to verify the basic formulae from the design tool. The calculation vs. experimental values have to match with an acceptable range;
- Find possible mistakes by assessing the test vs. calculation comparison;
- Check the test results again. If these are correct;
- Look for errors in the calculations

Prototype validation was made by calculating dimensions of BabyN using the design tool equations. The results should match within acceptable limits.

By evaluating the comparison between the measured and calculated dimensions, equations in the design tool were validated.

The prototype design that was sent to the workshop was the result of preliminary calculations and not final design tool values. As a result, some of the actual BabyN dimensions are different to what the current design tool version would set them to be. This compromise of constructing an early version of the prototype had to be made as the manufacturing process was estimated to and lasted one and a half years. Because half a year was planned for testing, the prototype design had to be submitted to the workshop at the end of the first of the three years of the period allocated for the research. Another reason is that the design approach is different using an existing machine. The force density is an input in Nessie design tool, but would be an output for designing BabyN.

By using design tool equations to calculate BabyN, scalable basic formulae used in Nessie Design tool are validated.

In the following Table 47 that contains the comparison between the actual and calculated dimensions of BabyN is discussed. The results are obtained by using formulae below with the parameters of the actual prototype. To goal is to obtain the other parameters of BabyN.

In the following, design tool formulae are discussed in relation to the prototype.

The rated full load electric power is calculated as (eq 141):

$$P_{el} = \sqrt{3} \cdot I_{max_{line}} \cdot Vout_{rated}\,[W] \qquad \text{eq 141}$$

The mechanical power is calculated as (eq 142):

$$P_{mec} = \frac{P_{el}}{efficiency}[W] \qquad \text{eq 142}$$

The turbine torque can be calculated as (eq 143):

$$T_{turbine} = \left(\frac{P_{mec}}{2 \cdot \pi \cdot f}\right) \cdot PolePairs[Nm] \qquad \text{eq 143}$$

From the finite element model, the Torque vs Angle curve at synchronous speed was determined Figure 120.

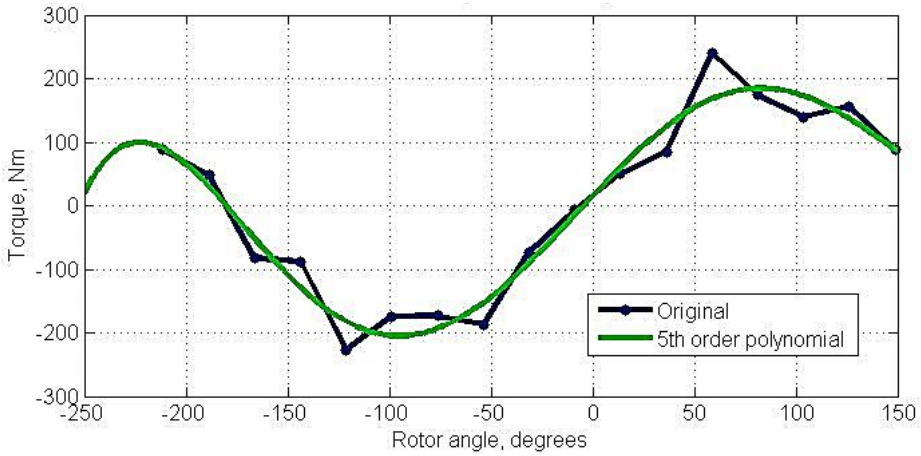

Figure 120:Baby N FEM Load Torque As Function Of Angle At 30.8A

The value for the rated full load torque was chosen 150 Nm to leave room for overload and to provide for the ideal vs real machine differences.

Where the number of pole pairs (eq 144):

$$PolePairs = round\left(60 \cdot \frac{f}{n_{rpm}}\right) = round\left(60 \cdot \frac{50}{500}\right) = \ 6 \qquad \text{eq 144}$$

The number of slots (eq 145):

$$Q_s = SlotPolePhase \cdot poles \cdot m = 1 \cdot 12 \cdot 3 = 36 \qquad \text{eq 145}$$

The bore diameter is calculated using eq 146:

$$D_{bore_{Estimated}} = \sqrt[3]{2\frac{T_{turbine}}{\pi \cdot LStackToDgapAvg \cdot Fd}} \qquad \text{eq 146}$$

The bore diameter needed to adjusted when calculating BabyN by using an adjustment factor (eq 147):

$$DboreAjustmentFactor = \frac{D_{bore_{BabyN}}}{D_{bore_{Estimated}}} = 1.16 \qquad \text{eq 147}$$

With this, the bore diameter becomes (eq 148):

$$D_{bore} = \ D_{bore_{Estimated}} \cdot DboreAjustmentFactor \qquad \text{eq 148}$$

Where the force density Fd is determined by eq 149

$$F_d = \frac{1}{2} \cdot \frac{B_{gapAV}^2}{\mu_0}\left[\frac{\mathrm{N}}{\mathrm{m}^2}\right] \qquad \text{eq 149}$$

The average B in the air-gap is (eq 150):

$$B_{gapAV} = B_{gap} \cdot markspaceratioofB[T] \qquad \text{eq 150}$$

The material used for the PM is samarium cobalt. The following BH curve is associated with the material (Figure 121).

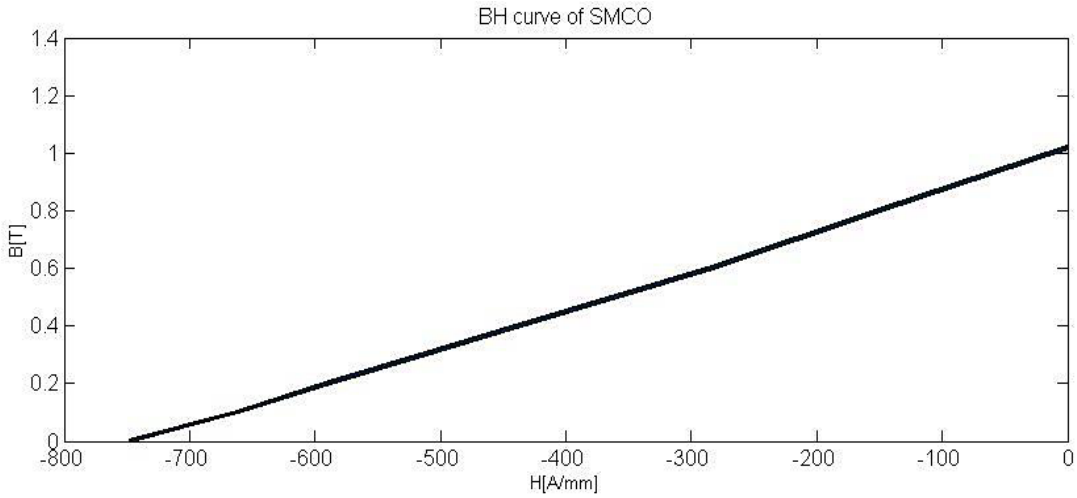

Figure 121: BH curve of the Samarium Cobalt PM used in BabyN

From the pole to pole pitch ratio or by observing Figure 122, the marks to space ratio of Bap was found to be 0.4.

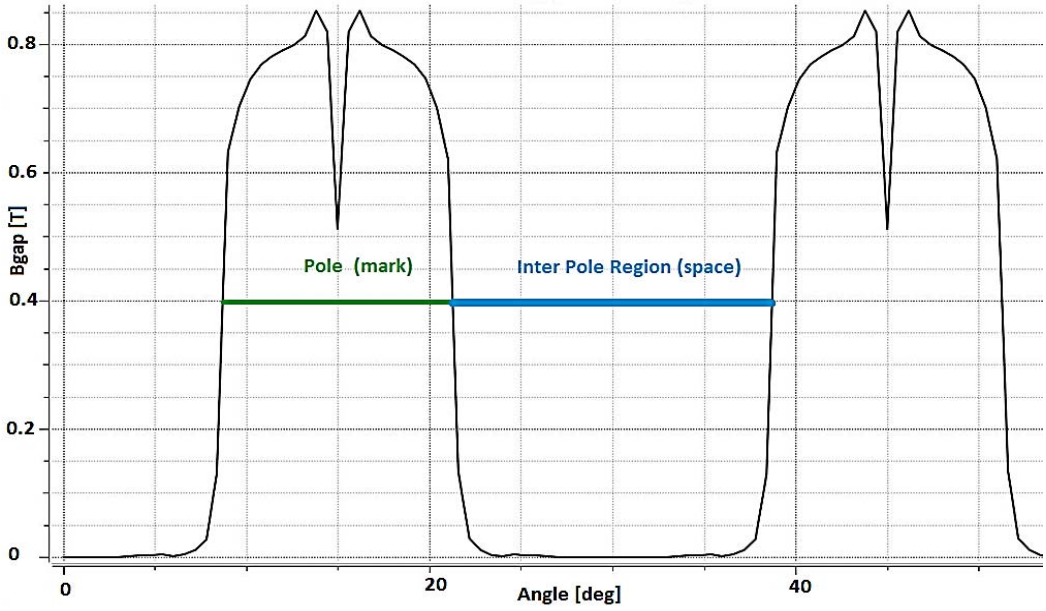

Figure 122: B_{gap} at no Load-FEM Result for BabyN

The pole pitch (eq 151):

$$PolePitch = \pi \cdot \frac{D_{bore}}{poles} \quad \text{eq 151}$$

The core length (eq 152):

$$L_{overallCore} = \frac{L_{usefull}}{stackingFactor}[mm] \quad \text{eq 152}$$

The value for the stacking factor was 0.95

The useful length (eq 153):

$$L_{usefull} = \frac{2 \cdot \mu_0 T_{turbine}}{D_{bore}^3 \cdot B_{gapavg}^2 \cdot \pi}[mm] \quad \text{eq 153}$$

As for the D_{bore}, an adjustment factor was needed for the machine length (eq 154):

$$LusefullAjustmentFactor = L_{Core_{BabyN}} \frac{stackingFactor}{L_{usefull}} = 0.61 \quad \text{eq 154}$$

With this, the useful length becomes (eq 155):

$$L_{usefull} = L_{usefull} \cdot LusefullAjustmentFactor[mm] \quad \text{eq 155}$$

The phase resistance is calculated (eq 156, eq 157):

$$R_{phase_{DC}} = \left(\frac{rho_{CuFunctionTemperature} \cdot L_{wirePhaseDistributed}}{CrossSectionWire}\right)[\Omega] \quad \text{eq 156}$$

where

$$rho_{CuFunctionTemperature} = rho_{copper20} \cdot \left(1 + \left(\frac{1}{273.15}\right) \cdot (temperature - 20)\right) \quad \text{eq 157}$$

The copper resistance at the room temperature at 20C (eq 158):

$$rho_{copper20} = 1.75e - 8\ [\Omega m] \quad \text{eq 158}$$

The length of the wire is (eq 159):

$$L_{wirePhaseDistributed} = turnsperphase \cdot \left(L_{Core} \cdot 2 + L_{overhang_{1Coil}}\right) = 172\ [m] \quad \text{eq 159}$$

The length of the overhang (eq 160):

$$L_{overhang1Coil} = 2 \cdot \left(2 \cdot height_{overhang} + coilsteplength\right) = 0.51[m] \quad \text{eq 160}$$

The correction coefficient 1.7 was used to adjust the estimated length of the conductors per phase.

To test this coefficient, the weight of the phase winding is checked against the specification of the manufacturer

$$MassCu = m \cdot L_{wirePhaseDistributed} \cdot CrossSectionWire \cdot copper_{density} = 10[kg] \quad \text{eq 161}$$

This is the mass of the pure copper (eq 161). To calculate the mass of the entire winding, the insulation should be taken into account. 40% was considered for the insulation. With this, the total mass of the winding is (eq 162):

$$Mass_{Winding} = MassCu \cdot 1.4 = 14[kg] \quad \text{eq 162}$$

With the lacquer insulation, the 15 kg for the windings quoted by the manufacturer checks out.

The required volume of PM (eq 163):

$$V_{magnetRequired} = -\left(\frac{\left(B^2_{magRequired}\right) \cdot V_{gap}}{\mu_{0mm} \cdot B_{wkg} \cdot H_{wkg}}\right) \quad \text{eq 163}$$

The inductance for the machine was measured to be L_{phase}= 18.53 with L_d and L_q eqal to 27.8. see determination in Appendix 11

To calculate the phase inductance the following was used (eq 164):

$$L_{Ph} = L_{magnetising_{Ph}} + L_{Leakage_{Ph}} + L_{Leakage_{Overhang_{Ph}}}[H] = 18.53[mH] \quad \text{eq 164}$$

With eq 165, eq 166, eq 167 and eq 168:

$$L_{magnetising_{Ph}} = \left(\frac{\left(D_{bore} \cdot L_{usefull} \cdot \mu_0 \cdot \pi \cdot (turnsperphase \cdot windingFactor)^2\right)}{4 \cdot gap_{equivalent_{length}} \cdot PolePairs^2}\right)[H] \quad \text{eq 165}$$

$$L_{Leakage_{Ph}} = \frac{Flux_{Wasted_{Ph}}}{Curent_{Ph}}[mH] \quad \text{eq 166}$$

$$Flux_{WastedPh} = \frac{Flux_{WastedInSlot} \cdot Qs}{m} \quad \text{eq 167}$$

$$Flux_{WastedInSlot} = \mu_0 conductorsPerSlot^2 \cdot CurrentPerConductor \cdot SpecificPermeance_{Slot} \cdot L_{usefull} \quad \text{eq 168}$$

The slot specific permeance for the BabyN slot Figure 123 was calculated with eq 169:

$$SpecificPermeanceOfSlot = \frac{h4}{w4} + \frac{2 \cdot h3}{w4 + w2} + \frac{2 \cdot h2}{3 \cdot (w3 + w1)} + \frac{\pi}{6} \quad \text{eq 169}$$

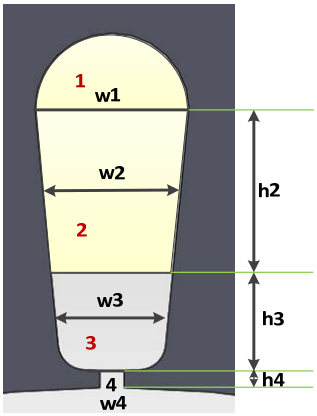

Figure 123: BabyN Slot for Specific permeance

For the overhang in cm (eq 170)

$$L_{leakage_{Overhang_{Ph}}} = \left(\frac{1.3}{2\sqrt{2}} \frac{\left(turnsperphase^2 \cdot windingFactor \frac{L_{overhang1Coil}}{2} \right)}{poles} \right) 10^{-9} \ [H] \quad \text{eq 170}$$

The moment of inertia is calculated with eq 171:

$$InertiaMoment = \frac{RotorWeight \cdot R_{rotor}^2}{2} = \frac{17.35 \cdot 0.09223^2}{2} = 0.0738 \ [Kg \cdot m^2] \quad \text{eq 171}$$

Another way of determining the moment of inertia is through the CAD program.
For the flux of the PM per phase measured is(eq 172):

$$Flux_{PM}Ph = \frac{\sqrt{2} \cdot Vout_{ratedPhase}}{n_{rads_{el}} \cdot poles} [Wb \ turns] \quad \text{eq 172}$$

Figure 124 show the flux linkages phase caused only by the PM undisturbed by current in the winding. It can be seen that the PM gives a flux linkage of 0.19 WbTurns and the lowest value (between the poles) is 0.04
Analytically, the flux of the PM per phase is ()

$$Flux_{PM}Ph = TurnsInSeriesPerPhase \cdot windingFactor \cdot FluxPerPole \ [Wb \ turns] \quad \text{eq 173}$$

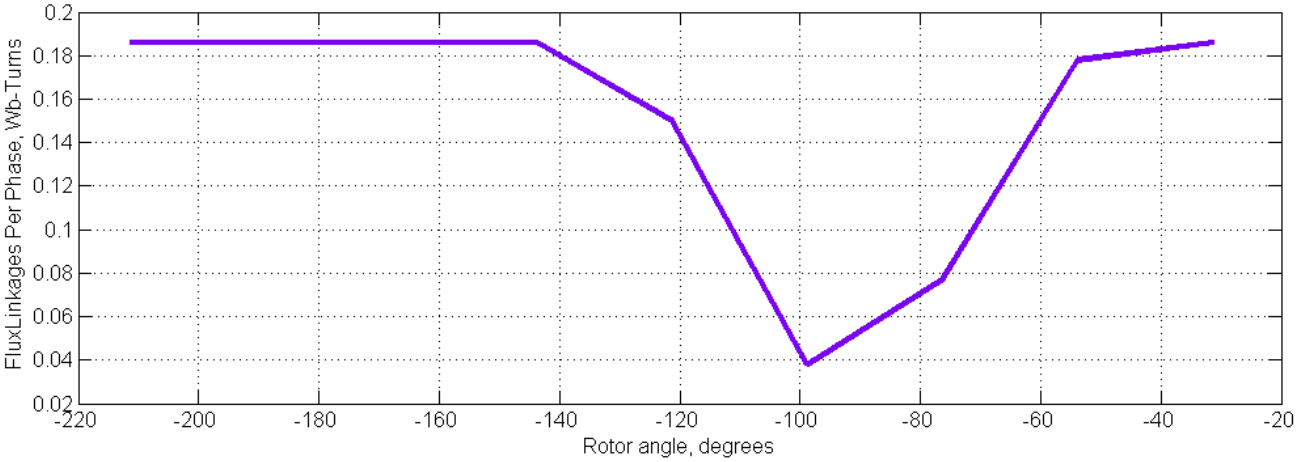

Figure 124: FEM BabyN No Load Flux Linkages Per Phase

Figure 125 shows the generated voltage in one phase at no load.

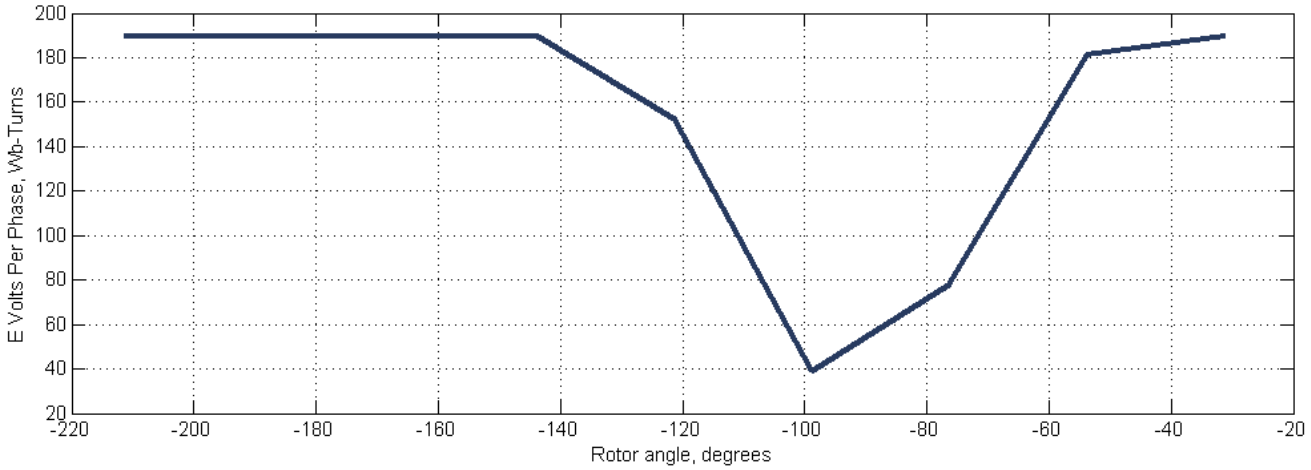

Figure 125: FEM BabyN No Load Volts Per Phase

Figure 126 shows the cogging torque as function of rotor angle as calculated from FEM. The values displayed are for the sum all tooth + magnet interaction in the entire machine. The negative value of the cogging torque correspond to the leading edge and the trailing edge of the magnet approaching the tooth

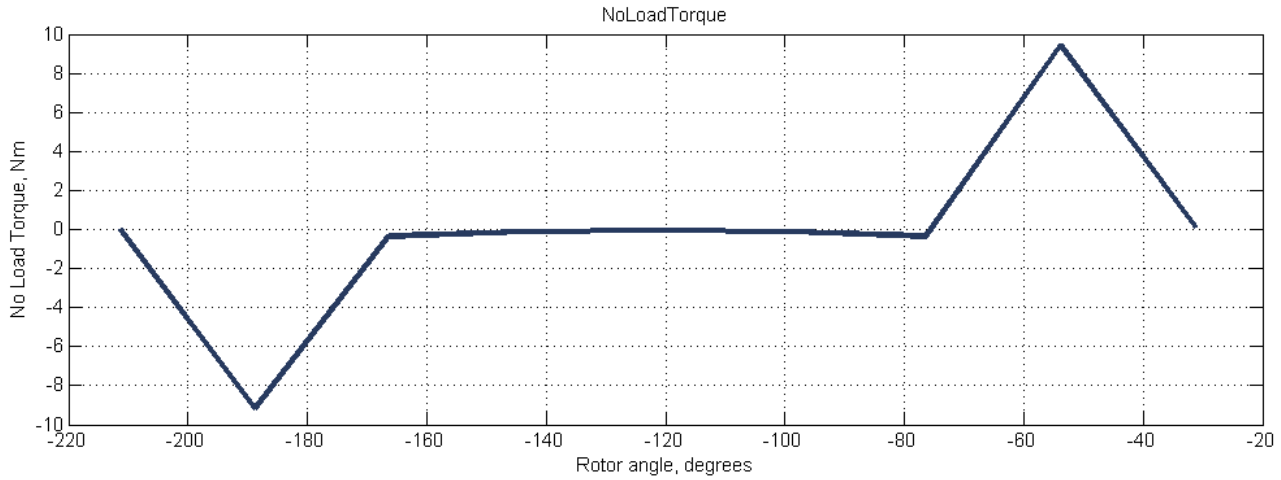

Figure 126: FEM BabyN No Load Torque-Cogging Torque

	Design	Prototype	Obs
Characteristics			
PM Material	SmCo	SmCo	
Specifications			
Tmechanichal[Nm]	150	150	*1
Pmec[kW]	8.8	8.8	
Pel[kW]	8	8	
phases	3	3	
Rotational speed [rpm]	500	500	
Terminal Voltage (50Hz)@ full load I, Rload[V]	150	150	
Rated Current(max)[A]	30.8	30.8 A	
Number of pole pair [-]	6	6	
Number of slots[-]	36	36	
Frequency [Hz]	50	50	
Nr. of slots per pole per Phase[-]	1	1	
Dimensions			
Bore diameter D_{bore} [mm]	162	186	*2
Air-gap length [mm]	1	1	
Stacking factor	0.95	0.95	
Machine length(rotor core length)[mm]	130	130	*2
Lumped Parameters			
cold/warm R/ph[Ω]	0.71/8.2	0.7/0.86	*3
Direct /Quadrature inductance [mH]	26.3	27.8	
PM flux linkage [Wb turns]	0.19	0.187	*4
Inertia[kg·m^2]	0.0738	0.077	
Iron			
Width tooth middle[mm]	7.9	7.9	
Height tooth[mm]	26	26	
Width slot middle[mm]	11	11	
Stator Height slot[mm]	Height tooth	Height tooth	*5
Stator yoke height [mm]	Wtooth midd	10	
Rotor yoke height [mm]	Wtooth midd	67	
PM			
PM height [mm]	6	6	*6
Rotor pole width(width of PM)[mm]	11	18.5	
Mass [kg]			*7
Stator windings	15	15	*8
PM Total	1.42	1.42	
Lamination stator/	13.6	13.9	*9
Lamination rotor	15.8	15	*10
Fixing plates for PM	0.88	0.93	*11
Mass of the rotor	17.35	18.1	
Mass of active material(PM+Fe+Cu)	**46.7**	**46.25**	

Table 47: Prototype Validation of the Design Tool

*1 from FEM

*2 Values for the calculated machine were obtained by considering an adjustment factor

*3 the temperature of 60 C was used to calculate the warm resistance

*4 analytical design

*5 set by manufacturing cost constraints. These dimensions were not locked design wise at the time of ordering the lamination

*6 the density of the PM was determined by weighing the PM and then trying to match the density in the CAD model. The Density was found to be 8200 kg/m^3 . the total number of PM=8per plate X 12number of poles=96. The weight of one PM according to the CAD is 14.88

*7 the calculation weights were taken from the solid works model. This is the method for assessing the weights for Nessie as well. It is concluded that this is a fairly accurate method of finding the weights as

opposed to constructing formulae to calculate the volume of the geometry. The library of materials is easier to manage in solid works.
*8 according to manufacturer-design and construction
*9 the density of the lamination material was determined similarly to the PM one. The value obtained for the PM support plate Density=5850 kg/m^3 The number of lamination in the stack-approximately 200
*10 the thickness of one lamination is 0.65 and an approximate number of 190 laminations per stack were considered. This corresponds to a stacking factor of 95%
*11 the density of the plate was determined similarly to the PM one. The value obtained for the PM support plate Density=7800 kg/m^3 .The total number of plates is 12

Conclusions

The validation of the design tool from several viewpoints was done. Comparison between literature reports of direct drive machines and output design of the Nessie tool were performed.

Representation, evaluation and analysis of the analytic design were made in CAD to make the design concept better understood to the users and developers (design tool developers, engineering colleagues, public, conferences and workshops).

The prototype validation was used to check whether or not the weights delivered by the CAD program can be trusted and used. Material densities can be approximated using the CAD model. As shown in Table 47, the difference between the calculated and the measured active mass is very little.

The diameter and lengths of the actual machine have been verified by the design tool formulae. Adjustments have been made to the calculation tool equations as a result of the prototype validation method.

Appendix 11: BabyN Prototype

In this appendix, the Deep Wind prototype (BabyN) used to verify the design tool is presented. The idea is to have a generator and then, knowing the specification of the constructed machine (geometrical and material characteristics), to design the machine using the calculation tool. Compare the actual machine with the result of the calculation. As a result of the analysis, a verification of the accuracy of the calculation tool should be made. At first, a description of the machine is made. The laboratory tests and results are presented and discussed.

The prototype, although small scale is intended to verify the design tool at a basic level: overall suitability of the formulae used for sizing. Taking in account the relatively low budget allocated and the development stage of the design tool, the 6 kW prototype was considered enough for validation. A larger scale prototype would be feasible if the sizing calculations for the overall turbine are more mature.

An important advantage of building this prototype is that the materials used can be individually tested and data from the suppliers is available. This would not be the case for an off the shelf machine. The geometry for BabyN was influenced by the designer hence adjustments like a future second rotor could be accommodated.

From a construction and testing point of view, the prototype has a different geometry than the geometry intended for the 6 and 20 [MW] Nessie. An example of the geometry difference is the shape of the slots-bar coils would be inappropriate for the construction of BabyN due to the extreme low scale of the latter. Another example would be the permanent magnets to be glued on the rotor.

Due to limited time and resources, the prototype needed to be designed, constructed and tested quickly. The prototype was finished 1½ years after the design was ready for submitting to the workshops. To allow for a minimum of one year of testing and documenting, within 3 years of project allocated time, a complete design of design the prototype had to be finished around the middle of the first year of project. At that time, limited knowledge about the desired technical specifications for the downscale machine were known as suitable concepts for the 5 and 20[MW]machines were still being discussed. The design tool was in the process of being built, debugged and validated.

The purpose of BabyN is to:

1. Verify the design algorithm to be included in the Nessie design tool
2. Evaluate a key idea relatively quickly-decide whether or not an idea is considering for Nessie)
3. Demonstrate the feasibility of an idea or of a high risk concept or element for the Nessie design Tool
4. Assess if the design tool code is reliable enough to build to the next level
2. Get an idea of the real machine that can be made from the existing tool (No perfection needed for the prototype).
3. Combine stators and rotors to learn about problems and benefits of each rotor solution
4. Learn about manufacturing issues-how to adapt a design to something that can be produced in the workshop
5. Test BabyN: Characteristics, performance
6. BabyN as feedback for the Generator design tool

A. The strategy for BabyN

To be able to successfully carry out the prototype validation of what would be the design tool the following approach was taken:

- Locate an existing test bench that is set up for testing prototype machines of ratings that the project could afford to build. The setup should have a drive machine that can be controlled in a closed loop: torque and speed control. Access to the control of the drive should be available-modification of parameters and possibly adding of new control. Active logging of the measurement results should be available. It is desired to obtain logged data in a file to hand written values.
- arrange for the existing setup to be borrowed at the time when the prototype is estimated to be finished
- the prototype would fit with minimum adjustments in the test bench. The most important aspect was that the outside diameter of the prototype case would fit onto the fixing plate of the existing setup
- starting from this diameter the machine was designed and built
- with this set of arrangements, from the machine being set up onto the bench and getting the first set of test results one week has passed.
- Complete testing of the machine took around two months. This is considerably less than the time that would have been needed to build a setup bench with its control.
- Having tested the machine, validation of the design tool is done by designing the prototype using the now finished calculation set. By comparing the numbers obtained from the design tool with the laboratory measurements, an assessment of the calculation accuracy can be evaluated. Compared to the initial design of the prototype, the geometry was slightly altered to comply with manufacturing requirements and constraints. These alterations are to be taken into account when evaluating the difference between the calculated and the measured quantities of the prototype. At the stage of the design tool documented here, the hypothesis of general design calculations was accepted. As stated in the future work section, manufacturing considerations are to be worked into the design tool influencing the basic calculations. For now, a general calculation of the machine parameters was considered sufficient as a first step in the development of the calculation algorithm.
- To be able to design the prototype using the calculation tool, rated values and inputs must be known: rated Power, speed, desired output voltage (rated voltage), materials specifications and geometrical specifications e.g. winding type and PM displacement. These are determined by either observing or testing the prototype machine.

B. Prototype Description

Two machines were planned to be evaluated: permanent magnet (Figure 127) and wound rotor synchronous (Figure 128) generators. To cut down on prototyping costs and to be able to accurately compare the performance of the PM and Wound concept, one single stator is to be made. The rotors should be interchangeable.

Due to financial and organisational impediments (laboratory renovations), only the PM version was assembled, the wound rotor was left for future work (laminations cut; encoder prepared, winding not made)

As a choice between the two rotors had to be made, the PM one was chosen for construction and testing. With this, the verification of the design tool was possible for the PM modules.

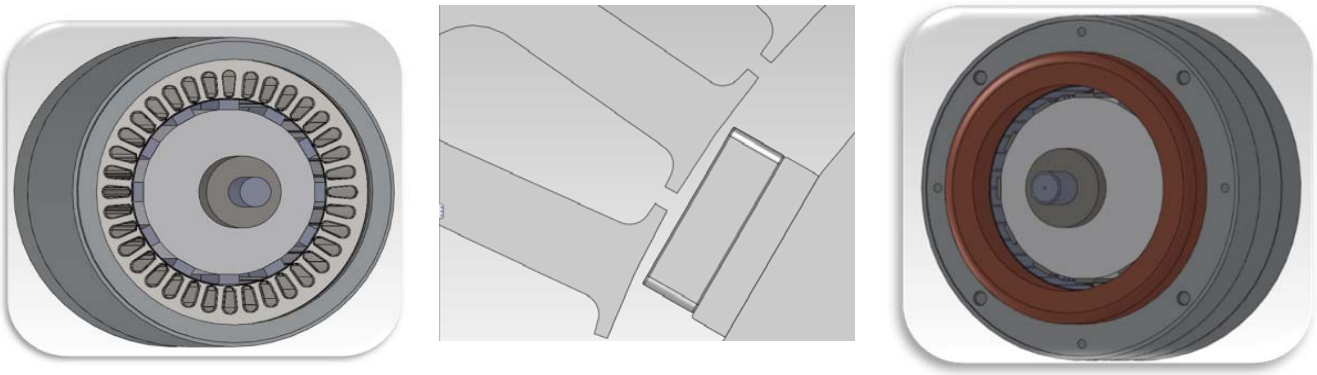

Figure 127:PM BabyN- CAD Model

Table 48 shows the list of common components for both machines. Table 49 is a components list for the PM one and Table 50 for the wound rotor generator. The latter is given as documentation in case the wound prototype is to be constructed in the future.

Figure 128:Wound Rotor BabyN

Name	Quantity	Material	Observations
Stator housing	1 [pcs] in total	aluminium	Just one stator housing
Stator Terminal connectors	4 [pcs]	standard	
Support Legs	[pcs]	steel	
Shaft	1[pcs]	steel	-Should be the same length as for the other machine+-functional features
Support legs	[pcs]	steel	Support legs
Housing-midplates screws	4	standard	Total of 4-only one stator housing
Endplate screws	8		8 in total for both BabyNs-4 for the drive end endplate; 4 for the non-drive end endplate

Table 48: Common Parts List

Name	Quantity	Code	Material	Observations
bearings	2 [pcs]	skf 62306	Like in specification	See specifications in the file set
washers	[pcs]			standard
PM	120[pcs]	S1035-350	Sintered SmCo	Supplied by Sintex.dk
End plates	2[pcs]		aluminium	Same type for both BabyNs
Shaft	1[pcs]		steel	-Should be the same length as for the other machine+-functional features
Glue PM plates	1 bottle	Loctite 620		Glue magnets on the rotor
PM mounting plates	12		Sheet steel	

Table 49: Part List PM BabyN

Name	Quantity	Code	Material	Observations
bearings	[pcs]	skf 62306	Like in specification	See specifications in the file set
washers	2[pcs]			Standard
Stator wire	[m]		copper	Windings done by TransElectro Probably
Rotor wire	[m]			
End plates	2[pcs]		aluminium	Same type for both BabyNs
Slipring and Brush Holder	1		standard	Nordjysk Diesel-Elektro A/S;Hjulmagervej 38; 9000 Aalborg, Dk 98 12 09 11; boschaalborg.dk
Rotor Terminal connectors	2[pcs]		standard	
Shaft	1[pcs]		steel	-Should be the same length as for the other machine+-functional features
midplate screws	4 [pcs]		standard	Total of 4-only one stator housing

Table 50: Wound BabyN part List

C. BabyN PM Machine Specifications

The PM BabyN specifications are listed in Table 51.

The winding diagram is shown in Figure 129. The winding manufacturer has supplied information regarding the coils (Table 51)

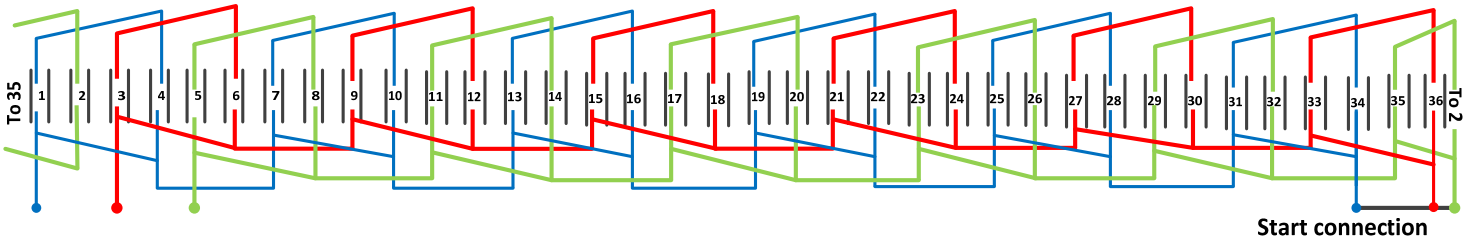

Figure 129:BabyN Winding Diagram

poles	12
phases	3
Stator slots	36
PM rotor	
- type	Sintered SmCo
- total number of PM	8PMx12poles=96
Winding type-stator	distributed
• 37 turns per coil	
• 6 coils in each phase	connected in series
• 4 parallel wires	ø1.4 [mm]
• Enamelled copper wire	2L 200 C rating
• Coil step	3(1-4)
Iron	
- Number of laminations	200
- Lamination stack length	130 mm
- Single lamination thickness	0.65mm
Masses[kg]	
- Stator windings	15
- PM Total	96 x 77.5g=0.74 kg
- Total Lamination	
o Lamination stator	200 x 69.8g=13.96 kg
o Lamination Rotor	200 x 78.9g=15.78 kg
- Fixing plates for PM	12 x 77.5g=0.93 kg
- Rotor with shaft and bearings	31
- Overall weight of active material(PM+Fe+Cu)	45.48

Table 51: BabyN PM Prototype Specifications

The stator rotor and the machine on the assembling bench are showed in Figure 130.

To be able to compare the theoretical dimensions (electromagnetic and mechanical) with the actual ones, the following set experiments were carried out. The purpose of each experiment is stated.

Determination of rated values

To be able to design the machine using the calculation tool, input values are need. Values for the rated power, current density, force density, speed and frequency are needed.

Other inputs like LstackToDgapAvg, (see design rules in Appendix 9)

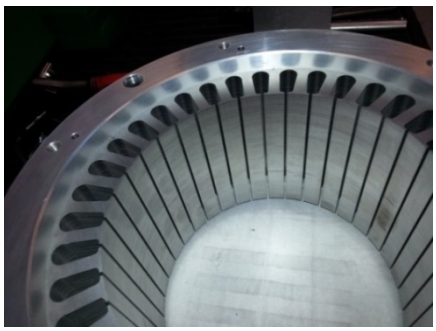

Unwound stator

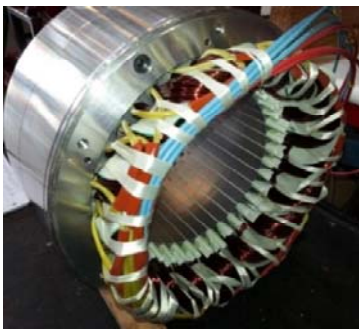

Wound stator

PM rotor

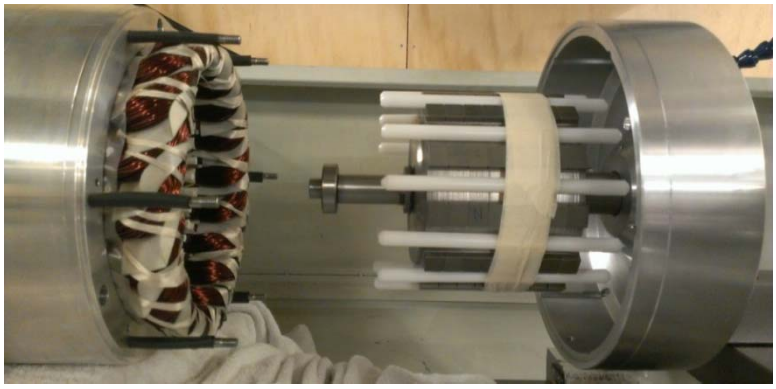

PM BabyN Being Assembled

Figure 130: PM BabyN –Actual Machine

The prototype parameters were determined by measuring the machine and interpreting the results.

The value for the maximum current that the windings of the prototype can withstand is related to the value of the current density considered in the design process.

The cross section of the round conductor- diameter of 1.4-used in the winding is (eq 174):

$$A_{conductor} = \frac{4 \cdot \pi \cdot D_{conductor}{}^2}{4} = \frac{4 \cdot \pi \cdot 1.4^2}{4} = 6.157[mm^2] \qquad \text{eq 174}$$

For a current density of 5 A/mm^2 and a round conductor, I_{max} becomes (eq 175):

$$I_{max} = j \cdot A_{conductor} = 5 \cdot 6.157 = 30.8[A] \qquad \text{eq 175}$$

The rated power calculated with $V_{terminals}$ (measured for generator mode at the rated speed) is (eq 176):

$$P_{max} =\cdot \sqrt{3} \cdot V_{terminals} \cdot I_{load} = \sqrt{3} \cdot 110 \cdot 30.8 = 5.87[kW] \qquad \text{eq 176}$$

If the load is purely resistive, X_q (magnetisation component) is the component that one cam measure because the load is at unity power factor (eq 177, Figure 131):

$$Z_{windings} = R + X_q[\Omega] \qquad \text{eq 177}$$

The X_d and X_q axis are defined as shown in Figure 132.

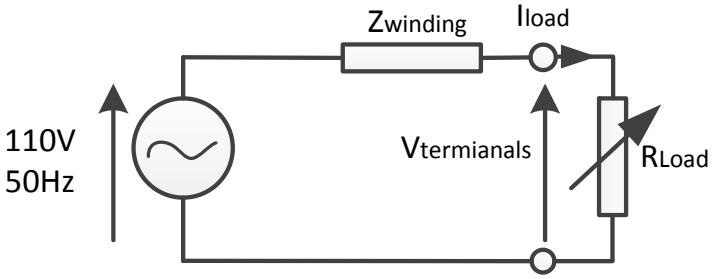

Figure 131:EMF-Terminal Voltage Diagram

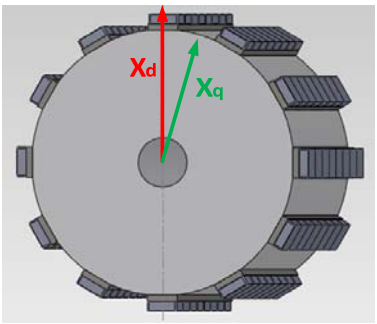

Figure 132:BabyN d and q Axis Reactances

D. BabyN Tests

In the following, the set of tests performed on the prototype are presented. The overall purpose of testing is the determination of parameters and validation of the design tool. Individual objectives are stated for each test as well as the methodology and results.

a. Cold Resistance of BabyN Test

The purpose of the test was to determine the cold resistance of the prototype. The result was intended to be compared to the value calculated using the design tool.

The instruments used were

- DC power supply SM 70-22 Delta Electronica AAU83245
- PPA 5530 KinetiQ-Precission Power Analyser AAU98209

The layout used is presented in Figure 133. A dc power supply was used to supply the prototype. Using ohm's law and with the measured voltage and current (Table 52), the resistance was calculated. The phase and line resistance are presented in Table 53.

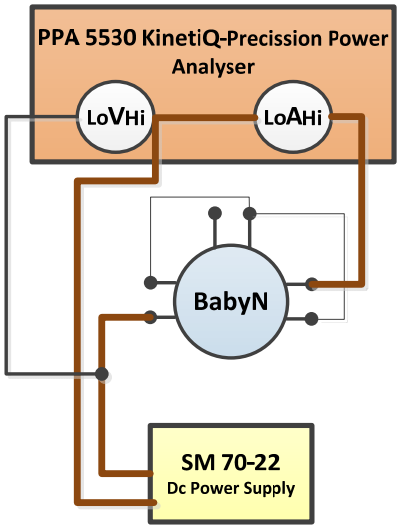

Figure 133:BabyN Cold Resistance Test Setup

V	1.5	2.89	4.2	5.6	7.15	14.25
A	1	2	3	4	5	10
R BabyN	1.5	1.44	1.4	1.4	1.43	1.425

Table 52: Prototype Cold Resistance Test Values

Phase Cold Resistance	0.7 [Ω]
Line Cold Resistance	1.4 [Ω]

Table 53: Cold Resistance of PM BabyN

b. Inductance measurement BabyN Test

The inductance measurement of a phase winding was done to match the experimental results with the results of the calculation. The goal is to verify that the analytic formula gives reliable results.

A phase winding was connected to a DC power supply (Figure 134). The current and voltage applied to the winding were measured using an oscilloscope.

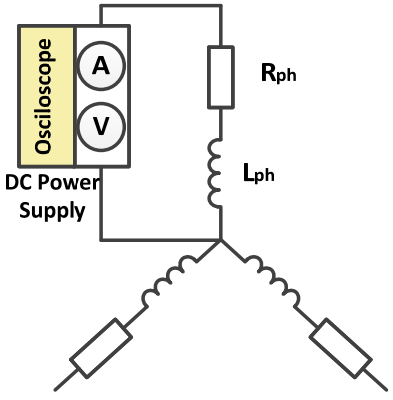

Figure 134:Induction Measurement Setup

The instruments used were a DC Power supply, Fluke 8845A for measuring the resistor, Calibrated standard resistor 1Ohm to test the precision of the ohmmeter and an oscilloscope.

The inductance is determined from the time constant of the experimental RL circuit eq 178.

$$\tau = \frac{L}{R}; \quad L = \tau R \qquad \text{eq 178}$$

The resistance of the winding was measured using the Fluke 8845A. To make sure of the measured value of the resistance, a standard 1 Om resistance was used to calibrate the Ohm meter. The value of the resistance was R_{ph}=0.7415 Ω.

The time constant is found from the current rise in the coil after applying a voltage step. At 63,2% and a current value of 1.817 A , the time was 25 ms - Figure 135

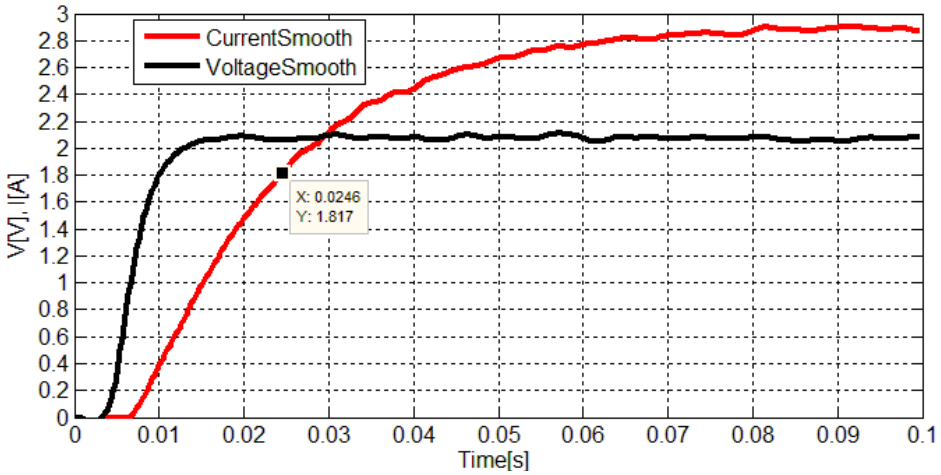

Figure 135: Time Constant Measurement

With this, the phase inductance was calculated from eq 178.

$$L_{phase} = \tau R_{phase} = 25 \cdot 0.7415 = 18.53\ [mH] \qquad \text{eq 179}$$

Even though the fixing plates for the magnets will give some saliency, this was found to be very small so for the direct and quadrature inductance were considered equal eq 180:

$$L_d = L_q = \frac{3}{2} L_{phase} = 27.8[mH] \qquad \text{eq 180}$$

Summary

Table 54 lists the measured parameters of the prototype

Lumped Parameters	cold/warm R/ph[Ω]	0.7/0.86
	Direct /Quadrature inductance [mH]	27.8
	Moment of Inertia[kg·m^2]	0.077
Mass [kg]	Stator windings	15
	PM Total	1.42
	Lamination stator/	13.9
	Lamination rotor	15
	Fixing plates for PM	0.93
	Mass of the rotor	18.1
	Active materials(PM+Fe+Cu)	**46.25**

Table 54: Prototype Measured Parameters

Conclusion

In this appendix, the prototype built for the validation of the design tool equations was presented. The concept of the prototype, the geometry and construction were discussed. Tests for determining the resistance and inductance were presented.

Appendix 12: Optimisation Tools

The current Appendix presents the background of the optimisation module of the design tool. The principles of the Particle Swarm Optimisation (PSO) and Genetic Algorithms (GA) are presented. Implemented elements are listed and linked to the theory.

A tool is needed for adjusting the design in a certain direction. The problem of finding the best suited algorithm for machine optimisation was investigated.

By comparing the two algorithms most discussed in the literature –genetic algorithms (GA) and particle swarm optimisation (PSO), the one best suited has proved to be the particle swarm algorithm [223]

Both GA and PSO were integrated in the design tool and are available for use. [27], [28], [29].in the following the concept of each method is outlined. The features used to carry out the present study are presented. An example of optimisation by using both methods is shown.

A. Particle Swarm Optimisation (PSO)

a. PSO Theoretical Concept

PSO is a method that is used for optimising almost every problem that has an explicit form including nonlinear systems. The concept of the algorithm imitates the behaviour of a flock of birds or a fish school that are seeking food. These groups are referred to as swarms. A Swarm is a set of individuals that tend to move in a cluster in an apparently disorganised manner. The individuals of the group are communicating between each other transmitting the information of the food location. Each particle has a defined position, velocity, acceleration and a distance to move [27], [224]. Figure 136 a shows the initial situation of the process and b shows the convergence (final situation) when the particles are positioned close to the solution.

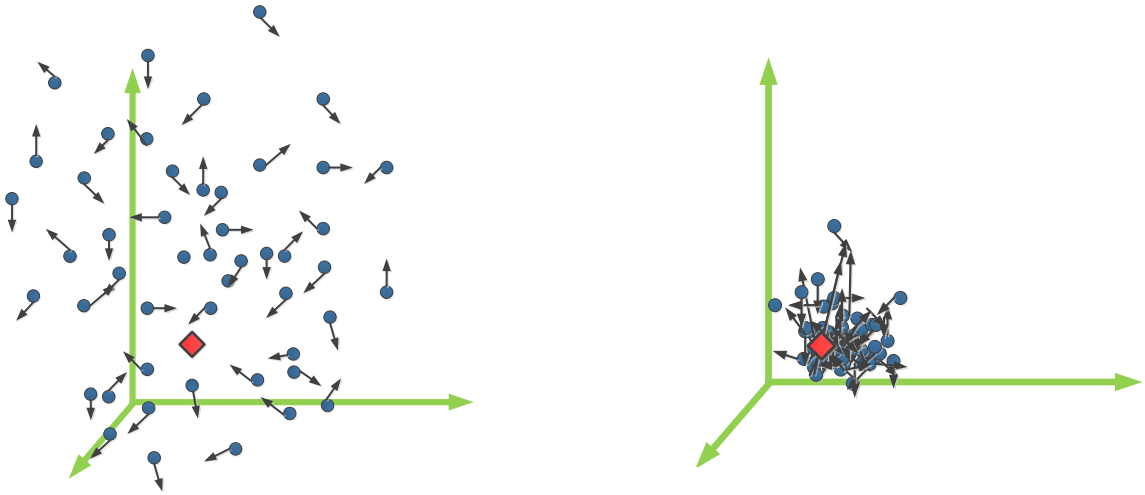

(a) initial situation (b) Convergence

Figure 136: PSO Elements Overall Concept: Particles And Solution

As initial conditions, the particles are assigned random positions and velocities within a space. Each particle remembers the best position that it had within that space. The highest fitness positions are attributed to the best individual in the population and the best in the neighbourhood at each point in time, each individual accelerates towards one of the best places listed above.

Steps of the PSO are the following [225], [225]:

1. Define the solution space
2. Define the fitness function
3. Initialise the population
4. Evaluate the fitness of each particle
5. Modify the velocities based on individual, population and neighbourhood bests.
6. Stop due to condition
7. Evaluate- retake step 2

The advantages that particle swarm can bring to machine optimisation are, [224]:

- Very simple calculations are involved
- Easy to implement
- The algorithm uses real numbers It is reported to be fast as the main parameter monitored is the speed of the particle

The disadvantages of the method are:

- Often some particles migrate towards a false optimum
- Cannot be used on non-coordinate systems life fields
- Is still being developed-the mathematical ground has not been thoroughly laid down yet

The main elements of the PSO are presented and discussed in the following. The following notations were used:

t-time **i**-particle number **k**-dimension **d**-dimension of the vector

- **Swarm** : is the population of all moving particles.
- **Particle *X(t)*:** is a possible solution represented by a *d*-dimensional real-value vector.
  The position of the particle is (eq 181):

$$X_i(t) = [x_{i,1}(t), \quad x_{i,2}(t), \dots, x_{i,d}(t)] \qquad \text{eq 181}$$

- **Velocity *V(t)*:** is the velocity of the moving particles (eq 182):

$$V_i(t) = [v_{i,1}(t), \quad v_{i,2}(t), \dots, v_{i,d}(t)] \qquad \text{eq 182}$$

- **Personal best *P(t)*:-** the position with the best value of fitness the a particle has achieved during the movement throw the search space. For each iteration, each particle searches whether the new position produces a better fitness result. If the new fitness is better than the personal best, the personal best is replaced with the new particle. The personal best vector is (eq 183):

$$P_i(t) = [p_{i,1}(t), \quad p_{i,2}(t), \dots, p_{i,d}(t)] \qquad \text{eq 183}$$

- **Neighbour best *B(t)*:** is the best position among a distinct set of neighbours of a particle, achieved so far. The neighbours can be determined using different approaches. The neighbour best can consist of all particles in the swarm, and then $B(t)$ is the global best or it can consist of only a few particles from the swarm, for which there are numerous techniques of selection, and then $B(t)$ is the local best [226]. The neighbour best of the i^{th} particle can be described as (eq 184):

$$B_i(t) = [b_{i,1}(t), \quad b_{i,2}(t), \dots, b_{i,d}(t)] \qquad \text{eq 184}$$

- **Stopping criteria**: if this/these conditions are met, the process stops. There are two types of stopping criteria
  - . if the change of the best particle over a number of generations will not be greater than a pre-specified error.
  - the maximum number of iterations was reached

The velocity eq 185 and position eq 186 updates are

$$v_{id}(t) = v_{id}(t-1) + c_1\varphi_1(p_{id} - x_{id}(t-1)) + c_2\varphi_2(b_{id} - x_{id}(t-1)) \qquad \text{eq 185}$$

$$x_{id}(t) = x_{id}(t-1) + v_{id}(t) \qquad \text{eq 186}$$

, where: c_1 and c_2 are social parameters 1 and 2 (usually both have the value 2);

φ_1 and $\varphi_2$positive random numbers between 0.0 and 1.0;

As can be seen from Figure 137 the velocity $v_i(t)$ is determined by three components [227]:

- momentum $v_i(t-1)$: previous velocity term. This parameter tends to carry the particle in the direction it was traveling so far.
- cognitive component $c_1\varphi_1(p_{id} - x_{id}(t-1))$: tendency to return to the best position visited so far;
- social component $c_2\varphi_2(b_{id} - x_{id}(t-1))$: tendency to be attracted towards the best position found in the neighbourhood.

An example using particles with two dimensions problem is presented in Figure 137.

From the initial position, by adding the three elements of the velocity equation, the new position of the particle is obtained. The components of the updated vector are: the last velocity of the particle, (green arrow), the distance from the current position to the best previous position (dark blue) and the distance from the current position to the best neighbour (light blue).

This basic PSO has a big drawback. The velocity has the tendency to "explode" to a large value see Figure 138 [141], [228].

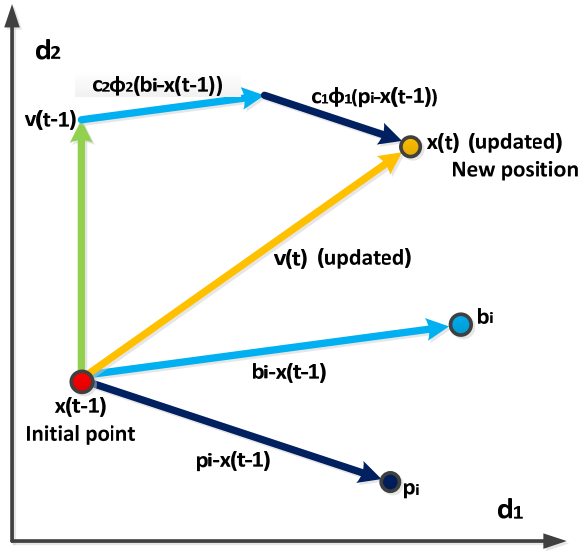

Figure 137: Particle Movement In The Search Space [229]

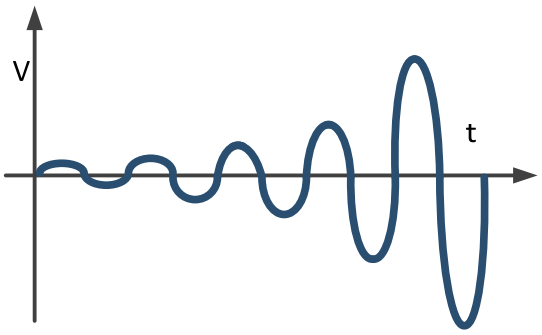

Figure 138: Particle Velocity In Time [228]

To overcome this drawback of the velocity increase, the following solutions are proposed.(for future implementation)

Inertia weight $w(t)$: is a parameter that is used to control the influence of the previous velocities on the current velocity (eq 187):

$$v_{id}(t) = w(t)\cdot v_{id}(t-1) + c_1\cdot\varphi_1\cdot(p_{id} - x_{id}(t-1)) + c_2\cdot\varphi_2\cdot(b_{id} - x_{id}(t-1)) \qquad \text{eq 187}$$

This is an adaptive variable that controls the exploration of the search space and changes linearly with the number of iterations [141]. At the beginning of the search a higher value (typically 0.9) allows the particles to move freely towards a global optimum. After the particle has arrived in the optimum region, the value of the inertia weight can be decreased (typically 0.4). This is done in order to limit the search.

The down side of a linear reduction of the inertia weight is that the swarm loses its ability to search a new region as it is no longer in exploration mode. The constriction factor is employed to compensate for this short coming.

The **Constriction factor χ** represents a method to control the "explosion" effect of the swarm [230]. (eq 188 and eq 189)

$$v_{id}(t) = \chi \cdot \left[v_{id}(t-1) + c_1 \cdot \varphi_1 \cdot (p_{id} - x_{id}(t-1)) + c_2 \cdot \varphi_2 \cdot (b_{id} - x_{id}(t-1)) \right] \quad \text{eq 188}$$

$$\chi = \frac{2 \cdot k}{\left| 2 - \varphi - \sqrt{\varphi^2 - 4\varphi} \right|}, \varphi_1 + \varphi_2 = \varphi > 4.0 \quad \text{eq 189}$$

By modifying φ, the convergence characteristic of the system can be controlled [230]. With $= 1$, $\varphi_1 = \varphi_2 = 2$, and $\varphi = 4.1$, give a constriction factor of $\chi = 0.729$.[230], [229], [231]

For the implemented optimisation program for the design tool, the constriction factor and the maximum velocity will be set to the value of the maximum position as suggested in [232]

. The topology of the PSO is an important element and represents the method to determine the best neighbour of a particle in the swarm. Knowing the topology, neighbours for every particle are defined, see Figure 139.

Particles have mainly been studied in two main types of topologies: global best Figure 139 a (particles influenced by the best particle in the swarm) and local best (particles are attracted by the best particle in a local neighbourhood) [232], [229]

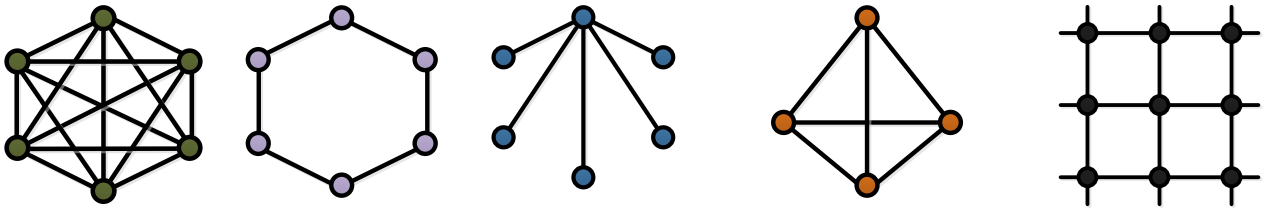

(a) Global best. (b) Ring (c) Wheel (d) Pyramid (e) Von Neummann

Figure 139: Particle Neighbour Topologies [233]

According to [229] the global best version converges fastest, but has a high possibility of getting stuck in a local optimum point. The local best neighbourhood version has a bigger chance to find the global optimum, but a slower conversion is to be expected.

By investigating all topologies from Figure 139, [234] concluded that the best results occurred in a randomly generated neighbourhood with an average number of 25% particles.

For each given problem, an appropriate topology must be associated. For the generator design tool, the random generated structure of neighbours was used. The number of neighbours for every particle will be set to 1/4 of the swarm size.

b. Implemented PSO algorithm

The algorithm implemented is presented in Figure 140. The program was written in Matlab R2011b (7.13.0.564) 32-bit (win 32).Using object orientated programming a 'particle' class was created containing the following fields.

The class 'particle' has the following properties:

X	- position vector
V	- velocity vector
P	- personal best vector
B	- neighbour best vector
fitness	- current position fitness
fitnessP	- best fitness of particle until now
fitnessB	- best fitness of neighbours until now
insideDomain	- shows if the particle is inside the search domain

A set of functions were written for the PSO algorithm.

1) **particle(designLimits, nrDimensions)**
   -constructs the class
   -initialises the particles in the swarm
   -best particle- only the best particle in the swarm at every iteration is memorised.

2) **updateVelocity(obj,designLimits,nrDimensions,ConsFactor,c1,c2)**
   - updates the velocity of every particle with eq 187.
   -controls the value of the velocity and consequently the 'explosion' by limiting the velocity in the velocity in the $+V_{max}/-V_{max}$ range.

3) **updatePosition(obj,designLimits,nrDimensions)**
   - updates the position of every particle in the swarm using
   - checks if the updated particle is in the search space. If not, the velocity of the particle is made zero.
   -informs other functions whether the particle is in the search space or not
   -checks if the particle is moving in a feasible direction. If not, the velocity of the particle is made zero.
   - informs other functions whether the particle is in moving towards a feasible direction or not

4) **updateBestNeighbour(obj,obj2)**
   - updates the best neighbour position of every particle
   -fitness of the neighbour to be better than the fitness of the current best neighbour update.

5) **updatePersonalBest(obj)**
   -checks the fitness of the current position against the best fitness of the position found so far(update possible if the current position is inside the search space).

   -updates the personal best position of every particle

The input variables for the program are: fitness function, PSO variables, convergence test parameters, velocity variables and the design limits. The program starts to create the swarm of particles and the best particle. As a next step, the algorithm starts iterating for the optimum solution.

For each iteration, the following sequence is repeated:

- What is the fitness of each particle in the swarm?
- Update personal best of each particle
- Are the particles in the search space?
- Update best neighbour position for each particle-
- Stores all the values of the best particle from the swarm in the independent best particle element
- Update the velocity and position of each swarm particle
- Convergence test;

The best fitness from every iteration is stored in the best particle vector.

The convergence check is done by comparing the variation between two results with a tolerance set by the user.

If the convergence event does not occur, the program stop when the maximum number of iterations set by the user is reached.

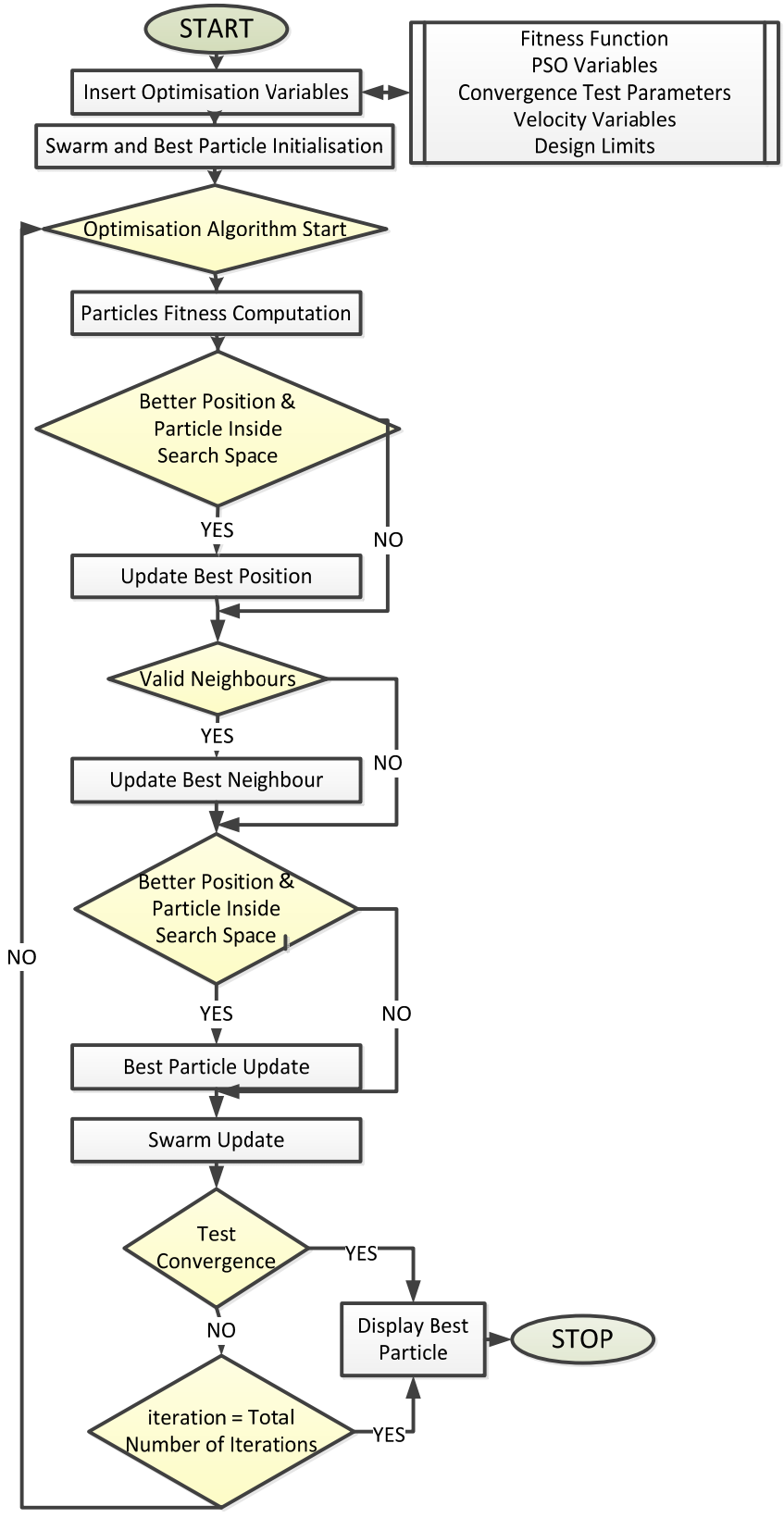

Figure 140: Optimisation Program Flow-Chart

B. Genetic algorithms (GA)

a. GA Theoretical Concept

Genetic algorithms are stochastic optimisation methods built on the evolutionary metaphor.

The main idea behind GA is that the fittest individuals have a higher probability to produce offspring for the next generation. They are the ones that transmit the information contained in their chromosomes to the next generation.

The individual, also known in the literature as chromosome, is created using is created using dedicated operators: selection, crossover, mutation.

GA can be implemented in binary and real coding of the information in the chromosome. The latter method was considered more suitable for the Nessie design tool because the design variables were used directly in the algorithm.

In the following, the terminology used in genetic algorithms is listed. The vocabulary clearly shows the link to the biological background [225], [235], [236], [237], [238]

Cost Function=the mathematical function expressing the objective of the optimisation process

Fitness = the performance of the cost function for a specific point in the search domain:

Individual =in the search domain: points, chromosome;

Population= all the individuals in one generation;

Search Domain=domain of definition of the optimization problem

Descendent = a new point in the search domain produced by the individuals present in the current generation using the reproduction operators;

Parent = individual in the current generation, which was selected to produce offspring.

Generation= One iteration in the search process. See Figure 144

Chromosome=a set of characteristics (genes) of an individual. It is represented as an array of binary or real numbers [239]. In Figure 144, Individual 1 has 3 genes.

Genes =part of a chromosome. They are represented by the Nessie design variables

Genetic operator = a tool to manipulate the individuals;

The GA operators are:

Selection - selects chromosomes from the population for reproduction. Fittest chromosomes are more likely to be chosen. There are several methods of selection [237]

Crossover – the process of creating one or more offspring from two parents, selected from the current generation.

Mutation produces new individuals by exchanging some of the genes in a chromosome. Mutation can change the information in an offspring, after crossover. A new individual is created by altering the current one.

Figure 141 presents the concept of genetic algorithms in a nutshell. From the current generation, fit parents are selected. Through the operators of Crossover and Mutation, the next generation is created. This will replace the old generation.

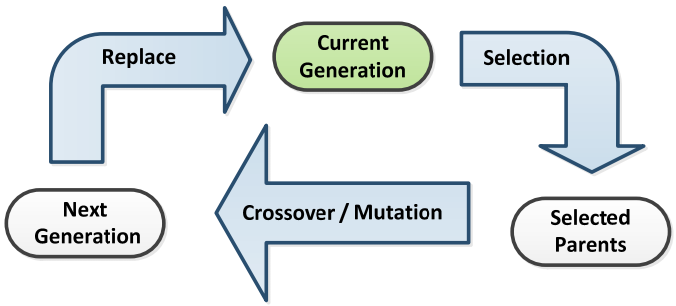

Figure 141:GA Concept

Figure 142 shows the algorithm to be implemented.

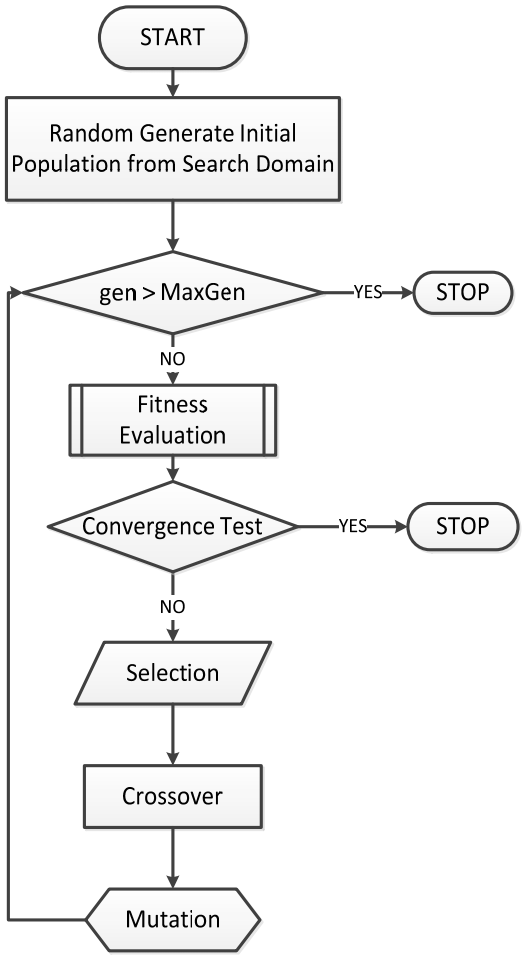

Figure 142:GA Algorithm

- First, the initial population is randomly selected from the search domain.
- The individuals in the first population are evaluated against the chosen fitness function.

The stochastic search process starts here:

- A process of selection is applied on the individuals to choose the best parents for the next generation.
- The new offspring are updated using the crossover operator, which is applied to the parents;
- Mutation is also used to alternate the offspring. (Usually mutation is set to have a very small probability, rarely affects the offspring).
- The old generation is replaced by the new generation;
- The fitness value of each new individual is determined.
- The STOP condition is tested. As STOP condition the program can have: maximum number of generations, convergence condition, or even both.
- The process is repeated until the STOP condition is true.

While the search condition is not satisfied changes are made:
-chromosomes are selected from the current generation to form the new population
- crossover operator and mutation operators are applied
-the current population is updated by replacing the old individuals with the new individuals. with this, the new generation is formed
-all the individuals in the new population are evaluated against the chosen fitness function;

The procedure repeats until the search condition is satisfied. The stop condition for genetic algorithms is set by the number of generations chosen at the start of the program

b. Implemented GA

For the Nessie design tool the following was implemented. A short definition of each is presented

Selection operators:

1. **Monte Carlo**-the random selection of individuals with a probability influenced by their performance indicator. An analogy is made with the roulette disk. The disk is divided in sectors equal to that of the

number of individuals. The dimension of each sector is proportional to the probability of that individual. This probability is given by the fitness level of the individual. The roulette is spun n times, where n is the number of individuals desired in the new population. After each spin, one individual is selected.[240]

2. **Tournament** –a predefined number of individuals are randomly selected from the population and the individual with the best fitness value is selected as a parent for the next generation. This process is repeated until all the parents are selected. [238].

3. **Elitist preserving**- preserves a predefined number of the best individuals from the current generation to the next one while the rest of the offspring are generated using another selection method, usually Monte Carlo.

4. **Stochastic universal sampling** – to each individual, a segment is allocated, equal in length to the fitness value. Segments are afterwards sorted in decreasing order. To select the parents a number of pointers equal to the population number are generated. To determine the placement of the pointers, first the interval between them is calculated, and the position of the first pointer is randomly generated in the [0, Pointer 1] interval. The selected individual corresponds to the segment where the pointer is placed. [239]

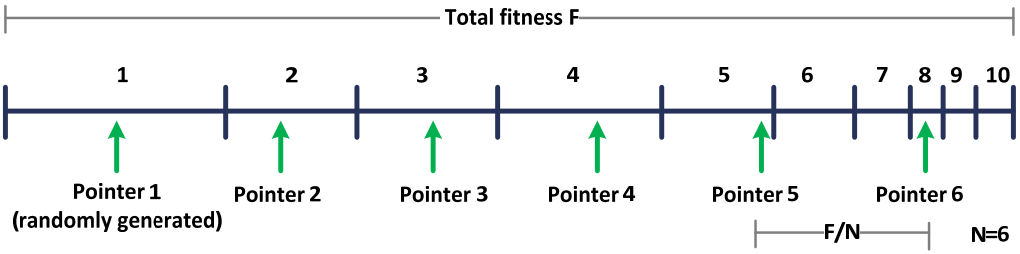

Figure 143:Stochastic Universal Sampling

Crossover types [241]:

1. **Single Point** – a cut point is chosen randomly and two new individuals are created by keeping the information until the cut point and exchanging the information after the cut point (see also Figure 144)

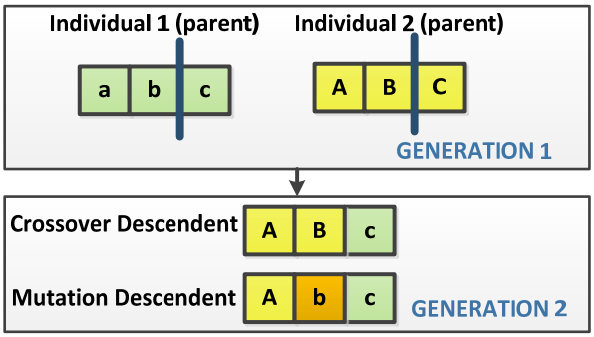

Figure 144:GA Dictionary- Single Point Crossover Example-

2. **Two Point** –as single, but two cut points are chosen
3. **N Point** –n cut points are chosen
4. **Average** – starting from two parents, and with a crossover probability, certain genes are randomly selected to be modified. The new genes are obtained by averaging the gene value of the two parents. The genes which are not selected to be averaged are transferred unchanged from the parents to the offspring.
5. **Arithmetic (convex**) – the two offspring are generated from two parents and a parameter (m) selected from the interval [0, 1], using the following two equations eq 181, eq 182:

$$a_i' = a_i \cdot m + (1 - m) \cdot b_i \qquad \text{eq 190}$$

$$b_i' = a_i \cdot (1 - m) + m \cdot b_i \qquad \text{eq 191}$$

, where: $a_i' \; and \; b_i'$ are the new individuals, $a_i \; and \; b_i$ are the parents;

6. **Uniform (guaranteed uniform) -** The value of each gene in the offspring is found by the random uniform choice of the values of this gene in the parents. – see Figure 145

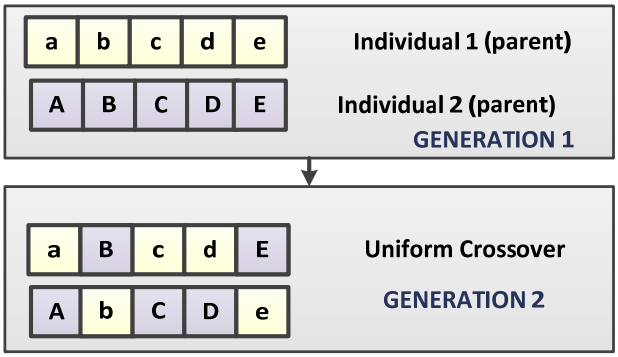

Figure 145:Uniform Crossover

7. **Little Creep** [237] – the new offspring is generated from only one individual. Each gene in the parent is varied in the ± 10% interval to obtain the new gene for the offspring. The variation of each gene is determined randomly.

8. **Big Creep** – procedure is similar as for the Little Creep crossover, only the interval of variation is ± 20%.

9. **BLX-α (Blend Crossover)**(α =0.3) –

In this method each new gene is randomly selected from the interval $[a_i - \alpha(b_i - a_i),\ b_i + \alpha(b_i - a_i)]$.

By setting the value for α, the exploratory characteristic of the method can be chosen. (Chen, 2003, unpublished manuscript). [242], [243]

10. **BLX- α (α =0.5)** The method is similar with BLX-α (α =0.3), only α is different. By setting α to a bigger value the exploratory characteristic is increased. This is advantageous especially at the beginning, when the search domain is unknown, and especially when the search domain is large.11. BLX- α (α =0.3)(2-16-2) – from each two parents 16 offspring are created using the same principle as for BLX-α(α =0.3). From the 16 offspring the best two are selected to be transferred to the next generation.

12. **BLX- α (α =0.5)**(2-8-2) - the method is similar with BLX-α(α =0.3)(2-16-2), only α is 0.5, to increase the exploratory characteristic, and the number of initial offspring is 8, from which only the best two are passed to the next generation.

Mutation Types:

1. Random: from each individual only one gene is randomly selected for the mutation. To determine if the mutation will affect this gene a number is randomly generated, and if the number is below the selected probability the gene is changed, if not, the gene remains the same. The probability is constant and is selected by the user, usually it is a small value <7%.
2. Scale-local or global :
   - Total Scale: All the parameters in an individual have a 50% chance to be affected by mutation; If the parameter will be affected by mutation it has a 50% chance of being increased with 10% or decreased with 10%.
   - Limited Scale: Only one parameter, of an individual, will be affected by mutation; Once the parameter is randomly selected the coefficient which will vary the parameter is randomly selected from the [0,2] interval;
3. Order Based: Consists of four different manipulation techniques: insert, swap, inversion and scramble. The type of manipulation applied is selected randomly for each individual in the population.
4. Non-Uniform: the method is similar to random mutation. The only difference is that the mutation probability is reduced while the number of generations is increasing.

Conclusions

In this appendix, the philosophy of the optimisation process and the optimisation methods applied were presented. The most suitable algorithms for Nessie were briefly discussed- genetic algorithms and particle swarm optimisation.

As stated in the overall concept of the design tool, the author does not seek to design a machine or to perform the final optimisation. The focus is to develop a reliable, flexible and transparent tool that can be further developed in complexity and that enables the design of certain machines in relatively broad power and speed ranges. The present work presents an exercise in using the optimisation module.

The optimisation module needs a set of values to be modified within a certain range to get a minimisation of a desired quantity.

Following an analysis of the structure of the analytical design and the optimisation algorithm, it was concluded that at this stage, only a restrictive set of inputs can be safely fed to the process.

A list of valid input and output parameters were chosen for the optimisation process. With these and an analytic design path shaped so that the optimisation process can repeatedly run it until convergence provided an optimised version of the machine.

Appendix 13: Dynamic Simulation Models for the Generator System

This section presents the simulation model used to test the machine parameters generated by the design tool.

The overall simulation model is presented in Figure 146. The main components of the model are the PM machine and the field oriented control [244].

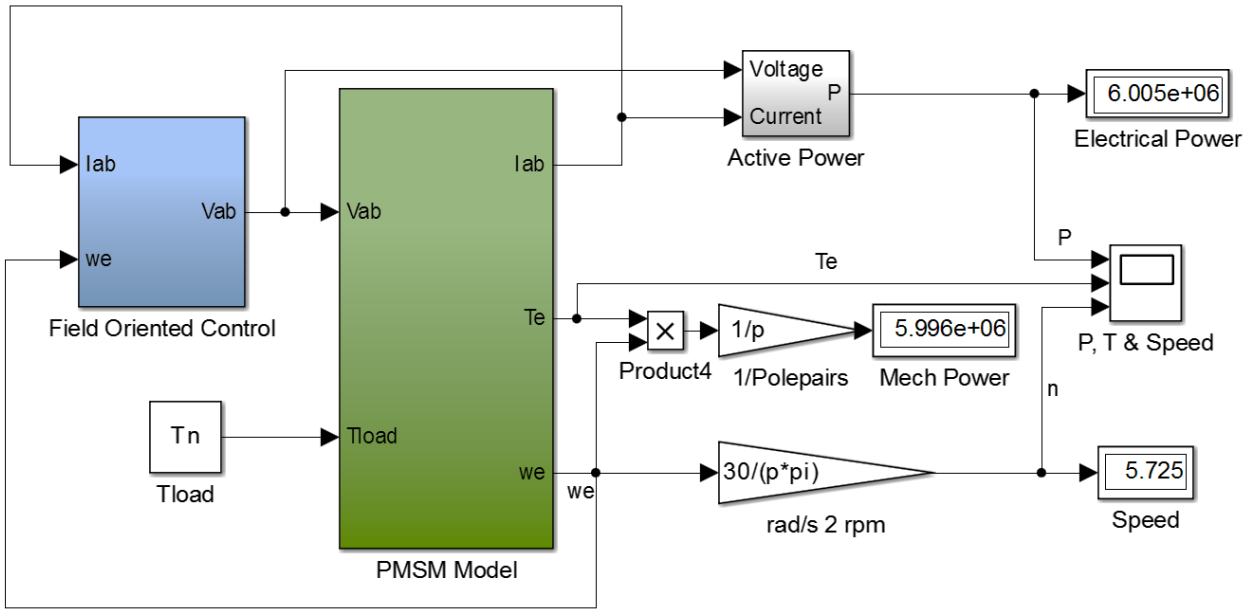

Figure 146: Dynamic Model-Main Model

The PMSM model comprises the voltage, electromagnetic torque and speed equations.

For modelling the machine the 3 phase equations are transformed into dq axis through park. The d and q equivalent circuit diagrams are presented in Figure 147and Figure 148 respectively.

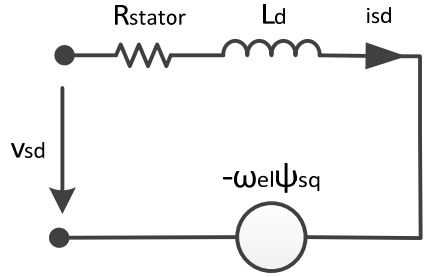

Figure 147:d Axis Equivalent Circuit

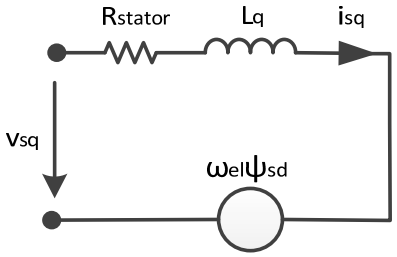

Figure 148:q Axis Equivalent Circuit

Where -i_{sd} and i_{sq} are the stator d and q axis currents;

-v_{sd} and i_{sq} are the stator d and q axis currents

-ω is the electrical speed

The modelling equations [212], [212], [23] are presented in the following.

The voltage equations in dq are (eq 192, eq 193):

$$v_d = R_{stator} \cdot i_{sd} + \frac{d\psi_{sd}}{dt} - \omega_{el}\psi_{sq} \quad \text{eq 192}$$

$$v_{sq} = R_{stator} \cdot i_{sq} + \frac{d\psi_{sq}}{dt} + \omega_{el}\psi_{sd} \quad \text{eq 193}$$

Where the flux equations are (eq 194, eq 195):

$$\psi_{sd} = L_{sd} \cdot i_{sd} + \psi_{PM} \quad \text{eq 194}$$

$$\psi_{sq} = L_{sq} \cdot i_{sq} \qquad \text{eq 195}$$

The mechanical equation (eq 196):

$$T_{el} = \frac{3}{2} p\left(\psi_{sd} \cdot i_{sq} - \psi_{sq} \cdot i_{sd}\right) = \frac{J}{p} \cdot \frac{d\omega_{el}}{dt} + T_{mec} \qquad \text{eq 196}$$

Where

J is the assembly moment of inertia
p – pole pairs
T_{el} is the electromagnetic torque
T_{mec} is the mechanical torque

The Simulink model of the PMSG is shown in Figure 149.

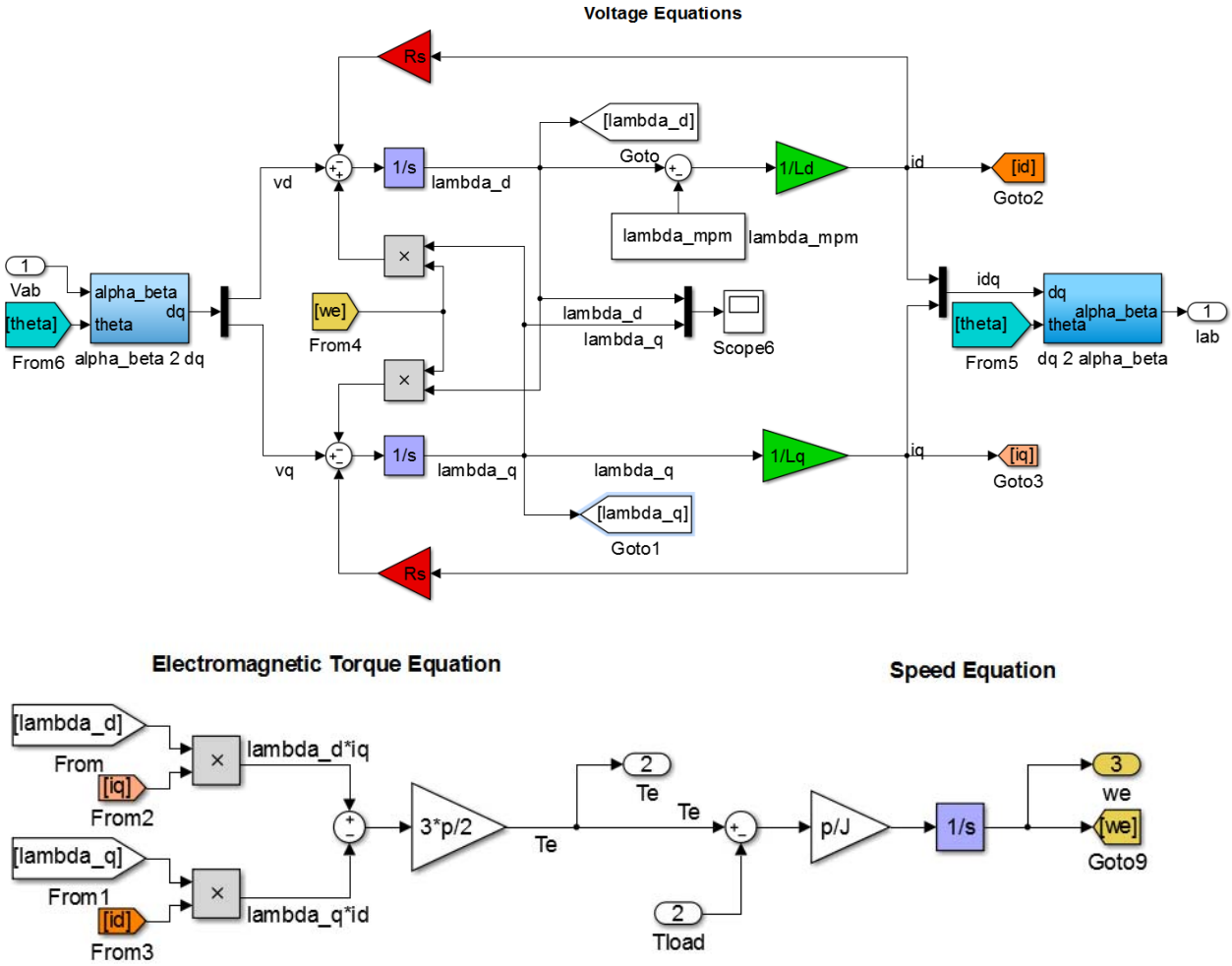

Figure 149: Dynamic Model-PMSM Model

Where p represents the pole pairs and J-the moment of inertia.1/s represent integrators
Figure 150 shows the model of the field oriented control

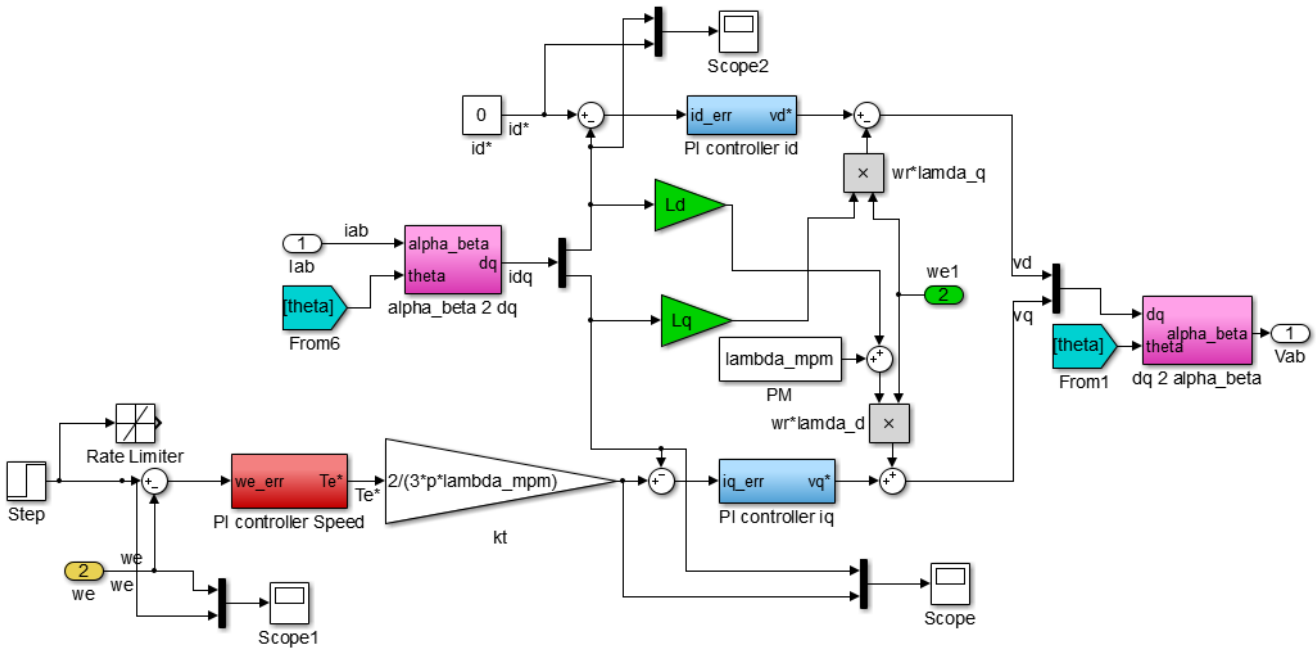

Figure 150: Dynamic model-Field Oriented Control Box

Where the PI controllers for the i_d and i_q are depicted in Figure 151.

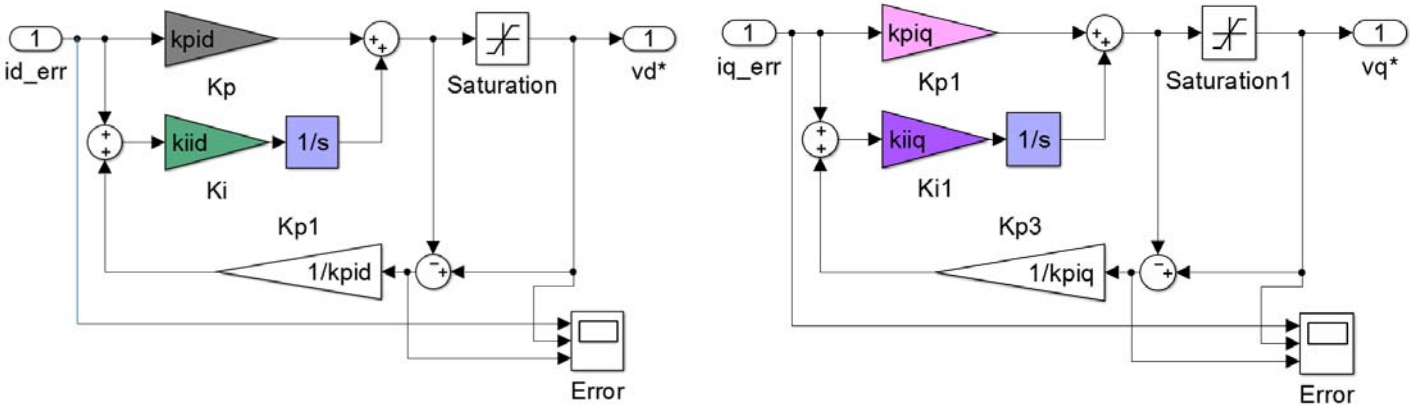

Figure 151: Dynamic model-PI Controller id and iq

The speed controller is shown in Figure 152. To tune the PI controllers the Matab Control System Tuning' tool was used.

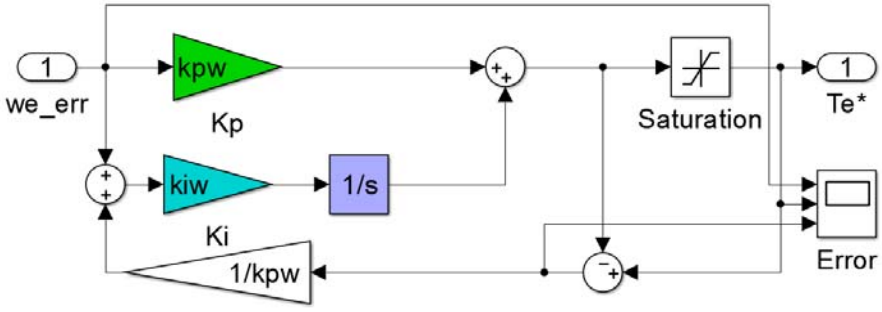

Figure 152: Dynamic model- Speed PI Controller

The First step was to determine the time constant of the plant. Based on that, the PIs are toned so that the response of the system is faster.

The transfer function for the electric circuit (In: Voltage; Out : Current)[245]-eq 197:

$$H_{iq} = \frac{1}{L_q s + R_s} \quad \text{eq 197}$$

Where

L_q – q inductances

R_s –stator resistance

The mechanical transfer function is(eq 198):

$$H_{tn} = \frac{p}{J \cdot s} \quad \text{eq 198}$$

The open loop transfer function for the mechanical circuit is (In: Torque; Out: Speed)-eq 199:

$$H_{torque} = H_{tn} \cdot H_{i_q} \quad \text{eq 199}$$

Where the current transfer function is (eq 200):

$$H_{i_q} = \frac{k_{proportional_i} \cdot s + k_{integrator_i}}{L_q \cdot s^2 + \left(Rs + k_{proportional_i}\right) \cdot s \cdot k_{integrator_i}} \quad \text{eq 200}$$

The values for the proportional and integrator constants for the speed and current controllers are presented in Table 55

	Classic RF	**Double Airgap**
$\boldsymbol{k_{proportional_i}}$	1	4
$\boldsymbol{k_{integrator_i}}$	0.3	8
$\boldsymbol{k_{proportional_{speed}}}$	500	350
$\boldsymbol{k_{integrator_{speed}}}$	20	35

Table 55: PI Tuning of Electrical System-Double Airgap Nessie

Conclusion

This appendix presented the dynamic model of the generator implemented in MATlab Simulink. With this, the Classic RF and the Double Airgap machines were analysed (see Chapter 3: 6 [MW] Candidates).

The purpose of this model is to show that the analytic design tool can successfully be linked with the simulation model. With this relationship, the parameters calculated analytically were checked (see Appendix 10: Validation of the Design Tool)

Appendix 14: Complete Data Sheets

A complete set of values are presented for the Classic RF Benchmark (unoptimised) machine This is an example of a raw design data sheet that is produced by the Nessie Calculation Tool.

Dimension Name	Symbol	Value	[units]
Machine Parameters			
	Machine type	Classic Radial flux PM	
Active power generated	Pactive	5.75	[MW]
	Pmec	6.2	[MW]
	Vout_rated	13.5	[kV]
frequency	f	15	[Hz]
number of phases	m	3	[-]
number of pole pairs	PolePairs	157	[-]
rated speed	n_rpm	5.73	[rpm]
rated speed	n_rad_s	0.6	[rad/s]
turbine torque	Tturbine	10	[MNm]
force density	Fd	0.255	[N/mm^2]
actual force density	ForceDensityActual	0.183	[N/m^2]
power factor	cosfi	0.950	[-]
current density	j	6	[A/mm2]
Resulting Ratios			
	DboreToDstatorActual	0.976	[-]
	LStackToDgapAvgActual	0.691	[-]
	PM2PolePitchActual	0.85	[-]
	SlotPerSlotPitchActual	0.456	[-]
	SlotWidthPerHightActual	0.644	[-]
	CoilWidthPerHightActual	0.3	[-]
Diameters			
rotor diameter	Drotor	5.988	[m]
stator diameter	Dstator	6.145	[m]
average air-gap diameter	Dgap_avg	5.994	[m]
bore diameter	Dbore	6	[m]
	DrotorCore	5.948	[m]
	DrotorIn	5.884	[m]
Lengths			
	gap_length	6	[mm]
	LoverallCore	4.142	[m]
effective length of the core	Lusefull	3.852	[m]
Yokes			
	hRotorYoke	31.74	[mm]
	hStatorYoke	31.74	[mm]
Pitches			
	slotPitch	55.6	[mm]
	polePitch	60	[mm]
	coilPitch_slots	1	[-]
Stator Tooth			
height of tooth	hStatorToothTotal	40.6	[mm]
Width of tooth	wStatorToothTotal	29	[mm]
	Btooth	1.4	[T]
Stator Slot			
SlotType	Open, Square slot bottom (parallel sided slot)		
number of stator slots	Qs	339	[-]
stator fill factor	slot_fill	0.5	[-]
slot/pole and phase	q	0.36	[-]
	SlotPerSlotPitch	0.5	[-]
	SlotWidthPerHight	0.3	[-]
	wStatorSlotTotal	26	[mm]
	hStatorSlotTotal	51	[mm]
total area-with insulation	AstatorSlotTotal	382	[mm2]
	spaceBetweenNeighbourCoils	4.8	[mm]
	slotClosureLength	5	[mm]

Winding			
ConductorCrossSection	Bar conductors for winding		
	SlotPolePhase	0.36	[-]
	Nr_of_concentrated_coils	339	[-]
	Nr_coils_in_Series_per_Phase	113	[-]
	CoilsPerPole	1.08	[-]
	VDesiredPerCoil	69	[V]
	windingFactor	0.95	[-]
	ChordingColilSpanFactor	0.993	[-]
	distributionFactor	0.955	[-]
	NrTurns1Coil	8	[-]
	NrTurnsTotal	2712	[-]
	turnsInSeriesPerPhase	904	[-]
	wCoilInsulated	11	[mm]
	hCoilInsulated	36	[mm]
	LconductorTotal	25930	[m]
	Lconductor1ConcentrCoil	76.5	[m]
	spaceBetweenNeighbourCoils	4.8	[mm]
Permanent Magnet			
	PMTypeMSG	NDFEBO	
	Brem	1	[T]
	Bwkg	0.8	[T]
	Hwkg	-220	[A/m]
	VmagnetRequired	1.654	[m3]
center angle of PM Opening	AngleCenterPMdeg	0.976	[deg]
center angle of PM Opening	AngleCenterPMrad	0.017	[rad]
width of PM	wpm	51	[mm]
height of PM	hpm	20	[mm]
	ApmAtGap	211366	[mm2]
	PM2PolePitch	0.85	[-]
	PM2PolePitchActual	0.85	[-]
	poles	314	[-]
	FluxLinkagePM	58.507	[Wb turns]
Insulation			
	Insulation Class	H	
	slotInsulThick	1	[mm]
	slotClosureThick	5	[mm]
	interTurnsInsul	1.5	[mm]
	interDiffPhasesInsul	3	[mm]
Max insulation temperature	teta_max	180	[degC]
Currents			
curret in one slot	Islot	518.602	[A]
curret in one coil	Icoil	259	[A]
phase curret	Iphase	259	[A]
Line Current	IoutEl	259	[A]
Inductions			
	Bmax	1.7	[T]
	Bgap	0.68	[T]
	average induction in the irgap Bgapavg	0.68	[T]
	actual induction obtained in the air-gap BgapActual	0.68	[T]
	BbackIron	1.2	[T]
	Btooth	1.4	[T]
working induction flux	BwkgCoefficient	0.8	[-]
working point B of PM	Bwkg	0.8	[T]
Flux			
	FluxPerCoil	0.155	[Wb]
	FluxPerPole	0.144	[Wb]
	CoilsPerPole	1.080	[Wb]
Flux Linkage			
(magnetic calculation)	PMfluxLinkagePhase	145	

Flux Leakage-Wasted			
	FluxWastedPerPhase	62	[Wb]
	FluxWastedIn1Slot	0.54	[Wb]
Inductances			
	InductanceLPerPhase	0.29	[H]
	LtotalPhase	0.29	[H]
	LmagnetisingPerPhase	0.057	[H]
	LinductanceLeakageWastage	0.718	[H]
	LWastedOverhang	0H]	[H]
	Ld	0.44 [H]	[H]
	Lq	0.44 [H]	[H]
EMFs			
output line voltage desired	EMFLineNeeded	13.18	[kV]
	EMFLineGenerated	14.217	[kV]
	EMFdesired-generated	-1.08	[kV]
	EMFdesired_Per_Coil	69	[V]
	EMFin1ConcentratedCoilGenerated	72.6	[V]
	VdesiredCoil-generatedCoil	-3.66	[V]
Voltages			
	Vout_rated line	13.5	[kV]
output line voltage desired	Vout_ratedDesired	13.5	[kV]
	VgeneratedLine	17.839	[kV]
	Vdesired-generated	-0.717	[kV]
Lumped Parameters-For Dynamic Simulation			
	Rph	0.054	[Ohm]
	Ld=Lq	0.44	[H]
	InertiaMoment	86084757	[kgm^2]
	FluxLinkagePM	134	[Wb]
Generator Power			
	Pmec	6	[MW]
	Qreactive	1.9	[MW]
	Pactive	5.7	[MW]
	Sapparent	6	[VA]
	powerFactor	0.95	[-]
Losses			
	PCu	9153	[W]
	Peddyst	0.77	[W]
	Physteresis	0.097	[W]
	Piron	0.868	[W]
	PadditionalLoss	36000	[W]
	PtotalLosses	45154	[W]
Performance			
	Pmec	6.2	[MW]
	Pactive	6	[MW]
	PtotalLosses	0.045	[MW]
	EfficiencyGenerator	0.965	[%]
Weights			
	MassCu	10.78	[ton]
	MassFe	35.68	[ton]
	MassPMtotal	9.6	[ton]
	MassActiveMaterialTotal	56.6	[ton]
Cost/Kg			
	costCu	15	[euros/kg]
	costFe	3	[euros/kg]
	costPM	50	[euros/kg]
Cost of Generator Material Estimation			
	costCuGenerator	161.7	[keuros]
	costFeGenerator	107.04	[keuros]
	costPMGenerator	480	[keuros]
	costActiveMaterialTotal	748.74	[keuros]

Table 56: Dimensions table for Generator

References

[1] Bang D, Polinder H, Shrestha G, Ferreira J. Review of generator systems for direct-drive wind turbines. 2008:1-11.

[2] Islam MR, Guo Y, Zhu J. A review of offshore wind turbine nacelle: Technical challenges, and research and developmental trends. Renewable and Sustainable Energy Reviews 2014;33:161-76.

[3] Alexandrova Y, Semken R, Pyrhönen J. Permanent Magnet Synchronous Generator Design Solution for Large Direct-Drive Wind Turbines. International Review of Electrical Engineering 2013;8.

[4] Deep Wind project Team. *Deep wind call-Future Deep Sea Wind Turbine* Technologies THEME [ENERGY.2010.10.2-1][Future Emerging Technologies for Energy Applications (FET)] Grant agreement for: Collaborative project* Annex I - "Description of Work"Grant agreement no: 256769; Date of preparation of Annex I (latest version): 2010-07-15 Date of last change: 2010-07-15 .

[5] Bilgili M, Yasar A, Simsek E. Offshore wind power development in Europe and its comparison with onshore counterpart. Renewable and Sustainable Energy Reviews 2011;15:905-15.

[6] Semken RS, Polikarpova M, Roytta P, Alexandrova J, Pyrhonen J, Nerg J et al. Direct-drive permanent magnet generators for high-power wind turbines: Benefits and limiting factors. Renewable Power Generation, IET 2012;6:1-8.

[7] Stander JN, Venter G, Kamper MJ. Review of direct-drive radial flux wind turbine generator mechanical design. Wind Energy 2012;15:459-72.

[8] Polinder H, Van der Pijl FFA, De Vilder GJ, Tavner PJ. Comparison of direct-drive and geared generator concepts for wind turbines. Energy conversion, IEEE transactions on 2006;21:725-33.

[9] BANG D.
Design of Transverse Flux PM Machines for Large Direct-Drive Wind Turbines.. Busan, Korea : Master of Engineering, Pukyong National University, 2010. ISBN 978-90-5335-336-3.

[10] Deok-je Bang HP. *RESEARCH REPORT on Rough Design of 10 and 20 MW Direct-drive Generators* (Deliverable No.: D 1B2.b.hp1, 2008).

[11] Li H, Chen Z. Overview of different wind generator systems and their comparisons. Renewable Power Generation, IET 2008;2:123-38.

[12] Maples B, Hand M, Musial W. Comparative Assessment of Direct Drive High Temperature Superconducting Generators in Multi-Megawatt Class Wind Turbines. Contract 2010;303:275-3000.

[13] Banham-Hall D, Smith C, Taylor G, Irving M. Meeting modern grid codes with large direct-drive permanent magnet generator-based wind turbines—low-voltage ride-through. Wind Energy 2012.

[14] Tsili M, Papathanassiou S. A review of grid code technical requirements for wind farms. Renewable power generation, IET 2009;3:308-32.

[15] Erlich I, Bachmann U. Grid code requirements concerning connection and operation of wind turbines in Germany. 2005:1253-7.

[16] Teodorescu R, Liserre M, Rodríguez P. Grid converters for photovoltaic and wind power systems. : Wiley, 2011.

[17] Altın M, Goksu O, Teodorescu R, Rodriguez P, Jensen B, Helle L. Overview of recent grid codes for wind power integration. 2010:1152-60.

[18] Pyrhonen J, Jokinen T, Hrabovcová V. Design of rotating electrical machines. : Wiley, 2009.

[19] Krøvel Ø. Design of Large Permanent Magnetized Synchronous Electric Machines. NTNU Trondheim February 2011;Thesis for degree of Philosophae Doctor:Norwegian University of Schience and Technology, Mathematics and Electrical Engineering,Dept. of Electric Power Engineering.

[20] Skaar S, Krovel O, Nilssen R. Distribution, coil-span and winding factors for PM machines with concentrated windings. ICEM 2006 2006:2-5.

[21] Ugade Rosillo G. Study on Concentrated Windings Permanent Magnet Machines for Direct Drive Applications. Doctoral Thesis;University of Mondragon, Spain.

[22] I.M. Postnikov. *Design of electrical machines*-translated from Russian Roumania: Publisher: State Energy, 1954.

[23] Boldea I. Transformers and Electrical Machines (Transformatoare si Masini Electrice). ISBN 973-9389-97-X ed. Timisoara, Romania: Editura Politehnica Timisoara, 2002.

[24] Boldea I. Variable speed generators. ISBN: 0-8493-5715-2 ed. USA: CRC Press, 2006.

[25] Bianchi N, Durello D, Fasolo A. Relationship between rotor losses and size of permanent magnet machines. Diagnostics for Electric Machines, Power Electronics & Drives (SDEMPED), 2011 IEEE International Symposium on 2011:251-7.

[26] Bianchi N, Dai Pre M. Use of the star of slots in designing fractional-slot single-layer synchronous motors. Electric Power Applications, IEE Proceedings - 2006;153:459-66.

[27] Nica FTV, Ritchie E, Leban KM. Comparison between Genetic Algorithms and Particle Swarm Optimization Methods on Standard Test Functions and Machine Design. Proceedings of the 10th Jubilee International Symposium on Advanced Electrical Motion Systems-Electromotion 2013 Cluj-Napoca, Romania 2013;Volume 20, Number 1-4 January-December 2013:ISSN 1223-057x.

[28] Nica FVT, Leban K, Ritchie E. Direct drive TFPM wind generator analytical design optimised for minimum active mass usage. 8th International Symposium on Advanced Topics in Electrical Engineering, ATEE 2013.

[29] Nica FTV, Ritchie E, Leban K. A comparison between two optimized TFPM geometries for 5 MW direct-drive wind turbines. Advanced Topics in Electrical Engineering (ATEE), 2013 8th International Symposium on IEEE 2013.

[30] Köfler H. Losses in Electrical machines Post- Graduate Course
. Faculty of Electrical Engineering Laboratory of Electromechanics Helsinki University of Technology Otaniemi 1990;ISBN 951-22-0157-7 ISSN 0784-4662 TKK OFFSET.

[31] Deok-je Bang HP.
Electromagnetic Optimization of Direct-drive generators.. s.l. : Project UpWind, 2010. Deliverable No.: D 1B2.b.hp2. .

[32] Lu K, Rasmussen PO, Ritchie E. Design considerations of permanent magnet transverse flux machines. Magnetics, IEEE Transactions on 2011;47:2804-7.

[33] Alshibani S, Agelidis VG. Issues regarding cost estimation of permanent magnet synchronous generators for mega-watt level wind turbines. Electric Machines & Drives Conference (IEMDC), 2011 IEEE International 2011;ISBN 978-1-4577-0060-6; DOI 10.1109/IEMDC.2011.5994606:1629-34.

[34] Lu K, Rasmussen PO, Ritchie E. A simple and general approach to determination of self and mutual inductances for AC machines. 2011:1-4.

[35] Nethe A, Scholz T, Stahlmann H. Improving the efficiency of electric machines using ferrofluids. Journal of Physics: Condensed Matter 2006;18:S2985.

[36] Okaue Y, Yoshikawa G, Miyasaka F, Hirata K. Study on Analysis Method for Ferrofluid. Magnetics, IEEE Transactions on 2010;46:2799-802.

[37] Ho JE. Study the Relative Permeability of Ferrofluid with the Mean Value Analysis of Experimental Apparent Gravity. Advanced Materials Research 2011;194:533-6.

[38] Zhu GP, Nguyen NT, Ramanujan R, Huang XY. Nonlinear Deformation of a Ferrofluid Droplet in a Uniform Magnetic Field. Langmuir 2011;27:14834-41.

[39] Odenbach S. Ferrofluids. Journal of Physics: Condensed Matter 2006;18.

[40] Chen S, Zhu J, Zhou T, He B, Huang W, Wang B. Preparation and Properties Study of Polyaniline Conductive Anti-Fouling Coatings. Int.J.Electrochem.Sci 2012;7:8170-84.

[41] Şerban VA, Vuoristo P, Hulka I, Niemi K, Wolf J. Comparison of Structure and Wear Properties of Fine-Structured WC-CoCr Coatings Deposited by HVOF and HVAF Spraying Processes. Solid State Phenomena 2012;188:422-7.

[42] Wu MM, Lou BY. Preparation and Corrosion Resistance of Electroless Plating of Ni-Cr-P/Ni-P Composite Coating on Sintered Nd-Fe-B Permanent Magnet. Advanced Materials Research 2011;284:2187-90.

[43] Alexandrova Y, Semken RS, Pyrhönen J. Permanent magnet synchronous generator design solution for large direct-drive wind turbines: Thermal behavior of the LC DD-PMSG. Appl Therm Eng 2014;65:554-63.

[44] Fletcher J, Judendorfer T, Mueller M, Hassanain N, Muhr M. Electrical issues associated with sea-water immersed windings in electrical generators for wave-and tidal current-driven power generation. Renewable Power Generation, IET 2009;3:254-64.

[45] Judendorfer T, Fletcher J, Hassanain N, Mueller M, Muhr M. Challenges to machine windings used in electrical generators in wave and tidal power plants. 2009:238-41.

[46] Liserre M, Cardenas R, Molinas M, Rodriguez J. Overview of multi-MW wind turbines and wind parks. Industrial Electronics, IEEE Transactions on 2011;58:1081-95.

[47] Szabo C, Imecs M. Synchronous motor drive with controlled stator-field-oriented longitudinal armature reaction. 2007:1214-9.

[48] Samaan N, Zavadil R, Smith JC, Conto J. Modeling of wind power plants for short circuit analysis in the transmission network. 2008:1-7.

[49] Wu R, Blaabjerg F, Wang H, Liserre M, Iannuzzo F. Catastrophic failure and fault-tolerant design of IGBT power electronic converters-an overview. 2013:507-13.

[50] Bikfalvi P, Imecs M. Rotor Fault Detection in Induction Machines: Methods and Techniques-State-of-the-Art. 2006;1:199-204.

[51] Bazine IBA, Tnani S, Poinot T, Champenois G, Jelassi K. On-line detection of stator and rotor faults occurring in induction machine diagnosis by parameters estimation. Diagnostics for Electric Machines, Power Electronics & Drives (SDEMPED), 2011 IEEE International Symposium on 2011:105-12.

[52] Castelli-Dezza F, Maglio MM. A coil model for voltage distribution and electrical insulation analysis. Diagnostics for Electric Machines, Power Electronics & Drives (SDEMPED), 2011 IEEE International Symposium on 2011:444-50.

[53] Hong J, Lee SB, Kral C, Haumer A. Detection of airgap eccentricity for permanent magnet synchronous motors based on the d-axis inductance. Diagnostics for Electric Machines, Power Electronics & Drives (SDEMPED), 2011 IEEE International Symposium on 2011:378-84.

[54] Salon S, Salem S, Sivasubramaniam K. Monitoring and diagnostic solutions for wind generators. Power and Energy Society General Meeting, 2011 IEEE 2011:1-4.

[55] Romary R, Demian C, Schlupp P, Roger J, Szkudlapski T. Real scale experimental devices for stator core fault analysis. 2011:71-6.

[56] Thiringer T. Wind Power wind power Generator Systems wind power generator systems and Local Power System Interconnection. In: Anonymous Renewable Energy Systems: Springer; 2013, p. 1700-1739.

[57] Roshanfekr Fard P, Thiringer T, Lundmark S. Efficiency comparison of a 5 MW wind turbine PMSG-equipped generating system using various dc-link voltages. 2012.

[58] Max L, Thiringer T, Carlson O. Fault handling for a wind farm with an internal DC collection grid. Wind Energy 2012;15:259-73.

[59] Abdulahovic T, Thiringer T. Transformers internal voltage stress during current interruption for different wind turbine layouts. Power Electronics and Applications (EPE), 2013 15th European Conference on 2013:1-10.

[60] Yunus K, Thiringer T, Carlson O. Droop Based Steady State Control Algorithm for a Meshed HVDC Grid. 2013.

[61] Yunus K, Thiringer T, Carlson O. Steady State Controll Strategy for a Meshed HVDC Grid with Wind Power Plants. 2013.

[62] Imecs M, Szabó C, Incze II. Modelling and simulation of controlled bi-directional power electronic converters in a DC energy distribution line with AC grid-and motor-side active filtering. 2007:1-10.

[63] Liu H, Zhu Z, Mohamed E, Fu Y, Qi X. Flux-weakening control of nonsalient pole PMSM having large winding inductance, accounting for resistive voltage drop and inverter nonlinearities. Power Electronics, IEEE Transactions on 2012;27:942-52.

[64] Blaabjerg F, Liserre M, Ma K. Power electronics converters for wind turbine systems. Industry Applications, IEEE Transactions on 2012;48:708-19.

[65] Ma K, Blaabjerg F, Liserre M. Thermal analysis of multilevel grid side converters for 10 MW wind turbines under Low Voltage Ride Through. 2011:2117-24.

[66] Imecs M, Szabo C, Incze II. Modelling and simulation of a vector controlled synchronous generator supplying a DC energy distribution line coupled to the AC grid. 2008:544-9.

[67] Imecs M. **Vector control of the current-excited synchronous generators**. MACRo'2010- International Conference on Recent Achievements in Mechatronics, Automation, Computer Science and Robotics 2010.

[68] D. C. RUS, I. I. INCZE, Maria IMECS, Cs. SZABO. Vector Control Implementation for a Wound-Excited Synchronous Generator Neglecting the Damping Effect. ELECTROMOTION 2014.

[69] Imecs M, Incze II, Szabo C. Stator-Field Oriented Control of the Synchronous Generator: Numerical simulation. 2008:93-8.

[70] Maria IMECS, Ioan Iov INCZE and Csaba SZABO. Control of the energy flow in a dc distribution line, autonomous synchronous generator and ac grid by means of power electronic converters:modeling and simulation. International Carpathian Control Conference ICCC' 2008 Sinaia, ROMANIA May 25-28 2008.

[71] I. I. Incze, Cs. Szabó, Maria Imecs. Voltage-model-based flux identification in synchronous machine drives. International Carpathian Control Conference ICCC' 2009 Zakopane, Poland 2009.

[72] Meier F. Permanent-magnet synchronous machines with non-overlapping concentrated windings for low-speed direct-drive applications 2008.

[73] Johansson H, Berbyuk V. Statistical analysis of fatigue loads in a direct drive wind turbine. 2014.

[74] Aksenov YP, Proshletsov AP, Yaroshenko IV, Noe G. Practical results of on-line diagnostic methods synergy for motors and their efficacy. Diagnostics for Electric Machines, Power Electronics & Drives (SDEMPED), 2011 IEEE International Symposium on 2011:542-9.

[75] Yan J, Lin H, Feng Y, Zhu Z. Control of a grid-connected direct-drive wind energy conversion system. Renewable Energy 2014;66:371-80.

[76] Underwood SJ, Husain I. Online parameter estimation and adaptive control of permanent-magnet synchronous machines. Industrial Electronics, IEEE Transactions on 2010;57:2435-43.

[77] Zhang P, Du Y, Habetler TG, Lu B. A survey of condition monitoring and protection methods for medium-voltage induction motors. Industry Applications, IEEE Transactions on 2011;47:34-46.

[78] Yang W. Condition Monitoring the Drive Train of a Direct Drive Permanent Magnet Wind Turbine Using Generator Electrical Signals. Journal of Solar Energy Engineering 2014;136:021008.

[79] Wei X, Verhaegen M. Sensor and actuator fault diagnosis for wind turbine systems by using robust observer and filter. Wind Energy 2011.

[80] Yao Da, Xiaodong Shi, Krishnamurthy M. Health monitoring, fault diagnosis and failure prognosis techniques for Brushless Permanent Magnet Machines. Vehicle Power and Propulsion Conference (VPPC), 2011 IEEE 2011:1-7.

[81] Ly C, Tom K, Byington CS, Patrick R, Vachtsevanos GJ. Fault diagnosis and failure prognosis for engineering systems: a global perspective. 2009:108-15.

[82] Yang W, Tavner P, Wilkinson M. Condition monitoring and fault diagnosis of a wind turbine synchronous generator drive train. Renewable Power Generation, IET 2009;3:1-11.

[83] Nandi S, Toliyat HA. Condition monitoring and fault diagnosis of electrical machines-a review. 1999;1:197-204.

[84] Dai L. Safe and efficient operation and maintenance of offshore wind farms. 2014.

[85] May A, McMillan D. Condition based maintenance for offshore wind turbines: the effects of false alarms from condition monitoring systems. ESREL 2013 2013.

[86] Aziz MA, Noura H, Fardoun A. General review of fault diagnostic in wind turbines. Control & Automation (MED), 2010 18th Mediterranean Conference on 2010:1302-7.

[87] Judge A. Designing Permanent Magnet Machines for Ferrofluid Immersion. Energy Technology 2013: Carbon Dioxide Management and Other Technologies 2013:189-98.

[88] Engelmann S, Nethe A, Stahlmann TS. Concept of a new type of electric machines using ferrofluids. J Magn Magn Mater 2005;293:685-9.

[89] Franklin TA. WP3 technical status report oct 2012 DeepWind. Ferrofluid flow phenomena 2003.

[90] Meghini G. Optimization of a process for the magnetic density separation into multiple fractions. Thesis 2009;OAI identifier: oai:amslaurea.cib.unibo.it:365:Topics: Fac0021 :: Ingegneria :: Cdl0450.000.364 :: Ingegneria per l'ambiente e il territorio :: terza.

[91] Engelmann S, Nethe A, Scholz T, Stahlmann HD. Force enhancement on a ferrofluid-driven linear stepping motor model. J Magn Magn Mater 2004;272:2345-7.

[92] Nethe A, Scholz T, Stahlmann HD, Filtz M. Ferrofluids in electric motors-a numerical process model. Magnetics, IEEE Transactions on 2002;38:1177-80.

[93] Spałek D. Two theorems about electromagnetic force in activate anisotropic regions. 2010:1-6.

[94] Nethe A, Scholz T, Stahlmann HD. Theoretical evaluation of the ferrofluid-driven electric machine. J Magn Magn Mater 2005;293:709-14.

[95] Judge A. Air gap elimination in permanent magnet machines . Worcester Polytechnic Institute 2012;PhD Thesis.

[96] Greconici M. rese4arch Regarding Magnetic Bearings having ferrofluids(CERCETĂRI PRIVIND LAGĂRELE CILINDRICE CU LICHID MAGNETIC). Politechnical university of Timisoara, Romania 2003.

[97] Hadj NB, Kammoun JK, Fakhfakh MA, Chaieb M, Neji R. A Comparative Thermal Study of Two Permanent Magnets Motors Structures with Interior and Exterior Rotor. ELECTRIC VEHICLES–MODELLING AND SIMULATIONS 2011:333.

[98] Reichert T, Nussbaumer T, Kolar JW. Torque scaling laws for interior and exterior rotor permanent magnet machines. A A 2009;3:1.

[99] Technical University of Cuj-Napoca. invovative microsystem for rezidential wind energy conversion using direct drive generators - NNOWECS. Project PCCA NR 29 / 2012 2013.

[100] Argeseanu A. Direct Drive Transversal Flux Generator For Wind Turbine Deep Wind WP3. Deep Wind 2011.

[101] Polinder H, Ferreira JA, Jensen BB, Abrahamsen AB, Atallah K, McMahon RA. Trends in Wind Turbine Generator Systems. Emerging and Selected Topics in Power Electronics, IEEE Journal of 2013;1:174-85.

[102] Jensen BB, Abrahamsen AB. Modeling, construction, and testing of a simple HTS machine demonstrator. 2011:1636-40.

[103] Abrahamsen AB, Mijatovic N, Seiler E, Zirngibl T, Træholt C, Nørgård PB et al. Superconducting wind turbine generators. Superconductor Science and Technology 2010;23:034019.

[104] Abrahamsen AB, Jensen BB, Seiler E, Mijatovic N, Rodriguez-Zermeno VM, Andersen NH et al. Feasibility study of 5MW superconducting wind turbine generator. Physica C: Superconductivity 2011;471:1464-9.

[105] Karmaker H, Chen E, Chen W, Gao G. Stator design concepts for an 8 MW direct drive superconducting wind generator. 2012:769-74.

[106] Liu Y, Qu R, Wang J. Comparative Analysis on Superconducting Direct-Drive Wind Generators With Iron Teeth and Air-Gap Winding. Applied Superconductivity, IEEE Transactions on 2014;24:1-5.

[107] He J, Tang Y, Li J, Ren L, Shi J, Wang J et al. Conceptual Design of the Cryogenic System for a 12 MW Superconducting Wind Turbine Generator. 2014.

[108] Wang J, Qu R, Liu Y. Comparison study of superconducting generators with multiphase armature windings for large-scale direct-drive wind turbines. 2013.

[109] Snitchler G, Gamble B, King C, Winn P. 10 MW Class Superconductor Wind Turbine Generators. Applied Superconductivity, IEEE Transactions on 2011;21:1089-92.

[110] Schilling A, Cantoni M, Guo J, Ott H. Superconductivity above 130 K in the Hg-Ba-Ca-Cu-O system. Nature 1993;363:56-8.

[111] Bednorz JG, Müller KA. Possible highT c superconductivity in the Ba− La− Cu− O system. Zeitschrift für Physik B Condensed Matter 1986;64:189-93.

[112] Materials S. Image courtesy of Department of Energy - Basic Energy Sciences, http://www.ccas-web.org/superconductivity/#image1

[113] Stautner W, Fair R, Sivasubramaniam K, Amm K, Bray J, Laskaris E et al. Large Scale Superconducting Wind Turbine Cooling. 2013.

[114] Kirke BK, Lazauskas L. Limitations of fixed pitch Darrieus hydrokinetic turbines and the challenge of variable pitch. Renewable Energy 2011;36:893-7.

[115] Jang S, Jeong S, Ryu D, Choi S. Design and analysis of high speed slotless PM machine with Halbach array. Magnetics, IEEE Transactions on 2001;37:2827-30.

[116] Atallah K, Howe D, Mellor P. Design and analysis of multi-pole Halbach (self-shielding) cylinder brushless permanent magnet machines. 1997.

[117] Raich H, Blümler P. Design and construction of a dipolar Halbach array with a homogeneous field from identical bar magnets: NMR Mandhalas. Concepts in Magnetic Resonance Part B: Magnetic Resonance Engineering 2004;23:16-25.

[118] Jang S, Lee S, Yoon I. Design criteria for detent force reduction of permanent-magnet linear synchronous motors with Halbach array. Magnetics, IEEE Transactions on 2002;38:3261-3.

[119] Han Q, Ham C, Phillips R. Four-and eight-piece Halbach array analysis and geometry optimisation for Maglev. 2005;152:535-42.

[120] Davey K. Optimization shows Halbach arrays to be non-ideal for induction devices. Magnetics, IEEE Transactions on 2000;36:1035-8.

[121] Zhu Z, Howe D. Halbach permanent magnet machines and applications: a review. 2001;148:299-308.

[122] Liu X, Chau K, Jiang J, Yu C. Design and analysis of interior-magnet outer-rotor concentric magnetic gears. J Appl Phys 2009;105:07F101,07F101-3.

[123] Atallah K, Rens J, Mezani S, Howe D. A Novel “Pseudo” Direct-Drive Brushless Permanent Magnet Machine. Magnetics, IEEE Transactions on 2008;44:4349-52.

[124] Rasmussen PO, Andersen TO, Jorgensen FT, Nielsen O. Development of a high-performance magnetic gear. Industry Applications, IEEE Transactions on 2005;41:764-70.

[125] Atallah K, Calverley SD, Howe D. Design, analysis and realisation of a high-performance magnetic gear. Electric Power Applications, IEE Proceedings - 2004;151:135-43.

[126] Tsurumoto K, Kikuchi S. A new magnetic gear using permanent magnet. Magnetics, IEEE Transactions on 1987;23:3622-4.

[127] Niguchi N, Hirata K, Muramatsu M, Hayakawa Y. Transmission torque characteristics in a magnetic gear. 2010:1-6.

[128] Du S, Zhang Y, Jiang J. Research on a novel combined permanent magnet electrical machine. 2008:3564-7.

[129] Spooner E, Gordon P, Bumby J, French C. Lightweight ironless-stator PM generators for direct-drive wind turbines. 2005;152:17-26.

[130] Tavner P, Spooner E. Light structures for large low-speed machines for direct-drive applications. 2006:421.1,421.6.

[131] Deep Wind Project Team. www.deepwind.eu/The-DeepWind-Project. ;2014.

[132] Ritchie E, DTU R.
Deep Wind Demonstrator(Task 3.1)-update title.

[133] Polinder H, Bang D, van Rooij R, McDonald A, Mueller M. 10 MW Wind turbine direct-drive generator design with pitch or active speed stall control. 2007;2:1390-5.

[134] Trintis I. *Converter Design* (Task 3.5) -update title. Deep Wind 2011.

[135] Alger L. P. Induction machines, their behavior and uses. New York, Gordon and Breach 1970.

[136] J. Marques, H. Pinheiro, H. A. Gründling, J. R. Pinheiro and H. L. Hey. A SURVEY ON VARIABLE-SPEED WIND TURBINE SYSTEM.

[137] Delli Colli V, Marignetti F, Attaianese C. Analytical and Multiphysics Approach to the Optimal Design of a 10-MW DFIG for Direct-Drive Wind Turbines. Industrial Electronics, IEEE Transactions on 2012;59:2791-9.

[138] Abad G, López J, Rodríguez M, Marroyo L, Iwanski G. Doubly fed induction machine: modeling and control for wind energy generation. : John Wiley & Sons, 2011.

[139] Simoes MG, Farret FA. Renewable energy systems: design and analysis with induction generators. : CRC press, 2004.

[140] Lei T, Barnes M, Smith S. DFIG Wind Turbine Control System Co-ordination to Improve Drive-train Reliability.

[141] Xiang D, Ran L, Tavner PJ, Yang S. Control of a doubly fed induction generator in a wind turbine during grid fault ride-through. Energy Conversion, IEEE Transactions on 2006;21:652-62.

[142] Hansen AD, Michalke G. Fault ride-through capability of DFIG wind turbines. Renewable Energy 2007;32:1594-610.

[143] Draper A. Electrical machines. : Longmans, 1967.

[144] Bakshi MBU. DC machines and Synchronous Machines. : Technical publications, 2007.

[145] Dubois M. Optimized permanent magnet generator topologies for direct-drive wind turbines. PhD, Delft University 2004;142:143-82.

[146] Semken RS, Polikarpova M, Röyttä P, Alexandrova J, Pyrhonen J, Nerg J et al. Direct-drive permanent magnet generators for high-power wind turbines: benefits and limiting factors. Renewable Power Generation, IET 2012;6:1-8.

[147] Pyrhönen J, Nerg J, Kurronen P, Puranen J, Haavisto M. Permanent magnet technology in wind power generators. 2010:1-6.

[148] Luise F, Pieri S, Mezzarobba M, Tessarolo A. Regenerative Testing of a Concentrated-Winding Permanent-Magnet Synchronous Machine for Offshore Wind Generation—Part I: Test Concept and Analysis. Industry Applications, IEEE Transactions on 2012;48:1779-90.

[149] Xue YS, Han L, Li H, Xie LD. Optimal design and comparison of different PM synchronous generator systems for wind turbines. 2008:2448-53.

[150] Pyrhonen J, Alexandrova Y, Semken RS, Hamalainen H. Wind power electrical drives for permanent magnet generators—Development in Finland. 2012:9-16.

[151] EL-Refaie AM. Fractional-slot concentrated-windings synchronous permanent magnet machines: Opportunities and challenges. Industrial Electronics, IEEE Transactions on 2010;57:107-21.

[152] Lu K. Design Study for Controllable Electric Motor for Three Wheel Drive, In Wheel Mounting on Professional, Electric, Lawn Mower 2005.

[153] Lu K, Rasmussen PO, Ritchie E. An analytical equation for cogging torque calculation in permanent magnet motors. 2006.

[154] Lu K, Ritchie E. Preliminary comparison study of drive motor for electric vehicle application. 2001;2:995-8.

[155] Liserre M, Cárdenas R, Molinas M, Rodriguez J. Overview of multi-MW wind turbines and wind parks. Industrial Electronics, IEEE Transactions on 2011;58:1081-95.

[156] Nadine P, Richter A. SWOT Analysis - Idea, Methodology And A Practical Approach. ISBN 3640303032, 9783640303038 ed. : GRIN Verlag, 2009.

[157] Chen Y, Pillay P, Khan A. PM wind generator topologies. Industry Applications, IEEE Transactions on 2005;41:1619-26.

[158] Argeseanu A, Ritchie E, Leban K. Optimal design of the transverse flux machine using a fitted genetic algorithm with real parameters. Optimization of Electrical and Electronic Equipment (OPTIM), 2012 13th International Conference on 2012:671-8.

[159] Nica FVT, Leban K, Ritchie E. Direct drive TFPM wind generator analytical design optimised for minimum active mass usage. 2013:1-6.

[160] Sethuraman L, Venugopal V, Zavvos A, Mueller M. Structural integrity of a direct-drive generator for a floating wind turbine. Renewable Energy 2014;63:597-616.

[161] Shrestha G, Polinder H, Bang D, Ferreira JA. Structural flexibility: a solution for weight reduction of large direct-drive wind-turbine generators. Energy Conversion, IEEE Transactions on 2010;25:732-40.

[162] Versteegh C, Hassan G. Design of the Zephyros Z72 wind turbine with emphasis on the direct drive PM generator. 2004.

[163] Zavvos A, Bang D, McDonald A, Polinder H, Mueller M. Structural analysis and optimisation of transverse flux permanent magnet machines for 5 and 10 MW direct drive wind turbines. Wind Energy 2012;15:19-43.

[164] Bang D, Polinder H, Ferreira JA, Hong S. Structural mass minimization of large direct-drive wind generators using a buoyant rotor structure. 2010:3561-8.

[165] Seidel M. Jacket substructures for the REpower 5M wind turbine. 2007.

[166] Boglietti A, Cavagnino A, Staton D, Shanel M, Mueller M, Mejuto C. Evolution and modern approaches for thermal analysis of electrical machines. Industrial Electronics, IEEE Transactions on 2009;56:871-82.

[167] Stone G. Electrical insulation for rotating machines: design, evaluation, aging, testing, and repair. : Wiley-IEEE Press, 2004.

[168] Traxler-Samek G, Zickermann R, Schwery A. Cooling airflow, losses, and temperatures in large air-cooled synchronous machines. Industrial Electronics, IEEE Transactions on 2010;57:172-80.

[169] Luke GE. The cooling of electric machines. American Institute of Electrical Engineers, Transactions of the 1923;42:636-52.

[170] Li Zhenguo, Fu Deping, Guo Jianhong, Gu Guobiao, Xiong Bin. Study on spraying evaporative cooling technology for the large electrical machine. Electrical Machines and Systems, 2009 ICEMS 2009 International Conference on 2009:1-4.

[171] Siemens. *High-Voltage Machines Product-Overview*.

[172] Peng X, Guo H. Electromagnetic analyzing of slotless evaporative cooling generator. 2008:4192-4.

[173] Nerg J, Rilla M, Pyrhonen J. Thermal analysis of radial-flux electrical machines with a high power density. Industrial Electronics, IEEE Transactions on 2008;55:3543-54.

[174] Xyptras J, Hatziathanassiou V. Thermal analysis of an electrical machine taking into account the iron losses and the deep-bar effect. Energy Conversion, IEEE Transactions on 1999;14:996-1003.

[175] Staton DA, Cavagnino A. Convection heat transfer and flow calculations suitable for electric machines thermal models. Industrial Electronics, IEEE Transactions on 2008;55:3509-16.

[176] Keysan O, McDonald A, Mueller M. Integrated Design and Optimization of a Direct Drive Axial Flux Permanent Magnet Generator for a Tidal Turbine. 2010;10.

[177] Keysan O, Mueller M, McDonald A, Hodgins N, Shek J. Designing the C-GEN lightweight direct drive generator for wave and tidal energy. IET Renewable Power Generation 2012;6:161-70.

[178] Keysan O, McDonald AS, Mueller M. A direct drive permanent magnet generator design for a tidal current turbine (SeaGen). 2011:224-9.

[179] Pyrhönen J, Jokinen T, Hrabovcová V, Niemelä H. Design of rotating electrical machines. : Wiley Online Library, 2008.

[180] IEC 60085.

[181] IEC 600034-1.

[182] Naidu MS, Kamaraju V. High voltage engineering. 2nd ed. New York: McGraw-Hill, 1996.

[183] Zhu Z. Fractional slot permanent magnet brushless machines and drives for electric and hybrid propulsion systems. COMPEL: The International Journal for Computation and Mathematics in Electrical and Electronic Engineering 2011;30:9-31.

[184] Dosiek L, Pillay P. Cogging torque reduction in permanent magnet machines. Industry Applications, IEEE Transactions on 2007;43:1565-71.

[185] Zhu Z, Howe D. Influence of design parameters on cogging torque in permanent magnet machines. Energy Conversion, IEEE Transactions on 2000;15:407-12.

[186] Trifu I, Leban,Krisztina Monika, Ritchie, Ewen. Influence of Closed Stator Slots on Cogging Torque. Proceedings of the 10th Jubilee International Symposium on Advanced Electrical Motion Systems-Electromotion 2013 Cluj-Napoca, Romania;Volume 20, Number 1-4 January-December 2013:ISSN 1223-057x.

[187] Koo M, Jang S, Park Y, Park H, Choi J. Characteristic Analysis of Direct-Drive Wind Power Generator considering Permanent Magnet Shape and Skew Effects to Reduce Torque Ripple Based on Analytical Approach. Magnetics, IEEE Transactions on 2013;49:3917-20.

[188] Koivuluoto H. Microstructural Characteristics and Corrosion Properties of Cold-Sprayed Coatings. Tampereen teknillinen yliopisto.Julkaisu-Tampere University of Technology.Publication; 882 2010.

[189] Montgomery EL, Calle LM, Curran JC, Kolody MR. Timescale Correlation between Marine Atmospheric Exposure and Accelerated Corrosion Testing-Part 2. 2012.

[190] Wang Y, Jiang S, Zheng Y, Ke W, Sun W, Wang J. Effect of porosity sealing treatments on the corrosion resistance of high-velocity oxy-fuel (HVOF)-sprayed Fe-based amorphous metallic coatings. Surface and Coatings Technology 2011;206:1307-18.

[191] Tamaki S, Matsunaga H, Kato K, Ito S. Advance in Corrosion Protection and Its Material. Shinnittetsu Giho 2002:2-5.

[192] Zeng Z, Sakoda N, Tajiri T, Kuroda S. Structure and corrosion behavior of 316L stainless steel coatings formed by HVAF spraying with and without sealing. Surface and Coatings Technology 2008;203:284-90.

[193] Li Q, Yang X, Zhang L, Wang J, Chen B. Corrosion resistance and mechanical properties of pulse electrodeposited Ni–TiO< sub> 2</sub> composite coating for sintered NdFeB magnet. J Alloys Compounds 2009;482:339-44.

[194] Mueller M, Baker N. Direct drive electrical power take-off for offshore marine energy converters. Proc Inst Mech Eng A: J Power Energy 2005;219:223-34.

[195] www.iec.ch. International Standards and Conformity Assessment for all electrical, electronic and related technologies
. International Electrotechnical Commission;2014.

[196] Bang D. Design of transverse flux permanent magnet machines for large direct-drive wind turbines. Master of Engineering Pukyong National University, Korea 2010.

[197] Zhu Z. Course: 'Design of Electrical Machines'. University of Sheffield, UK spring semester 2013.

[198] Say MG, Pink EN. The performance and design of alternating current machines: transformers, three-phase induction motors and synchronous machines. : Pitman, 1958.

[199] El-Refaie AM. Fractional-Slot Concentrated-Windings Synchronous Permanent Magnet Machines: Opportunities and Challenges. Industrial Electronics, IEEE Transactions on 2010;57:107-21.

[200] Lindh PM, Jussila HK, Niemela M, Parviainen A, Pyrhonen J. Comparison of concentrated winding permanent magnet motors with embedded and surface-mounted rotor magnets. Magnetics, IEEE Transactions on 2009;45:2085-9.

[201] Brisset S, Vizireanu D, Brochet P. Design and optimization of a nine-phase axial-flux PM synchronous generator with concentrated winding for direct-drive wind turbine. Industry Applications, IEEE Transactions on 2008;44:707-15.

[202] Di Gerlando A, Perini R, Ubaldini M. High pole number, PM synchronous motor with concentrated coil armature windings. In: Anonymous Recent Developments of Electrical Drives: Springer; 2006, p. 307-320.

[203] El-Refaie AM, Jahns TM. Impact of Winding Layer Number and Magnet Type on Synchronous Surface PM Machines Designed for Wide Constant-Power Speed Range Operation. Industry Applications Conference, 2006 41st IAS Annual Meeting Conference Record of the 2006 IEEE 2006;3:1486-93.

[204] Fornasiero E, Alberti L, Bianchi N, Bolognani S. Considerations on selecting fractional—slot windings. 2010:1376-83.

[205] Bianchi N, Fornasiero E. Impact of MMF Space Harmonic on Rotor Losses in Fractional-Slot Permanent-Magnet Machines. Energy Conversion, IEEE Transactions on 2009;24:323-8.

[206] Bianchi N, Bolognani S, Pre MD, Grezzani G. Design considerations for fractional-slot winding configurations of synchronous machines. Industry Applications, IEEE Transactions on 2006;42:997-1006.

[207] Salminen P, Niemela M, Pyhonen J, Mantere J. Performance analysis of fractional slot wound PM-motors for low speed applications. 2004;2:1032-7.

[208] Abdel-Khalik AS, Ahmed S, Massoud A, Elserougi A. An Improved Performance Direct-Drive Permanent Magnet Wind Generator Using A Novel Single Layer Winding Layout. 2013.

[209] Hunh VX. Modeling of exterior rotor PM machine with concentrated windings. PhD Thesis, Delft University 2012;ISBN 9789088914690.

[210] Chee-Mun O. Dynamic simulation of electric machinery. 1998.

[211] Krovel O, Nilssen R, Skaar S, Lovli E, Sandoy N. Design of an Integrated 100kW Permanent Magnet Synchronous Machine in a Prototype Thruster for Ship Propulsion. ICEM 2004 2004:6-8.

[212] Kelemen, Árpád,Imecs, Mária,. Vector control of AC drives Vol. 2 Vol. 2. Budapest: Écriture, 1993.

[213] Hubert CI. Electric Machines: Theory, Operating Applications, and Controls (2nd Edition). ISBN: 0130612103 / 0-13-061210-3: Prentice Hall.

[214] Wildi T. Electrical Machines, Drives and Power Systems. Pearson plc 1999;0130824607 / 9780130824608 / 0-13-082460-7.

[215] Rahman T, Akiror JC, Pillay P, Lowther DA. Comparison of Iron Loss Prediction Formulae. parameters;3:4.

[216] Sarma MS. Electric Machines : Steady-State Theory and Dynamic Performance. ISBN-10: 0534938434 | ISBN-13: 9780534938437 ed. , 1994.

[217] Rasmussen C. Modeling and simulation of surface mounted PM motors. Technical University of Denmark, Aalborg University, Danfoss A/S , Graham A/S 1996;The Danish Energy Agency, The Sjelland Consortium of Power Stations:216.

[218] Ishak D, Zhu Z, Howe D. Eddy-current loss in the rotor magnets of permanent-magnet brushless machines having a fractional number of slots per pole. Magnetics, IEEE Transactions on 2005;41:2462-9.

[219] Brown D, Ma B, Chen Z. Developments in the processing and properties of NdFeB-type permanent magnets. J Magn Magn Mater 2002;248:432-40.

[220] Deok-je Bang, Polinder H, Shrestha G, Ferreira JA. Comparative design of radial and transverse flux PM generators for direct-drive wind turbines. Electrical Machines, 2008 ICEM 2008 18th International Conference on 2008:1-6.

[221] Deok-je Bang, Polinder H, Shrestha G, Ferreira JA. Promising Direct-Drive Generator System for Large Wind Turbines. Wind Power to the Grid - EPE Wind Energy Chapter 1st Seminar, 2008 EPE-WECS 2008 2008:1-10.

[222] Li H, Chen Z, Polinder H. Optimization of multibrid permanent-magnet wind generator systems. Energy Conversion, IEEE Transactions on 2009;24:82-92.

[223] Trifu I. Research on Reducing Cogging Torque in Permanent Magnet Synchronous Generators Used For Wind Systems. Dept of Electrical machines, Materials and Electric Drives, Politechnical University of Bucuresti, Romania 2013;Senate decision number 225 from 27.09.2013:138.

[224] Robinson J, Rahmat-Samii Y. Particle swarm optimization in electromagnetics. Antennas and Propagation, IEEE Transactions on 2004;52:397-407.

[225] Kennedy J, Mendes R. Population structure and particle swarm performance. 2002;2:1671-6.

[226] Bai Q. Analysis of particle swarm optimization algorithm. Computer and Information Science 2010;3:P180.

[227] Nima Madani. Design of a Permanent Magnet Synchronous Generator for a Vertical Axis Wind Turbine.

[228] Dr. Xiaodong Li,Professor Andries P.Engelbrecht,. Particle Swarm Optimization, A tutorial prepared for GECCO'07, An introduction and its recent developments. 2007.

[229] del Valle Y, Venayagamoorthy GK, Mohagheghi S, Hernandez JC, Harley RG. Particle swarm optimization: basic concepts, variants and applications in power systems. Evolutionary Computation, IEEE Transactions on 2008;12:171-95.

[230] Clerc M, Kennedy J. The particle swarm-explosion, stability, and convergence in a multidimensional complex space. Evolutionary Computation, IEEE Transactions on 2002;6:58-73.

[231] Settles M. An Introduction to Particle Swarm Optimization. Department of Computer Science, University of Idaho, Novembrer 2005.

[232] Eberhart RC, Shi Y. Comparing inertia weights and constriction factors in particle swarm optimization. 2000;1:84-8.

[233] Eberhart RC, Shi Y, Kennedy J. Swarm intelligence. : Morgan Kaufmann, 2001.

[234] Kennedy J. Small worlds and mega-minds: effects of neighborhood topology on particle swarm performance. 1999;3.

[235] Winston PH. Artificial intelligence. Reading, Mass.: Ad-dison-Wesley 1984.

[236] Melanie M. An introduction to genetic algorithms. Cambridge, Massachusetts London, England, Fifth printing 1999.

[237] Herrera F, Lozano M, Sánchez A. A taxonomy for the crossover operator for real-coded genetic algorithms: An experimental study. Int J Intell Syst 2003;18:309-38.

[238] Argeseanu A, Popa M. Genetic Algorithms. Theory and Applications. (roumanian). ISBN(10) 973-625-315-3, ISBN(13) 978- 973-625-315-7 ed. : Politehnica, Timisoara, 2006.

[239] Skaar S, Nilssen R. Genetic optimization of electric machines, a state of the art study. 2004.

[240] Goldberg DE, Deb K. A comparative analysis of selection schemes used in genetic algorithms. Urbana 1991;51:61801-2996.

[241] Pencheva T, Atanassov K, Shannon A. Modelling of a stochastic universal sampling selection operator in genetic algorithms using generalized nets. 2009:1-7.

[242] Smith JE, Fogarty TC. Operator and parameter adaptation in genetic algorithms. Soft Computing 1997;1:81-7.

[243] Herrera F, Lozano M, Pérez E, Sánchez A, Villar P. Multiple crossover per couple with selection of the two best offspring: an experimental study with the BLX-α crossover operator for real-coded genetic algorithms. Advances in Artificial Intelligence—IBERAMIA 2002 2002:392-401.

[244] Chen L. Real coded genetic algorithm optimization of long term reservoir operation. JAWRA Journal of the American Water Resources Association 2003;39:1157-65.

[245] González-Longatt F, Wall P, Terzija V. A simplified model for dynamic behavior of permanent magnet synchronous generator for direct drive wind turbines. 2011:1-7.

[246] Ogata K. Modern control engineering. : Upper Saddle River, N.J. : Prentice Hall, 2002.